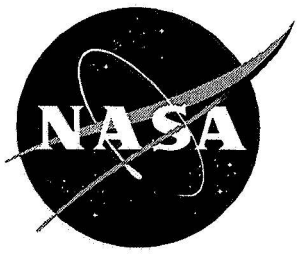

NASA Conference Publication 10139, Part 2
DOT/FAA/RD-94/14-II

Airborne Windshear Detection and Warning Systems

Fifth and Final Combined Manufacturers' and Technologists' Conference

Compiled by
V. E. Delnore
Lockheed Engineering & Sciences Company • Hampton, Virginia

Proceedings of a conference sponsored by the Federal Aviation Administration, Washington, D.C., and the National Aeronautics and Space Administration, Washington, D.C., and held in Hampton, Virginia
September 28–30, 1993

July 1994

Foreword

A dramatic improvement in the flight safety of transport aircraft worldwide has become possible through the development of sensor systems that detect hazardous wind changes miles ahead of an aircraft. This development--the result of a unique cooperation among NASA, the FAA, industry, and academia--involved fundamental breakthroughs in the understanding and measurement of commercial aviation's most lethal weather threat: microburst windshear.

One purpose of the meeting reported in these Proceedings was to spread the word: we were challenged with a need, joined forces to meet that need, and were enormously successful. U. S. avionics manufacturers small and large have capitalized on the results of our research and consulting guidance, and now have mounted independent sensor development efforts in the best entrepreneurial tradition. The technology applications include Doppler radar, lidar (laser radar), and infrared systems, each of which required groundbreaking advances in state-of-the-art design and signal processing. Many systems are now in the final stages of FAA production certification and commercial sales.

The meeting had another purpose: to open the next chapter in interagency and industry cooperation--this time for the development and application of sensors for wake vortices and for synthetic and enhanced vision systems. This too is reported in these Proceedings.

The windshear research reported here is the result of NASA and the FAA in 1986 setting a timetable for developing and demonstrating a solution to a problem then responsible for more than half the U. S. commercial aviation fatalities of the preceding decade. The success of this research, with flight tests completed two years ahead of schedule, ensures that, in the very near future, all airline passengers will travel with the threat of aviation's worst weather hazard effectively removed.

Contents

Part 1*

* Part 1 published under separate cover.

Session 4:

CERTIFICATION OF PREDICTIVE WINDSHEAR DETECTION AND AVOIDANCE SYSTEMS.

Chair: D. Hinton,

NASA Langley Research Center.

PT-2

Session 4:

CERTIFICATION OF PREDICTIVE WINDSHEAR DETECTION AND AVOIDANCE SYSTEMS.

Chair: D. Hinton, NASA Langley Research Center.

The FAA View. R. Passman and F. Rock, FAA

Windshear Certification Data Base for Forward-Look Detection Systems. G. Switzer, Research Triangle Institute, and D. Hinton and F. Proctor, NASA Langley Research Center

Certification Methodology Applied to the NASA Experimental Flight Sytem. C. Britt and G. Switzer, Research Triangle Institute, and E. Bracalente, NASA Langley Research Center

Certification of Windshear Performance with RTCA Class D Radomes. B, Mathews and L. Barnett, Westinghouse Electric Co.

Airport Surveillance Using a Solid State Coherent Lidar. M. Hufaker, Coherent Technologies, Inc.

The FAA View.

R. Passman and F. Rock,

FAA

[This presentation consisted of comments only;

no visuals are available for these Proceedings]

Windshear Certification Data Base for Forward-Look Detection Systems.

G. Switzer,
Research Triangle Institute,
and
D. Hinton and F. Proctor,
NASA Langley Research Center

WINDSHEAR DATABASE FOR FORWARD-LOOKING SYSTEMS CERTIFICATION

George F. Switzer*, Fred H. Proctor+, and

David A. Hinton+

* Research Triangle Institute

+NASA LaRC, Flight Management Division

September 29, 1993

Abstract

Described is an introduction to a comprehensive database (e.g., Switzer et al 1993) that is to be used for certification testing of airborne forward-look windshear detection systems. The database was developed by NASA Langley Research Center, at the request of the Federal Aviation Administration (FAA), to support the industry initiative to certify and produce forward-look windshear detection equipment. The database contains high-resolution, three-dimensional fields for meteorological variables that may be sensed by forward-looking systems. The database is made up of seven case studies that are generated by the Terminal Area Simulation System (e.g., Proctor 1987a, 1987b), a state-of-the-art numerical system for the realistic modeling of windshear phenomena. The selected cases contained in the certification documentation represent a wide spectrum of windshear events. The database will be used with vendor-developed sensor simulation software and vendor-collected ground-clutter data to demonstrate detection performance in a variety of meteorological conditions using NASA/FAA pre-defined path scenarios for each of the certification cases.

Included in the following are a brief outline of the contents and sample plots from the database documentation. These plots show fields of hazard factor, or F-factor (Bowles 1990), radar reflectivity, and velocity vectors on a horizontal plane overlayed with the applicable certification paths. For the plot of the F-factor field the region of 0.105 and above signifies an area of hazardous, performance decreasing windshear, while negative values indicate regions of performance increasing windshear. The values of F-factor are based on 1-Km averaged segments along horizontal flight paths, assuming an air speed of 150 knots (~75 m/s). The database has been released to vendors participating in the certification process. The database and associated document have been transferred to the FAA for archival and distribution and are available from the FAA.

References

Bowles, R. L., 1990: Reducing windshear risk through airborne systems technology. The 17th Congress of the ICAS, Stockholm, Sweden, 27 pp.

Proctor, F. H., 1987: The Terminal Area Simulation System, Volume I: Theoretical formulation. NASA Contractor Rep. 4046, NASA, Washington, DC, 176 pp. [Available from the National Technical Information Service, Springfield, VA, 22161.]

Proctor, F. H., 1987: The Terminal Area Simulation System, Volume II: Verification Experiments. NASA Contractor Rep 4047, NASA, Washington, DC, 112 pp. [Available from the National Technical Information Service, Springfield, VA, 22161.]

Switzer, G. F., F. H. Proctor, D. A. Hinton, and J. V. Aanstoos, 1993: Windshear Database For Forward-Looking Systems Certification. NASA Tech. Mem. 109012, 132 pp.

OUTLINE

- Introduction
- Overview of Database Cases
- Overview of Documentation
- Sample Plots
- Summary

DATABASE REQUIREMENTS

- Certification of forward-looking systems will require performance simulations
- Simulation requires sensor, windshear, & clutter models
- Certification database generated at FAA/industry request
- Database generated by NASA using Terminal Area Simulation System (TASS) numerical model
- Wide range of windshear conditions for testing LIDAR, radar, and infrared sensors

CERTIFICATION CONDITIONS MODELED

Wide variety of windshear conditions:

- High to low reflectivity microbursts (55 to 5 dBZ)
- Intervening rain cases
- Symmetrical, asymmetrical, and multiple core events
- Different life cycle stages
- Large scale and narrow core events
- Deep and shallow outflows
- Cold and warm thermal profiles
- Potentially hazardous gust front
- Contains 1-Km averaged F factor near "must not" and "must" alert levels

EVENTS REPRESENTED IN DATABASE

. 9 data sets derived from 7 events

1) DFW Accident Case, Wet Microburst, Rain and Hail
2) 6/20/91 Orlando, Florida, Wet Microburst
3) 7/11/88 Denver, Colorado, Multiple Microburst event
4) 7/14/82 Denver, Colorado, Stable Layer, Warm Microburst
5) 7/8/89 Denver, Colorado, Very Dry Microburst
6) Highly Asymmetric Florida Microburst
7) Montana Sounding, Gust Front

. 4 of 7 events represent observed events. 3 derived from soundings modified for specific objective.

VARIABLES CONTAINED IN DATABASE

Description

- 3 Components of Wind Velocity
- Temperature
- Radar-Reflectivity Factor
- Water Vapor
- Rainwater
- Hailwater
- Liquid Cloud-Droplet Water
- Radar Reflectivity Including Insects

F-factor diagnosed from winds along chosen path.

DOCUMENTATION CONTAINED WITHIN REPORT

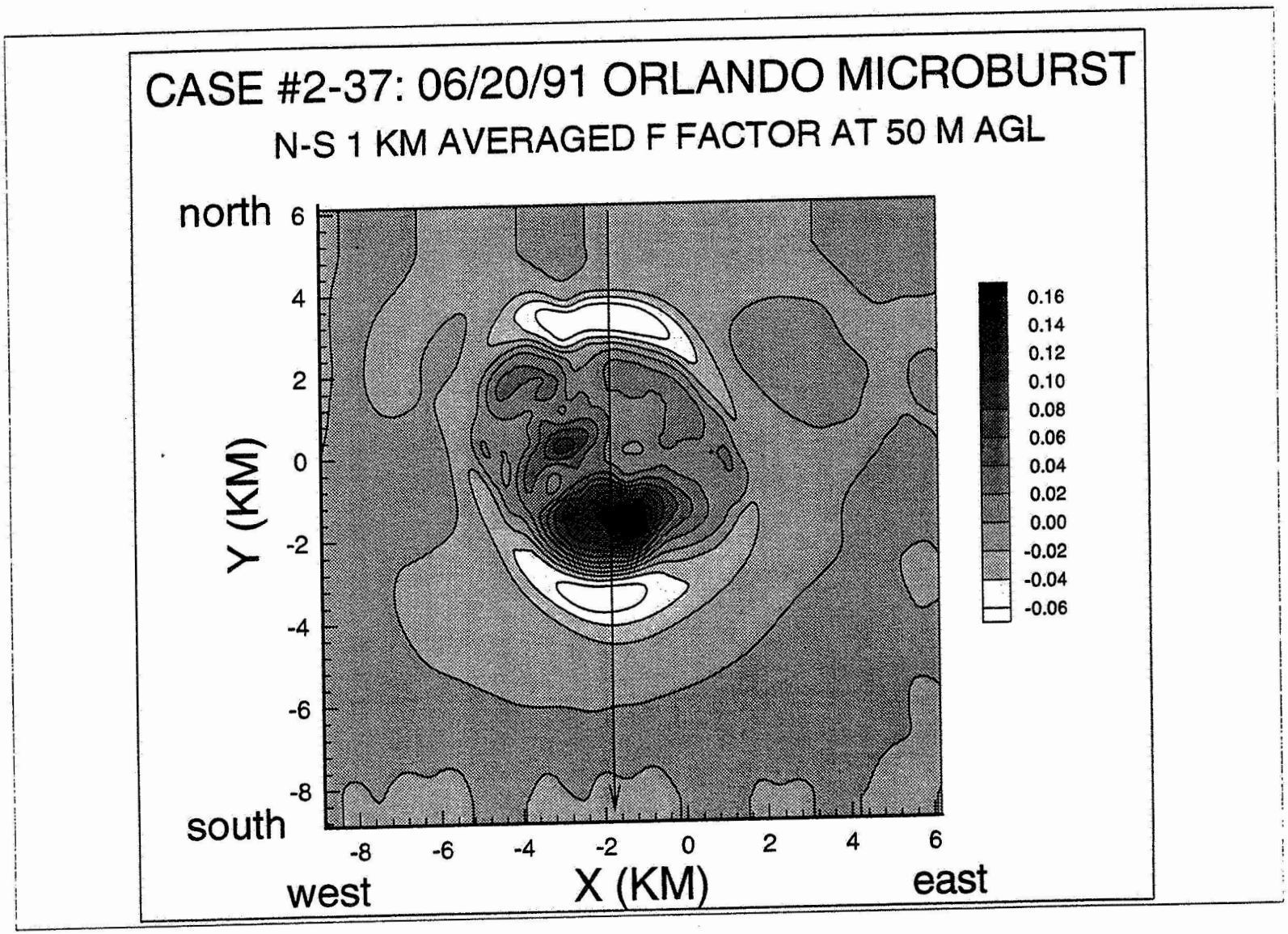
CASE #2-37: 06/20/91 ORLANDO MICROBURST
N-S 1 KM AVERAGED F FACTOR AT 50 M AGL
north
south
west
east
Y (KM)
X (KM)
6
4
2
0
-2
-4
-6
-8
0.16
0.14
0.12
0.10
0.08
0.06
0.04
0.02
0.00
-0.02
-0.04
-0.06

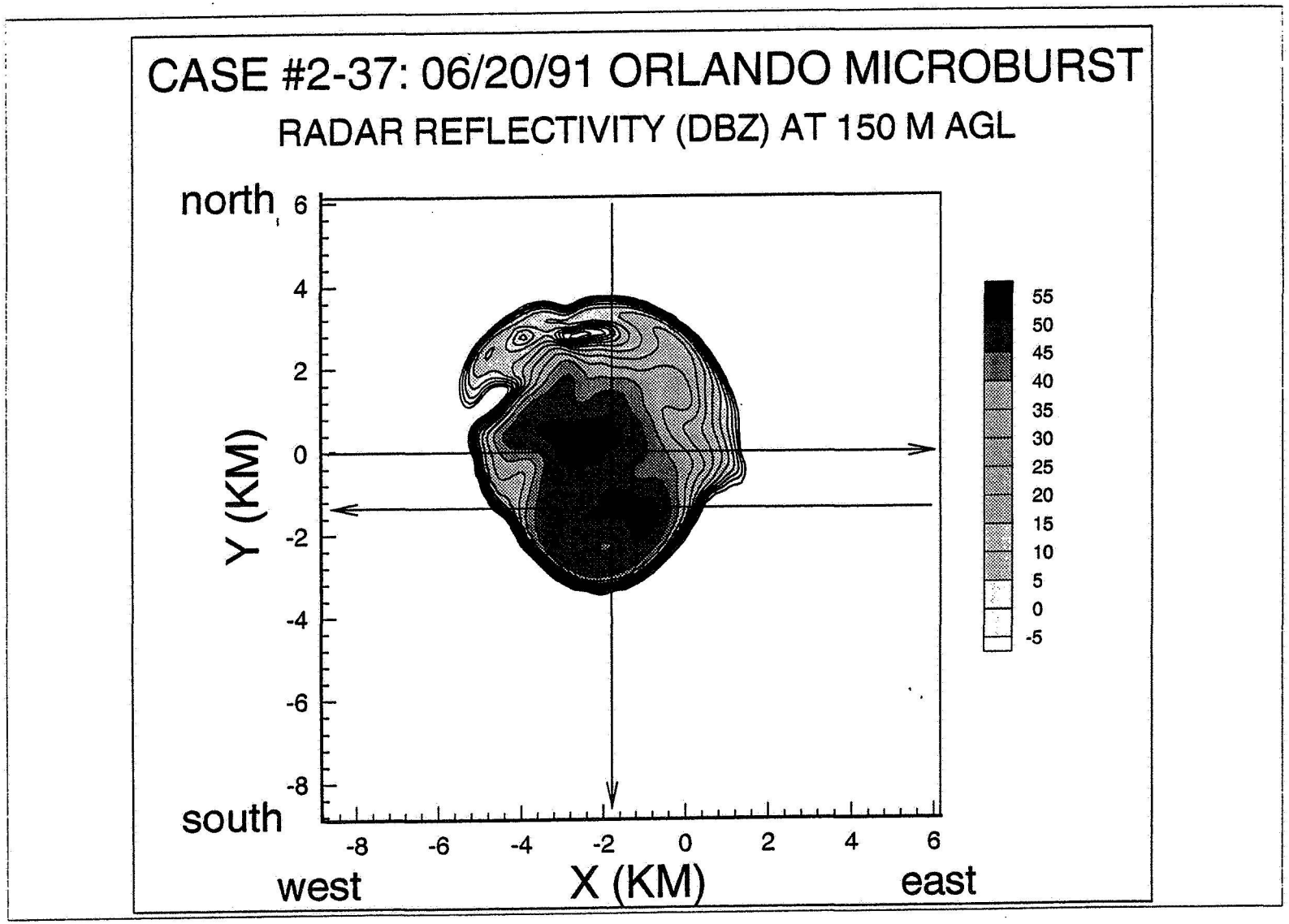
CASE #2-37: 06/20/91 ORLANDO MICROBURST
RADAR REFLECTIVITY (DBZ) AT 150 M AGL
north
south
west
east
Y (KM)
X (KM)
6
4
2
0
-2
-4
-6
-8
55
50
45
40
35
30
25
20
15
10
5
0
-5

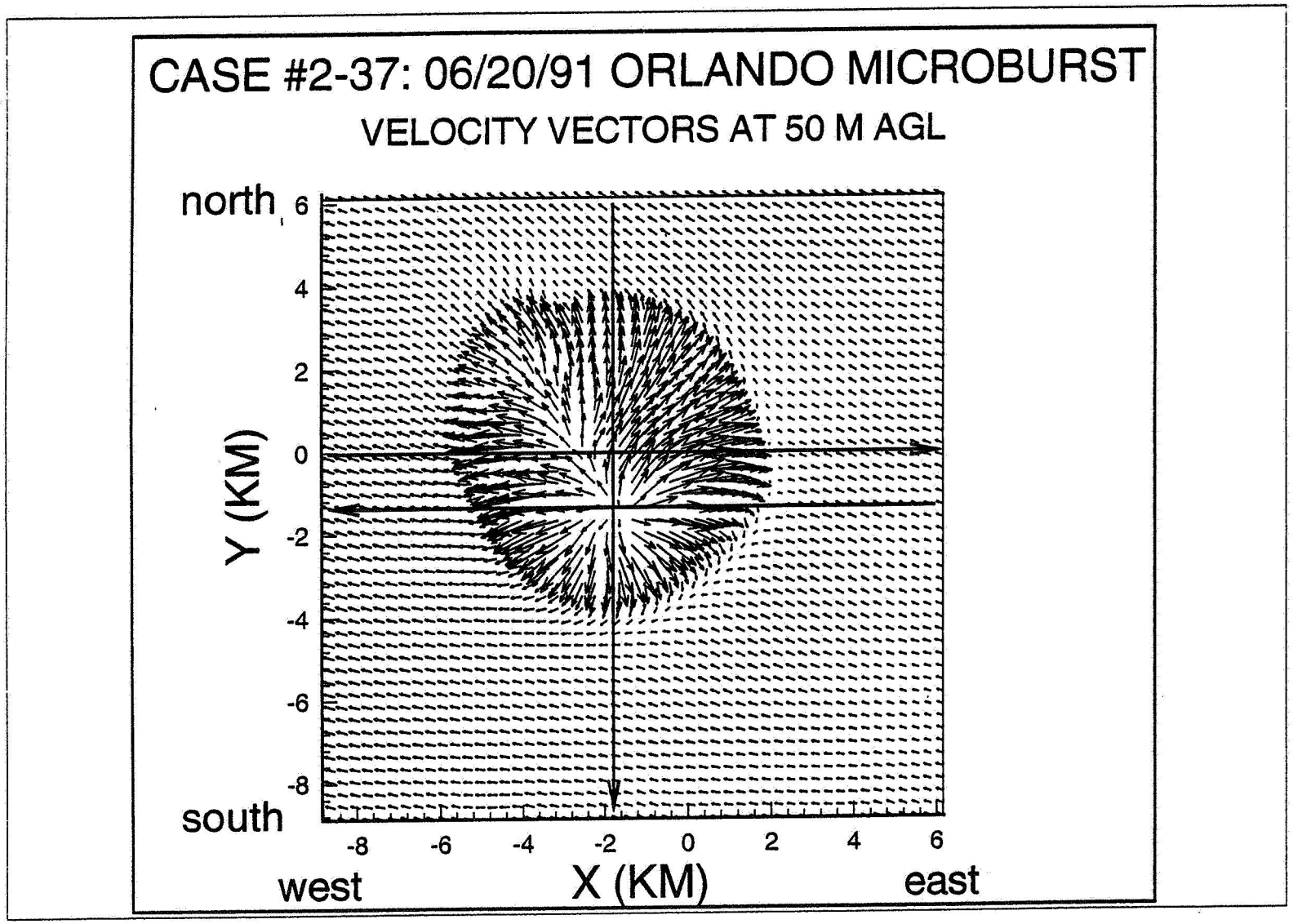
CASE #2-37: 06/20/91 ORLANDO MICROBURST
VELOCITY VECTORS AT 50 M AGL
north
south
west
east
Y (KM)
X (KM)
6
4
2
0
-2
-4
-6
-8
-8
-6
-4
-2
0
2
4
6

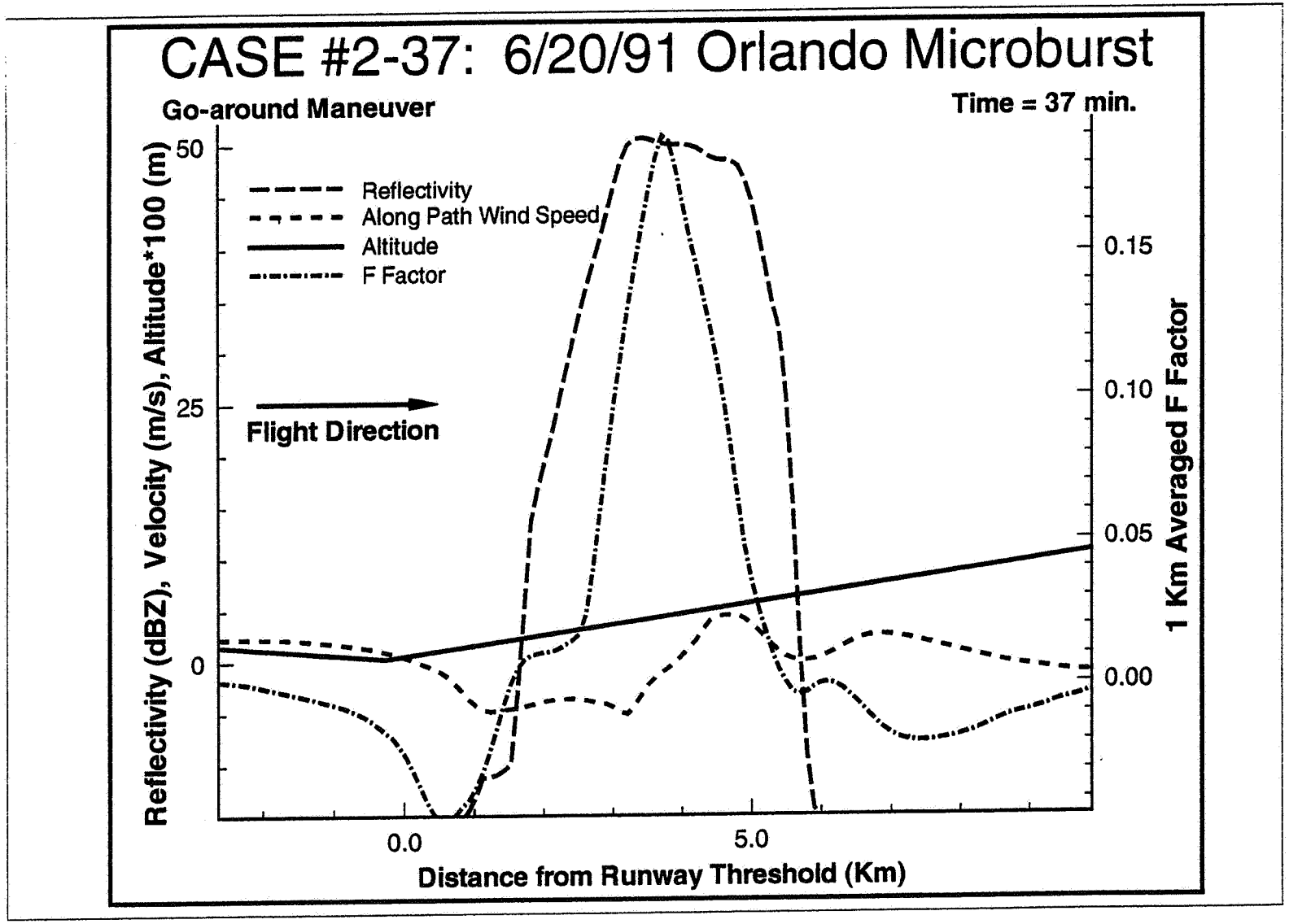
CASE #2-37: 6/20/91 Orlando Microburst
Go-around Maneuver
Time = 37 min.
Reflectivity
Along Path Wind Speed
Altitude
F Factor
Flight Direction
Reflectivity (dBZ), Velocity (m/s), Altitude*100 (m)
1 Km Averaged F Factor
50
25
0
0.15
0.10
0.05
0.00
0.0
5.0
Distance from Runway Threshold (Km)

SUMMARY

I. Database Size and Format
   A. Consists of two parts
      i. paper document
      ii. large computer data file (~ 1 gigabyte)

II. Current usage of Database
   A. Released to vendors that are actively participating in certification process
   B. Used by NASA to investigate radar performance

III. Database Availability
   A. Turned over to the FAA for archival and distribution

Certification Methodology Applied to the NASA Experimental Flight Sytem.

C. Britt and G. Switzer,
Research Triangle Institute,
and
E. Bracalente,
NASA Langley Research Center

ABS: next 2 pages

CERTIFICATION METHODOLOGY APPLIED TO THE NASA EXPERIMENTAL RADAR SYSTEM

Charles L. Britt, E. M. Bracalente & G. F. Switzer

5th Combined Manufacturers and Technologists
Airborne Wind Shear Review Meeting

September 28-30, 1993
Radisson Hotel
Hampton, VA

OVERALL RESEARCH OBJECTIVE: Low altitude wind shear has been identified as a major hazard to aircraft safety during landing and take-off. The FAA is requiring all commercial carriers to install a windshear hazard detection system on all aircraft in their fleet by 1995. The FAA, in 1986, in cooperation with NASA established a joint program to assess a variety of sensor technologies and develop those with significant potential for commercial application. One of these technologies was an airborne Doppler radar. An experimental Doppler wind shear radar was developed by NASA and flight tested during 1991 and 1992.

APPROACH: The specific objective of the research is to apply selected FAA certification techniques to the NASA Experimental wind shear radar system. Although there is no intent to certify the NASA system, the procedures developed may prove useful for manufacturers that plan to undergo the certification process. The certification methodology for forward-looking windshear detection radars will require estimation of system performance in several FAA-specified microburst/clutter scenarios as well as the estimation of probabilities of missed and false hazard alerts under general operational conditions. Because of the near-impossibility of obtaining these results experimentally, analytical and simulation approaches must be used.

ACCOMPLISHMENTS: Hazard detection algorithms were developed that derived predictive estimates of aircraft hazard from basic radar measurements of weather reflectivity and radial wind velocity. These algorithms were designed to prevent false alarms due to ground clutter while providing accurate predictions of hazard to the aircraft due to weather. A method of calculation of the probability of missed and false hazard alerts has been developed that takes into account the effect of the various algorithms used in the system and provides estimates of the probability of missed and false alerts per microburst encounter under weather conditions found at Denver, Kansas City, and Orlando. Simulation techniques have been developed that permit the proper merging of radar ground clutter data (obtained from flight tests) with simu-

ABS (cont'd)

lated microburst data (obtained from microburst models) to estimate system performance using the microburst/clutter scenarios defined by the FAA.

SIGNIFICANCE: The methodology described is specific to the detection techniques and algorithms used in the NASA experimental system. However, it will serve as a guide for calculations on other systems proposed for certification by various manufacturers of windshear detection systems. The methodology for calculation of false and missed alert probability will be included as an Appendix in the "General Certification Methodology and System Level Requirements for Airborne Windshear Predictive Systems" document published by the FAA.

FUTURE PLANS: A technical report will be issued documenting the techniques developed and the predicted performance of the NASA experimental system using the FAA-defined microburst/clutter certification scenarios.

Certification Methodology Applied to the NASA Experimental Radar System

Charles L. Britt
E. M. Bracalente
G. F. Switzer

VIEWGRAPH TITLES

Slide 1 - Title of the Presentation. NASA and Research Triangle Institute personnel participated with the FAA and interested manufacturers in the development of techniques for certification methodology for forward-looking windshear detection systems. The certification process presents unique problems because of the near-impossibility of testing the proposed systems in a realistic environment. While the NASA tests of the experimental system demonstrated the possibility of observing numerous hazardous windshears in flight tests, the windshears observed were not generally located in areas of severe ground clutter as may be encountered on a landing approach or takeoff. Also, safety and operational factors prohibit flight tests through hazardous windshear at low altitudes and slow aircraft speeds.

Slide 2 - Objective of the Study. The methodology finally developed by the FAA and NASA for certification of predictive windshear systems is being applied to the NASA experimental radar system to test the methodology.

Slide 3 - Sketch of the general methodology used to evaluate system performance using real and simulated data. The success of the NASA system and microburst simulation approach led to a certification methodology consisting of a combination of flight tests and simulation. In this concept, illustrated in the slide, ground clutter data will be collected by the manufacturers of systems being considered for certification at several severe clutter locations (e.g., Washington National, Newark, and Denver) and will be merged with simulated microburst data generated by the NASA TASS weather model. The merged data will then be subjected to the signal, data processing, display, and alert algorithms of the proposed system (using actual hardware) to determine the success of the system in meeting the FAA-specified performance goals.

Slide 4 - Illustration of the technique used by NASA in developing the computer code for merging real clutter data with simulated weather data. Modules from the NASA windshear simulation program (ADWRS) are incorporated into the radar flight data processing software.

Slide 5 - Example of a radar reflectivity map of case 2-37 of the FAA certification test cases. This map shows the "true" reflectivity from the TASS microburst database at a particular instant of time with no radar processing and no ground clutter incorporated.

Slide 6 - Radar reflectivity map similar to slide 5 (case 2-37) except the TASS data has been processed by the algorithms used in the NASA experimental radar system. This map shows the reflectivity from the TASS microburst database at a particular instant of time with normal radar clutter filtering but with no ground clutter incorporated.

Slide 7 - Radar reflectivity map similar to slide 6 (case 2-37) except the real ground clutter data from Philadelphia has been merged with the TASS data and has been processed by the algorithms used in the radar system. This map shows the reflectivity from the merged databases at a particular instant of time with normal radar clutter filtering.

Slide 8 - Hazard (F-factor) map of merged data (case 2-37) taken at the same time as the reflectivity map of slide 7. Two hazardous areas have been detected with a maximum averaged F-factor of 0.14. The windshear alert is given at a distance of approximately 8 km. from the hazard.

Slide 9 - Plots of wind velocity and hazard factor calculated from the merged data sets (case 2-37) as a function of radar range. The calculation is made along a azimuth line that passes through the hazardous windshear area shown on the radar F-factor map of slide 8. Radar calculated and "true" values are shown for comparison.

Slide 10 - Example of a radar reflectivity map of case 5-40 of the FAA certification test cases. This map shows the "true" reflectivity from the TASS microburst database at a particular instant of time with no radar processing and no ground clutter incorporated.

Slide 11 - Radar reflectivity map similar to slide 10 (case 5-40) except the TASS data has been processed by the algorithms used in the NASA experimental radar system. This map shows the reflectivity from the TASS microburst database at a particular instant of time with normal radar clutter filtering but with no ground clutter incorporated.

Slide 12 - Hazard (F-factor) map of merged data (case 5-40) taken at the same time as the reflectivity map of slide 12. A hazardous areas has been detected with a maximum averaged F-factor of 0.14. The windshear alert is given at a distance of approximately 3 km. from the hazard.

Slide 13 - Plots of wind velocity and hazard factor calculated from the merged data sets (case 5-40) as a function of radar range. The calculation is made along a azimuth line that passes through the hazardous windshear area shown on the radar F-factor map of slide 13. Radar calculated and "true" values are shown for comparison. Because of the low reflectivity of this microburst, the true and measured values do not compare as favorably as those shown for the wet microburst case of slide 9.

Slide 14 - Hazard Index definitions used in calculating the probability of false and missed hazard alerts.

Slide 15 - Probability density functions showing areas of the density corresponding to probabilities of false alerts, missed alerts and detection.

Slide 16 - Outline of the procedure used to estimate the probabilities of missed and false alerts.

Slide 17 - Methods of reducing false alerts used in the NASA experimental system. These methods must be considered when calculating the various probabilities.

Slide 18 - Plots of the standard deviation of the hazard (F-factor) measurement for the NASA system as a function of the radar range for three values of weather reflectivity.

Slide 19 - Probability density functions for F-factor and reflectivity (at three locations) used in the calculations.

Slide 20 - Averaged cumulative probabilities (log scale) of a missed detection of a hazardous windshear at Denver, Kansas City, and Orlando for microbursts with reflectivity exceeding 0 dBZ. The probabilities of false hazard alerts is estimated to be less than 10^{-6} when using the algorithms implemented in the NASA system.

CERTIFICATION METHODOLOGY APPLIED TO THE NASA EXPERIMENTAL WINDSHEAR RADAR SYSTEM

SEPTEMBER 29, 1993

C L. BRITT	RTI
E. M. BRACALENTE	NASA
G. F. SWITZER	RTI

Slide 1

OBJECTIVE

TO APPLY SUGGESTED FAA CERTIFICATION METHODOLOGY TO THE NASA EXPERIMENTAL WINDSHEAR RADAR SYSTEM

- PERFORMANCE EVALUATION IN SPECIFIED MICROBURST/CLUTTER SCENARIOS

- ESTIMATION OF THE PROBABILITY OF MISSED AND FALSE ALERTS PER MICROBURST ENCOUNTER

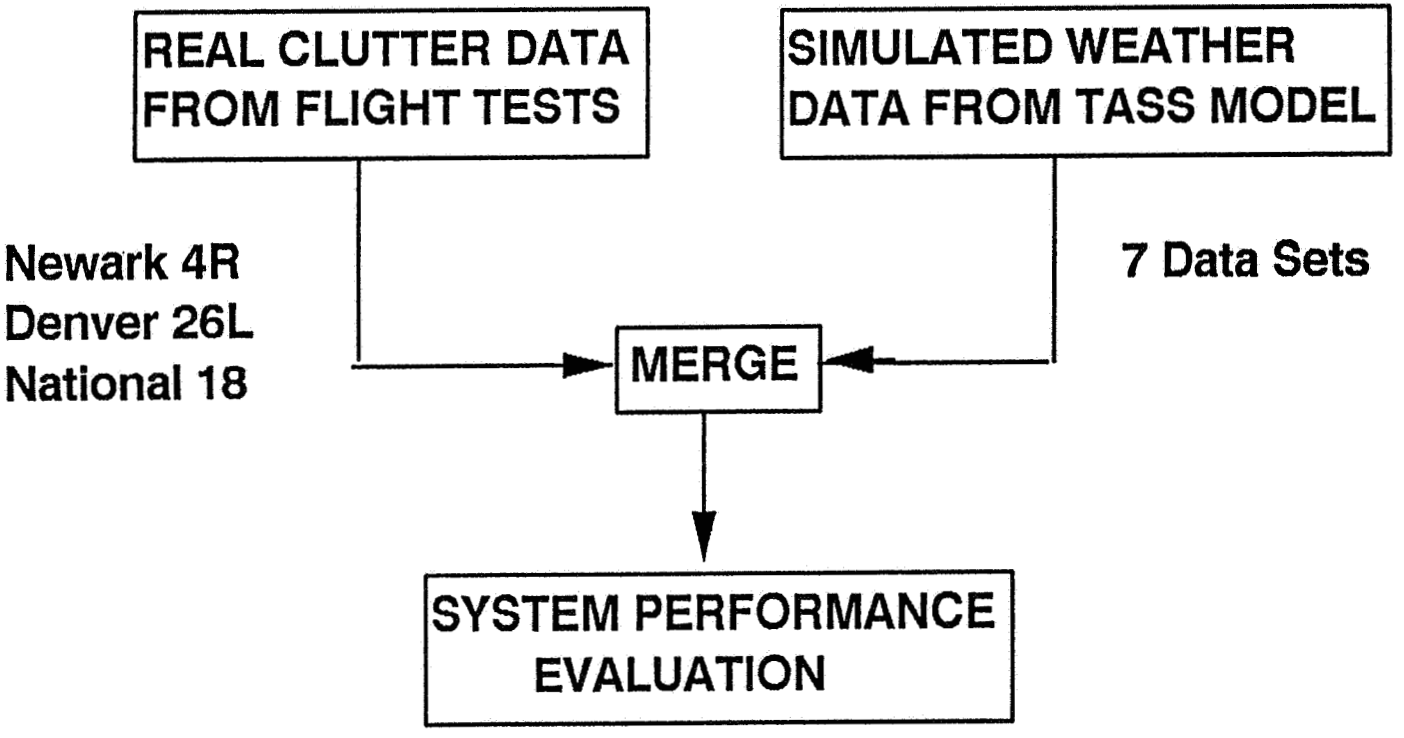

Approximately 40 Cases

Slide 3

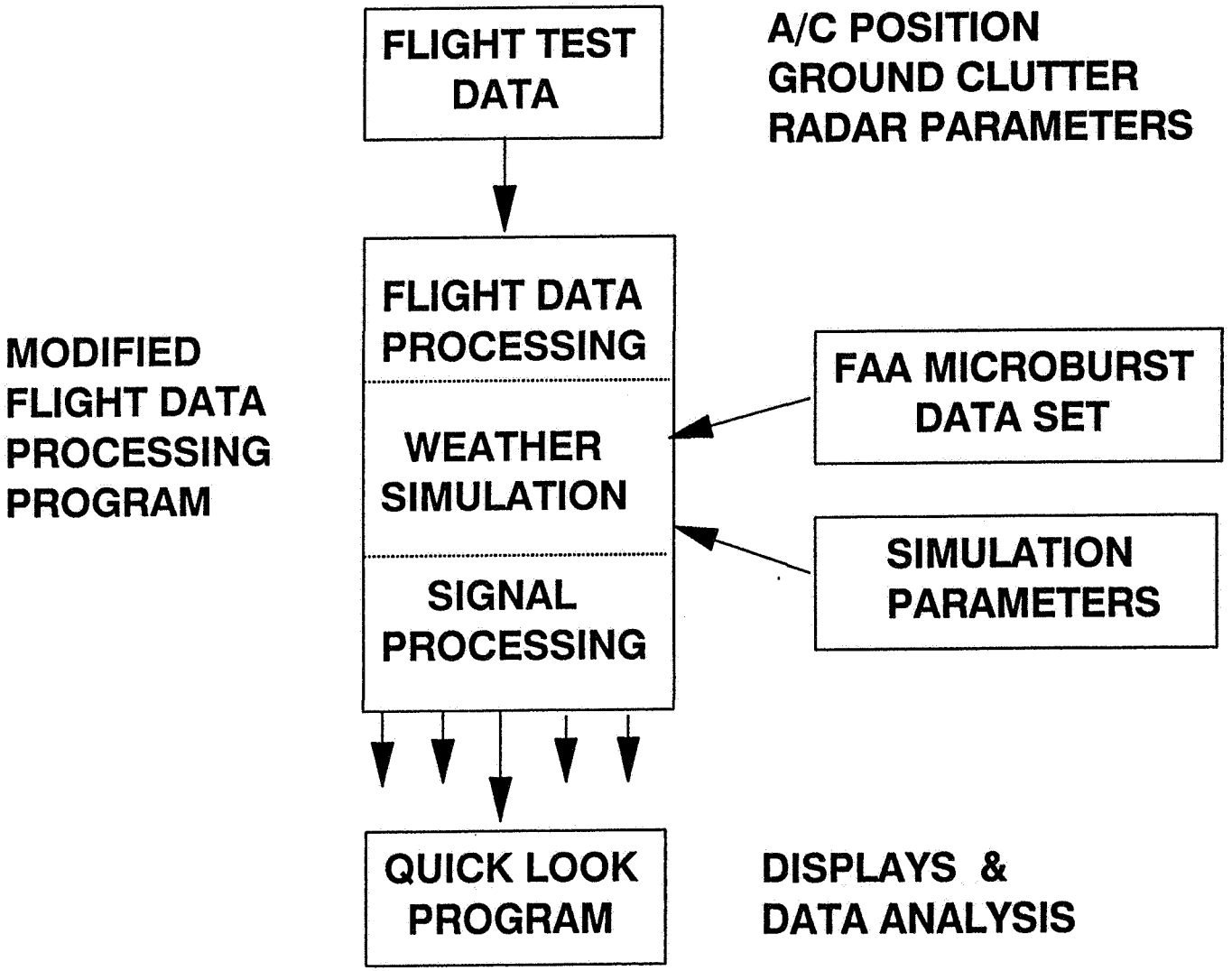
FLIGHT TEST DATA
A/C POSITION
GROUND CLUTTER
RADAR PARAMETERS
FLIGHT DATA PROCESSING
WEATHER SIMULATION
SIGNAL PROCESSING
FAA MICROBURST DATA SET
SIMULATION PARAMETERS
MODIFIED FLIGHT DATA PROCESSING PROGRAM
QUICK LOOK PROGRAM
DISPLAYS & DATA ANALYSIS

Slide 4

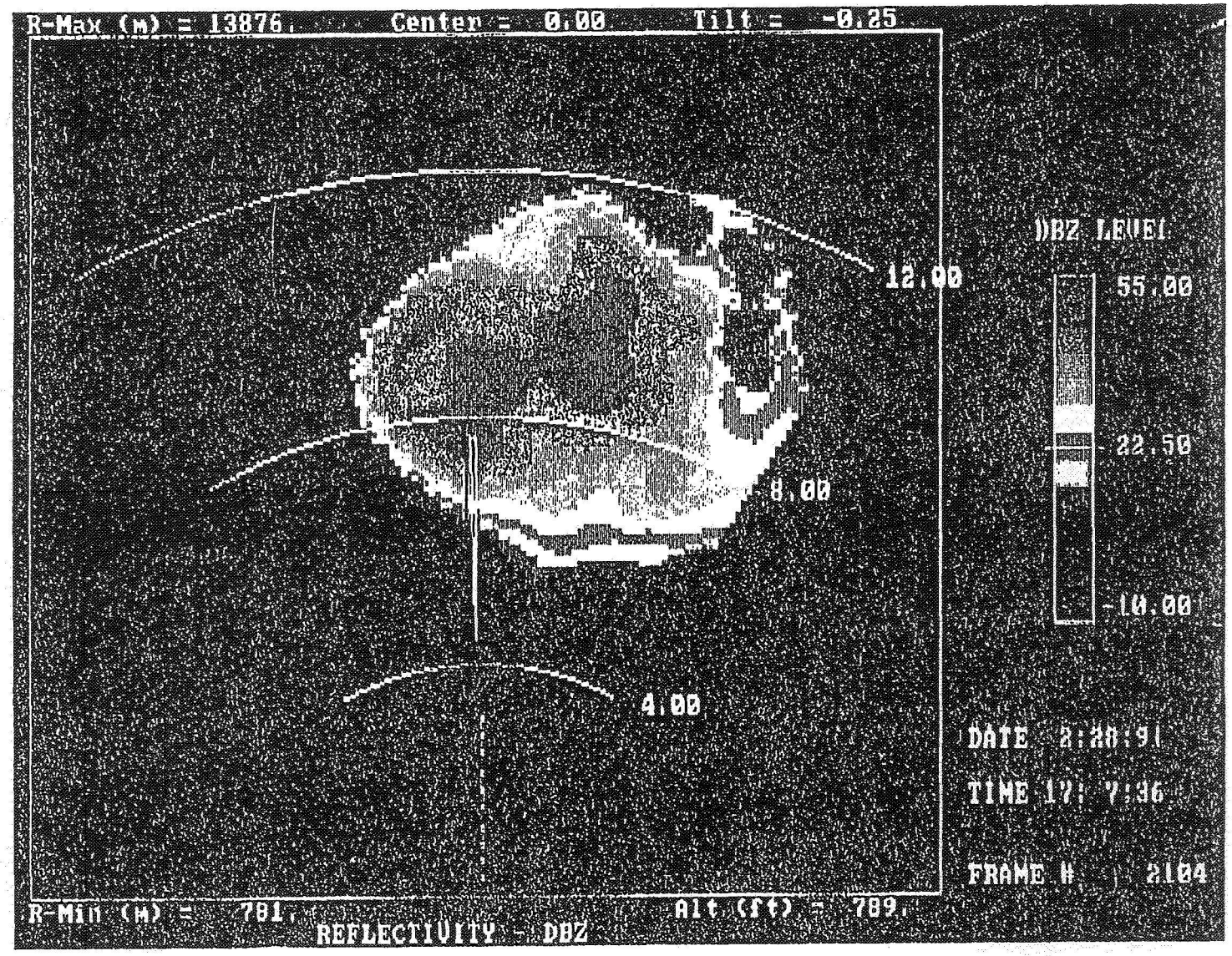
R-Max (m) = 13876.
Center = 0.00
Tilt = -0.25
12.00
8.00
4.00
DBZ LEVEL
55.00
22.50
-10.00
DATE 3:28:91
TIME 17: 7:36
FRAME # 2104
R-Min (m) = 781.
Alt (ft) = 789.
REFLECTIVITY - DBZ

Slide 5

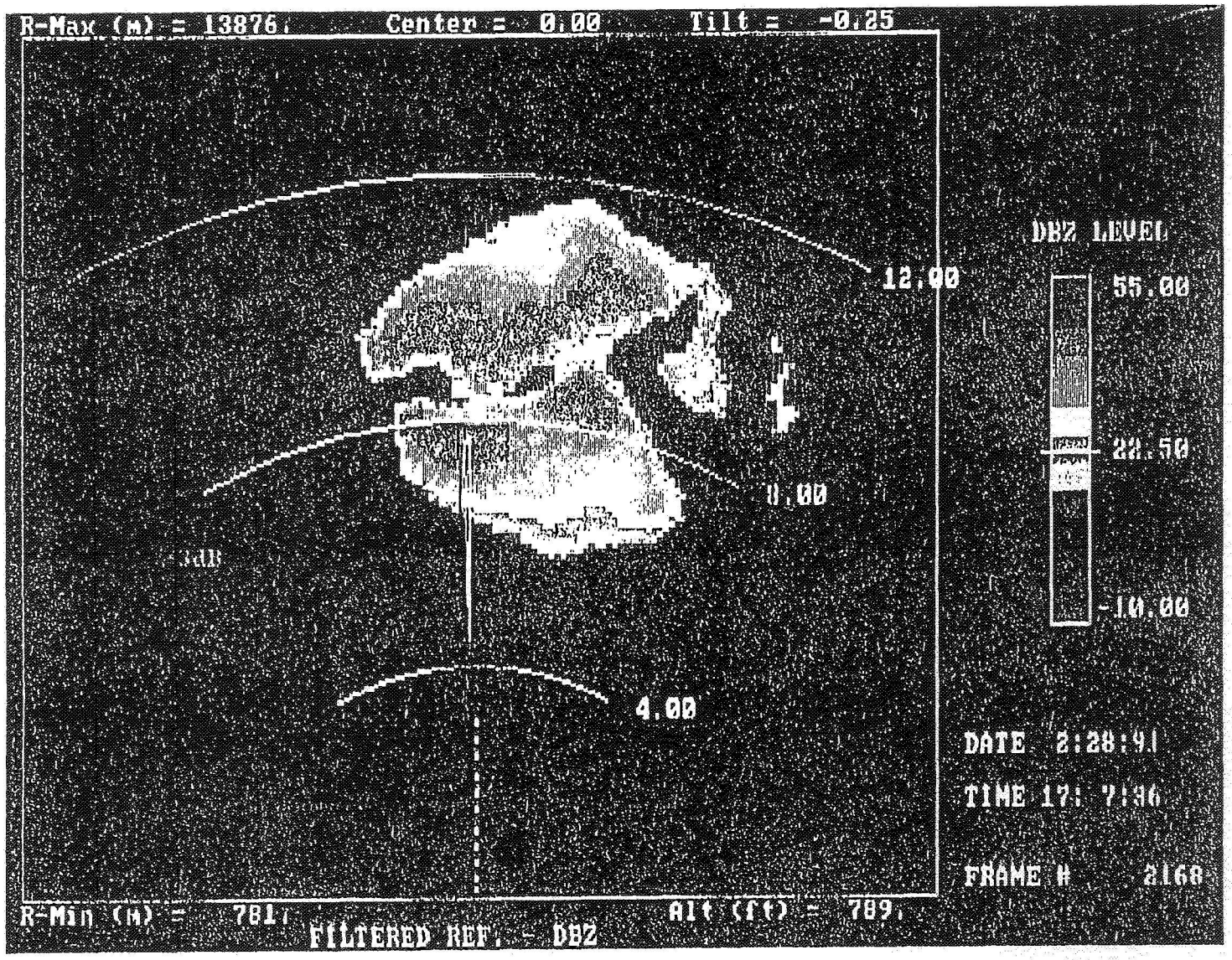
R-Max (M) = 13876.
Center = 0.00
Tilt = -0.25
12.00
0.00
-3dB
4.00
DBZ LEVEL
55.00
22.50
-10.00
DATE 2:28:91
TIME 17: 7:36
FRAME # 2168
R-Min (M) = 781.
Alt (ft) = 789.
FILTERED REF. - DBZ

Slide 6

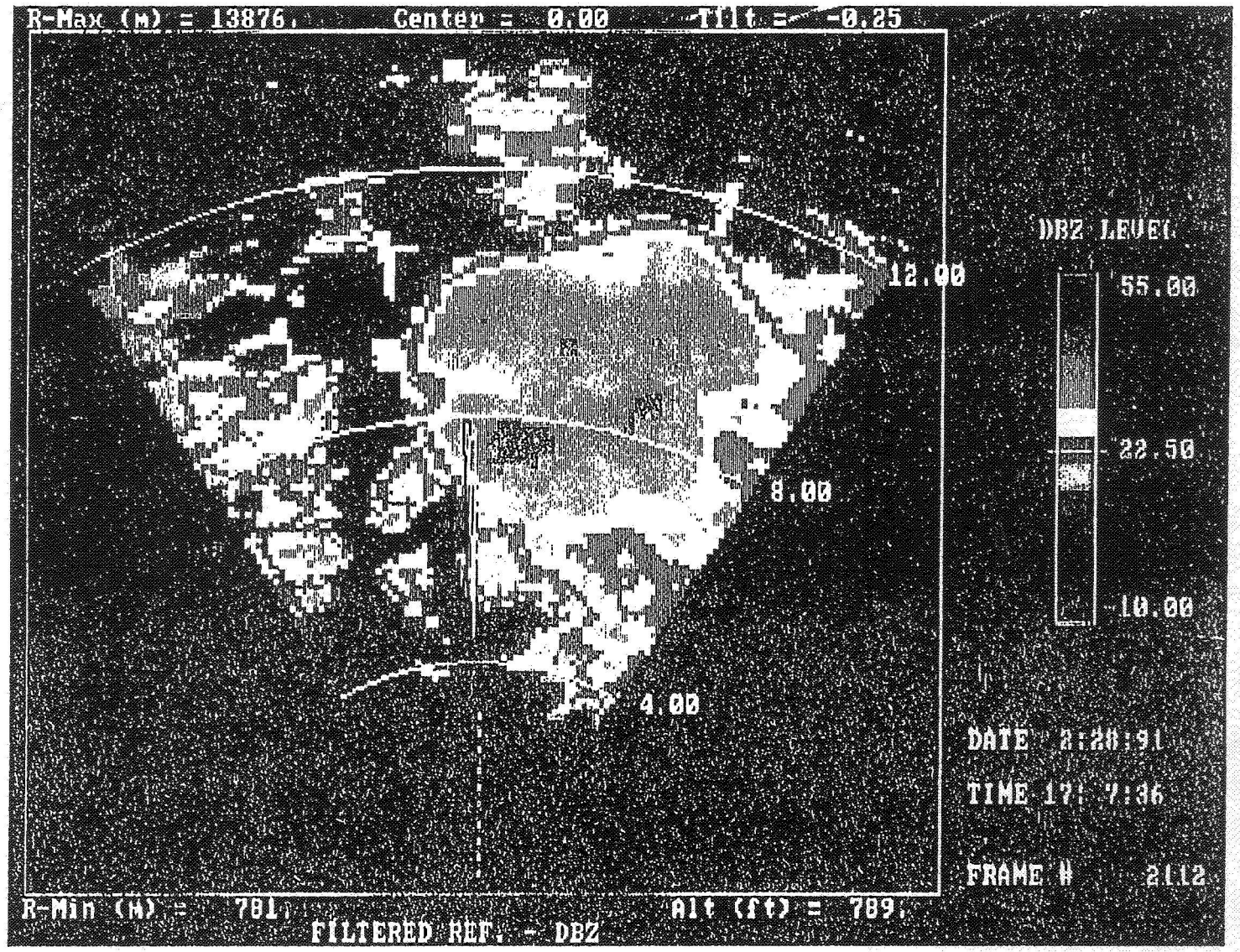
R-Max (m) = 13876.
Center = 0.00
Tilt = -0.25
12.00
8.00
4.00
DBZ LEVEL
55.00
22.50
10.00
DATE 2:28:91
TIME 17: 7:36
FRAME # 2112
R-Min (m) = 781.
Alt (ft) = 789.
FILTERED REF. - DBZ

Slide 7

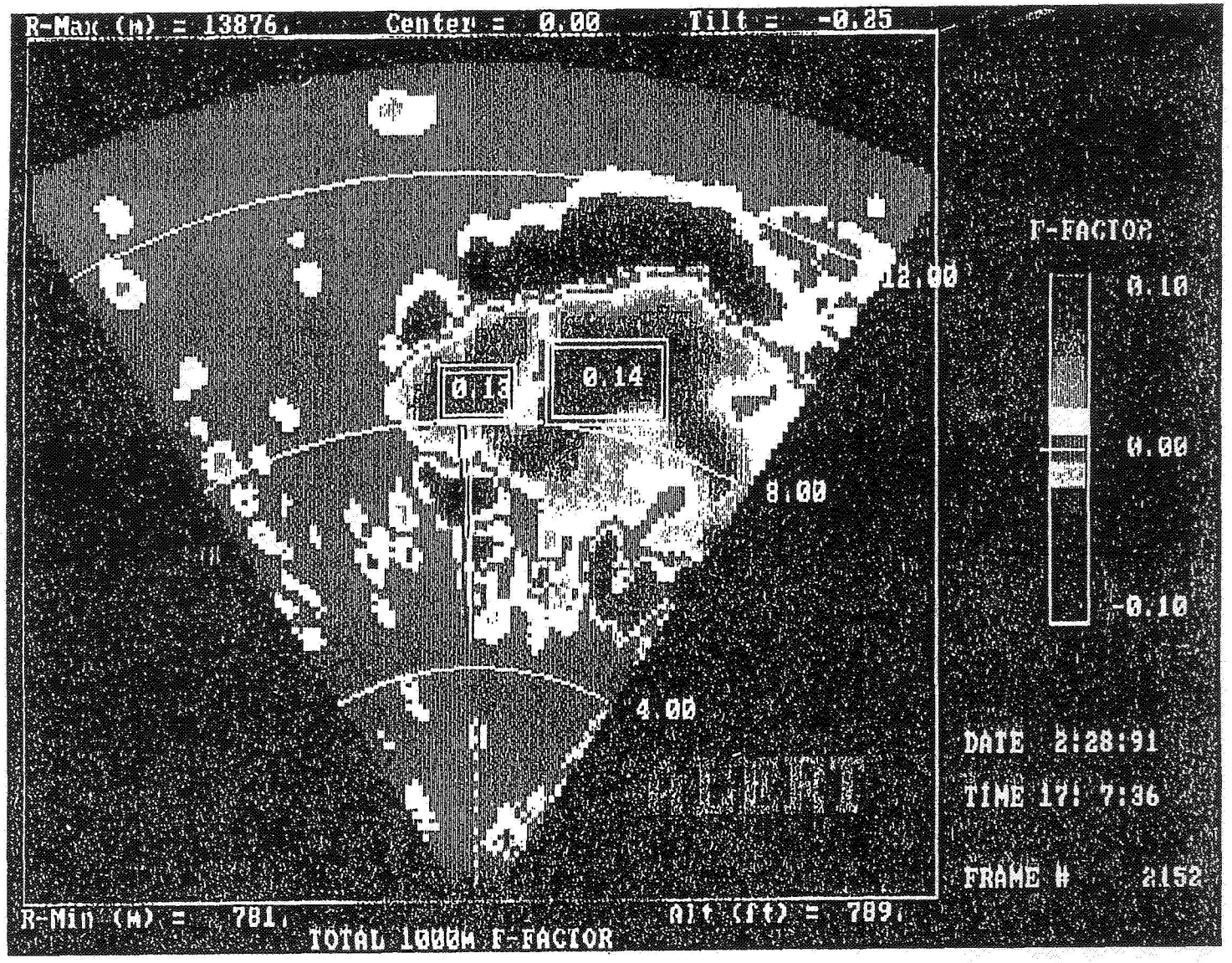
R-Max (M) = 13876.
Center = 0.00
Tilt = -0.25
12.00
8.00
4.00
0.13
0.14
F-FACTOR
0.10
0.00
-0.10
DATE 2:28:91
TIME 17: 7:36
FRAME # 2152
R-Min (M) = 781.
Alt (ft) = 789.
TOTAL 1000M F-FACTOR

Slide 8

SIMULATION CASE 2376: RADAR&TRUTH DATA VELOCITY & 1KM F-FACTOR

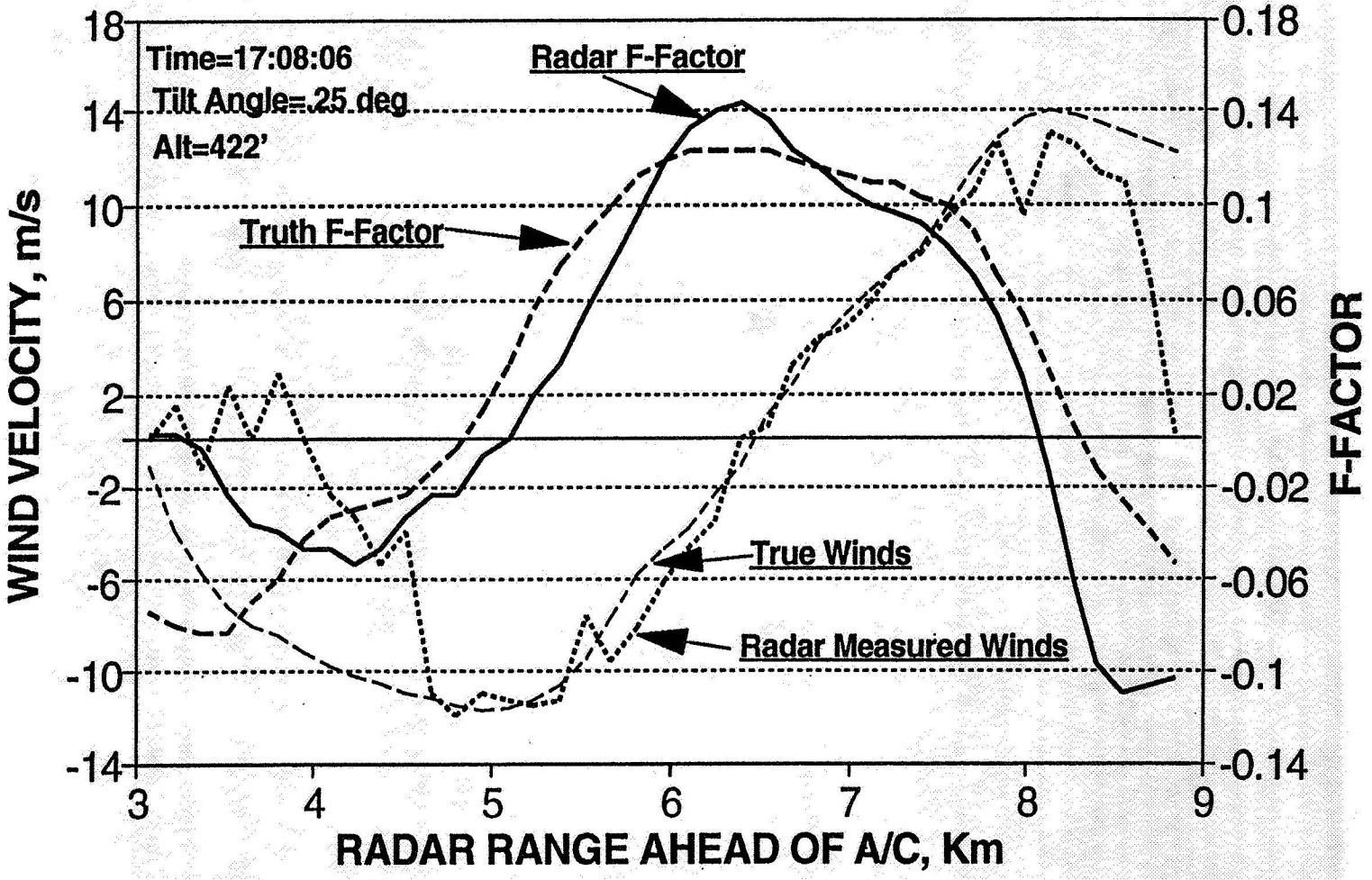

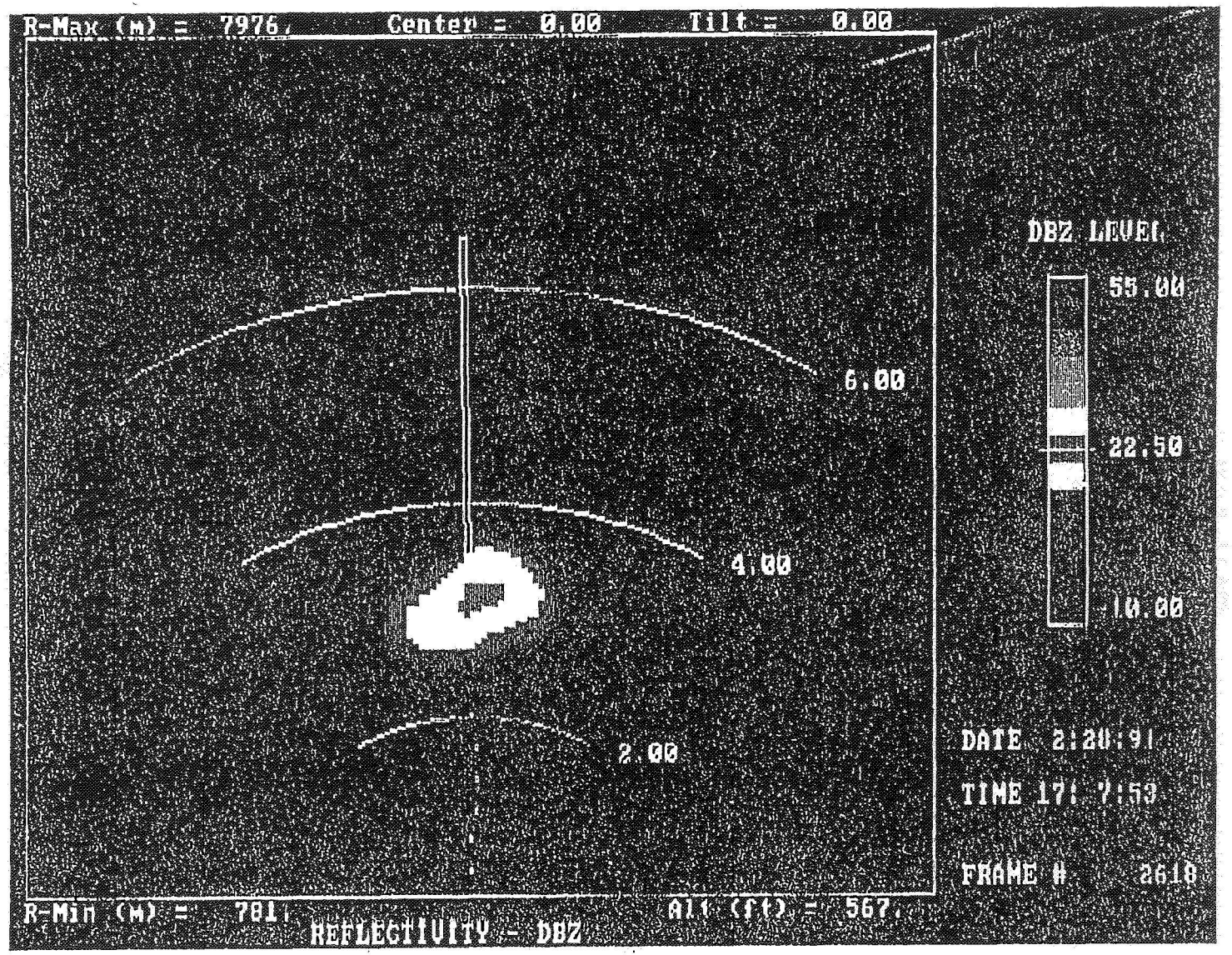
R-Max (M) = 7976.
Center = 0.00
Tilt = 0.00
6.00
4.00
2.00
DBZ LEVEL
55.00
22.50
10.00
DATE 2:20:91
TIME 17: 7:53
FRAME # 2618
R-Min (M) = 781.
Alt (ft) = 567.
REFLECTIVITY - DBZ

Slide 10

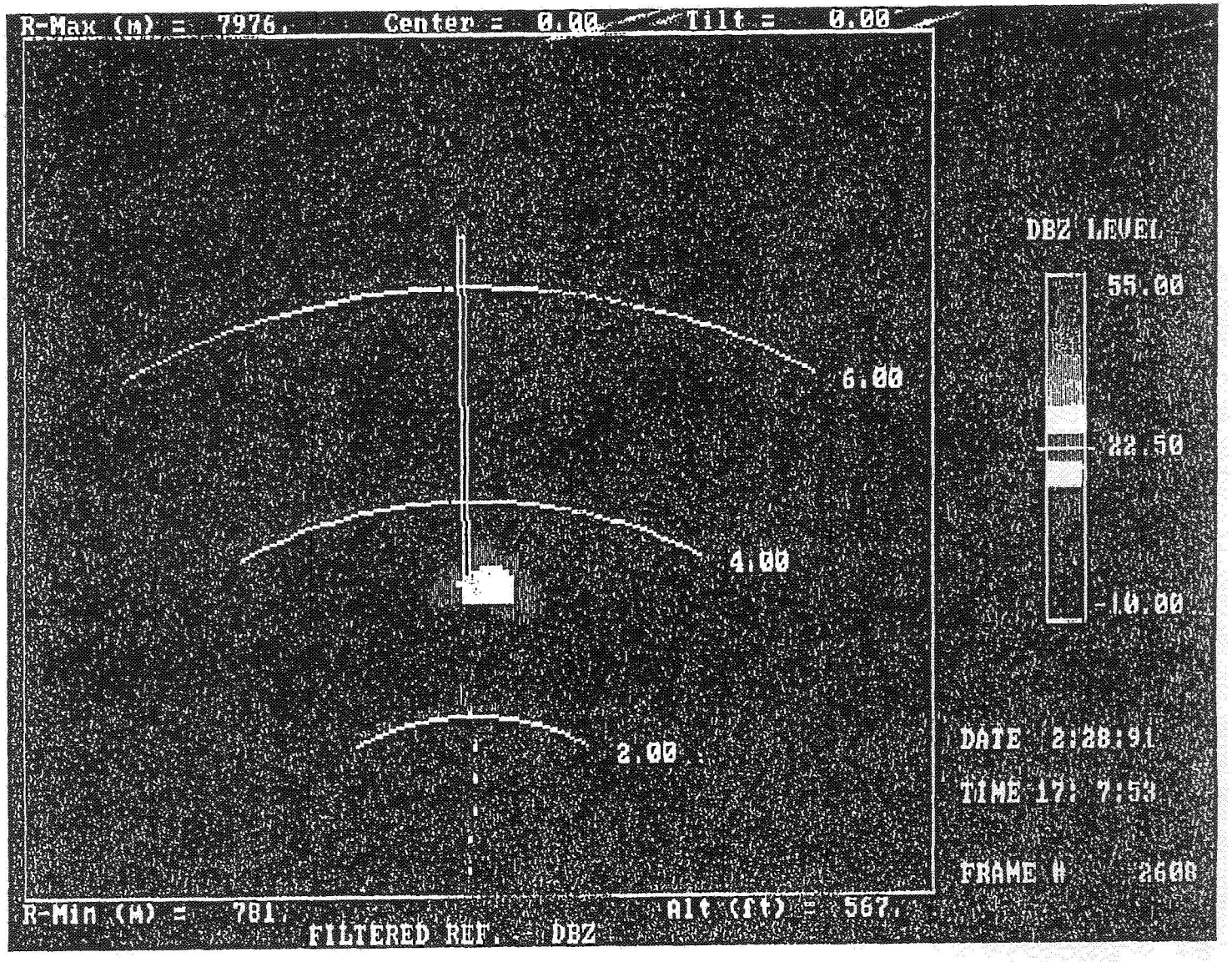
R-Max (m) = 7976.
Center = 0.00
Tilt = 0.00
6.00
4.00
2.00
DBZ LEVEL
55.00
22.50
-10.00
DATE 2:28:91
TIME 17: 7:53
FRAME # 2600
R-Min (M) = 781.
Alt (ft) = 567.
FILTERED REF. - DBZ

Slide 11

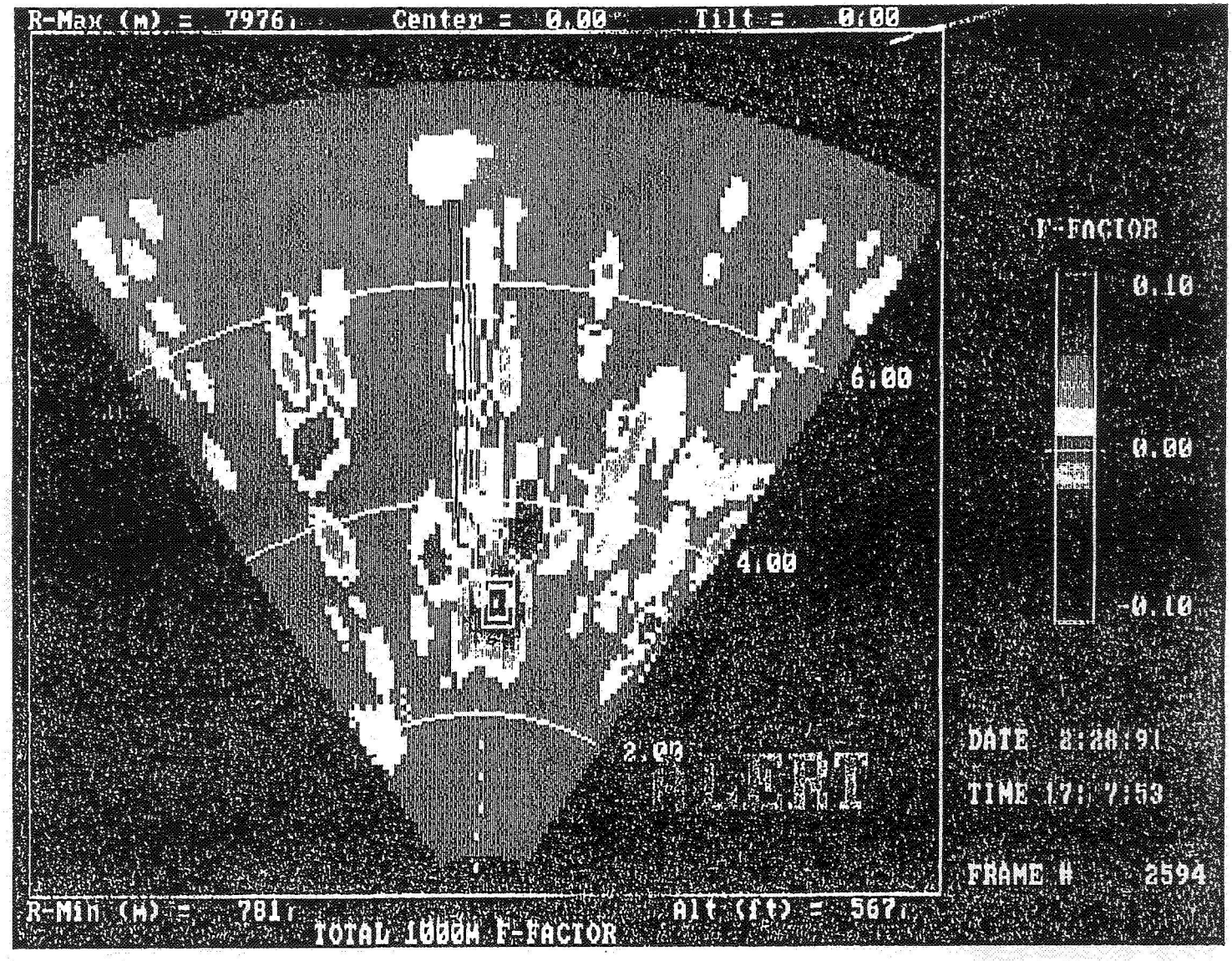
R-Max (m) = 7976.
Center = 0.00
Tilt = 0.00
F-FACTOR
0.10
0.00
-0.10
6.00
4.00
2.00
DATE 8:28:91
TIME 17: 7:53
FRAME # 2594
R-Min (m) = 781.
Alt (ft) = 567.
TOTAL 1000M F-FACTOR

Slide 12

SIMULATION CASE 5403: RADAR&TRUTH DATA VELOCITY & F-FACTOR

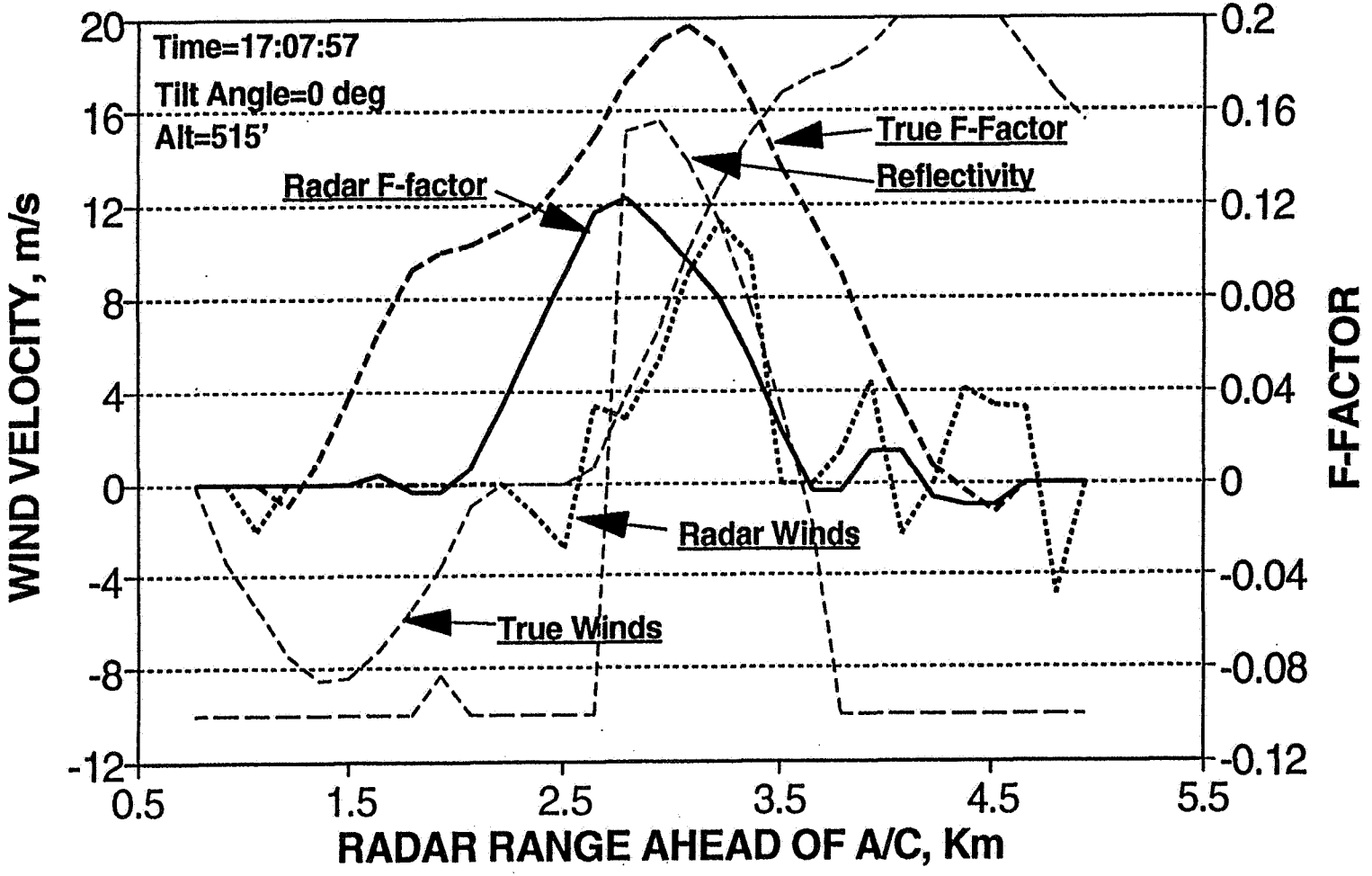

HAZARD INDEX

$$F = (V/g)\,(\text{SLOPE OF WIND VEL. VS. RANGE}) + \text{VERTICAL COMPONENT}$$

(AVERAGED OVER 1 KILOMETER)

MUST ALERT @ $F > .130$

MUST NOT ALERT @ $F < .085$

PROBABILITY FUNCTIONS

Detection and False Alert Probability

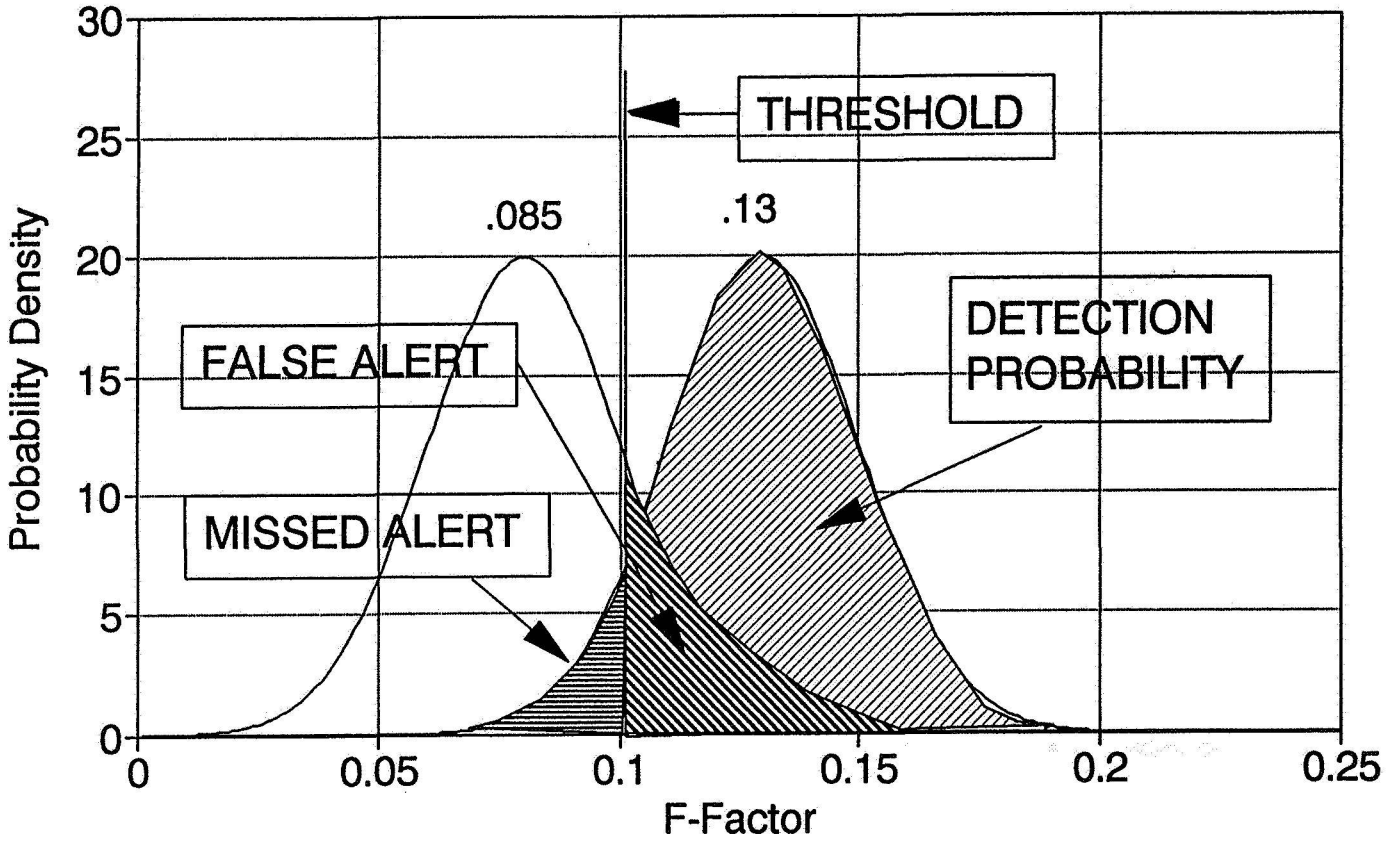

Slide 15

CALCULATION PROCEDURE

1. Single Pulse SNR vs Range
2. Std. Deviation of Velocity Meas. Errors
3. Std. Deviation of Hazard Factor Estimate
4. Single-Scan Probabilities - False & Missed Alerts
5. Multiple-Scan, Multiple-Pixel Probabilities
6. Cumulative Probabilities - False & Missed Alerts
7. Probabilities Averaged over a Population of Microbursts

FALSE ALERT REDUCTION

SIGNAL-TO-NOISE RATIO	> -3 dB
SPECTRAL WIDTH	< 8 m/s
HAZARD FACTOR	> .105
LEAST-SQUARES RESIDUAL	< 3 m/s
HAZARD AREA	> .2 sq km
PERSISTANCE	> 1 scan
TIME-TO-ENCOUNTER	< 30 secs

STANDARD DEVIATION OF AVR. F-FACTOR

FFT Processing, 128 Samples, SW = 3 m/s

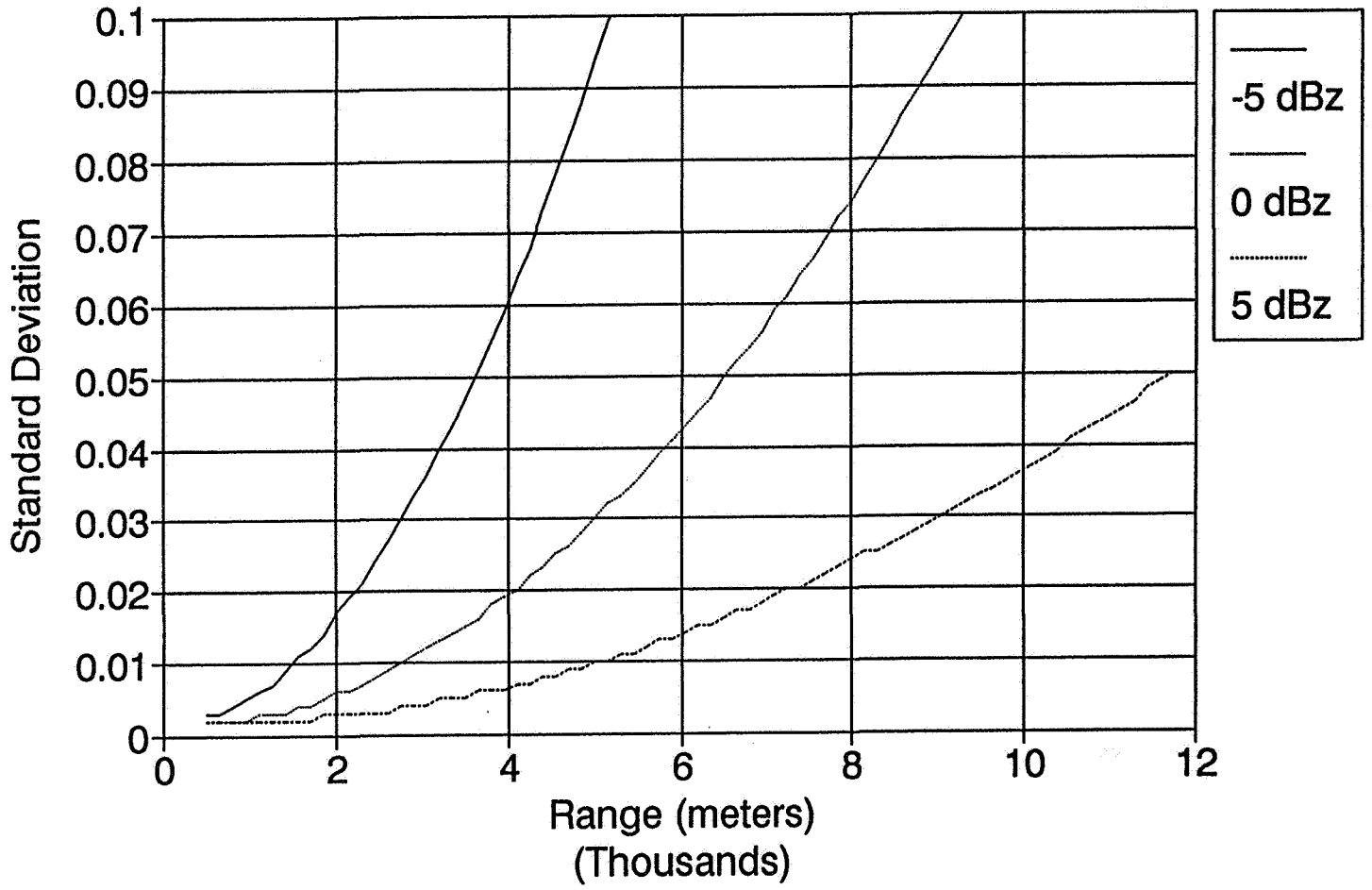

PROBABILITY DENSITY FUNCTION

Hazard Index (F-factor)

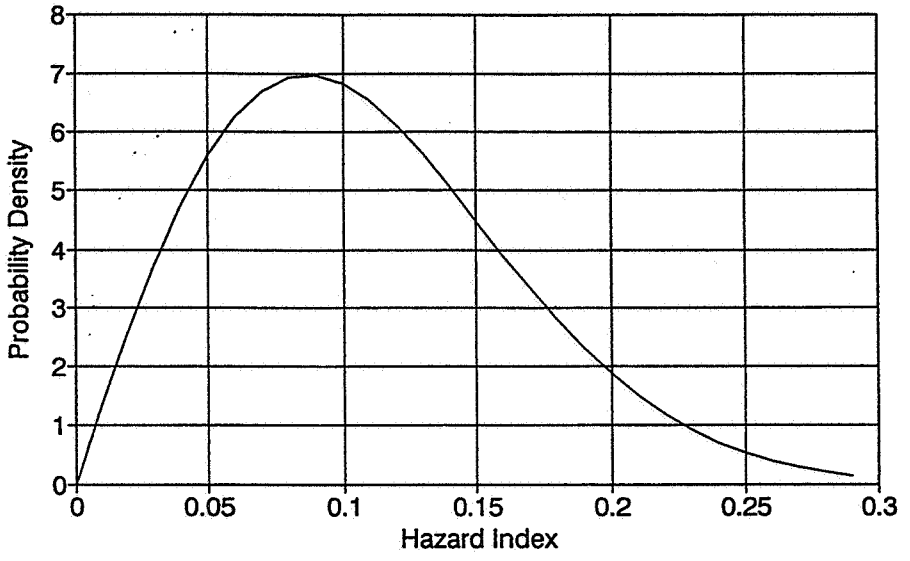

PROBABILITY DENSITY FUNCTIONS

Reflectivity @ Denver, Orlando, & KC

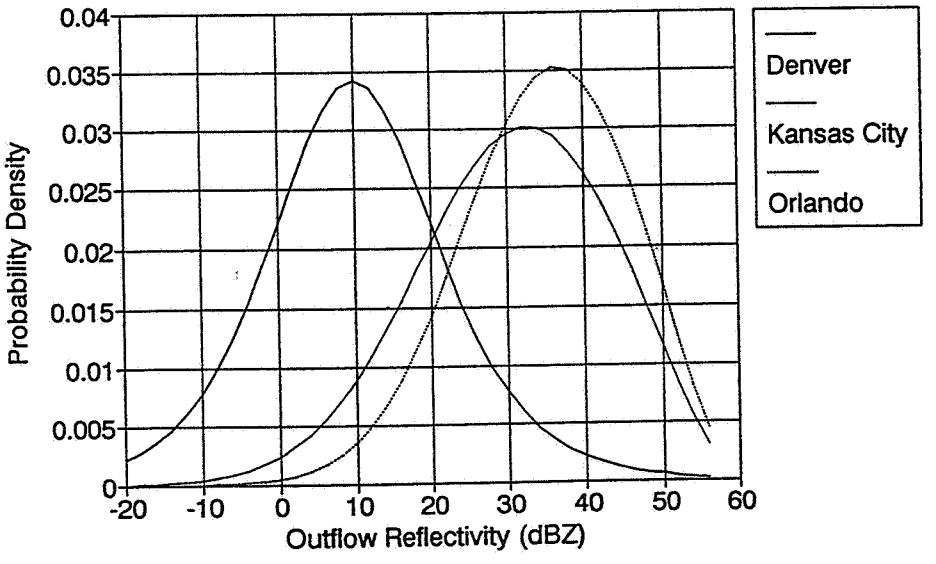

Slide 19

AVERAGED CUMULATIVE PROBABILITIES OF MISSED DETECTION (dBZ > 0)

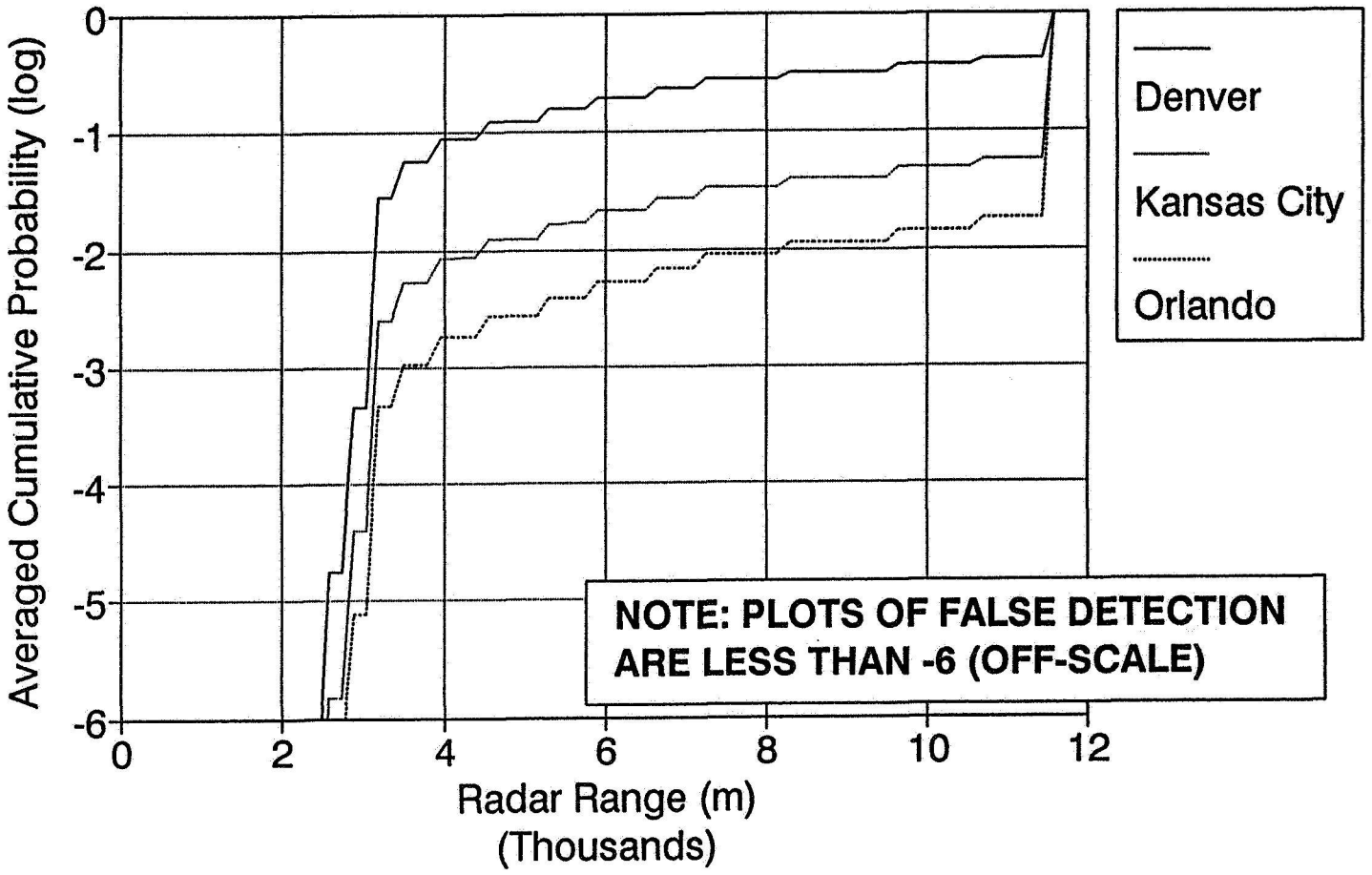

Certification of Windshear Performance with RTCA Class D Radomes.

B, Mathews and L. Barnett,

Westinghouse Electric Co.

ABS: next page

Overview and Highlights from Superposition Testing of MODAR 3000

by

Bruce Mathews, Fran Miller, Kirk Rittenhouse, Lee Barnett,
and William Rowe

Westinghouse Electric Corporation
Electronic Systems Group
Baltimore, MD

5th (and Final) Combined Manufacturers'

and

Technologists' Airborne Wind Shear Review Meeting

Radisson Hotel, Hampton, VA

Superposition testing of detection range performance forms a digital signal for input into a simulation of signal and data processing equipment and algorithms to be employed in a sensor system for advanced warning of hazardous windshear. For suitable pulse-Doppler radar, recording of the digital data at the input to the digital signal processor furnishes a realistic operational scenario and environmentally responsive clutter signal including all sidelobe clutter, ground moving target indications (GMTI), and large signal spurious due to mainbeam clutter and/or RFI respective of the urban airport clutter and aircraft scenarios (approach and landing antenna pointing). For *linear* radar system processes, a signal at the same point in the process from a hazard phenomena may be calculated from models of the scattering phenomena, for example, as represented in fine 3 dimensional reflectivity and velocity grid structures. Superposition testing furnishes a competing signal environment for detection and warning time performance confirmation of phenomena uncontrollable in a natural environment (see figure 1).

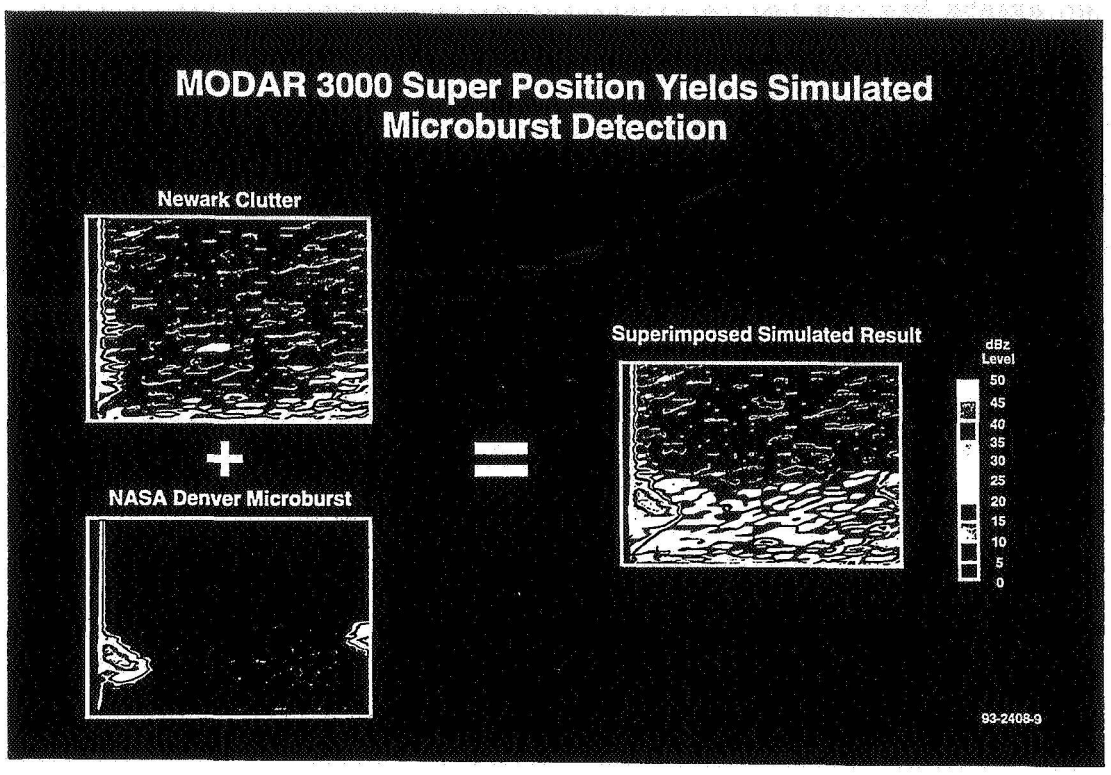

figure 1 Superposition Yields Simulated Microburst Detection in Urban Airport Environment

The range-Doppler power spectral density for clutter along a single, instantaneous antenna line of sight is recorded at the output of the FFT along with the antenna pointing angle and any other radar configuration and/or geometry necessary information. The range gated Doppler power spectral density of the microburst is calculated from the radar range equation using a fine three dimensional grid database and descriptions of the radar operation either from bench testing characterization and/or in-flight measurements. These plots show contours of signal-to-noise from 0 to 50 dB. with contours every 5 dB., for an upper bar scan in urban airport clutter.

The clutter signal recorded should represent the amplitude and phase stabilities and amplitude levels of the equipment conditions for the intended function and installations. The sensor system includes many other aircraft system assets besides the receiver-transmitter-processor unit. A pulse Doppler radar is preferably dependent upon INS data for clutter positioning and antenna pointing. Furthermore, pulse-Doppler radar performance is sensitive to the level of returns from antenna sidelobe directions. In all cases, this level is dependent upon antenna and radome characteristics.

In response to the practices and wishes of the commercial airlines, the RTCA committee on windshear has revised the MOPS for weather radar radomes. Essentially, the airlines have reacted to the introduction of a radar with windshear detection capability and a call for better radomes by insuring that existing (older) weather radomes and practices are not invalidated by a statement of new, improved standards. Especially older aircraft with allegedly satisfactorily maintained radomes may exhibit degraded transmissivity and antenna sidelobe performance in exception of present standards. A class "D", category 2 radome has been defined as a two way transmissivity of 1.4 dB. loss and sidelobe degradations up to -20 dB. relative to the mainlobe, respectively (see fig. 2). This has the desired effect of prescribing new standards which the practices of the airlines can and apparently do comply with.

Figures 3 and 4 show the installation configuration of the MODAR 3000 weather radar with predictive windshear. To support certification, Westinghouse has modified a BAC-1-11 radome to conform to the definitions of the RTCA class "D", category 2 radome. An otherwise class "A", category 1 radome, i.e. a low loss and properly maintained radome of minimal antenna pattern distortion was "patched" with coarse fiberglass layers to simulate a history of repair producing insertion/dispersion losses and sidelobe degradation over the aperture window of the windshear mode operation. The repair was non-symetrically located and consisted of three overlapped layers of cemented fiberglass near the nose, within the scan area of the windshear mode. Layers were applied until the average transmissivity was suitably degraded.

Several attempts were made at achieving the sidelobe levels. As was remarked in the RTCA meeting by aircraft and radome companies, class "D", category 2 sorts of distortions are difficult to realize from properly and purely localized radome repairs.

First attempts included modification of the antenna amplitude distribution by slot taping to raise the sidelobe levels. These first efforts produced antenna sidelobe levels which exceeded -20 dB. levels in both azimuth and elevation. However, the weather radar performance in either weather or windshear introduced continual display of red-yellow reflectivity levels at all range scales, even over non-urban clutter areas. That radome degradation was judged to be too severe as surely it should have prompted a request for maintainence action. The current class "D", category 2 modifications utilize only radome modifications and employ no degradation of the antenna amplitude distribution. This has produced azimuth degradations (see fig. 5) raising the general sidelobe level 3 to 5 dB. and a pronounced increase in the near sidelobes on the side of the "repair", up to -19 dB. In the elevation

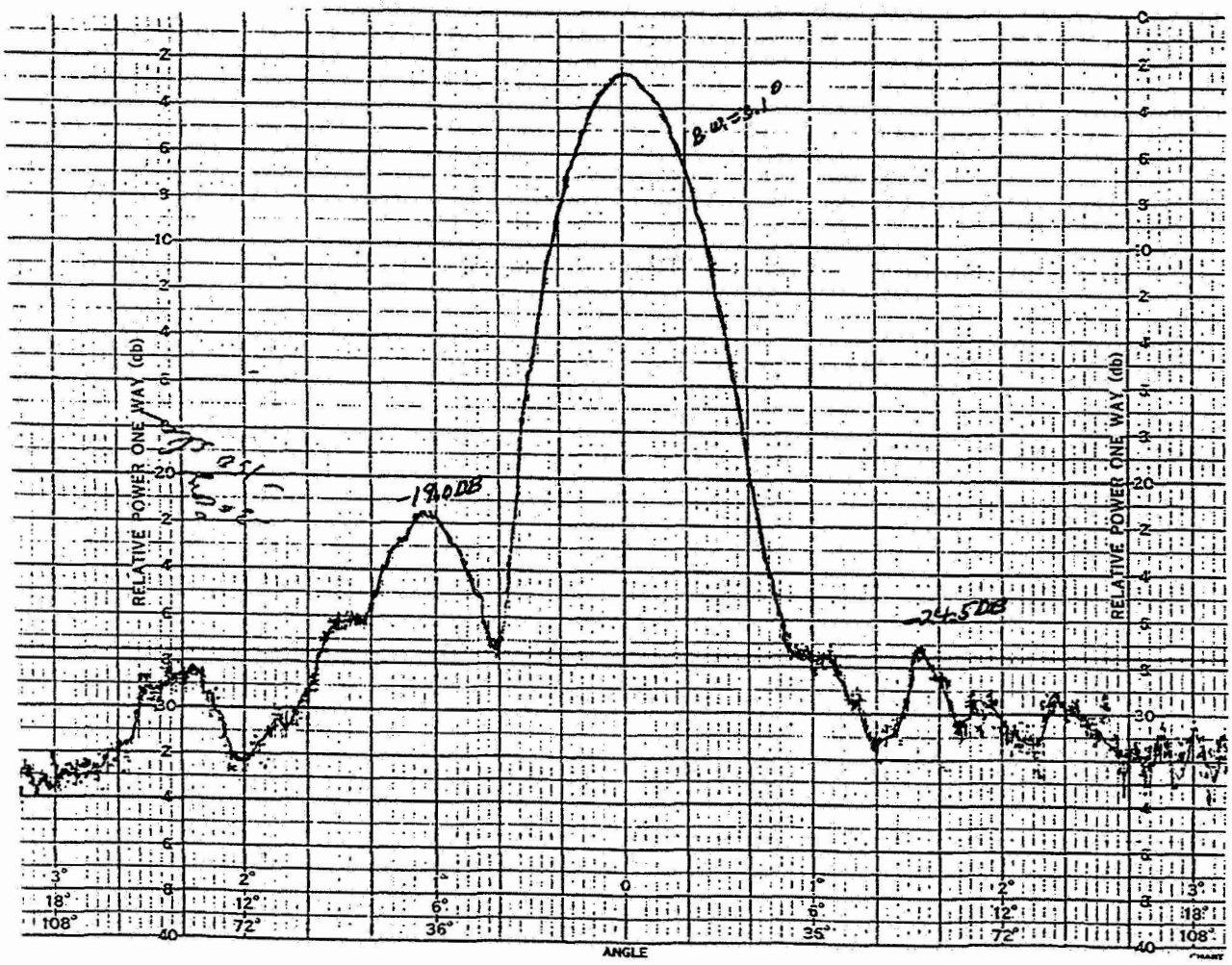

figure 2 **Airline Example RTCA Class D,category 2 Radome**

The RTCA class D,category 2 radome states that a degradation in the antenna sidelobe levels to within -20 dB. of the mainlobe should be acceptable. This also asserts that the dynamic range of weather radars need not be 50 dB. This is tantamount to a -40 dB. two way antenna sidelobe isolation rather than some -70 dB. min. two way isolation available from the phased array antenna.

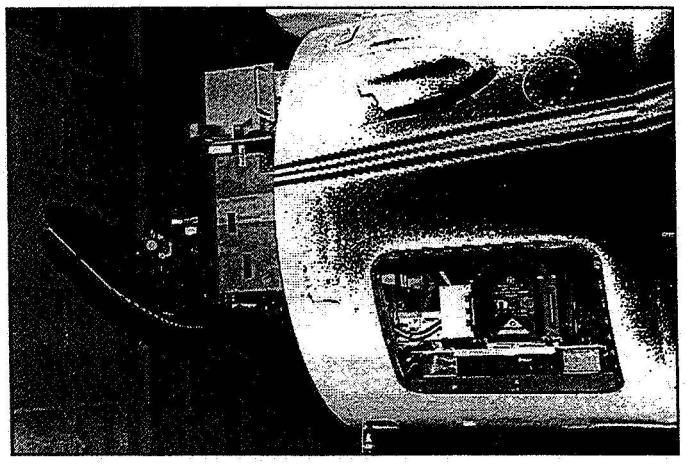

figure 3 MODAR 3000 Installation on the BAC-1-11

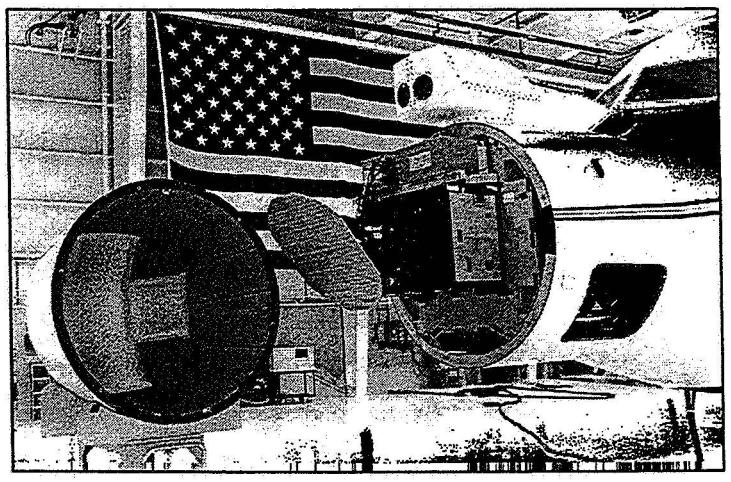

Front View - BAC1-11 MR 3000 Installed With Degraded (Class D) Radome

A932408-02 CD58A

figure 4 RTCA Class D,category 2 Radome

A spare radome for the BAC-1-11 was modified by cementing coarse fiberglass asymetrically near the nose. This furnished a decrease in the transmissivity and an increase in the antenna sidelobe for antenna pointing within the windshear mode window.

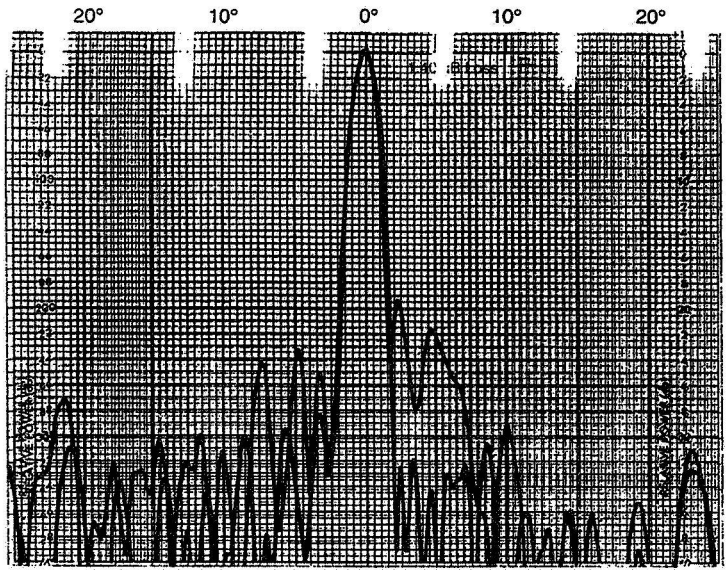

Azimuth Radiation Pattern Comparison

figure 5 **Azimuth Antenna/Radome Pattern**

Plots show a pronounced increase in the antenna first and near sidelobes. The degradation varies somewhat over the ±30 degree scan window.

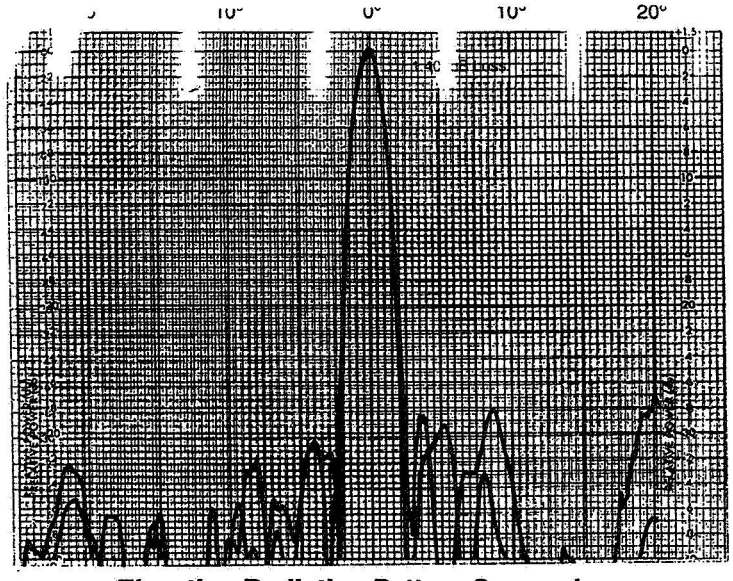

Elevation Radiation Pattern Comparison

figure 6 **Elevation Antenna/Radome Pattern**

dimension (see fig. 6), the general sidelobe level has also been raised, but the peak distortion is in the azimuth plane.

In-flight testing with this class "D" radome, most urban airports will introduce some sidelobe level leakage, evident on the weather display as spurious green spotting and/or smudge. Approaches into Newark, NJ from the southwest, however, produced displays with persistent, spatial correlating, small red and yellow spotting.

Westinghouse has been developing the MODAR 3000 to be certified with a Class D,category 2 radome. For the more prudent user of better and properly maintained radomes, certification to Class D,category 2 levels of radome performance would provide a sense of field degradation margin on detectability and false alarm performance. For the operator of older aircraft, an opportunity to equip with predictive is afforded.

To date, Westinghouse has collected clutter data for development purposes with the Class D,category 2 radome and has been evaluating detection performance degradations. Clearly, a class A radome will offer better warning time performance, especially against "drier" events, than a class D,category 2 radome, and, at this time, the prospects for detection certification of the class D,category 2 radome must be tentative. However, at the time of this paper, Westinghouse has completed flight test in Orlando with the FAA, with demonstration of 28 seconds of warning time on a must alert level hazard with this radome. Again with the FAA on board, Westinghouse has flown the BAC-1-11 and class D,category 2 radome into Newark, Washingtion National, and Philadelphia for the purposes of simulation path clutter collection. Westinghouse will claim FAA certification credit for demonstrating false alert free performance with a class D,category 2 radome during those flights. In summary, ***Westinghouse will claim certification credit for the flight test and false alert performance requirements for class D, category 2 or better radomes.*** By definition, a class E, category 2 radome will have the same sidelobe specifications but poorer transmissivity. Credit for class E, category 2 radome performance for certification might be claimed by using the clutter data collected with a class D, category 2 radome with a greater insertion loss in the weather return calculation.

The video shows the outputs from the superposion simulation expected for certification run cases. This video shows weather reflectivity and windshear hazard icon/anunciation with contours of true hazard against the NASA Denver multiple microburst during take-off using BWI class D, category 2 radome clutter data with a hazard located at 3 n.mi. The first segment is in the absence of clutter. The case begins just prior to brake release. The pilot's display initially shows only weak weather reflectivity and truth hazard contours. However, after scan-to-scan correlation, the simulation produces icons which conform generally to the size and shape of the hazard contours before/during brake release, giving the pilot warning well before he would have been committed to take-off. As the aircraft rolls down the runway and approaches in range, the truth hazard contours and the icon change. The radar begins to lose detection ability at nearer range, indicated by a scan without an icon, but the subsequent scan does furnish an additional icon. The next segment shows the same run with class D, category 2 radome clutter. There are

additional indications of green and yellow reflectivity due to leakage of ground clutter through the antena sidelobes. However, the radar performs detection and persistence in a fashion indistinquishable from the clutter free run, except the scan of icon recovery at near range is not produced.

The video also shows the format for certification presentation of results (see figure 7). The scenario is depicted in a plan view using N-S or E-W truth hazard contours of the dataset at the closest altitude. An *in situ* trace, based on the NASA *in situ* algorithm, is accumulated from the winds of the database at the position of the aircraft as a function of case run time. Warning time credit will be claimed from the difference in time at first warning (light and sound anunciation) and time of *in situ* encounter of the hazard edge.

For certification credit of icon scoring, the display will probably require modifications for slightly larger icons and coasted or otherwise artificial persistence of icons at nearest ranges.

At what point will airlines find sidelobe degradations unacceptable for in-route weather? Operation of an antenna and radome combination with the peak degradation only in the azimuth plane produces a weather map display of multiple distracting hazardous area portrayal which would seem very distracting in a high workload approach environment. A manufacturer of pulse Doppler radars and the community regulating their safe use must ultimately assume that user airlines will find it in their best interests to comply with some minimal standard of radome performence. In the case of a windshear detection capability, certification of detection and false alarm performance with a radome demonstrating compliance with the transmissivity and sidelobe degradations of class "D", category 2, especially with this instance of a BAC-1--11 modified radome, suggests that some predictive windshear capability may be obtained within the current "art" of radome maintenence. Furthermore, the pilots and crew on board aircraft with such radomes would have long been monitoring the symptoms of sidelobe degradations and might sense departures in the sidelobe performance from weather only observations.

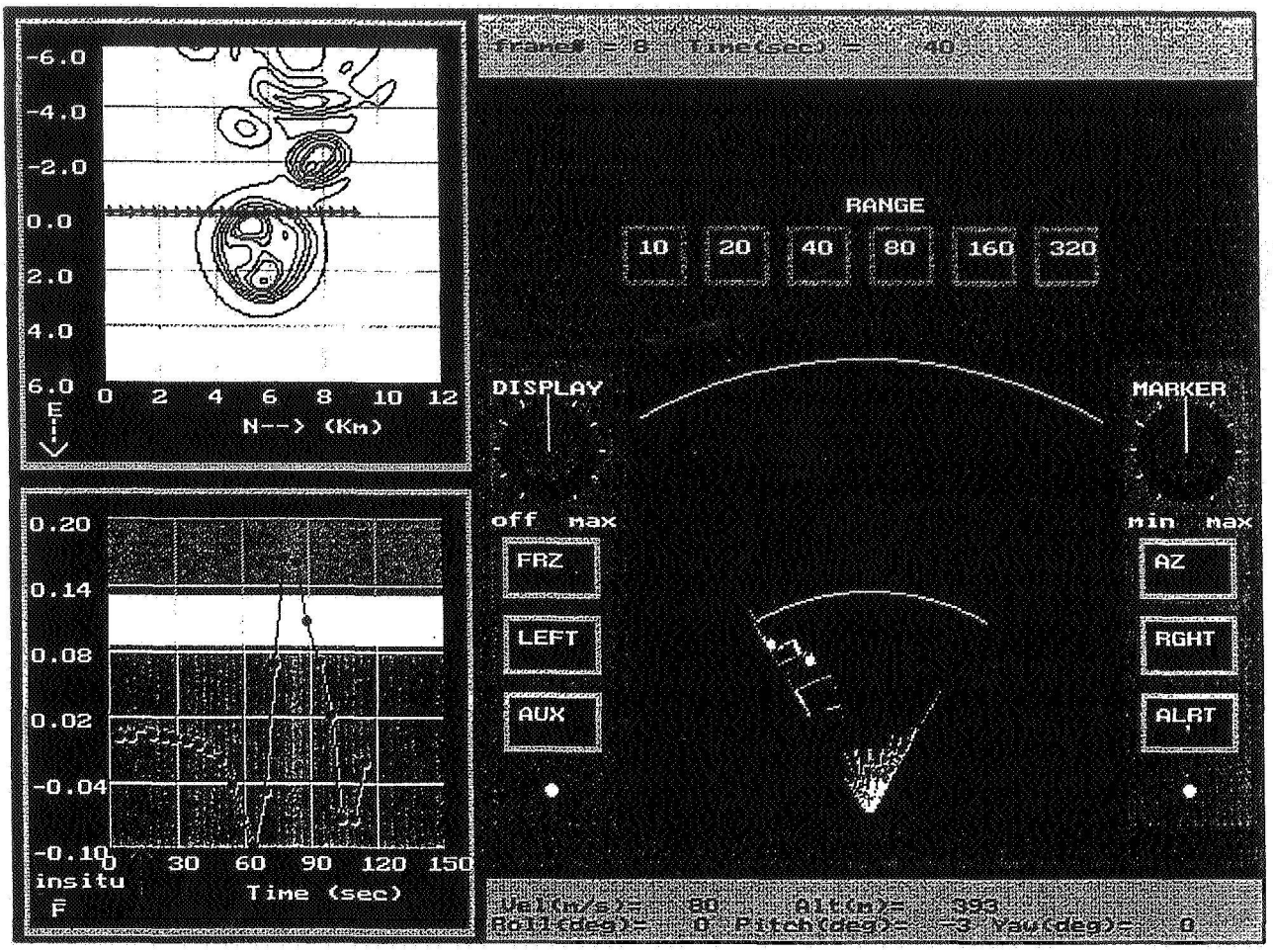

fig. 7 **Certification Simulation End Product**

Each simulation run is summarized by the plan view of the upper right, which shows the arrangement of NASA database E-W or N-S path hazard contours at the altitude closest to the scenario. The aircraft path will be described by a series of arrows, indicating its start and path through the event. The lower left furnishes a stripchart of NASA *in situ* hazard factor calculated from the database winds at the aircraft position as a function of time. The pilots display will show the weather reflectivity and icon at the time of initial position, some simulation runs may include production of a scan-by-scan sequence of the display as the event is approached for the judging of human factors. Credit for warning time is taken from the time difference of anunciation and *in situ* encounter, as delineated by markers on the *in situ* trace. True hazard contours along the expected flight path may be overlayed for observer orientation, but icon scoring will be a separate output.

Airport Surveillance Using a Solid State Coherent Lidar.

M. Hufaker,

Coherent Technologies, Inc.

No Abstract, Original Needed

AIRPORT SURVEILLANCE USING A SOLID-STATE COHERENT LIDAR

R. MILTON HUFFAKER
STEPHEN M. HANNON

COHERENT TECHNOLOGIES, INC.
BOULDER, COLORADO

FAA - Program Managers: James Rodgers
Lew Buckler

CONTRIBUTORS: J. Alex L. Thomson, J.R. Magee, G.W. Cox, and S.W. Henderson

PROGRAM SUMMARY

OBJECTIVE: *ASSESS THE UTILITY OF SOLID-STATE COHERENT LIDAR TO THE TASS PROGRAM*

APPLICATIONS: WAKE VORTICES; DRY AND WET MICROBURST WINDSHEAR; GUSTS; VERTICAL AND GENERAL WIND PROFILING; CLOUD CEILING

- TASK 1: SYSTEM PERFORMANCE MODELING
  - CONCEPT DEFINITION
  - SYSTEM SIZING
  - MEASUREMENT PLANNING
  - ALGORITHM AND GRAPHICS DISPLAY DEVELOPMENT
- TASK 2: FIELD DEMONSTRATION MEASUREMENTS
  - EXISTING MOBILE 2.09 μm COHERENT LIDAR SYSTEM
  - KENNEDY SPACE CENTER
  - STAPLETON INTERNATIONAL AIRPORT
- TASK 3: DATA ANALYSIS AND ASSESSMENT
- TASK 4: SYSTEM DESIGN SPECIFICATION

Instrument Mounted on Truck Top.

KENNEDY SPACE CENTER MEASUREMENTS

- NINE DAYS OF MEASUREMENTS WERE CONDUCTED DURING THE SPACE SHUTTLE ENDEAVOR MISSION (STS-54)
- COMPARATIVE WIND PROFILING EXPERIMENTS WERE CONDUCTED
  - LIDAR, RADAR WIND PROFILER, RAWINSONDES, ANEMOMETERS, SHUTTLE DATA
- MOBILE 2.09 μm COHERENT LIDAR SYSTEM USED DURING MEASUREMENTS
  - 27 mJ, 175 nsec, 5 Hz PRF, 10 cm APERTURE
- 2.09 μm COHERENT LIDAR SYSTEM LOCATED ADJACENT TO SHUTTLE LANDING FACILITY; ~7 km FROM THE LAUNCH PAD AND 8-10 km FROM ATLANTIC OCEAN
- PRIMARILY SPONSORED BY NASA/MSFC THROUGH THE AIR FORCE'S WRIGHT LABORATORY. DATA WAS ALSO COLLECTED AS PART OF THE TASS PROGRAM

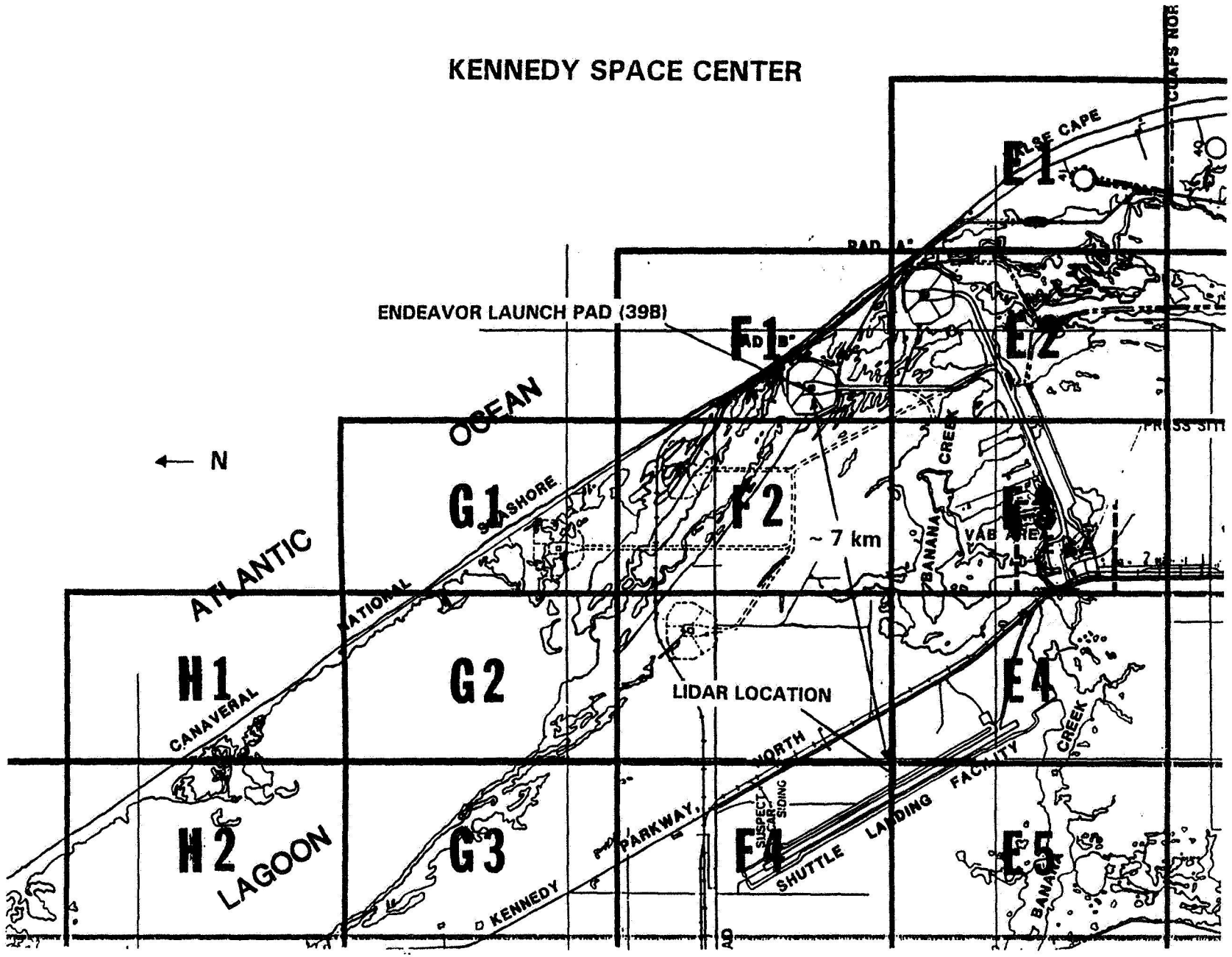
KENNEDY SPACE CENTER
CAPE CANAVERAL AIR FORCE STATION
ENDEAVOR LAUNCH PAD (39B)
PAD A
PAD B
OCEAN
ATLANTIC
N
~ 7 km
LIDAR LOCATION
VAB
BANANA CREEK
NORTH
SHUTTLE LANDING FACILITY
SUSPECT CARGO SIDING
PARKWAY
KENNEDY
LAGOON
E1
E2
E3
E4
E5
F1
F2
F3
F4
G1
G2
G3
H1
H2

19° PPI 30 MINUTES PRIOR TO LANDING

MEASURED RADIAL VELOCITY

(POSITIVE AWAY FROM LIDAR)

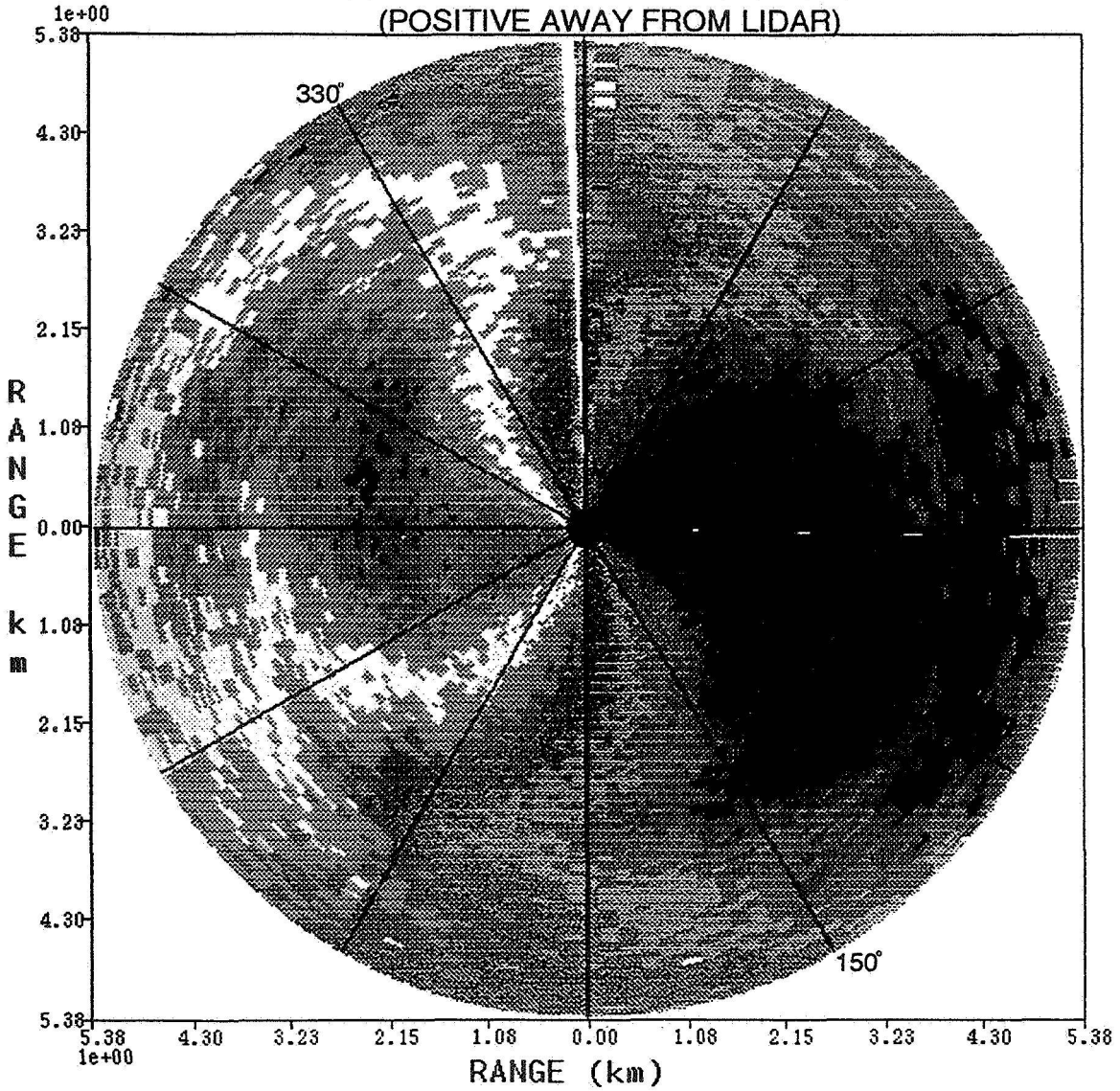

Jan 19 1993 08:04:02 0423 AZIM 094.455 ELEV 019.000

-8 0 8

RADIAL VELOCITY (m/sec)

SCAN RATE = 5°/sec
RANGE GATE = 100 m
N_{GATES} = 128
N_{AVG} = 3

PULSE WIDTH = 185 nsec
PULSE ENERGY = 27 mJ
PRF = 5 Hz
D = 8 cm

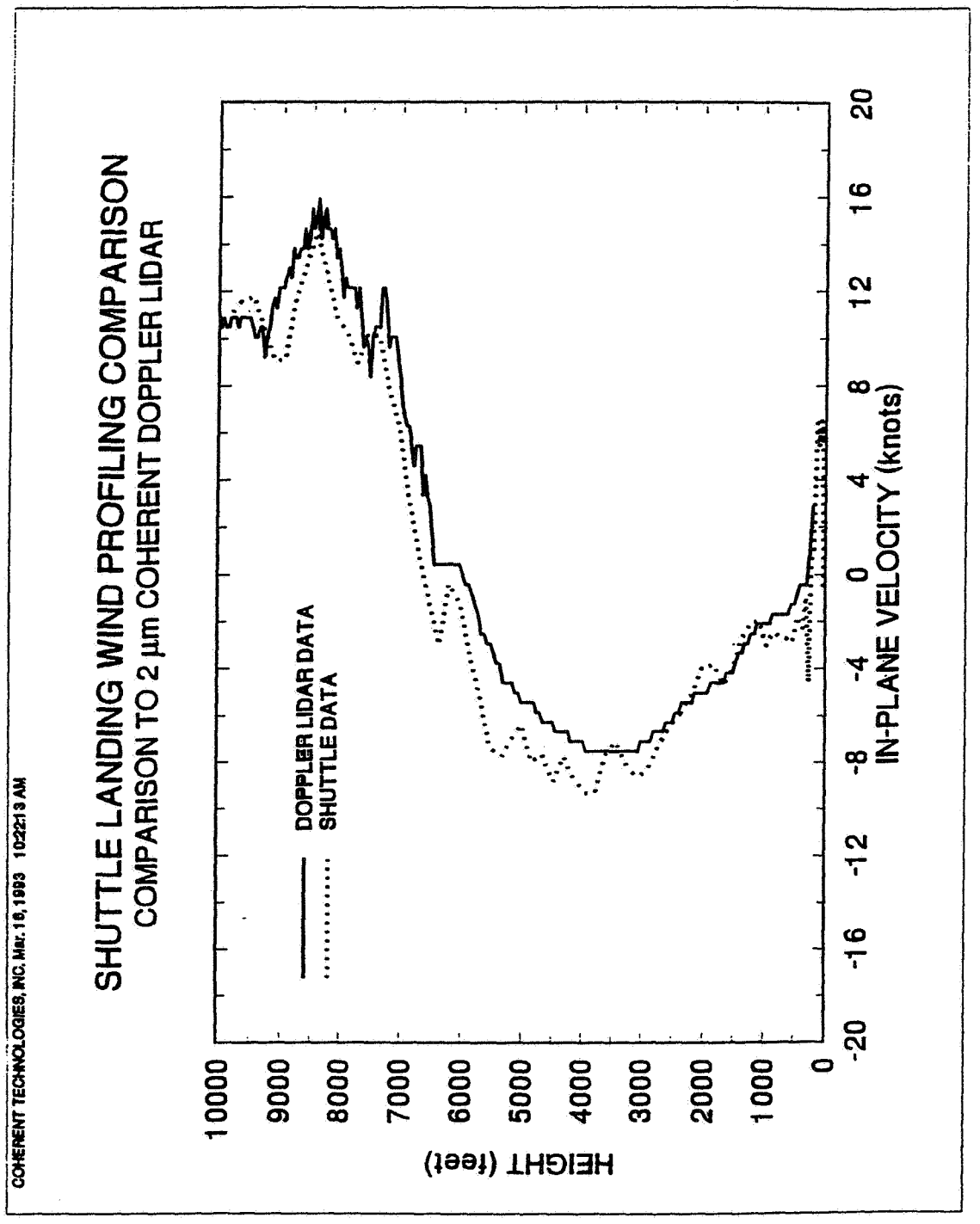
SHUTTLE LANDING WIND PROFILING COMPARISON
COMPARISON TO 2 µm COHERENT DOPPLER LIDAR
COHERENT TECHNOLOGIES, INC. Mar. 16, 1993 10:22:13 AM
DOPPLER LIDAR DATA
SHUTTLE DATA
HEIGHT (feet)
10000
9000
8000
7000
6000
5000
4000
3000
2000
1000
0
-20
-16
-12
-8
-4
0
4
8
12
16
20
IN-PLANE VELOCITY (knots)

PERFORMANCE IN RAIN, 27 mJ OPERATION

~6.3 mm/hr (VARIABLE, AVERAGED OVER ~30 min)

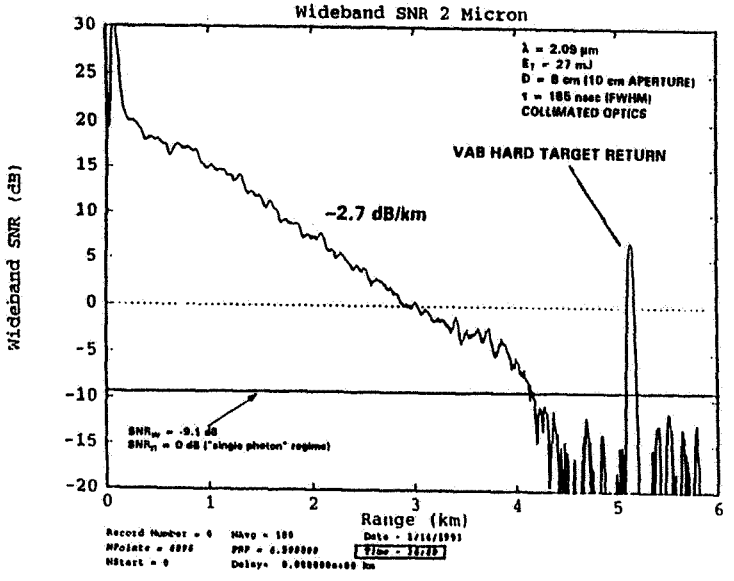

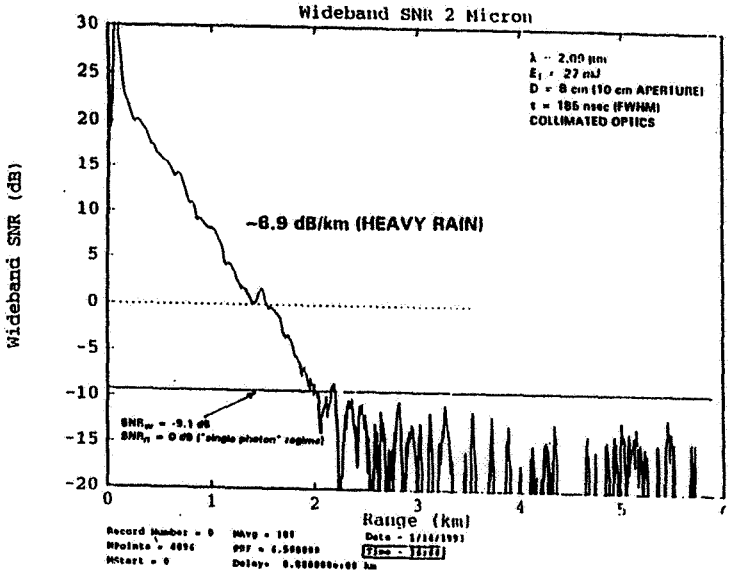

SCALE UP BY 4.3 dB FOR 500 nsec PULSE LENGTH

KENNEDY SPACE CENTER MEASUREMENTS—SUMMARY

- WIND PROFILING PERFORMANCE CLOSE TO THAT OBTAINED IN COLORADO
  - HIGHER HUMIDITY ENVIRONMENTS DO NOT SIGNIFICANTLY DEGRADE SYSTEM PERFORMANCE FOR A PROPERLY TUNED 2 μm COHERENT LIDAR

- 15-20 km HORIZONTAL RANGE FOR 27 mJ, 175 nsec OPERATION
  - COMPARES FAVORABLY WITH MODEL PREDICTIONS; NEGLIGIBLE REFRACTIVE TURBULENCE

- LIDAR WIND MEASUREMENT ACCURACY CONFIRMED THROUGH COMPARISONS WITH RADAR WIND PROFILER, SHUTTLE DATA, AND RAWINSONDES

- RAIN MEASUREMENTS YIELD FIRST 'QUANTITATIVE' EXTINCTION ESTIMATES AT 2 μm
  - COMPARES REASONABLY WELL WITH CHU AND HOGG (1968) DATA
  - SYSTEM MEASUREMENT RANGE OF ~2 km IN 1"/HOUR RAIN

STAPLETON MEASUREMENTS

- FOUR WEEKS OF MEASUREMENTS AT THE NATIONAL WEATHER SERVICE SITE ADJACENT TO STAPLETON AIRPORT (APRIL/MAY 1993)
- PRIMARY EMPHASIS ON WAKE VORTEX DETECTION/MONITORING/TRACKING
  - THREE VERTICAL SCAN PLANES, LANDING CONFIGURATION
  - EMPHASIZE 757, 767, AIRBUS, DC10
  - RETURN IN JUNE FOR ADDITIONAL MEASUREMENTS (MICROBURSTS)
- GROUND TRUTH DATA
  - RADAR WIND PROFILER
  - RAWINSONDES (TWO PER DAY)
  - RAS TEMPERATURE PROFILER (MINIMUM MEASUREMENT HEIGHT OF 100 m)
  - GROUND MET OBSERVATIONS (TEMPERATURE, WINDS, VISIBILITY, HUMIDITY)
- 30-60 MINUTES OF VORTEX DATA FOLLOWED BY A VERTICAL WIND PROFILE AND/OR A LOW-ALTITUDE PPI SCAN
- VERTICAL BACKSCATTER PROFILES AND LARGE AREA PPI SCANS

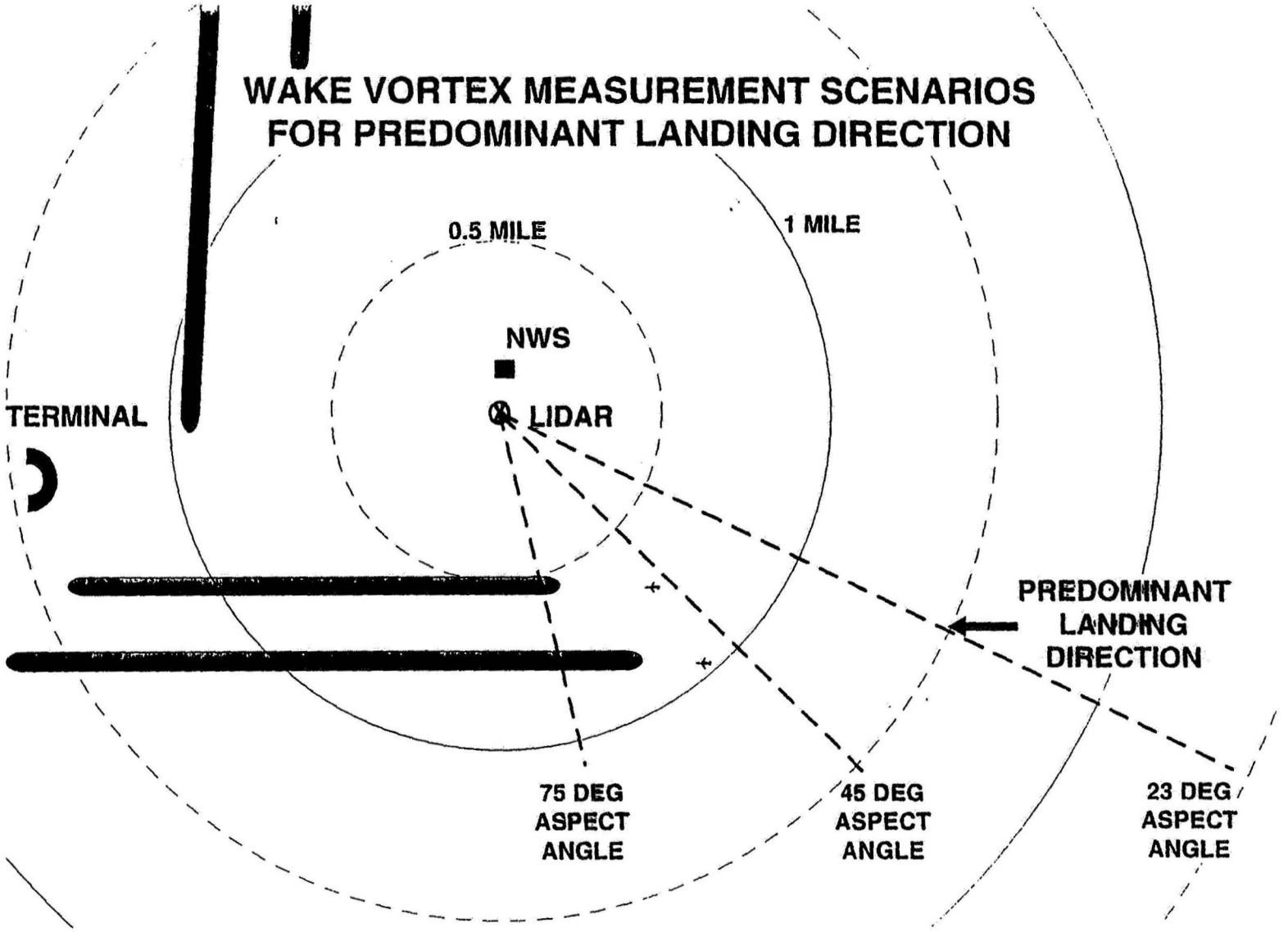
WAKE VORTEX MEASUREMENT SCENARIOS
FOR PREDOMINANT LANDING DIRECTION
0.5 MILE
1 MILE
NWS
LIDAR
TERMINAL
PREDOMINANT
LANDING
DIRECTION
75 DEG
ASPECT
ANGLE
45 DEG
ASPECT
ANGLE
23 DEG
ASPECT
ANGLE

Elev 42.82 Record Number 36
Range [km]
0.41
0.53
0.65
0.78
0.90
1.02
1.15
1.27
1.40
1.52
1.64
Frequency [MHz]
-50
-40
-30
-20
-10
0
10
20
30
40
50
SkyMode: lft
52
54.2
56.4
58.7
60.9
63.1
65.3
67.6
69.8
72

SPECTRAL SIGNATURES FOR DC10 WAKE VORTICES

RANGE-RESOLVED DOPPLER SPECTRUM (T + 24 sec)

(+30m/sec to -30 m/sec)

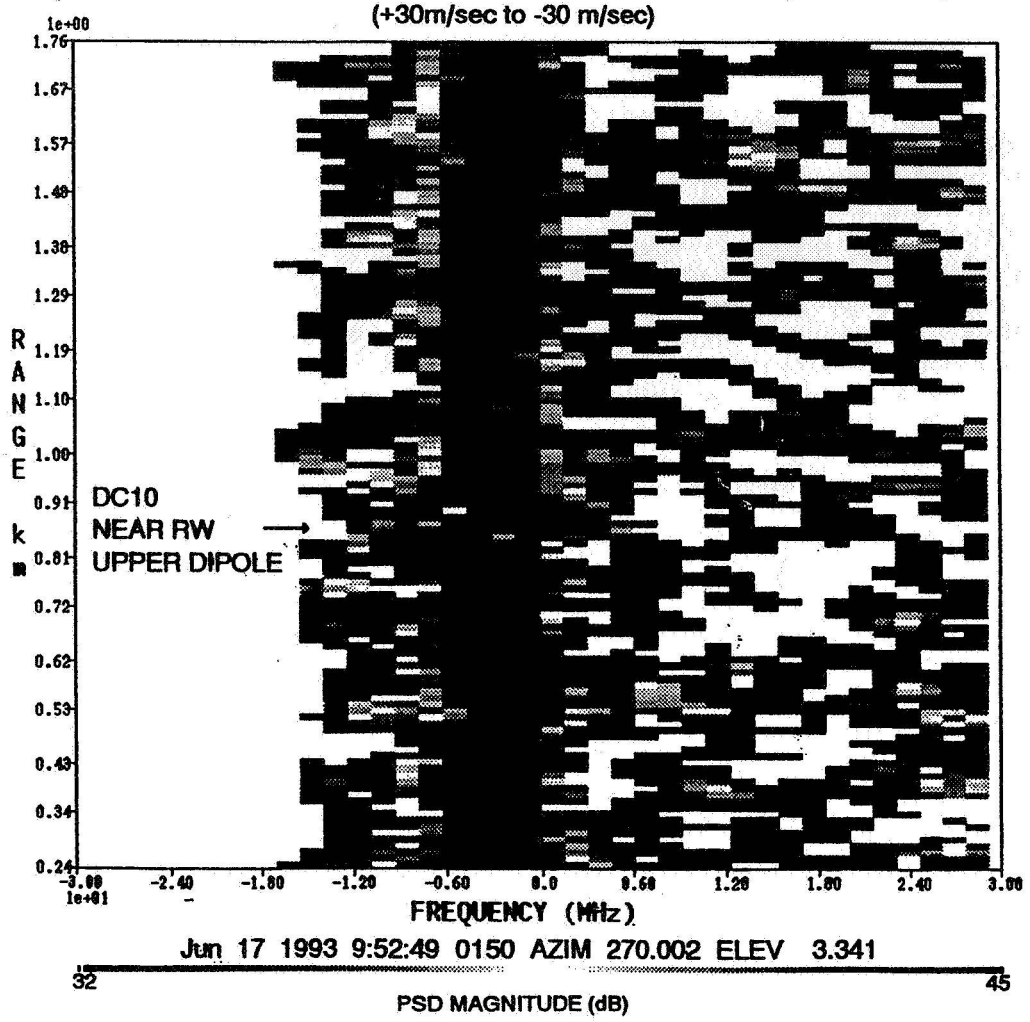

SCAN RATE = 0.6 /sec
RANGE GATE = 100 m
N_{GATES} = 128
N_{AVG} = 3

PULSE WIDTH = 165 nsec
PULSE ENERGY = 9 mJ
PRF = 5 Hz
D = 8 cm

SPECTRAL TRACKING RESULTS - DC10

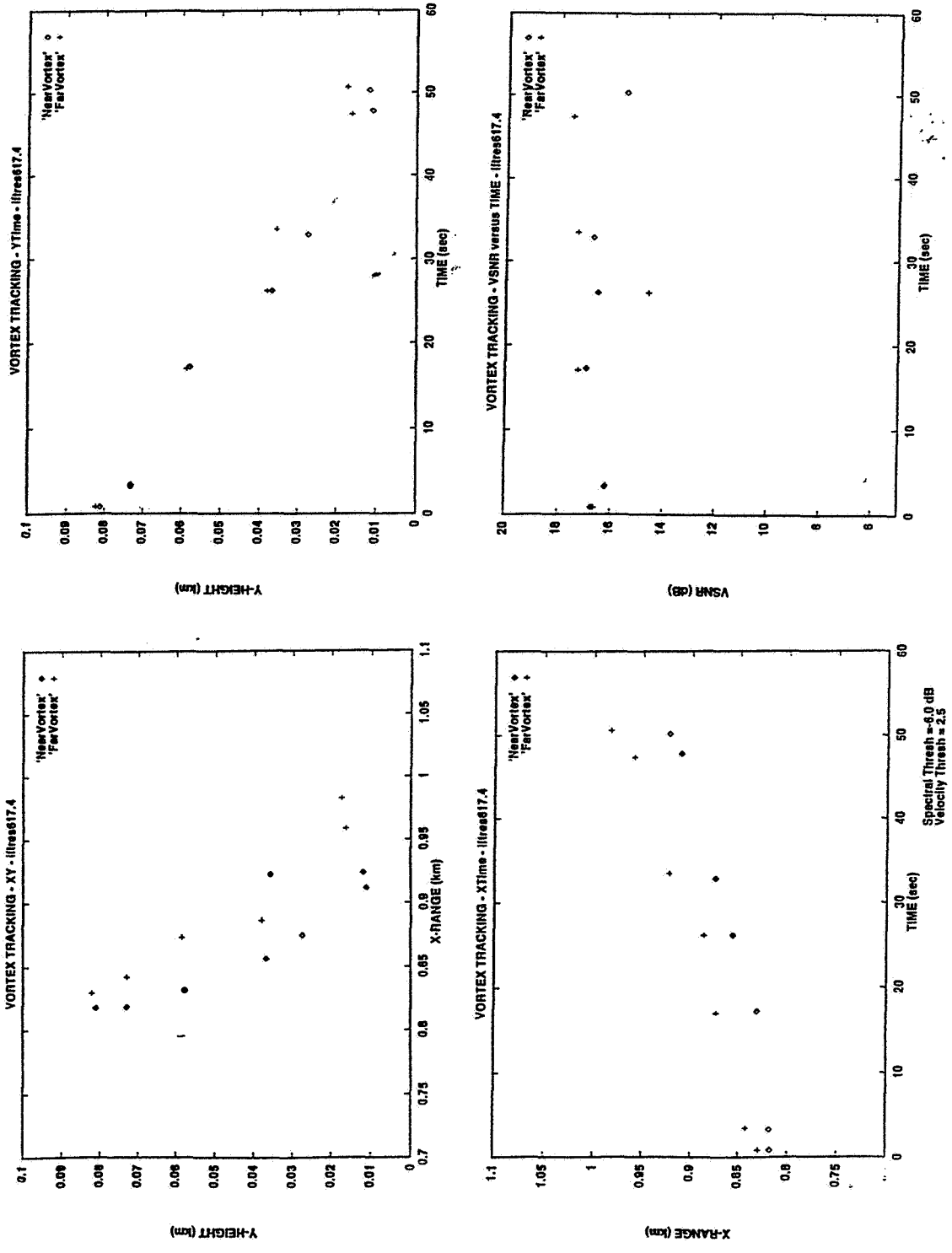

RHI @40° NEAR COLORADO FRONT RANGE

MEASURED RADIAL VELOCITY - TIME SLICE 1

(POSITIVE AWAY FROM LIDAR)

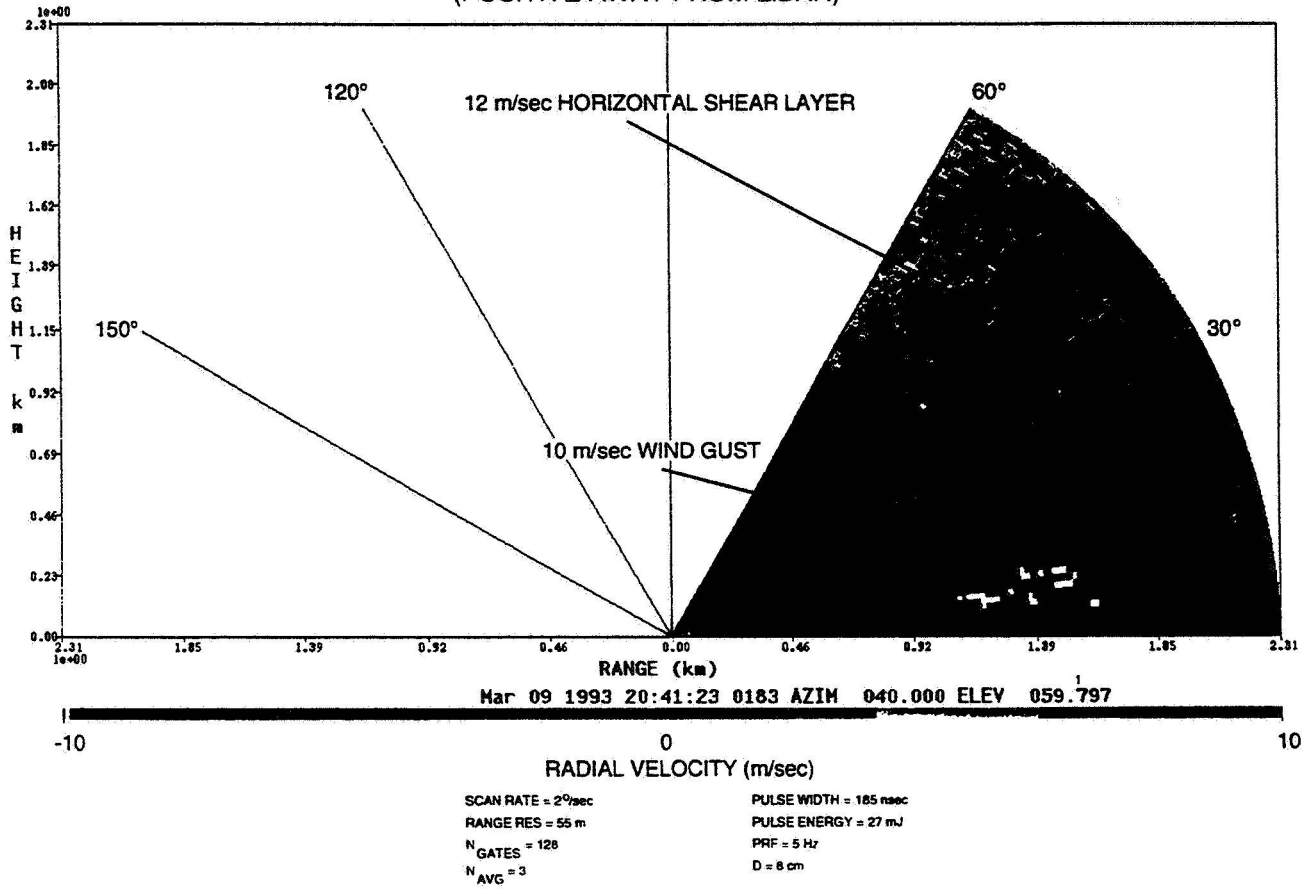

SCAN RATE = 2°/sec
RANGE RES = 55 m
N_{GATES} = 128
N_{AVG} = 3

PULSE WIDTH = 185 nsec
PULSE ENERGY = 27 mJ
PRF = 5 Hz
D = 8 cm

RHI @40° NEAR COLORADO FRONT RANGE

MEASURED RADIAL VELOCITY - TIME SLICE 2

(POSITIVE AWAY FROM LIDAR)

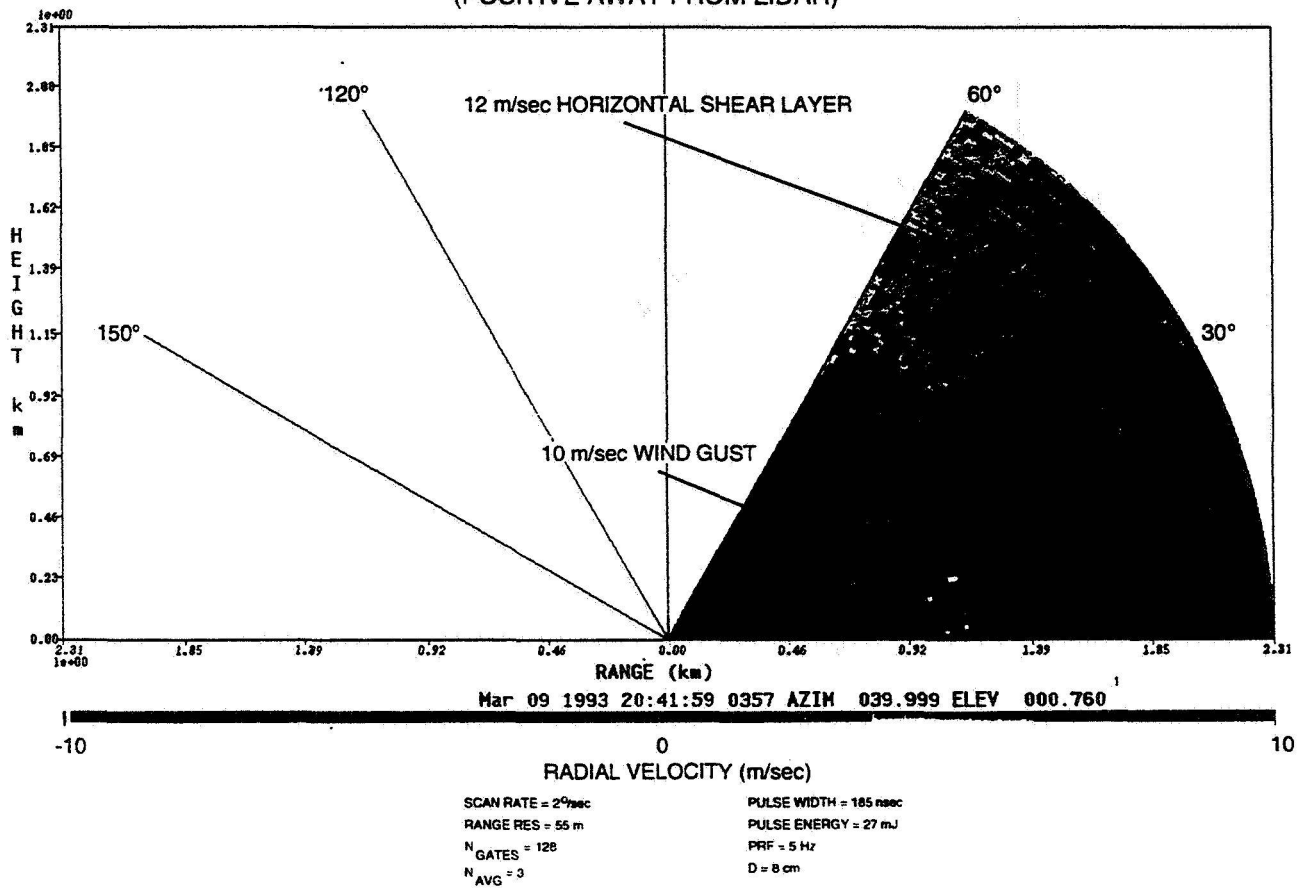

SCAN RATE = 2°/sec
RANGE RES = 55 m
N_{GATES} = 128
N_{AVG} = 3

PULSE WIDTH = 185 nsec
PULSE ENERGY = 27 mJ
PRF = 5 Hz
D = 8 cm

2° PPI SHOWING NUMEROUS INHOMOGENEITIES

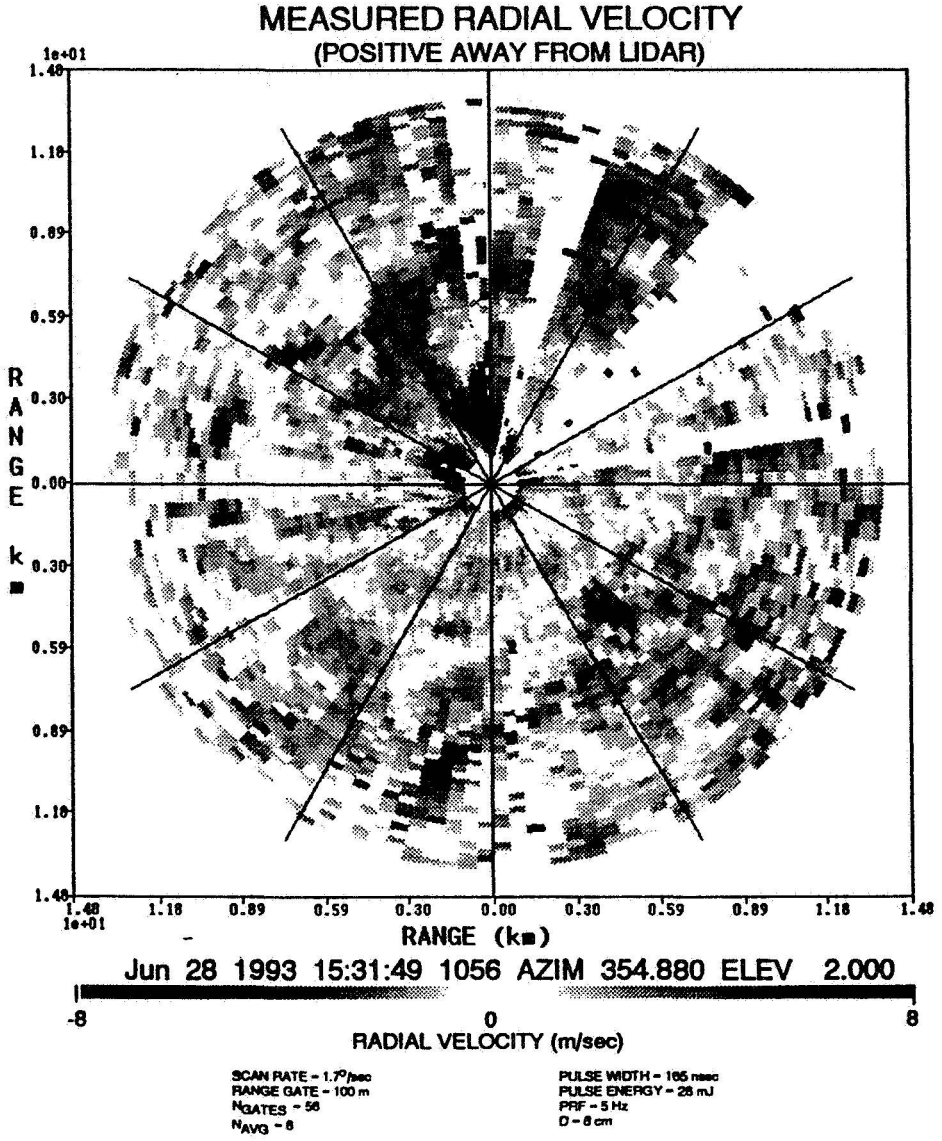

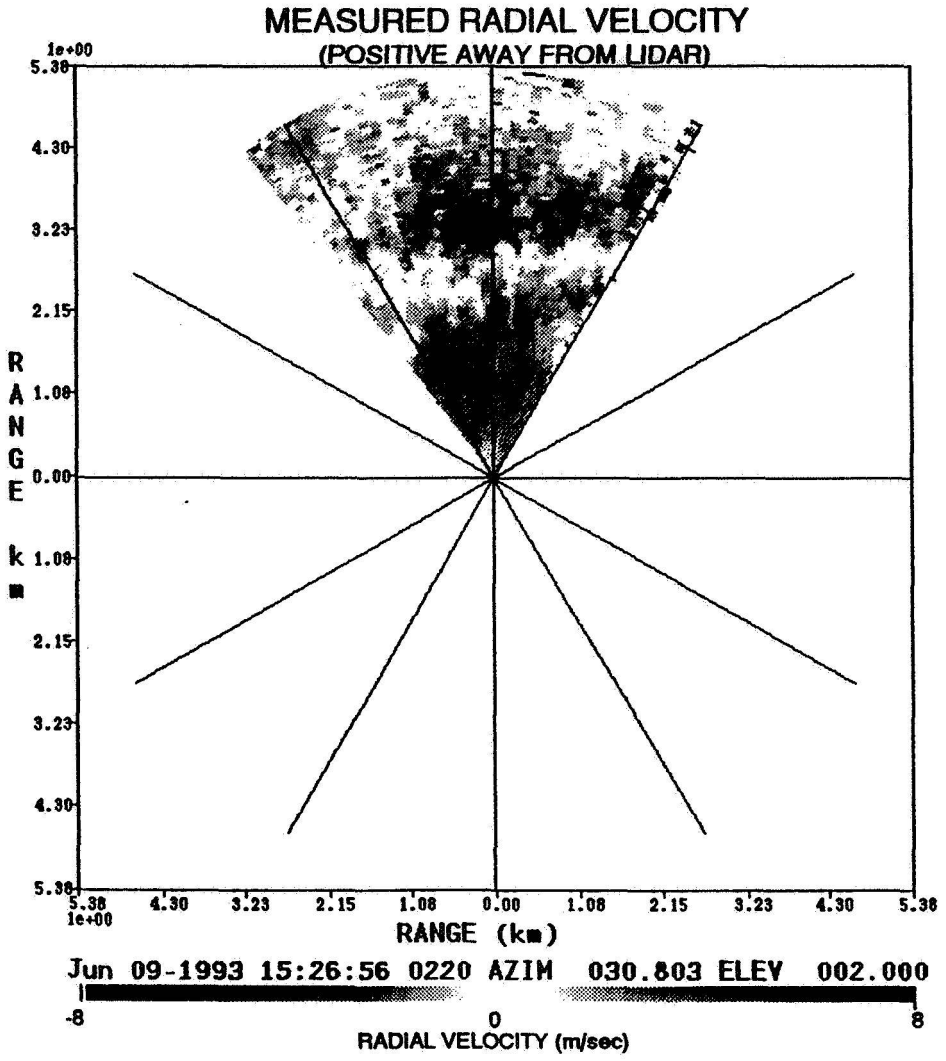
MEASURED RADIAL VELOCITY
(POSITIVE AWAY FROM LIDAR)
1e+00
5.38
4.30
3.23
2.15
1.08
0.00
1.08
2.15
3.23
4.30
5.38
RANGE km
5.38 4.30 3.23 2.15 1.08 0.00 1.08 2.15 3.23 4.30 5.38
1e+00
RANGE (km)
Jun 09-1993 15:26:56 0220 AZIM 030.803 ELEV 002.000
-8
0
8
RADIAL VELOCITY (m/sec)
SCAN RATE = 2°/sec
RANGE GATE = 100 m
NGATES = 128
NAVG = 4
PULSE WIDTH = 165 nsec
PULSE ENERGY = 9 mJ
PRF = 5 Hz
D = 6 cm

350° RHI SHOWING OUTFLOW DIPOLE

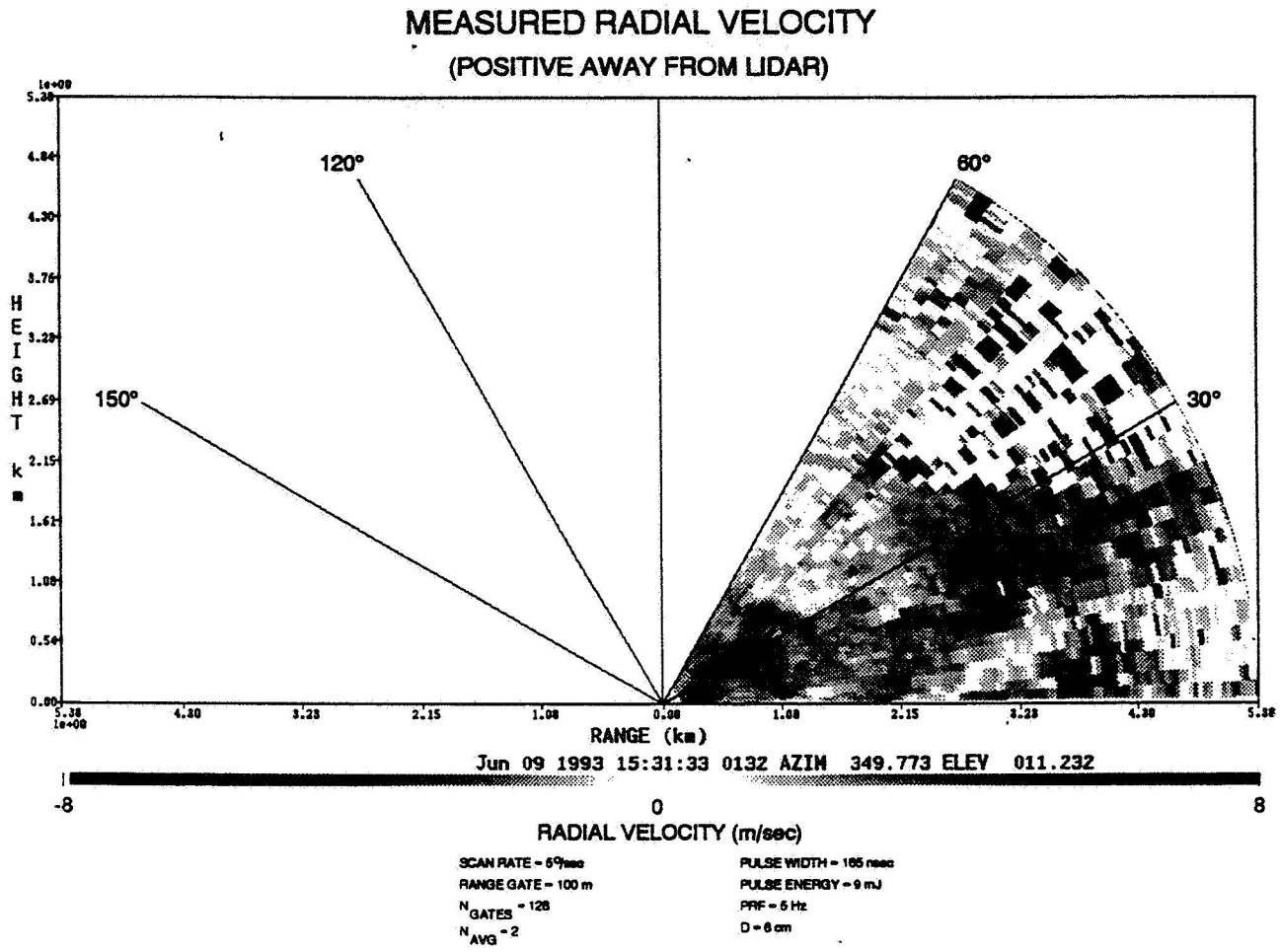

340° RHI 23 MINUTES LATER

MEASURED RADIAL VELOCITY

(POSITIVE AWAY FROM LIDAR)

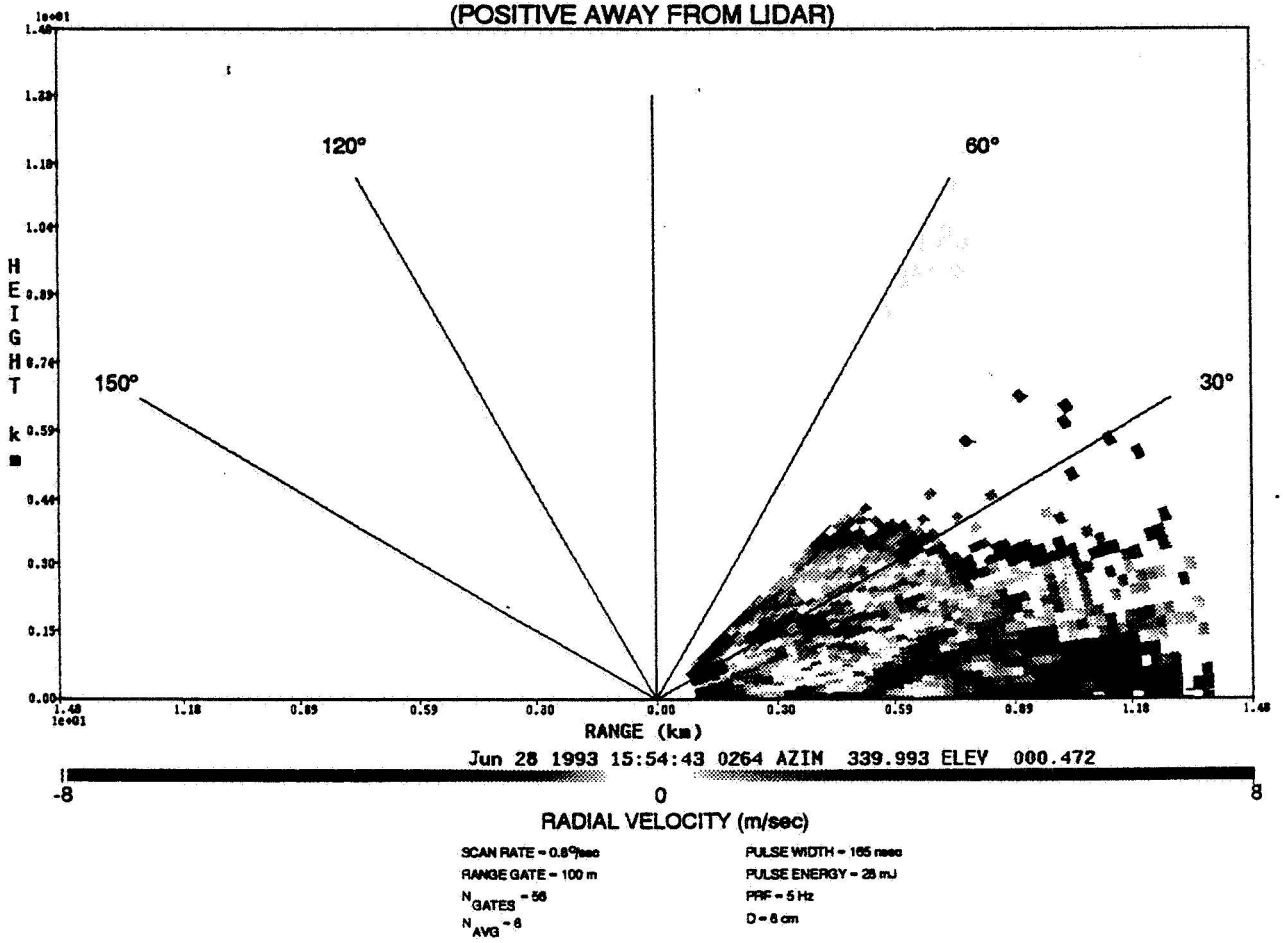

STAPLETON MEASUREMENTS—SUMMARY

- RELIABLE WAKE VORTEX DETECTION FOR EACH MEASUREMENT
  - LIDAR DETECTS WAKE EVERY TIME (~250+ LANDINGS)

- LARGE VORTEX DATABASE IS BEING COMPILED
  - THREE SCAN PLANES (ASPECT ANGLES)
  - LARGE AMOUNT OF METEOROLOGICAL DATA
  - CORRELATIONS BETWEEN ENVIRONMENT AND WAKE PERSISTENCE

- MULTIPLE SCAN PLANES CAN BE USED TO DETERMINE AXIAL FLOW SIGNATURE
  - TRANSVERSE FLOW MODEL PREVIOUSLY VERIFIED
  - AXIAL FLOW SIGNATURE IMPORTANT TO MAXIMIZE COVERAGE AREA WITH SINGLE-STATION LIDAR

- MEASUREMENT GEOMETRY NOT IDEAL
  - MINIMUM ELEVATION ANGLE OF 0.5° (8-15 m MINIMUM MEASUREMENT HEIGHT)
  - ELIMINATES ASPECT ANGLES BETWEEN 85° AND 45°)
  - ALTERNATE LOCATION NEAR NWS CONSIDERED FOR JUNE MEASUREMENTS

CANDIDATE SCANNING GEOMETRIES

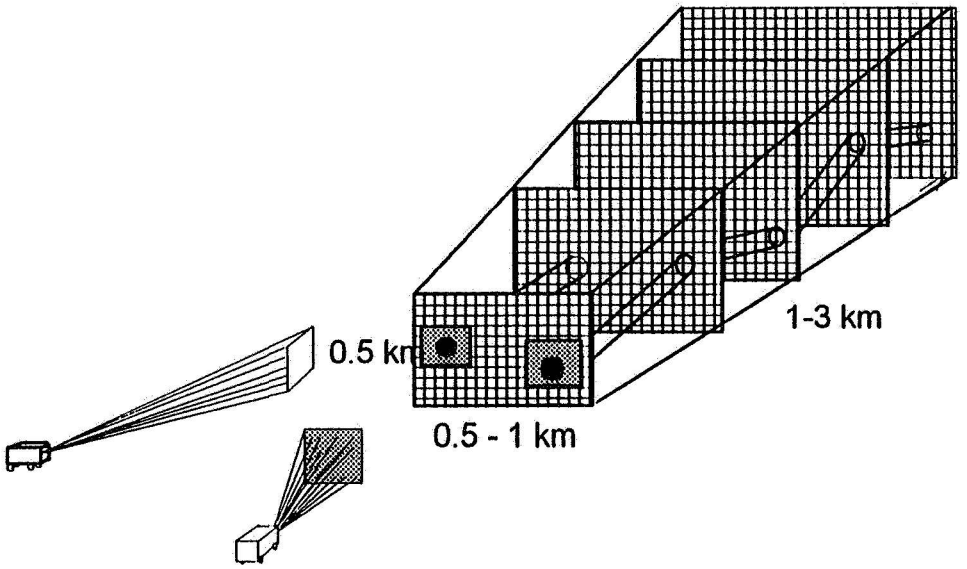

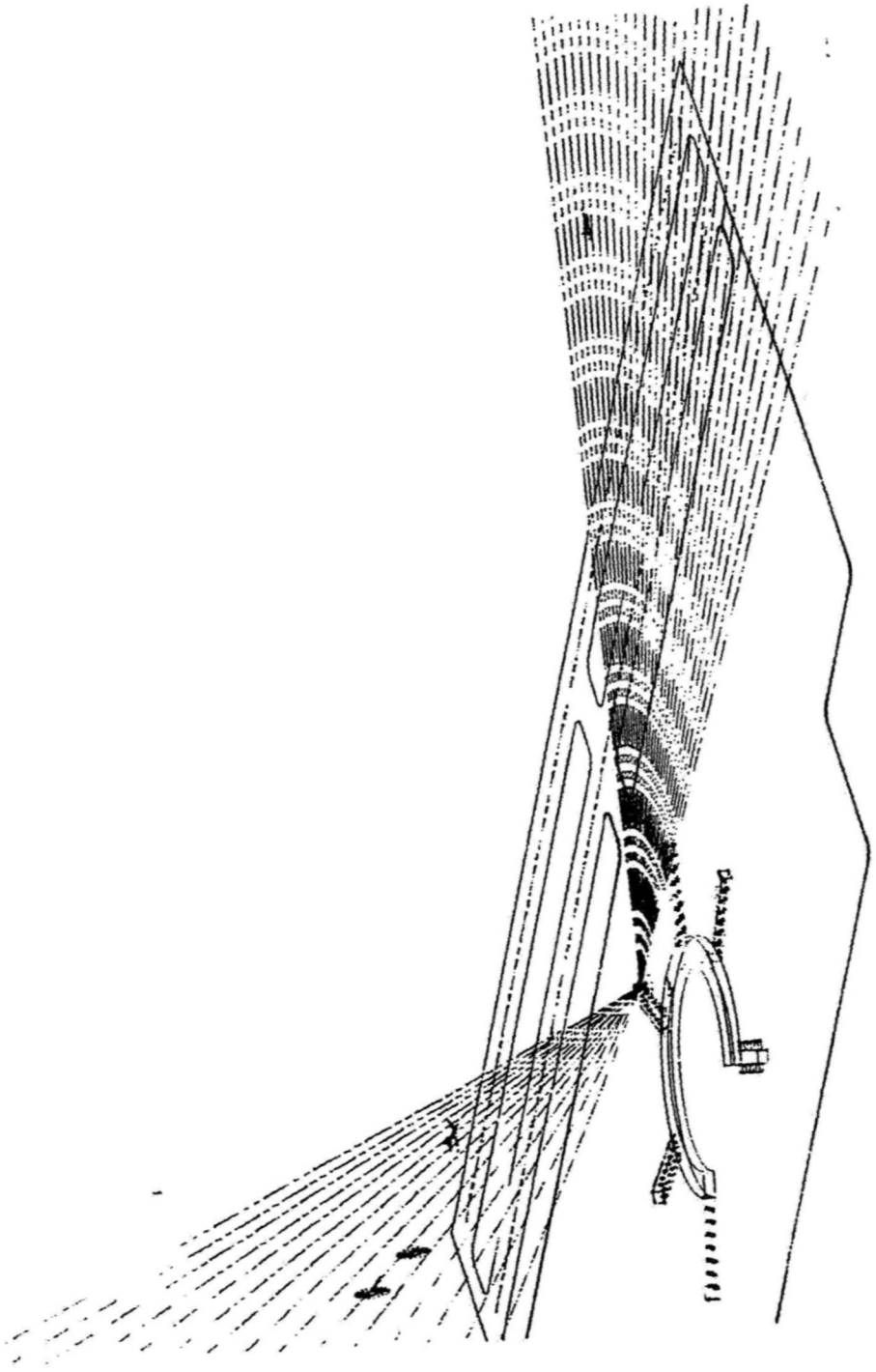

PRELIMINARY PERFORMANCE ASSESSMENT

- PULSED SOLID-STATE LIDAR BEST DEVICE FOR DETECTING AND TRACKING WAKE VORTICES
  - PULSE LENGTH 20-75 m TO MATCH WAKE DIMENSIONS
  - HIGH PRF SYSTEMS (>50 Hz) NEEDED TO MEET SPATIAL SAMPLING REQUIREMENTS (2 m)
  - PULSED OPERATION PERMITS MEASUREMENT TO RANGES OF A FEW KILOMETERS
  - RELIABLE ESTIMATES OF VORTEX LOCATIONS AND PERSISTENCE CAN BE ACHIEVED
- HIGH RESOLUTION WIND PROFILES VALUABLE FOR IN AIRPORT ENVIRONMENT (MICROBURST AND WIND GUST DETECTION AND TRACKING)
  - LARGE AREA OR SECTOR SCANS ON DEMAND
  - VOLUMETRIC SCANNING WITH SUFFICIENT PRF
  - VERTICAL WIND PROFILES ON DEMAND
- MODEST SYSTEM REQUIREMENTS
  - 10-20 mJ PULSE ENERGY; 10-15 cm APERTURE; 100-300 Hz PRF
  - EXISTING OR NEAR-TERM DIODE-PUMPED 2 μm TECHNOLOGY
  - CAPABLE OF FULL AIRPORT COVERAGE 10-15 km
- 3D VELOCITY 'IMAGES' ARE FEASIBLE
  - XYT DEMONSTRATED WITH 5 Hz PRF: $\Delta X = 35$ m; $\Delta T = 10$ sec
  - HIGH PRF SYSTEMS PERMIT XYZT WITH $\Delta X < 50$ m; $\Delta T < 10$ sec

Session 5:

FUTURE AERONAUTICS TECHNOLOGY RESEARCH PROGRAMS.

High Speed Civil Transportation Research.

M. Lewis,

NASA LangleyResearch Center

Session 5:

FUTURE AERONAUTICS TECHNOLOGY RESEARCH PROGRAMS.

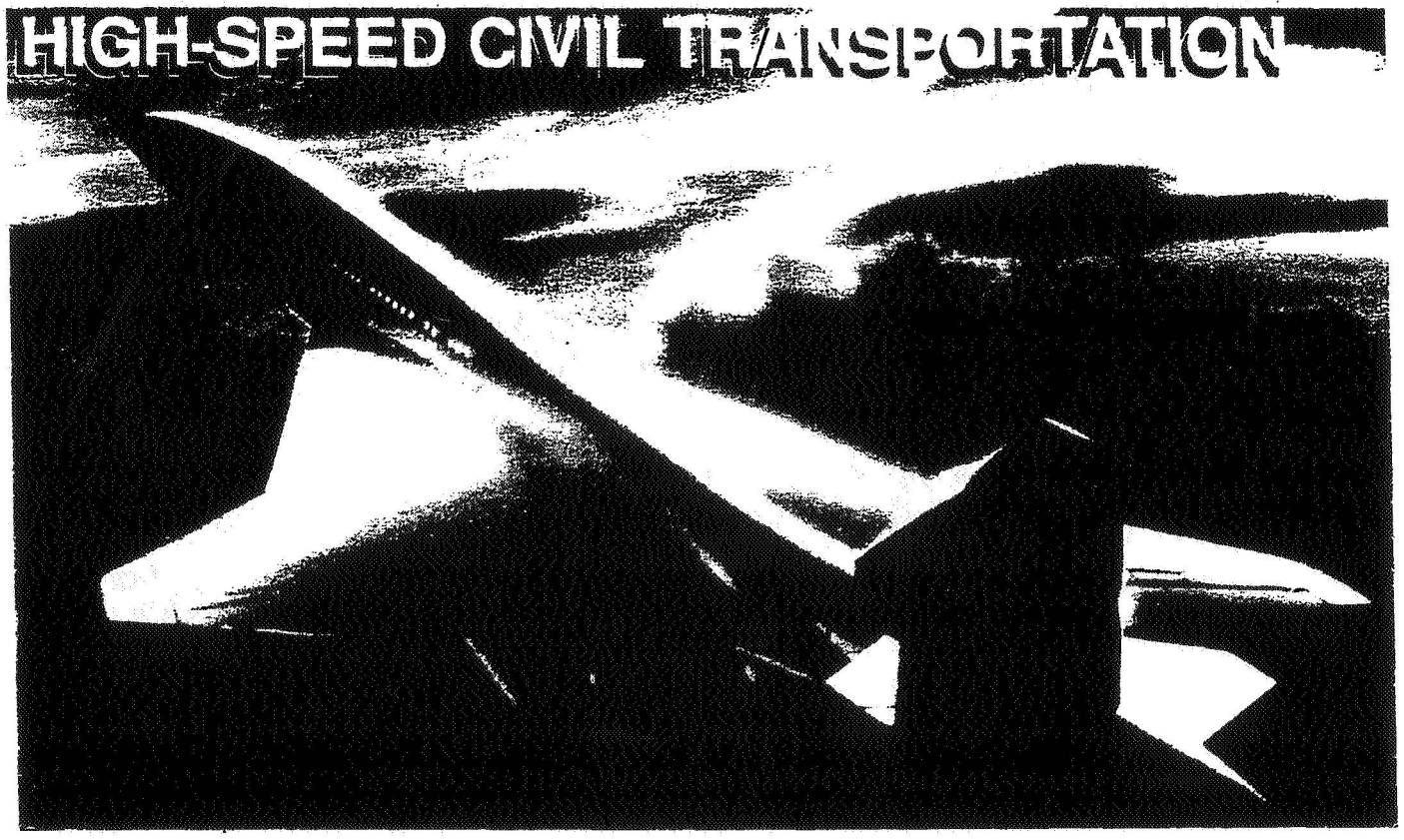

THE HIGH-SPEED CIVIL TRANSPORT MARKET

Range and Speed Impact

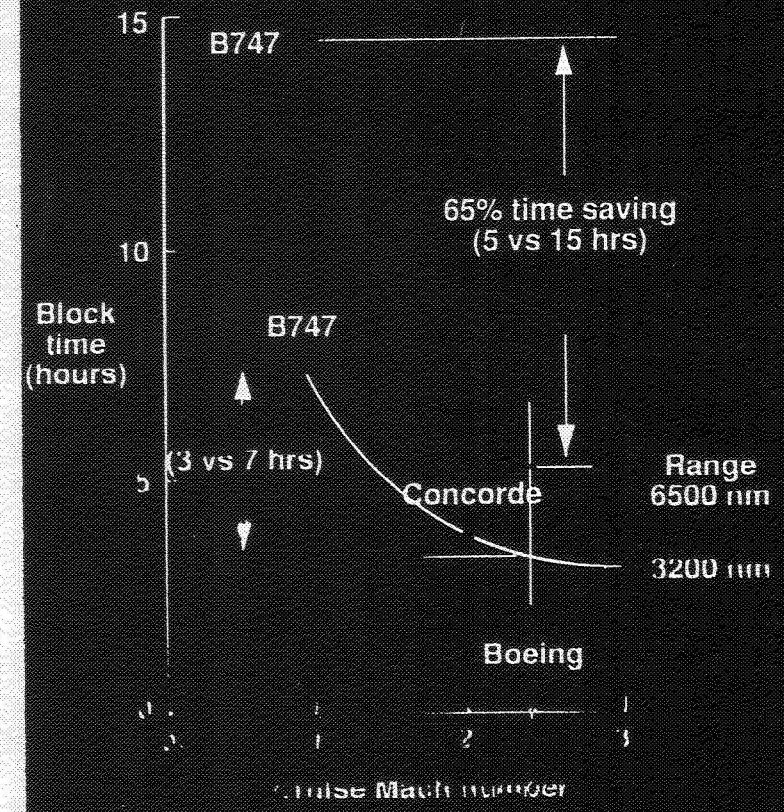

The Golden Triangle

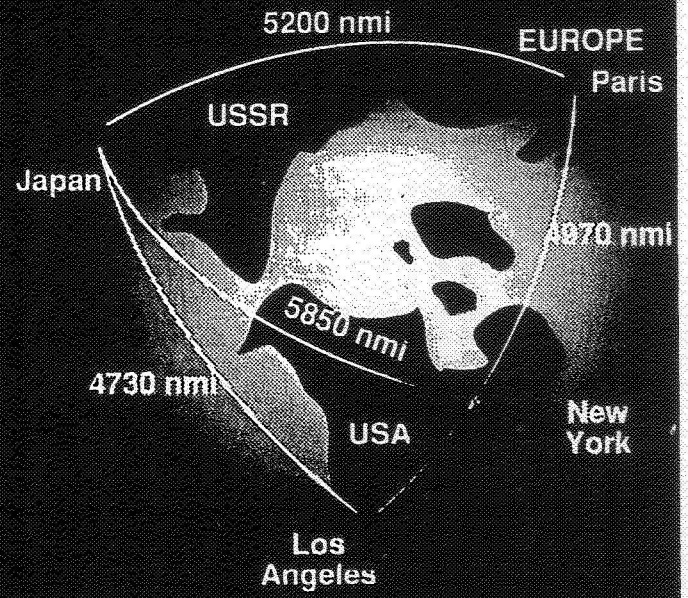

Source: M. Poisson-Quinton

HIGH-SPEED RESEARCH PROGRAM

Current Outlook

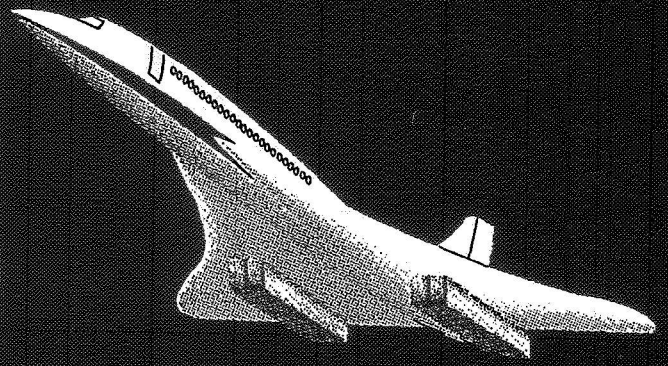

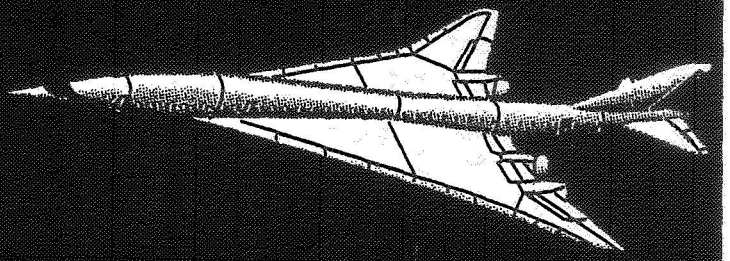

Concorde		HSCT Goals
3000	Range (N.Mi.)	5000 - 6500
100	Payload (Passengers)	250 - 300
400,000	Weight (Lb.)	750,000
87	Required Revenue (¢/RPM)	10
Premium	Fare Levels	Standard
Exempt	Community Noise Standard	FAR 36 - Stage III
20	Emissions Index (gm/Kg fuel)	3 - 8 (at HSCT efficiency)

VISION

Establish the technology foundation by 2001 to support the U.S. transport industry 2005 production of an environmentally acceptable, economically viable, 300 passenger, 5000 n.mi., Mach 2.4 aircraft.

HIGH-SPEED CIVIL TRANSPORT

PHASE I
ENVIRONMENTAL CONCERNS

- Prediction of HSCT ozone effects
- Feasibility of NO_x reduction
- Economical compliance with noise rules
- Sonic boom prediction/reduction
- Demonstrate supersonic LFC

PHASE II
ECONOMIC ENHANCEMENTS

- High-temperature, long-life composite materials
- Structural concepts
- Propulsion system development & performance
- High-lift & cruise aerodynamics
- Cockpit & flight management technology

Q-2

INTEGRATED HIGH-SPEED CIVIL TRANSPORT PLAN

The NASA HSR Program is Enabling Technology Development and Validation and Not Product Development

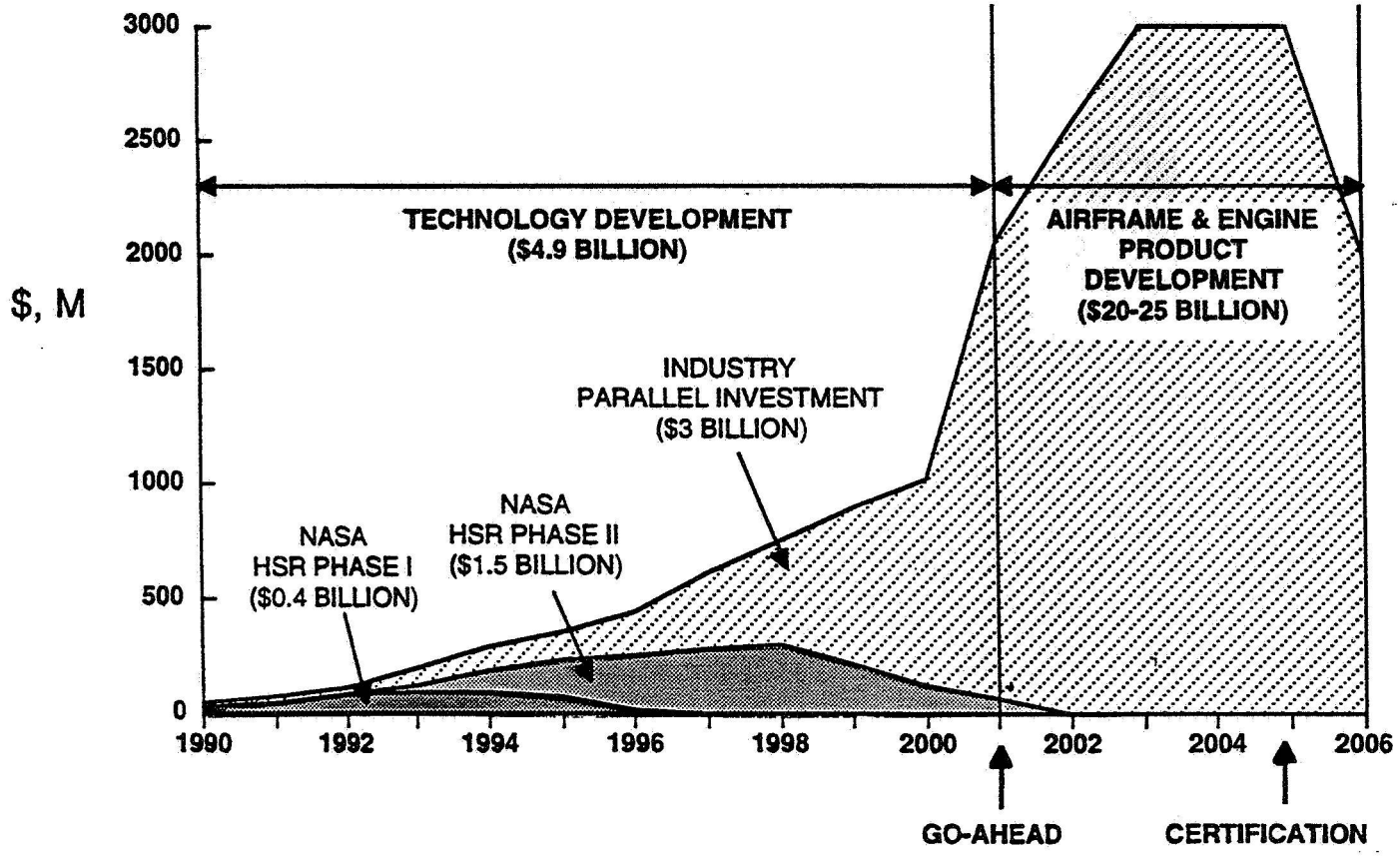

HIGH-SPEED RESEARCH PHASE II MILESTONES

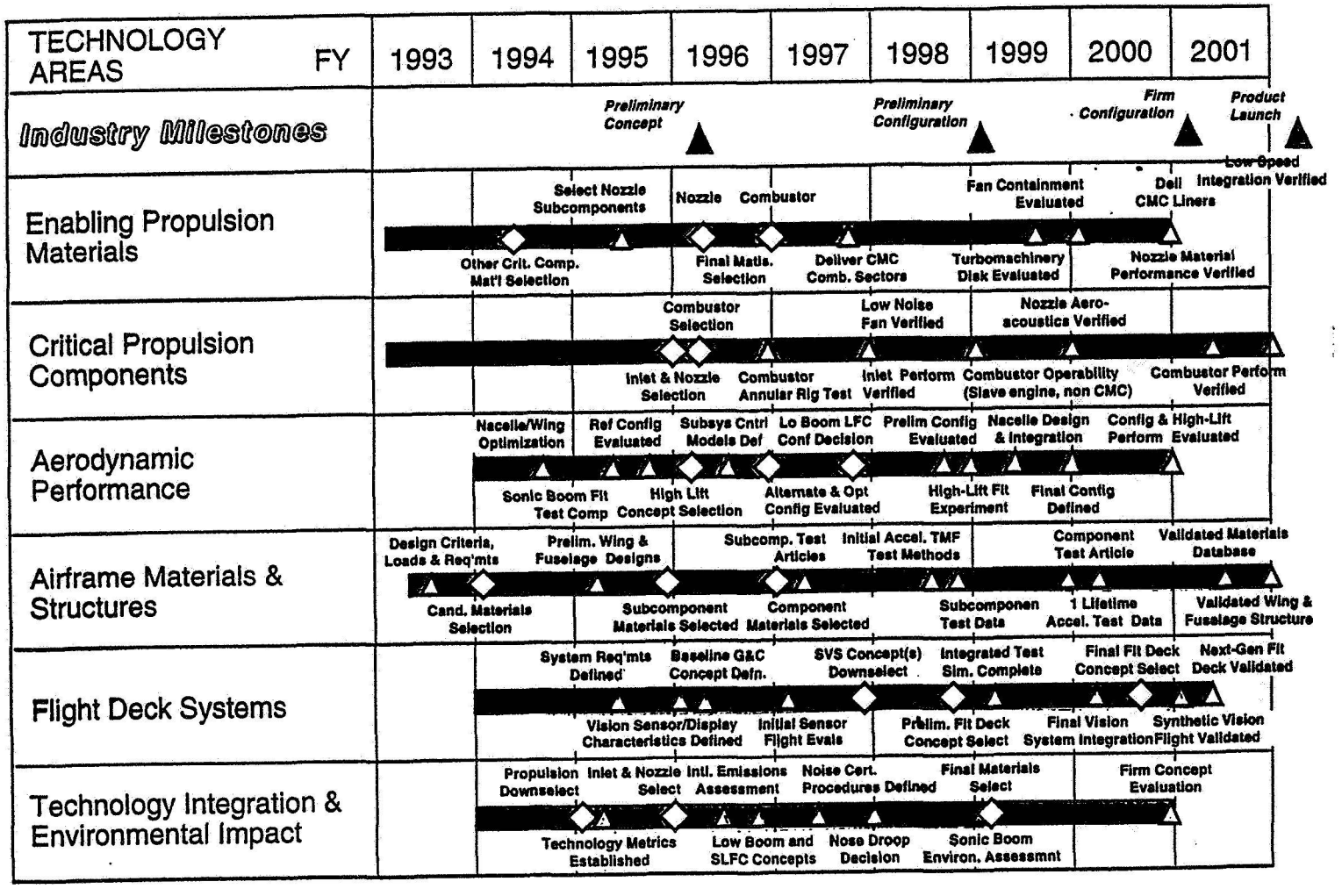

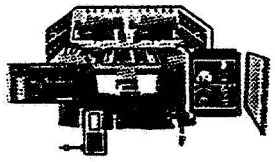

Flight Deck Systems

HSR-PHASE II

Objective: Provide validated flight deck systems technologies and certification guidelines to enable industry development of:

- Synthetic vision
- Next-generation flight deck

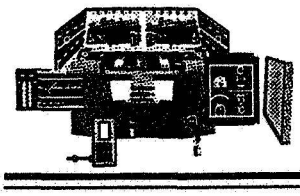

Flight Deck Systems

Issues & Problems

- RESTRICTED VISIBILITY
  - Approach & Landing
  - Ground Operations
  - Collision Avoidance (VFR, As Well As IFR)
- COCKPIT LOCATION
  - Optimization Of Flight Deck Volume/Shape
  - Cockpit Motion
  - Taxi Guidance & Control
- UNIQUE OPERATING REQUIREMENTS
  - Systems Management (Fuel, Temperature, Radiation)
  - Noise Management
  - ATC Integration
- LACK OF CERTIFICATION GUIDELINES
  - Synthetic Vision
  - Non-Evolutionary Cockpit

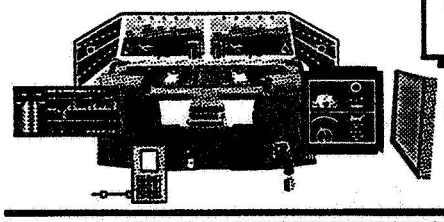

FLIGHT DECK SYSTEMS & CONTROLS

Constraints of Two Person Cockpits

HSR-PHASE II

Advanced Subsonic vs. Mach 2.4 HSCT

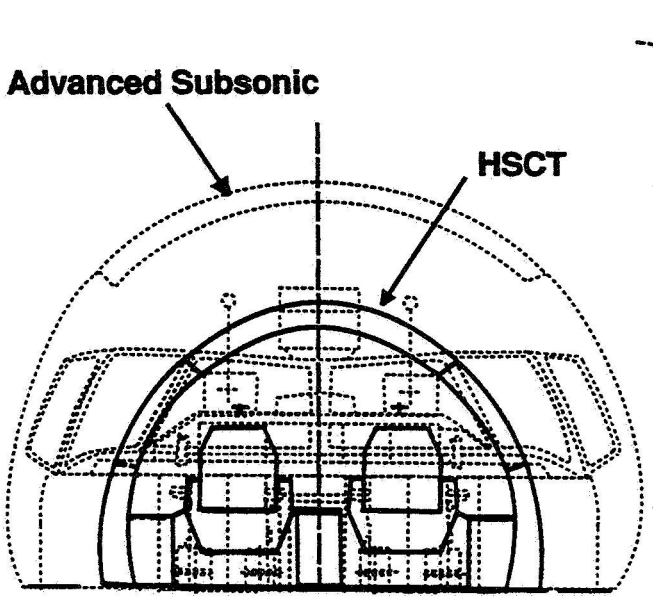

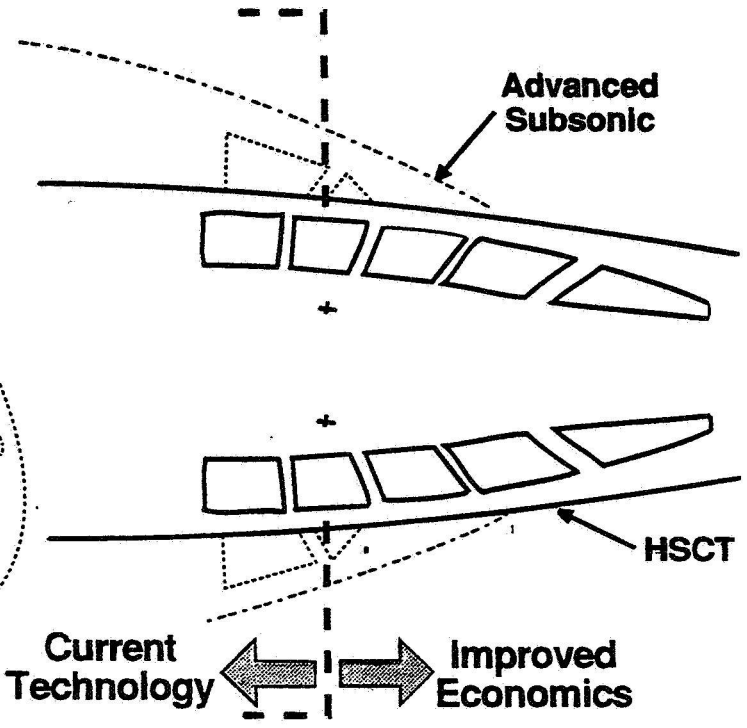

Flight Deck Volume/Shape

HSR-PHASE II

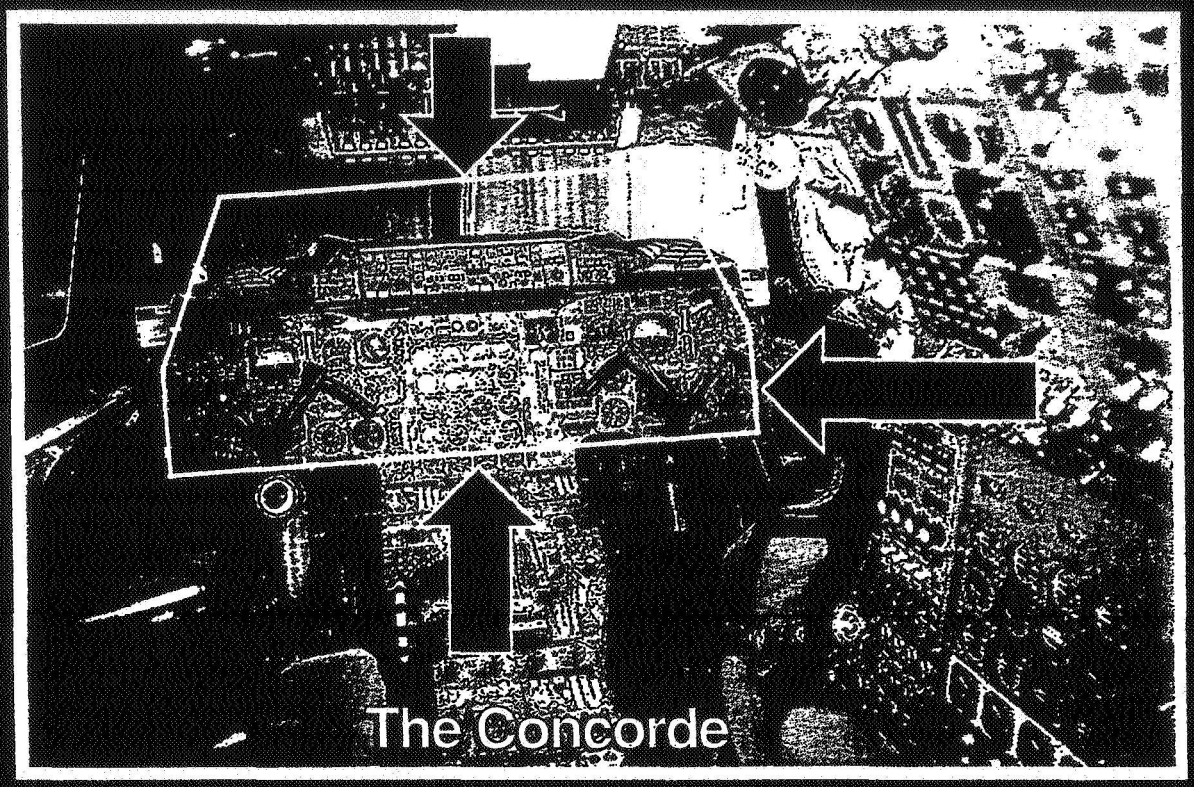

REDUCED FUEL RESERVES BENEFIT

ALL-SITE CAT IIIC OPERATIONAL CAPABILITY PROVIDED BY SYNTHETIC VISION

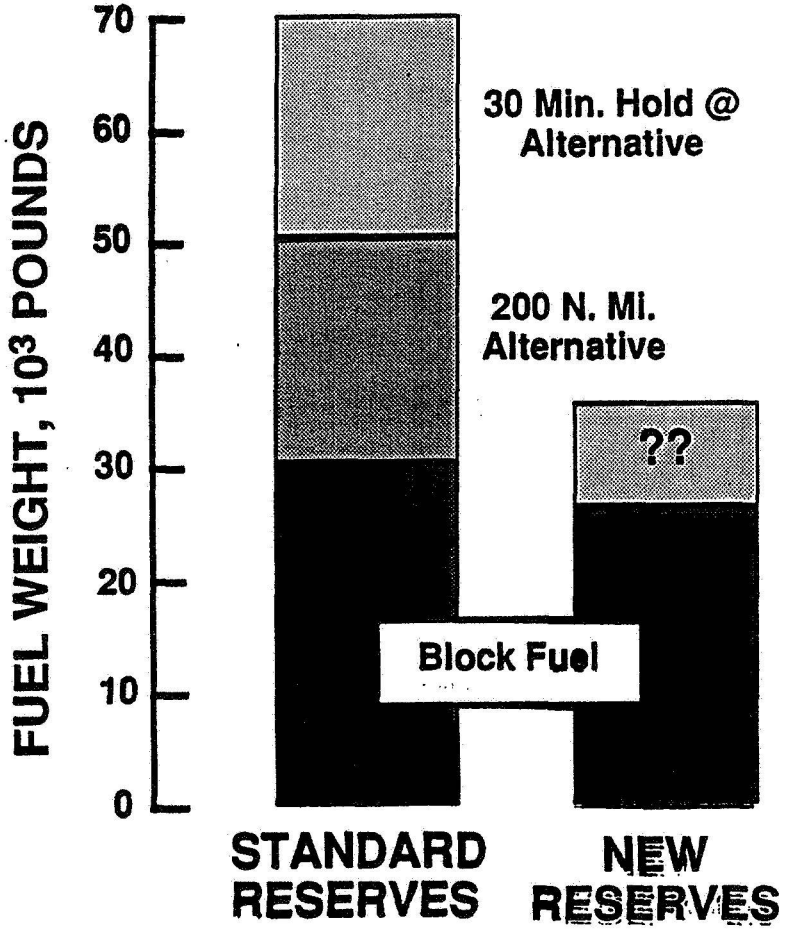

TOGW REDUCTION COULD EXCEED 15% !

SOURCE: Douglas Aircraft Co. Adv. Flt. Deck Configuration Study

Benefits of Integrated Flight Deck Systems

HSR-PHASE II =

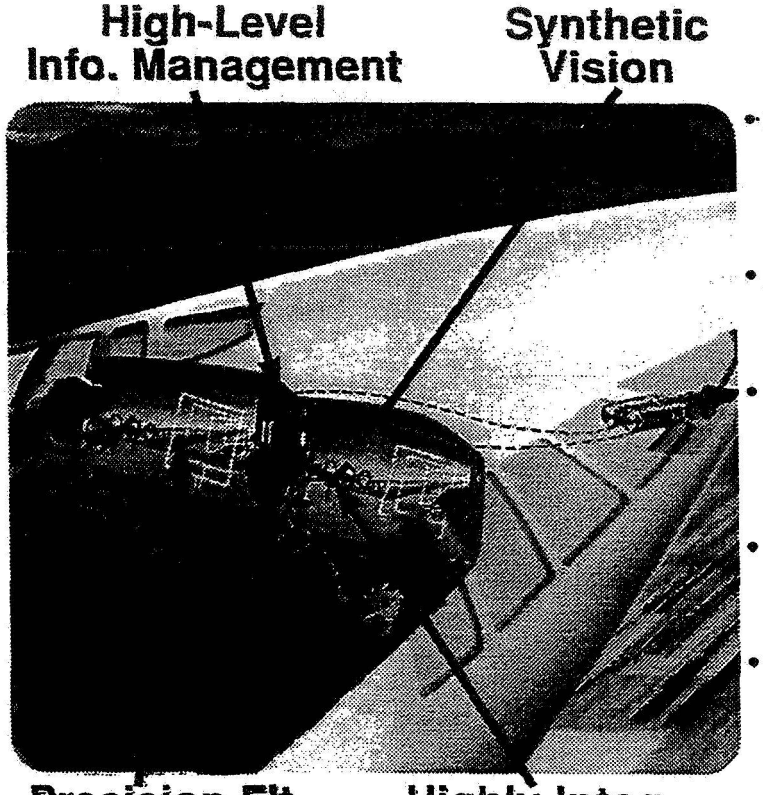

Payoffs

- *No Nose-Droop*
  (Saves 1,500 -2,000 Lbs.; 5,000 Lbs. In TOGW)
- *Additional Row of Seats*
  (2% Gain In Revenue)
- *All-Weather/All-Site Operations*
  (Schedule Reliability & Reduced Fuel Reserve)
- *Minimum Special ATC Handling*
  (No Throughput Impact)
- *Next-Generation Cockpit*
  (Technology Step-Change: Fewer Crew-Related Incidents)
- *Reduced Certification Time & Costs*

HSR-Phase II

FLIGHT DECK SYSTEMS

• Sim. Hdw. prov. by Industry

August 1993

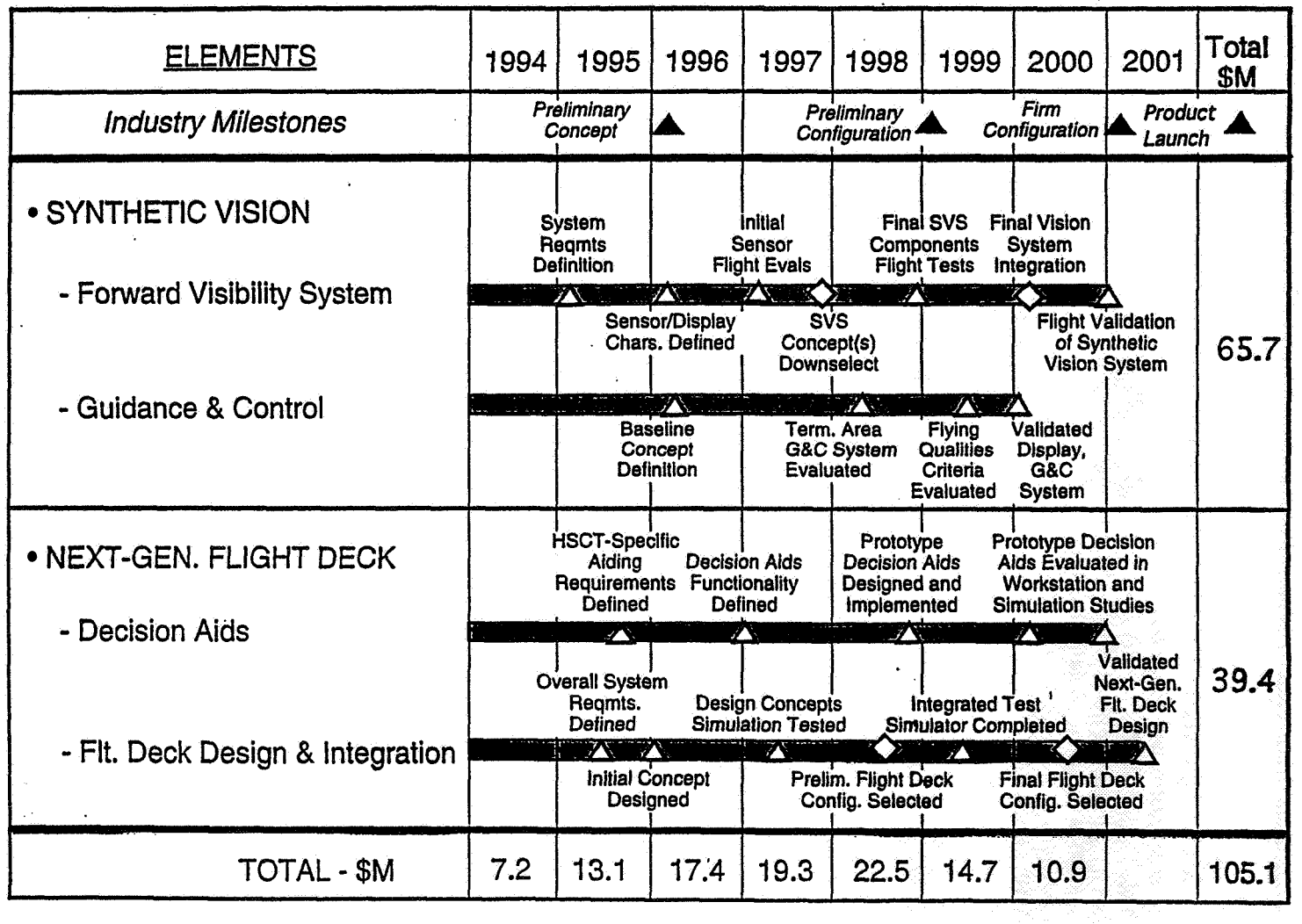

Terminal Area Productivity.

G. Steinmetz,
NASA Langley Research Center

[This presentation consisted of comments only;

no visuals are available for these Proceedings]

Session 6:

DEVELOPMENT AND APPLICATIONS OF SENSORS FOR AIRCRAFT WAKE VORTEX DETECTION AND AVOIDANCE.

Chair: R. Bowles,

NASA Langley Research Center.

Session 6:

DEVELOPMENT AND APPLICATIONS OF SENSORS FOR AIRCRAFT WAKE VORTEX DETECTION AND AVOIDANCE.

Chair: R. Bowles, NASA Langley Research Center.

Characteristics of Civil Aviation Atmos-pheric Hazards. R. Marshall and J. Montoya, Research Triangle Institute, and M. Richards and J. Galliano, Georgia Tech Research Institute

Ground-Based Wake Vortex Monitoring, Prediction, and ATC Interface. S. Campbell and J. Evans, Massachusetts Institute of Technology

Aircraft Wake RCS Measurement. W. Gilson, Massachusetts Institute of Technology

Wake Vortex Detection at Denver Stapleton Airport with a Pulsed 2-micron Coherent Lidar. S. Hannon and A. Thomson, Coherent Technologies, Inc.

Doppler Radar Detection of Vortex Hazard Indicators. J. Nespor, E. Hudson, and R. Stegall, Government Electronic Systems, Martin Marietta, and J. Freedman, MITRE Corp.

Remote Sensing of Turbulence in the Clear Atmosphere with 2-micron Lidars. R. Martinson, Lightwave Atmospherics, Inc., and J. Flint, Schwartz Electro-Optics, Inc.

Characteristics of Civil Aviation Atmospheric Hazards.

R. Marshall and J. Montoya,
Research Triangle Institute,
and
M. Richards and J. Galliano,
Georgia Tech Research Institute

ABS: next 2 pages

Characteristics of Civil Aviation Atmospheric Hazards

R. E. Marshall, M. A. Richards, J. A. Galliano, and J. Montoya

Abstract

Clear Air Turbulence, wake vortices, dry hail, and volcanic ash are hazards to civil aviation that have not been brought to the forefront of public attention by a catastrophic accident. However, these four hazards are responsible for major and minor injuries, emotional trauma, significant aircraft damage, and in route and terminal area inefficiency.

Most injuries occur during clear air turbulence. There is significant aircraft damage for any volcanic ash encounter. Rolls induced by wake vortices occur near the ground. Dry hail often appears as an area of weak echo on the weather radar.

ABS (cont'd)

This paper will present the meteorological, electromagnetic, and spatio-temporal characteristics of each hazard. A description of a typical aircraft encounter with each hazard will be given. Analysed microwave and millimeter wave sensor systems to detect each hazard will be presented.

Characteristics of Civil Aviation Atmospheric Hazards

R. E. Marshall, M. A. Richards, J. A. Galliano, and J. Montoya

Atmospheric Hazards

CAT as a Hazard to Aviation

- Major and minor injuries to passengers and cabin crew
- No deaths or crashes
- Unbelted passengers and flight attendants are especially vulnerable
- The service cart as well as hot liquids from it frequently injure flight attendants and passengers
- Flight crew safety harness bruises and flying manual injuries.
- Emotional trauma for crew and passengers
- Flights diverted to nearest airport for medical evaluation
- Pilots ignore ATC rerouting denials and search for calmer air

Atmospheric Hazards

CAT and the Atmosphere

- Air masses of different origins overlay one another near the jet stream at the tropopause.
- Layers formed may contain temperature inversions with strong vertical shear in the horizontal wind
- Layer characterized by the Richardson number. When Ri less than 0.25, turbulence is probable.
- Most frequently found along curved jet stream boundaries
- Thinning inversion layers (up to 10 deg K/km) appear to be good candidates for CAT.

Atmospheric Hazards

CAT Spatio-temporal Scales

- Cat layers may be 1 to 100 kilometers in the horizontal
- Cat layers may be 0.1 to 5 km in the vertical
- Turbulence may persist in a layer from 5 to 120 minutes

Atmospheric Hazards

RF Characteristics of CAT

- Bragg scattering from $\lambda/2$ turbulent eddys
- Radar reflectivity from -160 to -135 dB/m
- Scales of turbulence
  - Kolmogorov microscale
    - kinematic viscosity
    - eddy dissipation rate

At the surface
Severe: 0.4 cm » 37.5 GHz
Moderate: 0.6 cm » 25.0 GHz
Light: 0.8 cm » 18.8 GHz

At the tropopause
Severe: 1.0 cm » 15.0 GHz
Moderate: 1.7 cm » 8.8 GHz
Light: 2.2 cm » 6.8 GHz

Atmospheric Hazards

Hail as a Hazard to Aviation

- Majority of encounters are associated with takeoffs or landings
- Significant number of encounters involve a descrepancy between on board radar and ATC radar information
- *Safe areas* of lower reflectivity and brighter visibility often contain hail.
- Pitted and cracked radomes and windshields.
- Leading edge damage.
- Clogged pitot tubes.
- Turbulence

  +/- 400 to +/- 900 ft variations in altitude
  Minor and major injuries to mostly the flight attendants
  One death by heart attack

- No crashes

Atmospheric Hazards

Hail and the Atmosphere

- Hail is produced in convective clouds, normally cumulonimbus, with vertical velocities up to 20 m/sec.
- Mechanism for hail formation is controversial. Strong updrafts and prolonged balance between gravity and updraft velocity appear common to all theories.
- Most cloud charge generation theories involve solid precipitation such as hail.
- Hail may be embedded in any precipitation regime associated with cumulonimbus.

  Thrown out of top into clear air (*popcorn hail*)
  Dry falling hailshafts with surronding rain
  Rain and hail mixed
  Wet or spongy hail

- Hailstones range in size from 3 to 60 mm

* Hail Alley: Annual average of 8 days with hail. Common borders of Wyoming, Nebraska, and Colorado

Atmospheric Hazards

Hail Spatio-temporal Scales

- Hailshafts are between 0.1 and 2.0 km in diameter
- Hailshaft depths are from 1 to 5 km
- Hailshafts may persist from 5 to 30 minutes

Atmospheric Hazards

RF Characteristics of Hail

- X-band is at the Rayleigh - Mie transition
- Hail reflectivity is in excess of 40 dBZ
- Spherical hail produces 0 dB differential reflectivity
- Asymmetrical hail exists

  Asymmetry may increase with size
  Asymmetry for a given size may vary with location
  Orientation of falling asymmetrical hailstones is not well understood.

- For 1 cm hailstones, dry hail has approximately 7dB less reflectivity than for wet hailstones. The reflectivity of dry hailstones greater than 5 cm is greater than that of equal size wet hailstones

Atmospheric Hazards

Volcanic Ash as a Hazard to Aviation

- Encounters along vectors designed to avoid plumes
- Some or all engines flame out
- Clogged pitot tubes
- Clogged oil filters
- False cargo bay smoke alarms
- Pitted and cracked windshields
- Control surfaces pitted or permanently damaged
- St Elmo's fire around windows scares passengers
- One or all engines need replacement
- In rare cases the entire aircraft is condemned

Atmospheric Hazards

Volcanic Ash and the Atmosphere

- Explosive type volcanoes found along the Pacific *Ring of Fire*
- Ensembles of glass shards are blown up to 25 kilometers ASL
- 60 to 5 µm shards fall to earth 60 minutes after eruption
- 1 to 5 µm shards may exist in stratosphere up to 3 years
- Stratospheric ash clouds travel global distances
- 1 to 5 µm shards eventually fall into troposphere
- Tropospheric ash clouds persist less than 1 year
- Glass shards are often bathed in sulfuric acid 7 to 14 days after eruption

Atmospheric Hazards

Volcanic Ash Spatio-temporal Scales

- Horizontal scales may exist up to 100 km in the troposphere
- Horizontal scales may exist up to 1000 km in the stratosphere
- Ash cloud may exist up to 25 km ASL
- Normal atmospheric processes eventually produce layers of volcanic ash
- Volcanic ash may persist from months to years in the stratosphere
- Volcanic ash may persist from weeks to months in the troposphere

Atmospheric Hazards

RF Characteristics of Volcanic Ash

- Rayleigh scattering
- Radar reflectivity between -15 to 10 dBZ (measured at C-band)
- Asymmetrical ash particles
- Dielectric constant + 3.8

Atmospheric Hazards

Wake Vortex Aircraft Hazard

- Sudden and unexpected turbulent rolls up to 180 degrees.
- Most encounters occur on final approach or landing in clear air.
- Leading aircraft and parallel runway are sources.
- Winftip, landing gear, landing light, and propellar damage near ground.
- Short but frightening rolls at altitude hurl unrestrained passengers, cabin crew, and service carts.
- Minor injuries
- No deaths

Atmospheric Hazards

Wake Vortex and the Atmosphere

- Counter rotating vortices
  - Initially approximately 3/4 of a wingspan separation
  - 1 to 10 meter diameter core with strong laminar flow
  - Maximum core velocity on the order of 1/2 aircraft speed
  - Radial component of velocity orthogonal to tangential velocity
- Transport and decay highly dependent on atmospheric conditions
- Turbulent flow in the shear layer outside the core
- Turbulent flow in the shear layer outside the volume of air pushed down by the vortex pair (wake vortex system)
- At altitude, evidence indicates persistence of vortices 6 miles behind aircraft.

Atmospheric Hazards

Wake Vortex Spatio-temporal Scales

- Highly dependent on cross wind component and the stability of the atmosphere
- Core diameter between 0.01 and 0.1 wingspans
- Initial separation approximately 0.8 wingspans
- Out of ground effect the vortex lateral motion is primarily influenced by the cross wind.

  Calm to 1 knot: Vortices move away from one another at 2-4 knots
  3 to 5 knots: Upwind vortex may stall over runway
  Downwind vortex moves at 4 to 6 knots
  greater than 7 knots: vortices move with crosswind

- Initial descent rate is proportional to weight of aircraft and inversely proportional to the square of the wingspan. P3 ≈ 5 ft/sec.

- Characteristic decay time (Brunt-Vaisala)
  200 sec for near adiabatic
  55 sec for isothermal
  45 sec for a weak inversion
  19 sec for a strong inversion

Atmospheric Hazards

RF Characteristics of the Wake Vortex

- Reflectivity measurements between -120 and -140 dB/m
- Reflectivity measured in both the radial and transverse directions
- Scales of turbulence

  C-band measurements indicate non dissipating scales of 2.5 cm
  X-band scales of turbulence (1.5 cm) theoretically possible
  Ka-band scales of turbulence (0.5 cm) marginal in boundary layer

- Suggestions that there is a cold core in the vortex.

Atmospheric Hazards

Fog as a Hazard to Aviation

- Low or zero visibility landings and takeoffs
- Low or zero visibility taxiing

Atmospheric Hazards

Fog and the Atmosphere

- Cloud at the earth's surface
  - suspended 1 to 50µm diameter spherical water drops
  - 20 to 500 drops per cubic centimeter
  - 0.01 to 0.1µm diameter condensation nuclei in drops
  - LWC up to 0.4 grams per cubic meter in advection fog
  - LWC up to 1.0 grams per cubic meter in radiation fog

- 5 classifications based on the way fog forms
  - Radiation: Terrestrial radiation at night cools surface
  - Advection: Warmer moist air flows over cooler land or water
  - Upslope: Air flows up a slope and cools adiabatically
  - Precipitation: Cool air below a cloud evaporates falling raindrops increasing the dew point of the cool air
  - Steam: Cold air flows over warm water

- Annual average dense fog occurrence greater than 45 days
  - Coasts of WA, OR, CA, SE TX, ME, NH, MA, RI, CT, & Long Island. Mountains of VA, WV, TN & NC. N central FL.

Atmospheric Hazards

Spatio-temporal Scales

- Radiation Fog: Up to 10 m deep in calm air. Up to 100m deep with 3m/sec wind. Fog does not form when wind is above 3m/sec. Usually burns off by noon over flat terrain. May take longer in the mountains.
- Advection Fog: Depth increases with wind up to 7m/sec. After 7m/sec a stratus layer develops with possible drizzle. Larger horizontal extent and more persistent than Radiation Fog.
- Upslope Fog: Can be dense along mountain ridges.
- Precipitation: Dense with large horizontal extent. Fog at airports with rainy conditions.

Steam: Winter fog in unstable air. Fog is broken by downdrafts.

Atmospheric Hazards

RF Characteristics of Fog

- Rayleigh Scattering up to 500 GHz.
- Radar Reflectivity up to -14dBZ
- Attenuation Coefficients

  0.1 dB per km per gram of liquid water per cubic meter @ 10 GHz
  1.0 dB per km per gram of liquid water per cubic meter @ 35 GHz
  2.0 dB per km per gram of liquid water per cubic meter @ 50 GHz
  5.0 dB per km per gram of liquid water per cubic meter @ 95 GHz

- Visibility

  Light: less than 1000m visibility
  Moderate: less than 800m visibility
  Thick: less than 500m visibility
  Dense: less than 300m visibility

Ground-Based Wake Vortex Monitoring, Prediction, and ATC Interface.

S. Campbell and J. Evans,

Massachusetts Institute of Technology

Abs: next page

5th (and Final) Combined Manufacturers' and Technologists' Airborne Wind Shear Review Meeting
September 28–30, 1993
Hampton, Virginia

"GROUND–BASED WAKE VORTEX MONITORING, PREDICTION AND ATC INTERFACE"*

Steven D. Campbell and James E. Evans

Lincoln Laboratory
Massachusetts Institute of Technology
Lexington, Massachusetts
Telephone: 617/981–3386, E–mail: sdc@ll.mit.edu

This talk will discuss three elements of a proposed Wake Vortex Advisory Service: monitoring, prediction and ATC interface. The monitoring element is needed to ensure safety by warning controllers of hazardous wake vortex conditions. Such conditions exist when wake vortices persist in the approach/departure flight paths due to advection or to atmospheric conditions which prevent their decay. The prediction element is needed to provide ATC supervisors with advance warning that wake vortex separation conditions are about to change (i.e., require increased or decreased wake vortex separation). The ATC interface element is needed to provide controllers with adaptive wake vortex separations. The use of these adaptive wake vortex separations would lead to increased airport capacity under most conditions, while maintaining safety under conditions of wake vortex hazard.

A data gathering program is proposed to begin in the summer of 1994 at a major airport. A 10.6 μm CO_2 CW lidar system will be developed for characterizing the behavior of wake vortices in an operational airport setting. Wide–area weather data will be gathered by an Integrated Terminal Weather System (ITWS) testbed. Interface to the terminal ATC system will be accomplished using the TATCA (Terminal Air Traffic Control Automation) Interface Unit (TIU), which would allow wake vortex separation symbology to be inserted onto a TRACON controller's Full Digital ARTS Display System (FDADS) radar screen.

The proposed program would take advantage of the synergy between the Wake Vortex, ITWS and TATCA programs in achieving an integrated Wake Vortex Advisory System. An interim product of the program would be a characterization of the wake vortex separation requirements for different classes of aircraft in an operational setting. The ultimate aim of the program would be to achieve fielding of the proposed system.

* The work described here was sponsored by the Federal Aviation Administration under Air Force Contract No.F19628–90–C–002. The United States Government assumes no liability for its content or use thereof.

References:

1. Evans, J.E. and J.D. Welch: "Role of FAA/NWS Terminal Weather Sensors and Terminal Air Traffic Automation in Providing a Vortex Advisory Service", FAA International Wake Vortex Symposium, Washington, D.C., October 29–31, 1991.

2. Heinrichs, R.M., J.E. Evans and C.A. Primmerman: "Laser Systems for Characterization and Monitoring of Wake Vortices", FAA International Wake Vortex Symposium, Washington, D.C., October 29–31, 1991.

GROUND–BASED WAKE VORTEX MONITORING, PREDICTION AND ATC INTERFACE

STEVEN D. CAMPBELL

LINCOLN LABORATORY
MASSACHUSETTS INSTITUTE OF TECHNOLOGY

617/981–3386 (Phone)
617/981–0632 (FAX)
sdc@ll.mit.edu

OUTLINE

- MOTIVATION
  - INCREASE CAPACITY USING ADAPTIVE WAKE VORTEX SEPARATIONS
- APPROACH
  - SAFETY – MONITOR FOR UNSAFE CONDITIONS
  - PLANNING – PREDICT ADVECTION & DECAY
  - ATC INTERFACE – MINIMIZE CONTROLLER WORKLOAD
- PROGRAMS
  - WAKE VORTEX – NASA/FAA
  - INTEGRATED TERMINAL WEATHER SYSTEM (ITWS) – FAA
  - TERMINAL ATC AUTOMATION (TATCA) – NASA/FAA
- RESEARCH ORGANIZATIONS
  - NASA LANGLEY – WAKE VORTEX
  - VOLPE CENTER – WAKE VORTEX
  - NASA AMES – TATCA
  - LINCOLN – ITWS, TATCA, WAKE VORTEX (NASA LANGLEY)

WAKE VORTEX SEPARATIONS (nm)

LEADING AIRCRAFT

FOLLOWING AIRCRAFT	SMALL	LARGE	HEAVY	WEIGHT (lbs)
SMALL	3	4	6	<12,500
LARGE	3	3	5	12,500–300,000
HEAVY	3	3	4	>300,000

- CONSERVATIVE SEPARATIONS
- LIMITED CATEGORIES, INTEGER SPACINGS
- NON–ADAPTIVE

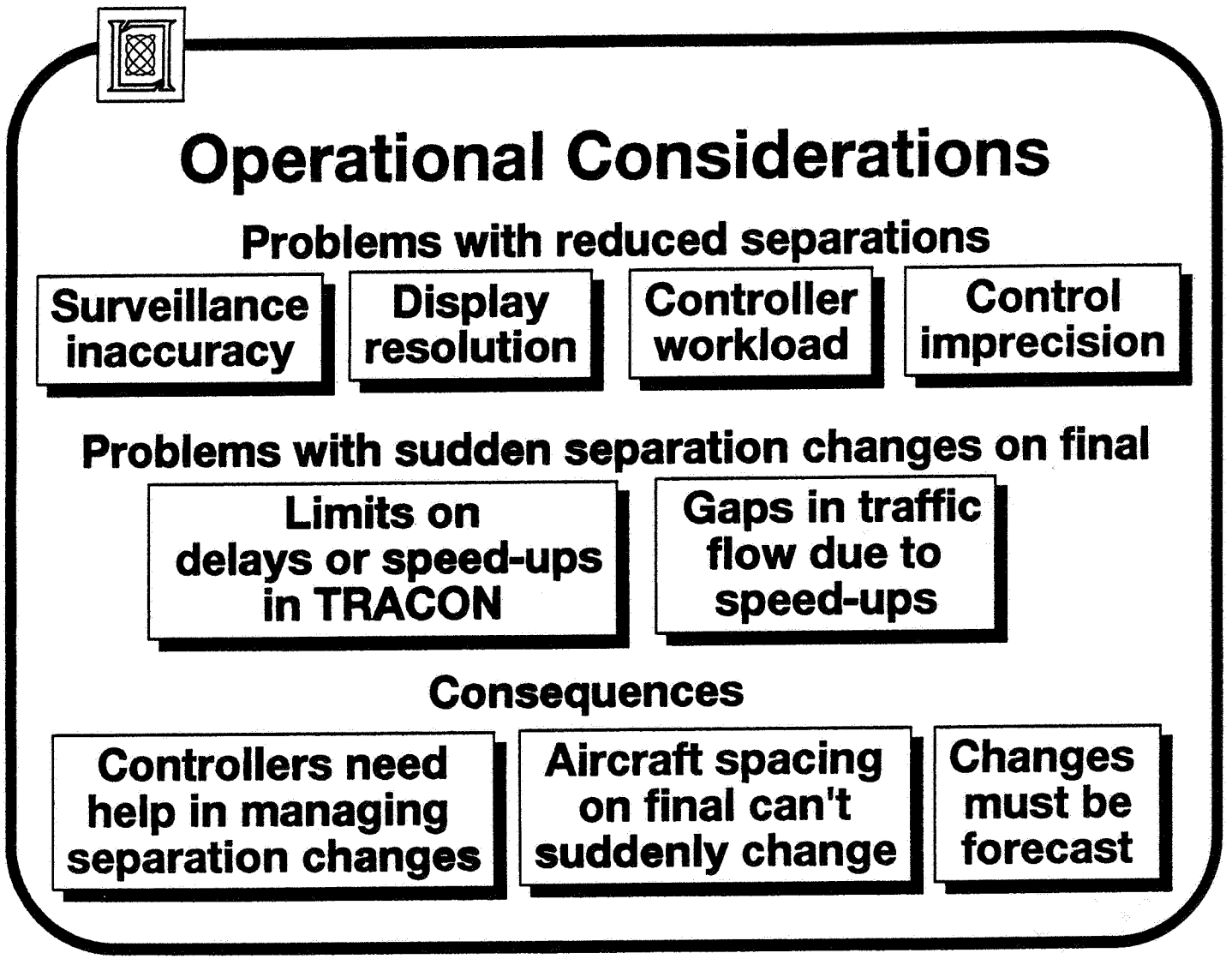
Operational Considerations
Problems with reduced separations
Surveillance inaccuracy
Display resolution
Controller workload
Control imprecision
Problems with sudden separation changes on final
Limits on delays or speed-ups in TRACON
Gaps in traffic flow due to speed-ups
Consequences
Controllers need help in managing separation changes
Aircraft spacing on final can't suddenly change
Changes must be forecast

Wake Vortex Advisory Service

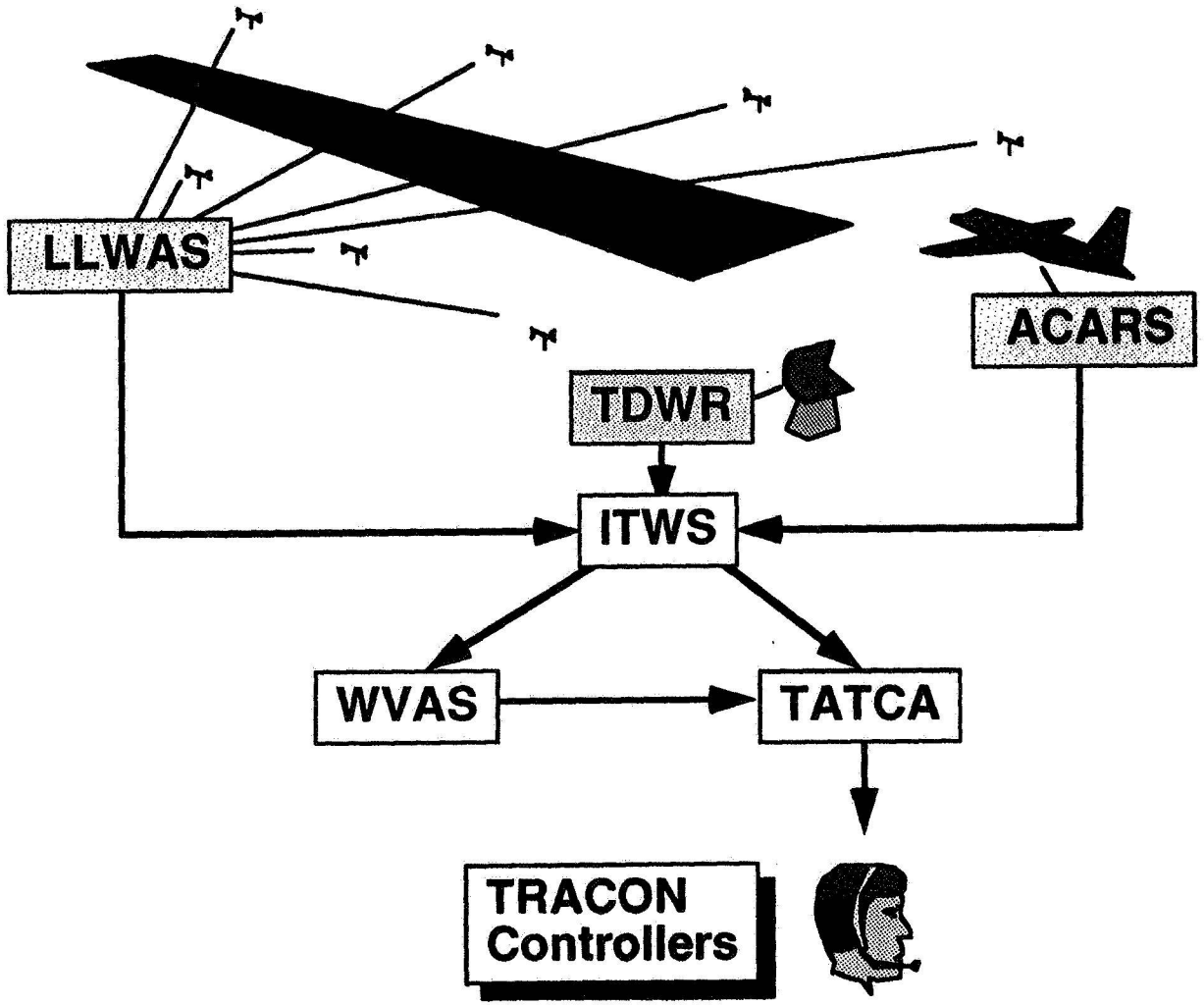

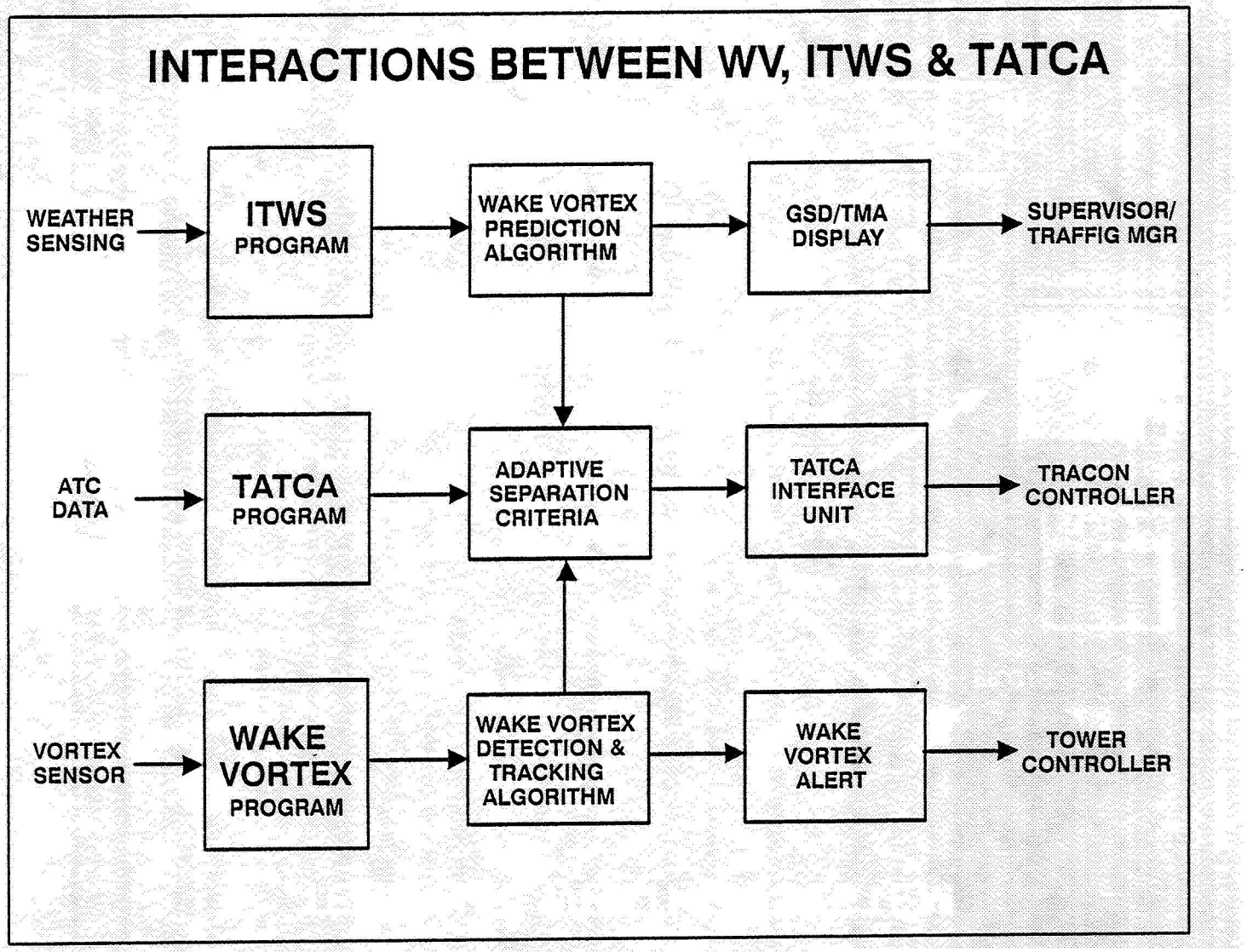
INTERACTIONS BETWEEN WV, ITWS & TATCA
WEATHER SENSING
ITWS PROGRAM
WAKE VORTEX PREDICTION ALGORITHM
GSD/TMA DISPLAY
SUPERVISOR/ TRAFFIG MGR
ATC DATA
TATCA PROGRAM
ADAPTIVE SEPARATION CRITERIA
TATCA INTERFACE UNIT
TRACON CONTROLLER
VORTEX SENSOR
WAKE VORTEX PROGRAM
WAKE VORTEX DETECTION & TRACKING ALGORITHM
WAKE VORTEX ALERT
TOWER CONTROLLER

TERMINAL WEATHER SYSTEM
PILOTS
CONTROLLERS
SUPERVISORS
WIND SHEAR
HAZARDOUS CELLS
WINDS
TORNADO
WAKE VORTEX
CEILING/VISIBILITY
TDWR/NEXRAD
ITWS PROCESSOR
TATCA
ASR-9
LLWAS
LIGHTNING
AIRCRAFT

ITWS RUNWAY WINDS

PRODUCT OVERVIEW

OPERATIONAL CONCEPT

Point Forecast: centerfield LLWAS

Path Forecast: runways and glide paths

Rapid (1–min) updates to 1– to 20–min forecasts

ANTICIPATED USES

Wake vortex advisories

Runway configuration management

SCHEDULE

Test in 1994 and 1995, DEMVAL in 1996

ITWS RUNWAY WINDS

PRODUCT OVERVIEW (CONT.)

INPUT DATA

- LLWAS observations
- Radar observations (TDWR + NEXRAD if avail.)
- ITWS Gridded Winds product

TECHNICAL APPROACH

- Space–time autocorrelation
- Simple physics (e.g., advection)
- Kalman Filter framework

T-LAPS WIND FIELD – 3530 feet AGL at the Airport Reference Point
T-LAPS GSD Playback
Overlay Options
Runways
Range Rings
Sensors
Landmarks
Geography
Observations...
Wind Vectors
Radar Options
Radar
TDWR
Background
Reflectivity
Layer
Surface only
Altitude
3200 ft AGL
Wind Scale
10 kts
Zoom:
2 km grid
Playback Options
Play
Rewind
Stop
Speed (frames per hour):
240
Source...
Time...
Load...
Site: Orlando
Date: 08/20/02
Time: 23:05:00
Messages
Displaying radar background
for 482 feet AGL
Hard Copy...

COLUMN MODEL PRODUCTS FOR WVAS

- COLUMN MODEL PROVIDES WVAS METEOROLOGICAL PRODUCTS
  - TEMPERATURE PROFILE
  - TURBULENT KINETIC ENERGY
- FINE VERTICAL RESOLUTION AND SHORT–TERM FORECAST (15 – 30 MINUTES)
- UNDER DEVELOPMENT FOR ITWS CEILING AND VISIBILITY
- CAN BE USED FOR OFF–LINE ANALYSIS OF MEMPHIS WVAS DATA
- PROFILER / RASS CAN BE USED FOR COMPARATIVE ANALYSIS AND COLUMN MODEL VALIDATION

Elements of TATCA

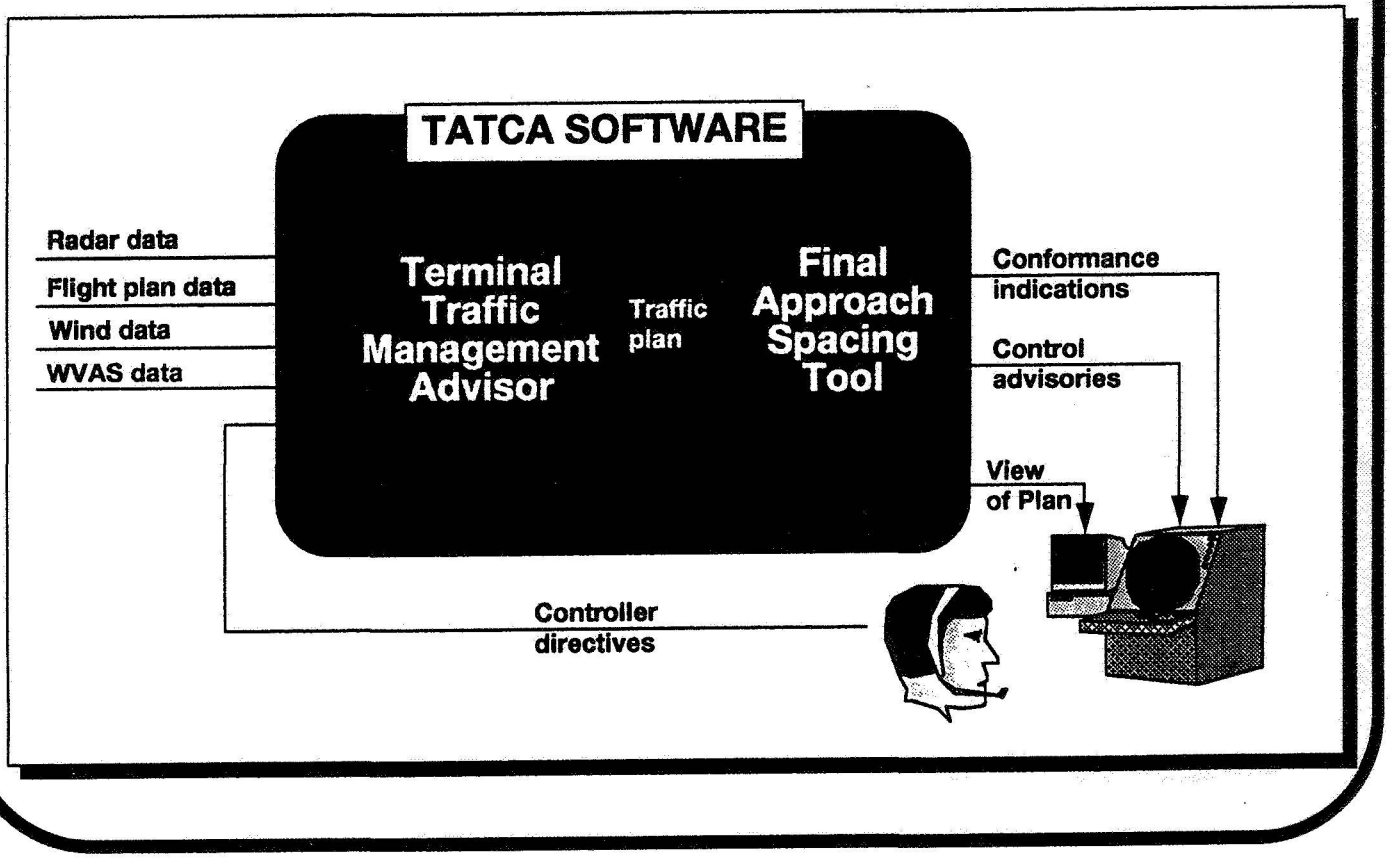

Interfacing FAST to Existing (ARTS) Radar Processing System

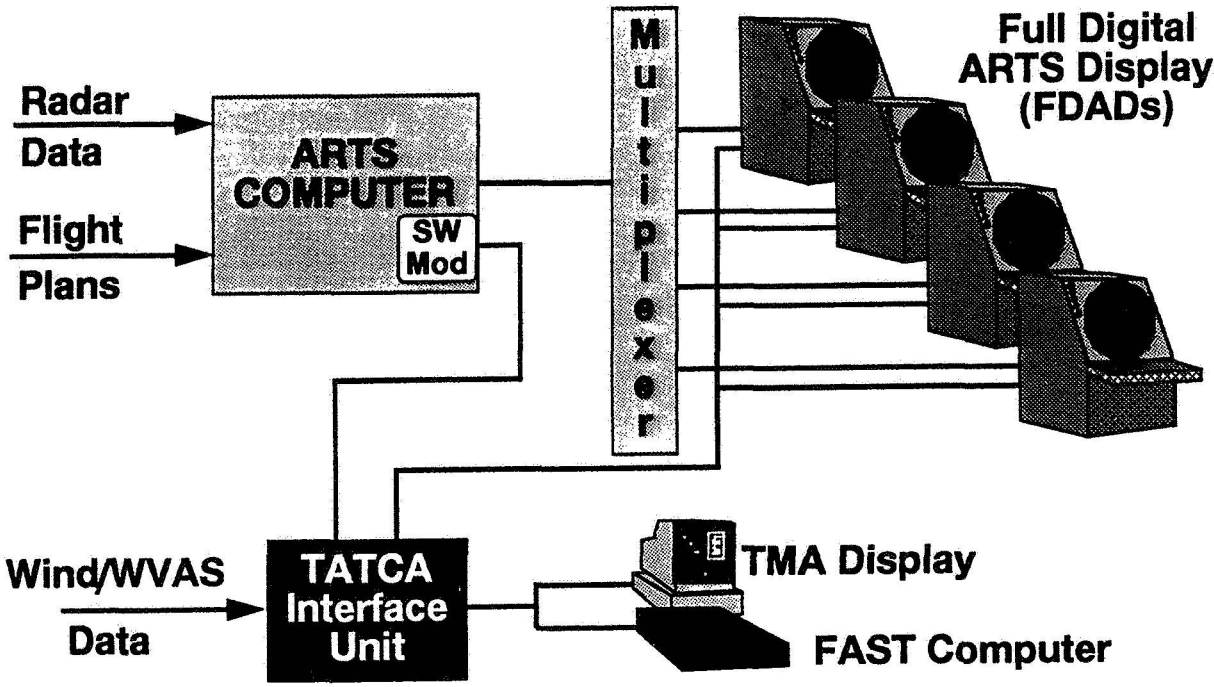

WAKE VORTEX MONITOR

- POTENTIAL SENSORS
  - ANEMOMETER ("SAFETY ELLIPSE")
  - LIDAR
    - PULSED
    - CW
  - MMW
  - ACOUSTIC

- POTENTIAL DEPLOYMENT STRATEGIES
  - HIGH–TRAFFIC AIRPORT: LIDAR
  - MODERATE–TRAFFIC AIRPORT: ANEMOMETER
  - DECISION BASED ON COST/BENEFIT TRADEOFF STUDIES

Table 1. Summary of major influences on wake vortex behavior (LDWR = Laser Doppler Weather Radar)

Wake vortex factor	How measured	Effect
Aircraft Parameters		Initial vortex attributes
Type (wingspan, C_D, vortex characteristics)	Beacon, aircraft data	Initial strength, separation, core turbulence
Weight		Initial strength
Speed	Beacon	Initial strength
Position	Beacon	Initial position
Flaps and landing gear		Core turbulence
Stratification (Lapse rate)	Temperature and humidity sensors	Decreased sink rate Increased decay rate
Turbulence	LDWR and anemometers for $\epsilon^{1/3}$ and Λ	Decreased sink rate Increased decay rate
Vertical Wind Shear	LDWR and anemometers	Solitary long-lived vortex
Ground effect	LDWR for vortex altitude	Rebound Travel along ground Increased decay rate
Advective winds	LDWR and anemometers	Travel along ground

FIELD MEASUREMENTS

- WAKE VORTEX BEHAVIOR
  - CW LIDAR
  - AUTOMATIC DETECTION & TRACKING ALGORITHM
- ATMOSPHERIC DATA
  - ITWS
    - WINDS (TLAPS, ANEMOMETER)
    - SOUNDING (MDCRS, SURFACE TEMP.)
  - LIDAR
    - BOUNDARY LAYER WINDS PROFILE
    - TURBULENCE PROFILE
  - TEMPERATURE PROFILE
    - TOWER OR RAS
- AIRCRAFT DATA
  - ATC
    - AIRCRAFT TYPE, POSITION, ALTITUDE, SPEED
  - ESTIMATE AIRCRAFT WEIGHT & CONFIGURATION

WAKE VORTEX LIDAR CONFIGURATION

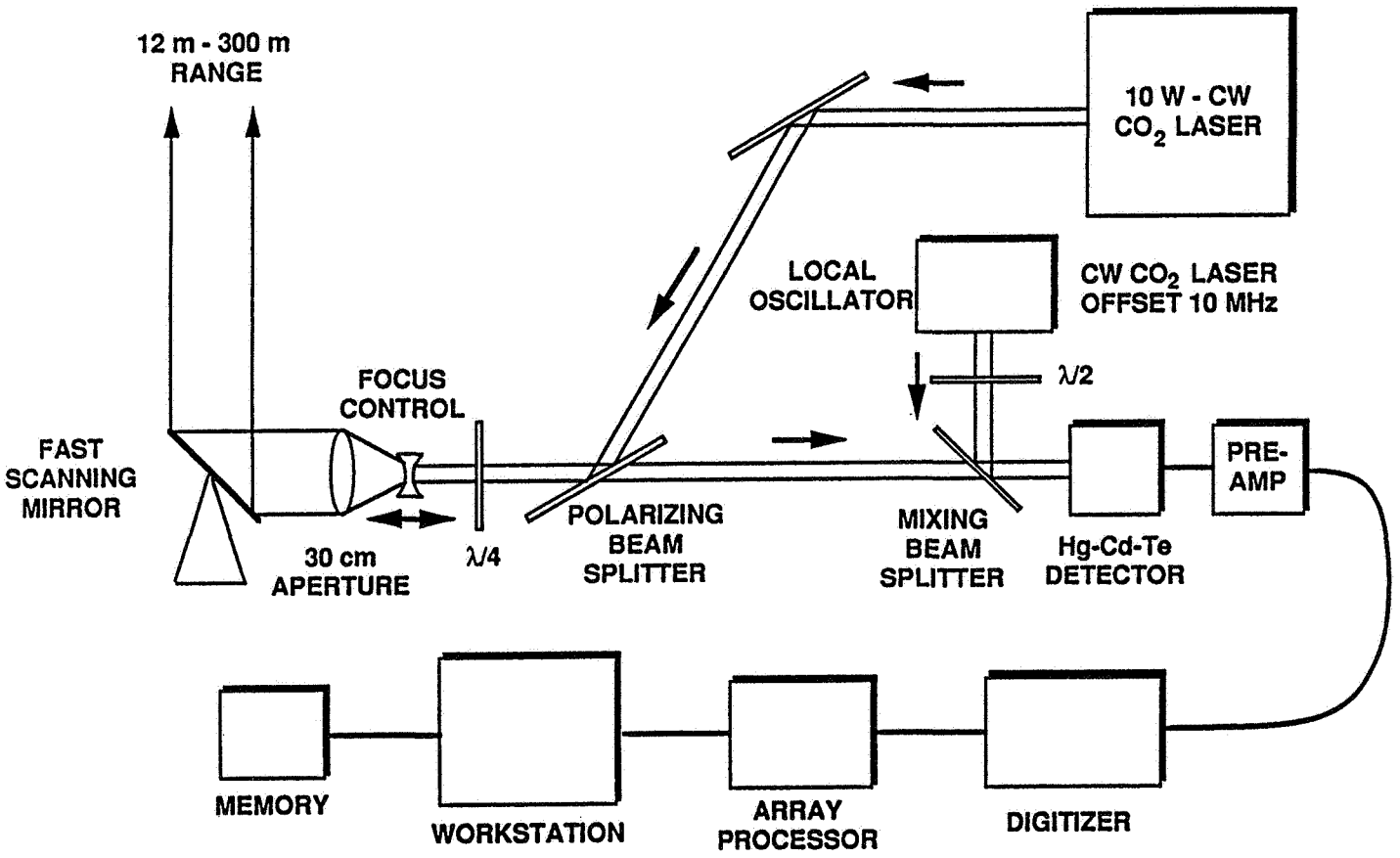

WAKE VORTEX LIDAR CONFIGURATION

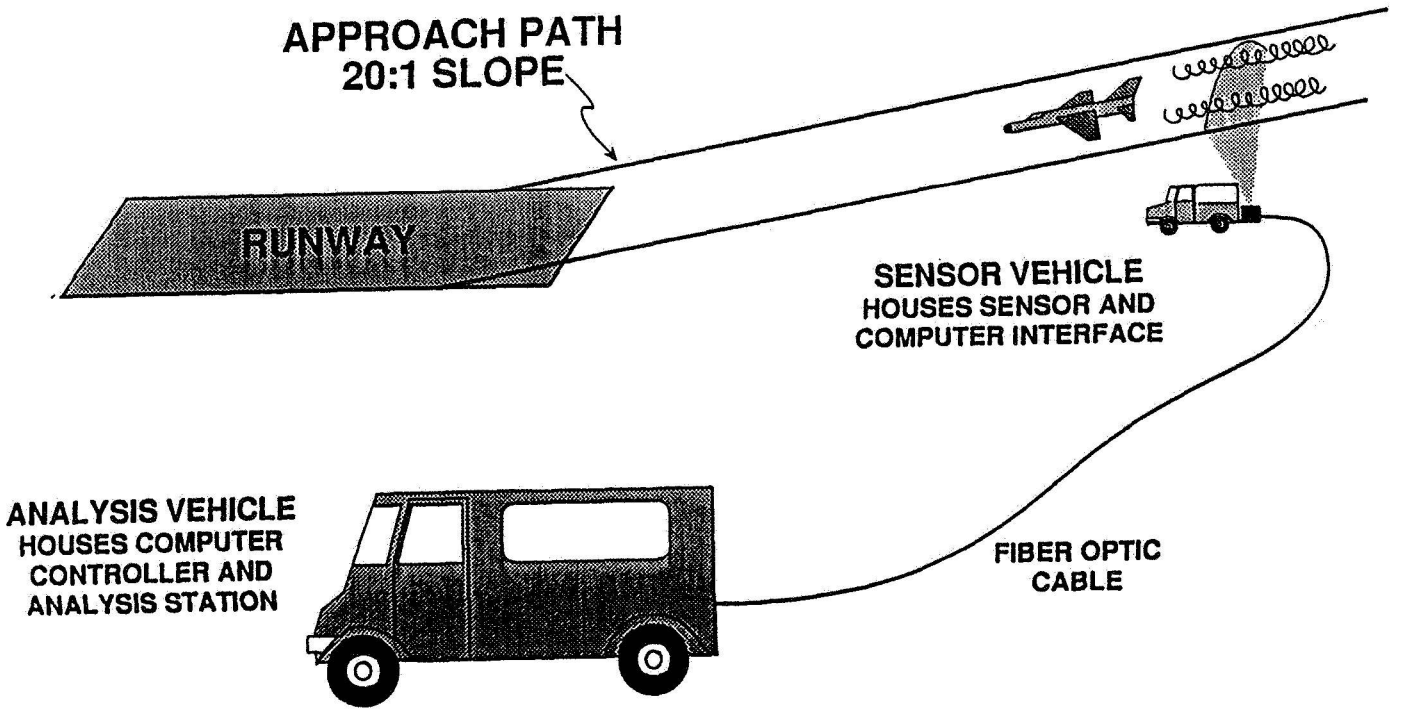

WAKE VORTEX SENSOR INTEGRATION

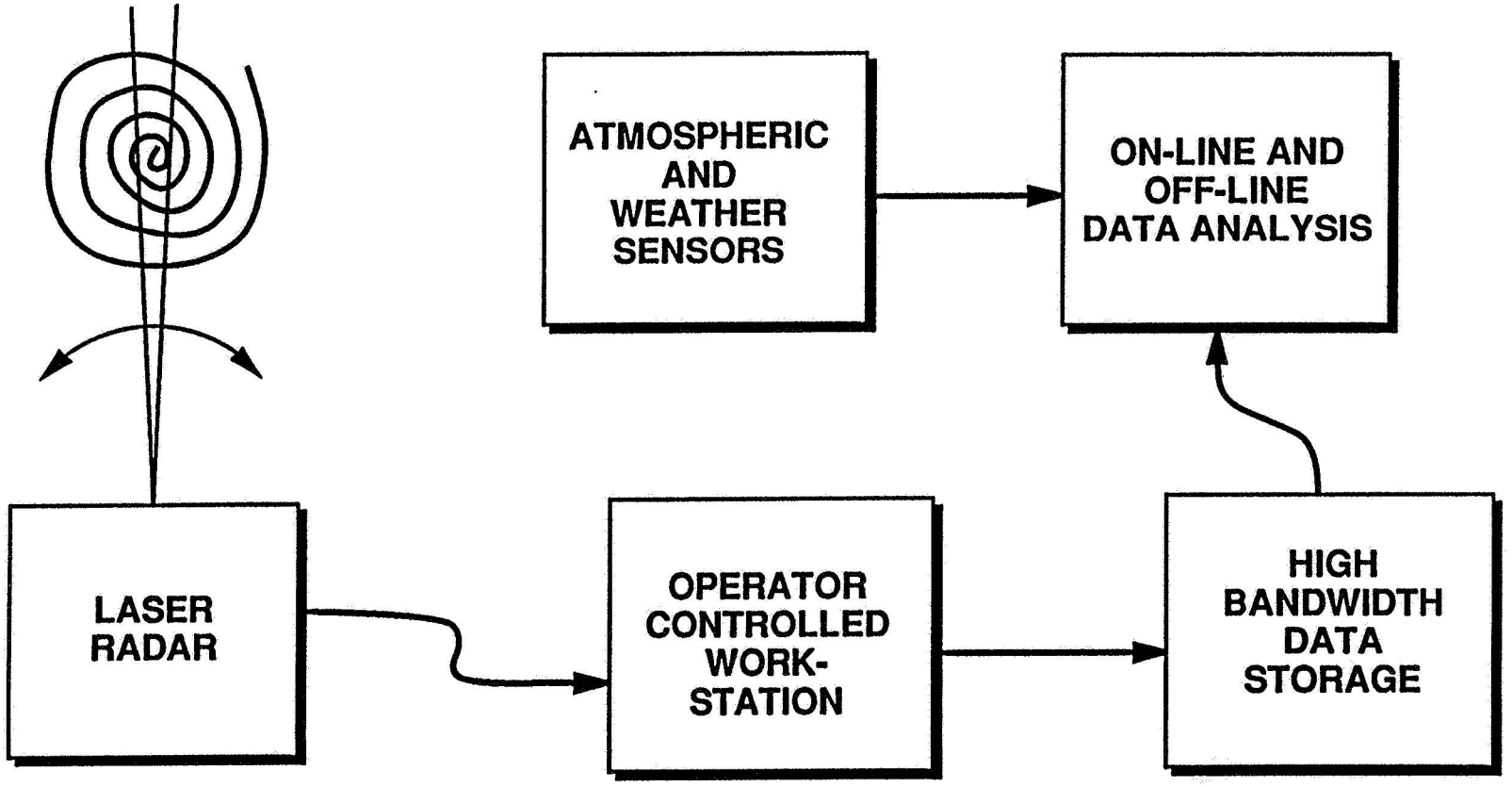

BACKSCATTER RETURN AND LASER POWER REQUIRED FOR VARIOUS ATMOS. PARAMETERS AT 10.6 μm

D = 30 cm, R = 200 m

ATMOSPHERIC MODEL	κ (Km^{-1})	$\beta\pi$ ($Km^{-1}Sr^{-1}$) ($x10^{-5}$)	P_{REC}/P_L ($x10^{-13}$)	P_L (Watts)
25 mm/hr RAIN	2.85	4.15	1.05	2.14
HAZE (98% RH)	0.61	4.15	2.58	0.87
MODERATE FOG 500 m VISIBILITY	1.96	62.9	22.8	0.1

- WAKE VORTEX LIDAR WITH 10-W LASER CAN OPERATE IN ALL THESE CONDITIONS

DOWNRANGE RESOLUTION VERSUS RANGE

D = 30 cm, λ = 10.6 μm

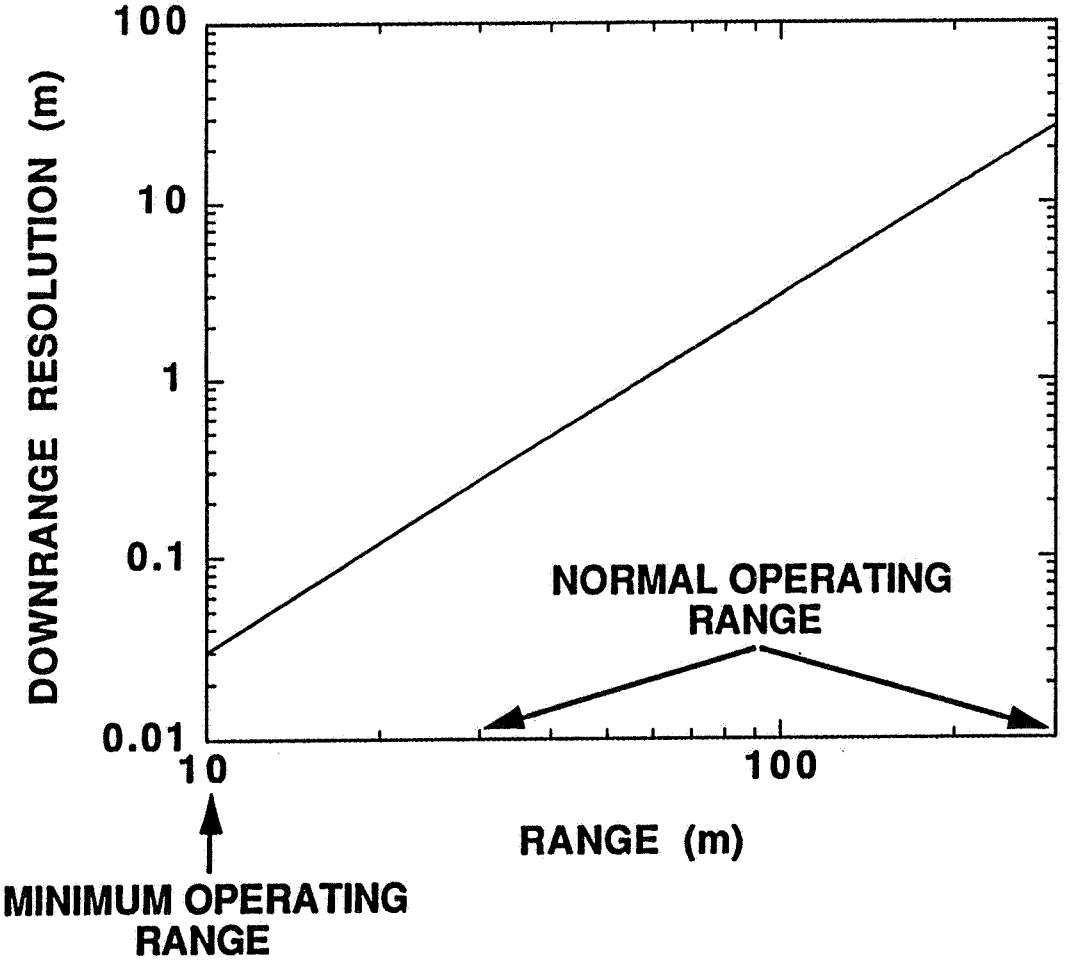

$$\Delta R = \frac{8}{\pi}\lambda\frac{R^2}{D^2}$$

VORTEX ACQUISITION AND TRACKING

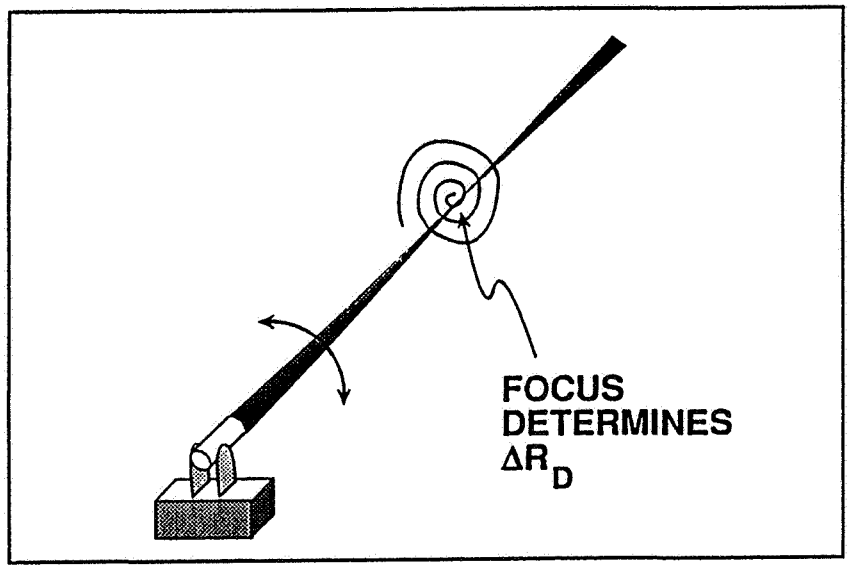

- SYSTEM FIRST PERFORMS WIDE AREA SCAN TO DETERMINE LOCATION OF VORTEX
  - USE SIGNATURE RECOGNITION ALGORITHMS DEVELOPED FOR ITWS
- ONCE VORTEX IS ACQUIRED, SYSTEM PERFORMS HIGH - RESOLUTION SCANS NEAR CORE TO ACCURATELY DETERMINE CIRCULATION VERSUS TIME

VORTEX PARAMETERS TO MEASURE

VORTEX DECAY TIME

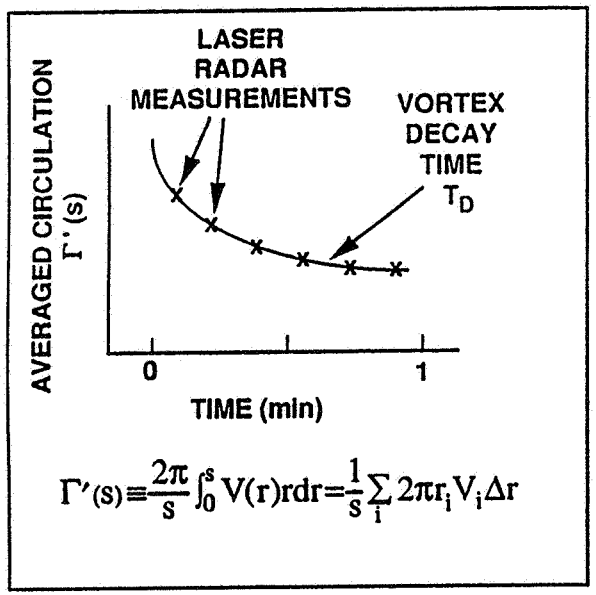

$$\Gamma'(s) \equiv \frac{2\pi}{s}\int_0^s V(r)rdr = \frac{1}{s}\sum_i 2\pi r_i V_i \Delta r$$

- VORTEX DECAY DUE TO TURBULENCE AND WIND SHEAR
- Γ'(s) ~ ROLL MOMENT ON WING SPAN 2s

VORTEX CLEARING TIME

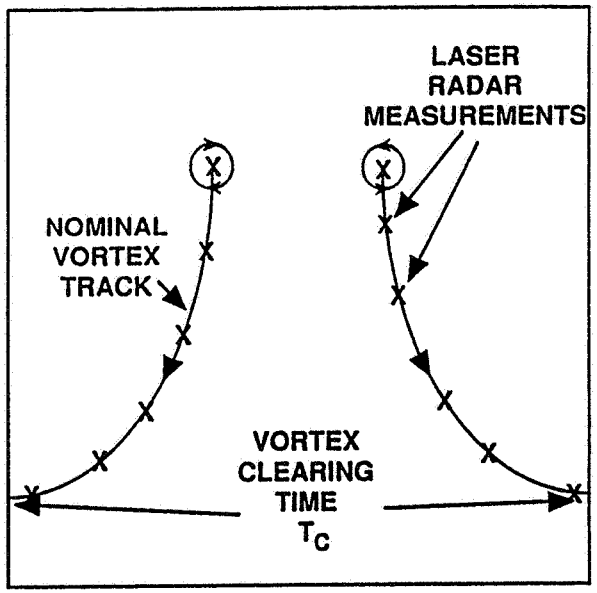

- VORTEX CLEARING TIME MODIFIED BY AMBIENT WINDS

- HAZARD OCCURS FOR PERSISTENT AND STATIONARY VORTICES

WAKE VORTEX SIGNATURE VERSUS LIDAR FOCUS

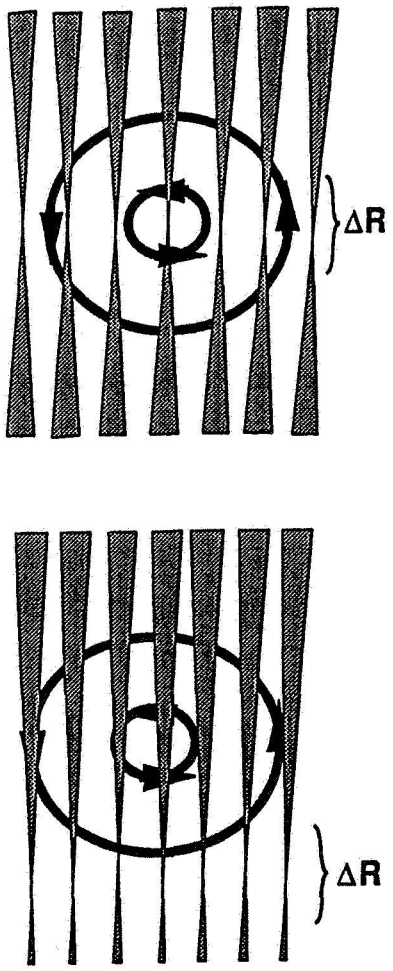

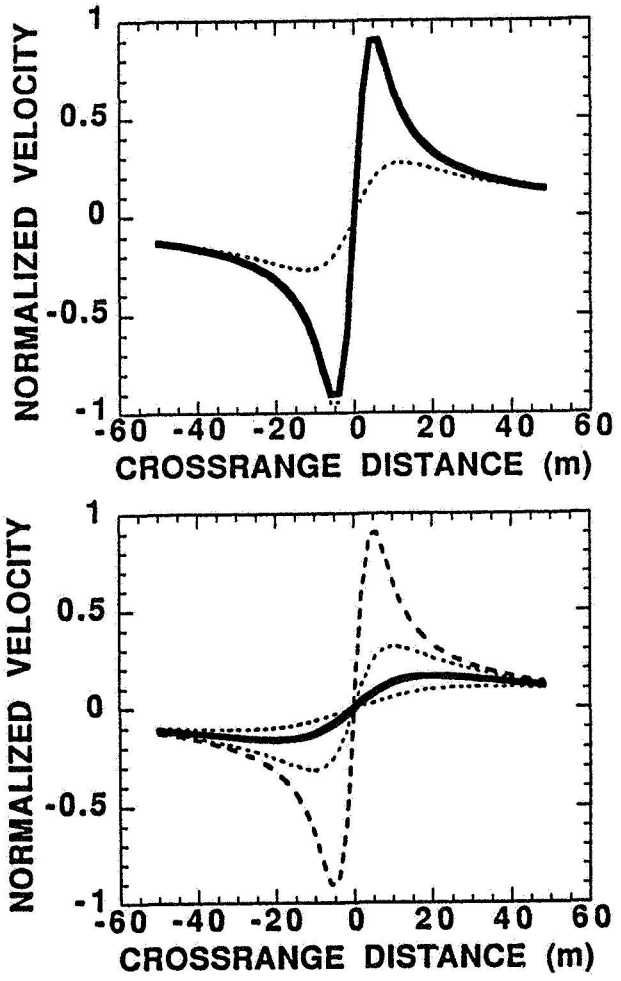

R_{VORTEX} = 200m

R_{FOCUS} = 200m

ΔR = 12m

——— PEAK OF SPECTRUM

------- EXTENT OF SPECTRUM

— — VELOCITY THROUGH CORE REGION

R_{VORTEX} = 200m

R_{FOCUS} = 180m

ΔR = 12m

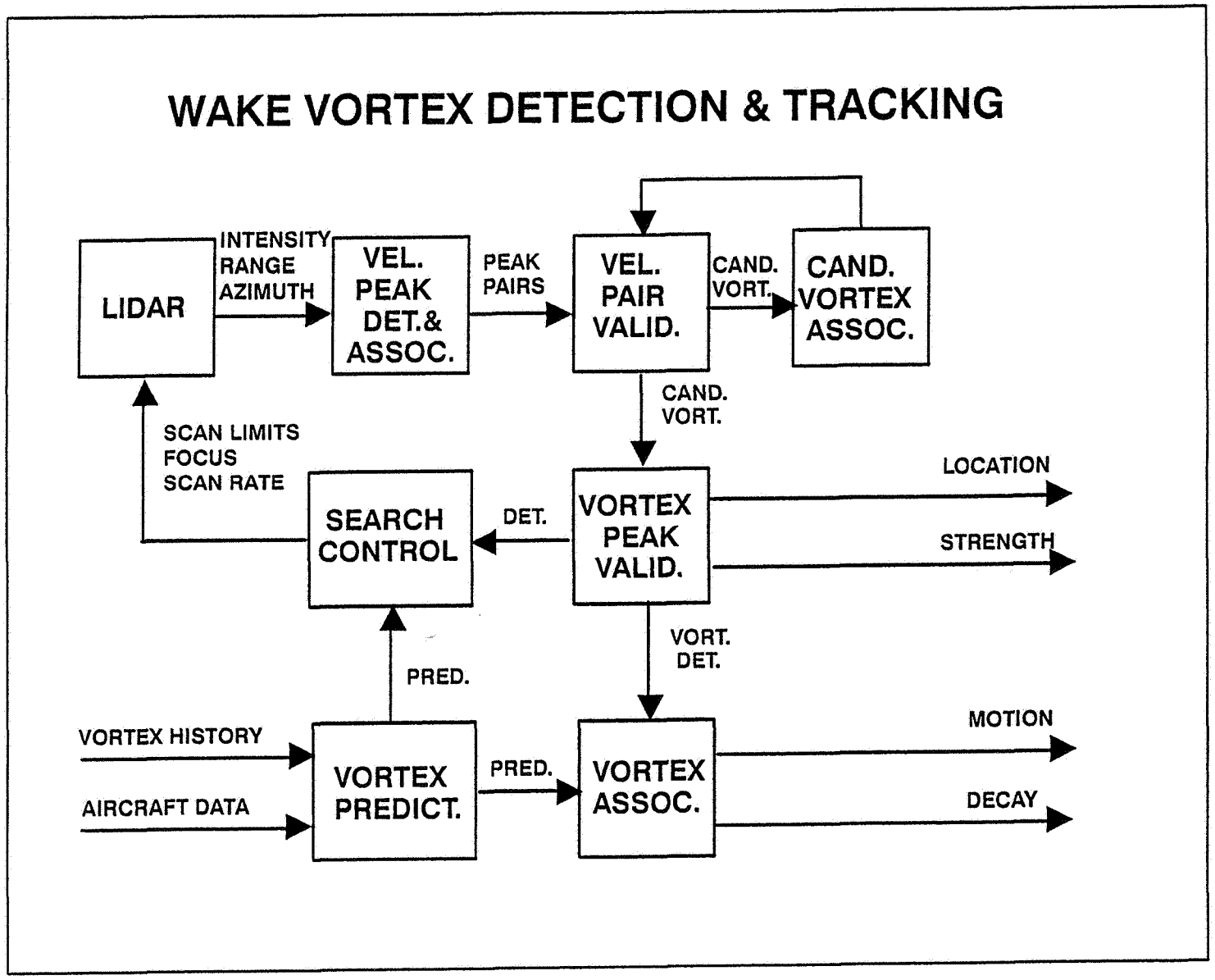
WAKE VORTEX DETECTION & TRACKING
LIDAR
INTENSITY
RANGE
AZIMUTH
VEL.
PEAK
DET.&
ASSOC.
PEAK
PAIRS
VEL.
PAIR
VALID.
CAND.
VORT.
CAND.
VORTEX
ASSOC.
CAND.
VORT.
SCAN LIMITS
FOCUS
SCAN RATE
SEARCH
CONTROL
DET.
VORTEX
PEAK
VALID.
LOCATION
STRENGTH
VORT.
DET.
PRED.
VORTEX HISTORY
AIRCRAFT DATA
VORTEX
PREDICT.
PRED.
VORTEX
ASSOC.
MOTION
DECAY

TURBULENCE DETECTION WITH COHERENT LASER RADAR

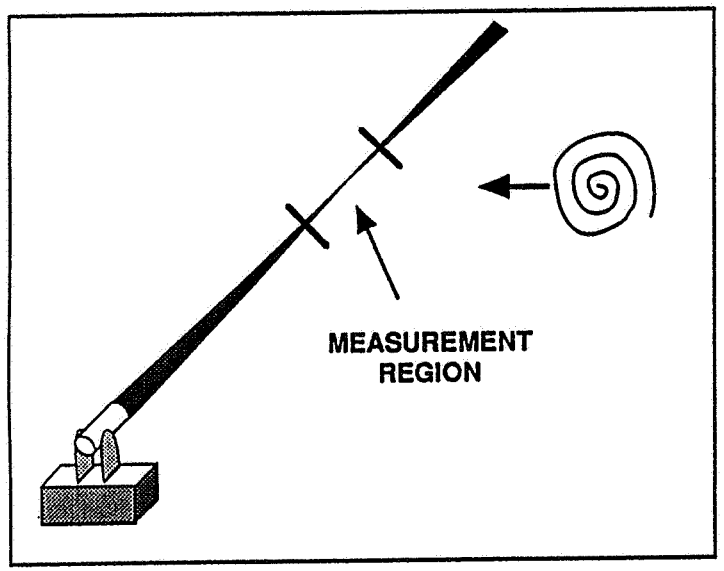

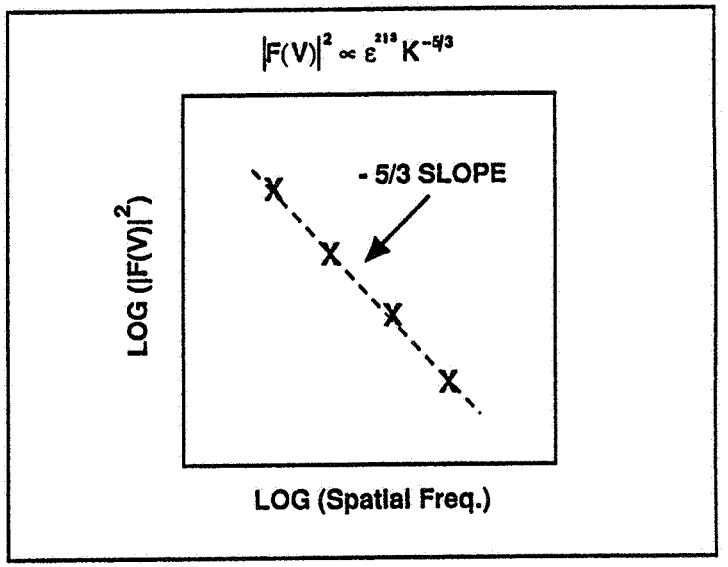

- MEASURE STRENGTH OF KOLMOGOROV TURBULENCE BY FITTING VELOCITY VERSUS SPATIAL FREQUENCY MEASUREMENTS TO -5/3 POWER LAW
  - SYSTEM CAN ACHIEVE $\Delta V \leq 5$ - 10 cm/sec WHICH IS ADEQUATE FOR MEASURING LOW TO MODERATE TURBULENCE
- LOOK FOR WIND SHEAR AND NON - KOLMOGOROV TURBULENCE (Deviation From Power Law Behavior) OVER SPATIAL SCALES COMPARABLE TO THE SIZE OF THE VORTEX

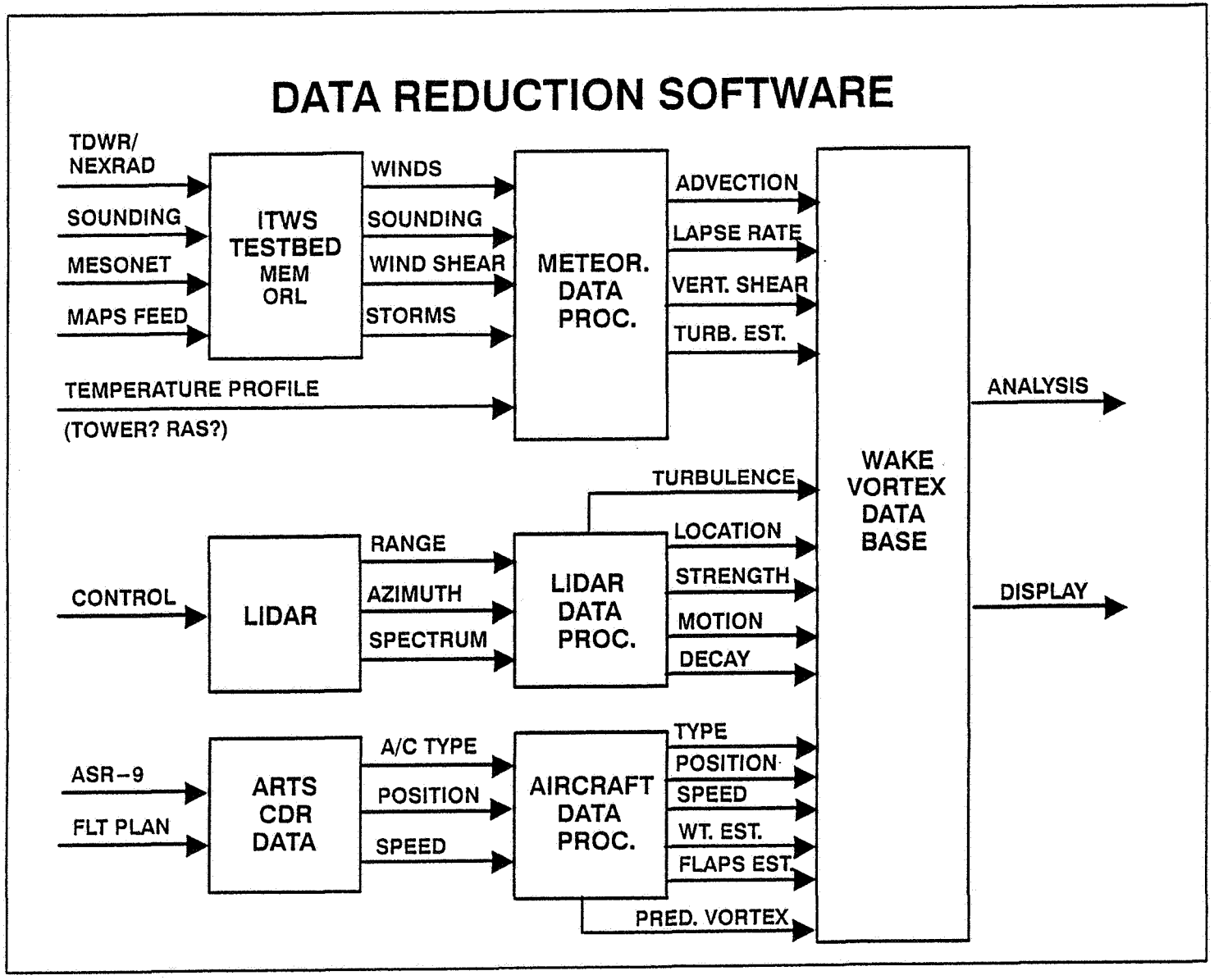
DATA REDUCTION SOFTWARE
TDWR/
NEXRAD
SOUNDING
MESONET
MAPS FEED
ITWS
TESTBED
MEM
ORL
WINDS
SOUNDING
WIND SHEAR
STORMS
METEOR.
DATA
PROC.
ADVECTION
LAPSE RATE
VERT. SHEAR
TURB. EST.
TEMPERATURE PROFILE
(TOWER? RAS?)
ANALYSIS
WAKE
VORTEX
DATA
BASE
TURBULENCE
CONTROL
LIDAR
RANGE
AZIMUTH
SPECTRUM
LIDAR
DATA
PROC.
LOCATION
STRENGTH
MOTION
DECAY
DISPLAY
ASR-9
FLT PLAN
ARTS
CDR
DATA
A/C TYPE
POSITION
SPEED
AIRCRAFT
DATA
PROC.
TYPE
POSITION
SPEED
WT. EST.
FLAPS EST.
PRED. VORTEX

PROTOTYPE ANALYSIS DISPLAY CONCEPT

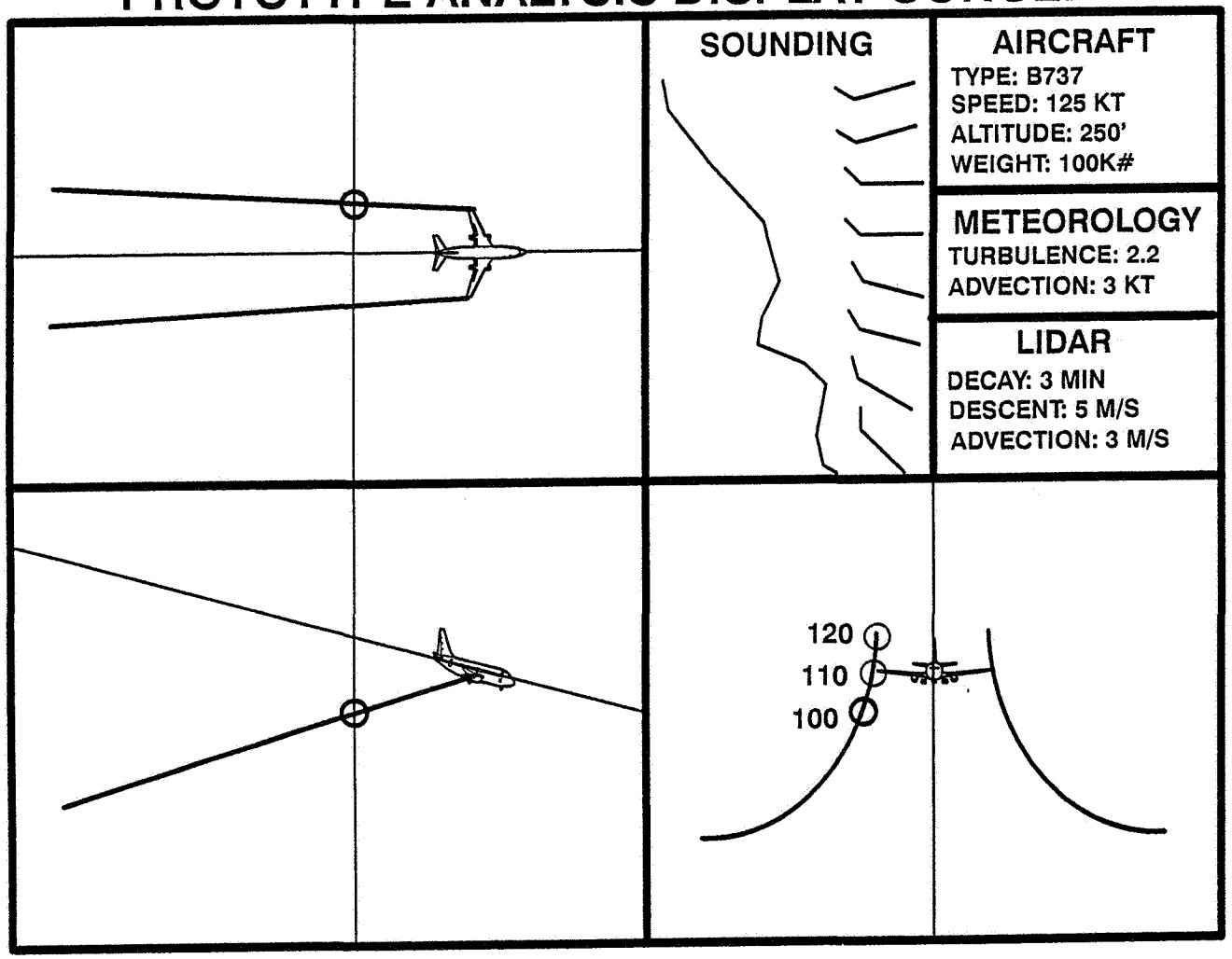

PROPOSED WAKE VORTEX PROGRAM PLAN

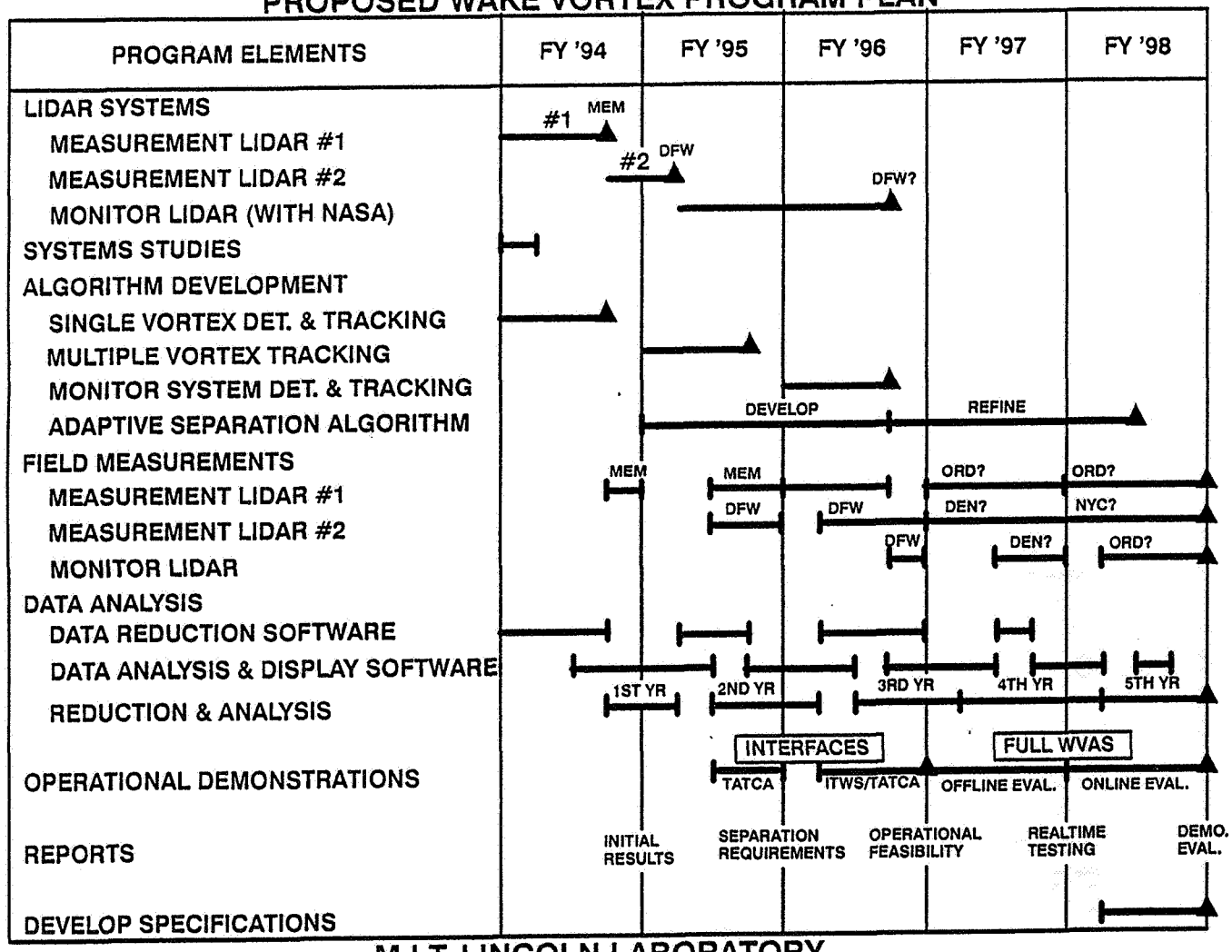

M.I.T. LINCOLN LABORATORY

SUMMARY

- ADAPTIVE WAKE VORTEX SEPARATION
  - REQUIRES INTERACTION BETWEEN WV, ITWS & TATCA
  - COLLABORATIVE EFFORT (NASA, FAA, LL, VOLPE)

- LINCOLN EFFORT IN FY '94
  - CONSTRUCT MEASUREMENT LIDAR SYSTEM BY SUMMER '94
  - DEVELOP VORTEX DETECTION & TRACKING ALGORITHM
  - OPERATE FOR ONE MONTH AT MAJOR AIRPORT (MEMPHIS?)
    COLLECT LIDAR, ATMOSPHERIC & AIRCRAFT DATA
  - BEGIN DATA REDUCTION & ANALYSIS
  - COLLABORATE WITH LANGLEY & VOLPE ON SYSTEM STUDIES

- LONGER–TERM
  - SECOND MEASUREMENT LIDAR AT DFW IN '95
  - BEGIN DEMONSTRATING OPERATIONAL FEASIBILITY IN '96

Aircraft Wake RCS Measurement.

W. Gilson,

Massachusetts Institute of Technology

ABS: next page

Radar Measurements of Aircraft Wakes at Kwajalein, R.M.I.

William H. Gilson
Lincoln Laboratory, Massachusetts Institute of Technology
244 Wood Street
Lexington, Massachusetts 02173-9108

ABSTRACT

A series of multi-frequency radar measurements of aircraft wakes at altitudes of 5,000 to 25,000 ft. was performed at Kwajalein, R.M.I., in May and June of 1990. Two aircraft were tested, a Learjet 35 and a Lockheed C-5A. The cross-section of the wake of the Learjet was too small for detection at Kwajalein. The wake of the C-5A, although also very small, was detected and measured at VHF, UHF, L-, S-, and C-bands, at distances behind the aircraft ranging from about one hundred meters to tens of kilometers. The data suggest that the mechanism by which aircraft wakes have detectable radar signatures is, contrary to previous expectations, unrelated to engine exhaust but instead due to turbulent mixing by the wake vortices of pre-existing index of refraction gradients in the ambient atmosphere. These measurements were of necessity performed with extremely powerful and sensitive instrumentation radars, and the wake cross-section is too small for most practical applications.

This work was sponsored by the Office of Naval Technology. The views expressed are those of the author and do not reflect the official policy or position of the U.S. Government.

AIRCRAFT WAKE RCS MEASUREMENTS

WILLIAM H. GILSON

LINCOLN LABORATORY
MASSACHUSETTS INSTITUTE OF TECHNOLOGY

THIS WORK WAS SPONSORED BY THE OFFICE OF NAVAL TECHNOLOGY. THE VIEWS EXPRESSED ARE THOSE OF THE AUTHOR AND DO NOT REFLECT THE OFFICIAL POLICY OR POSITION OF THE U.S. GOVERNMENT

OUTLINE

- BACKGROUND
- RADARS AND AIRCRAFT
- RADAR DATA EXAMPLES
- WAKE SIGNATURES
  - STRENGTH
  - POSSIBLE MECHANISMS
  - ARE WAKES USEFUL "TELL-TALES?"
- SUMMARY

AIRCRAFT WAKE STRUCTURE AND RADAR SCATTERING

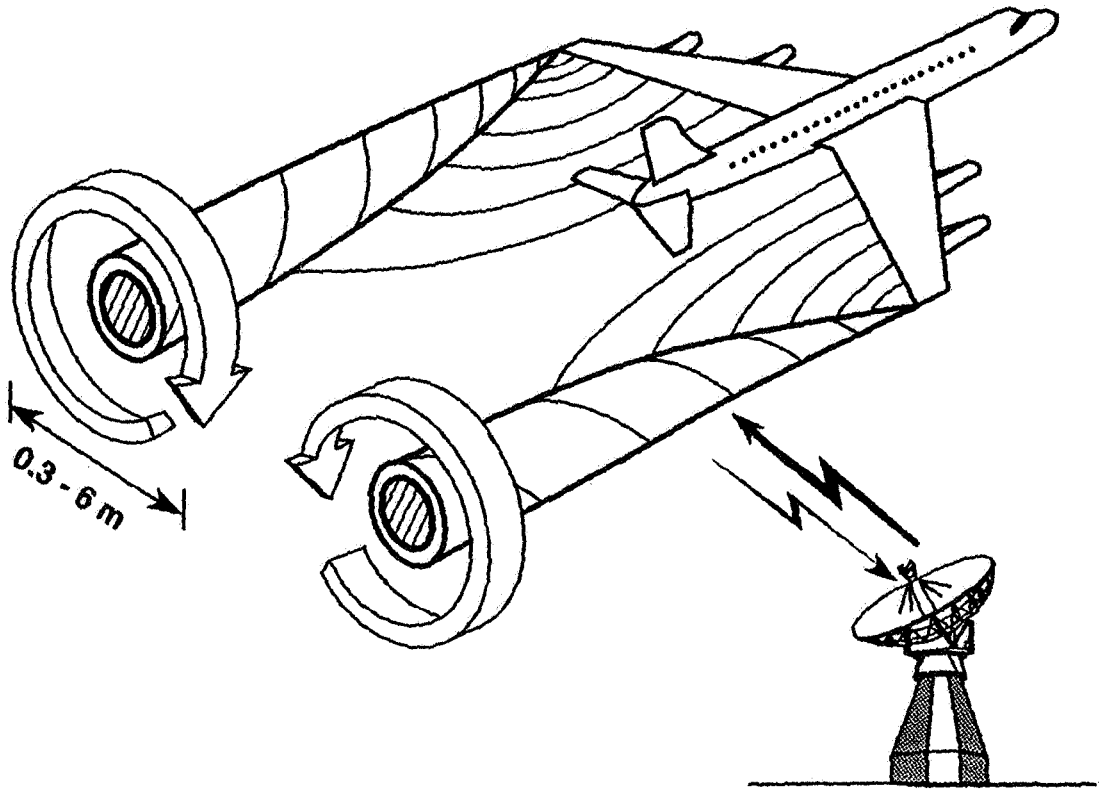

- WAKE STRUCTURES
  - — SENSITIVE TO AIRCRAFT CONFIGURATION
  - — INITIALLY LAMINAR FLOW DECAYS TO TURBULENCE
  - — UP TO 10 TO 20 km LONG

- POTENTIAL SCATTERING MECHANISMS
  - — REFRACTIVITY VARIATIONS
    - EXHAUST HEAT AND MOISTURE
    - MIXING OF ATMOSPHERIC STRATA
    - VORTEX DYNAMICS
  - — EXHAUST PARTICULATES AND AEROSOLS

AIRCRAFT WAKE SIGNATURE
PRIOR MEASUREMENTS AND CALCULATIONS

EXTRAPOLATION

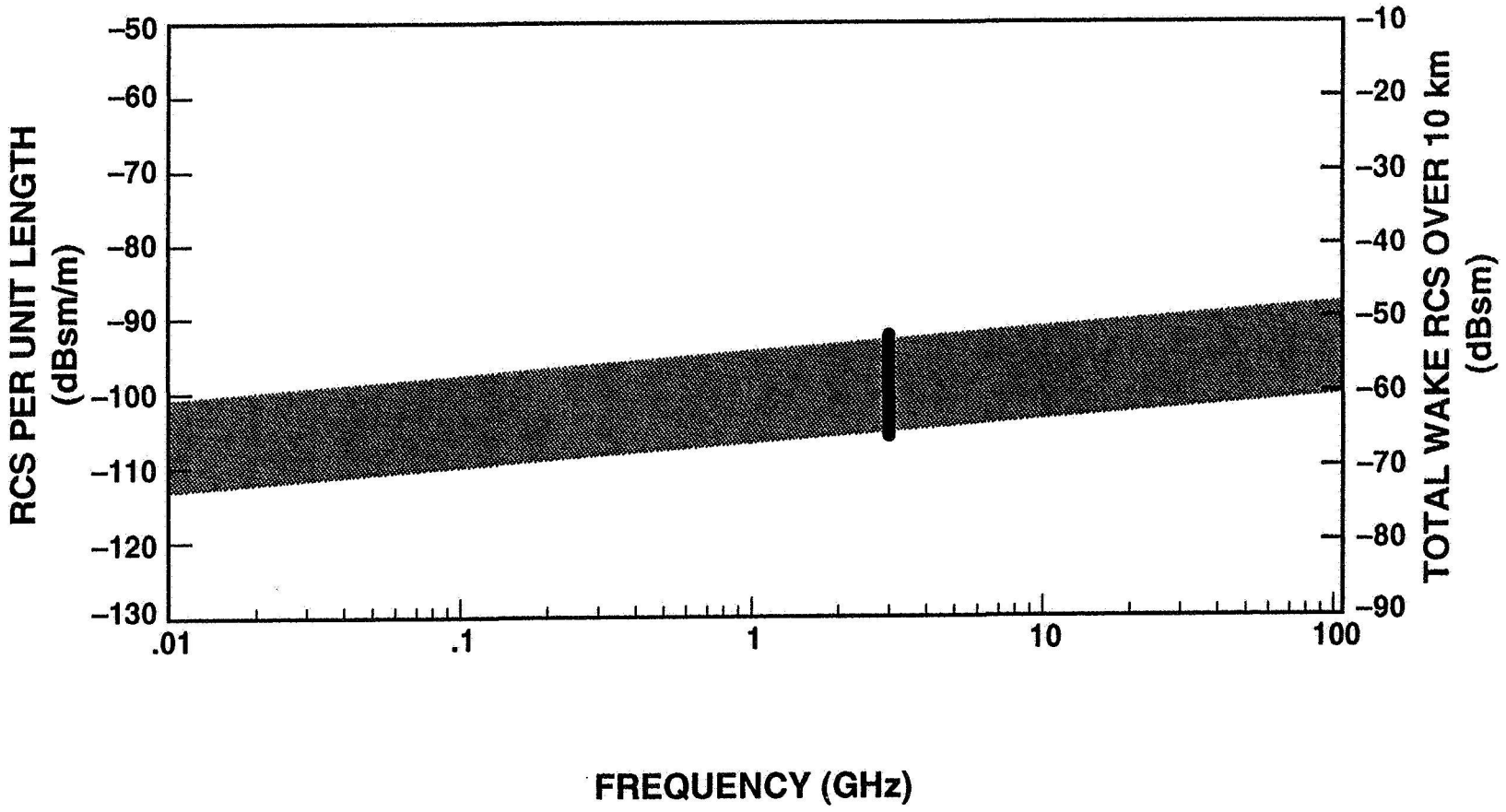

KWAJALEIN ATOLL
KWAJALEIN ISLAND
U.S.
HAWAII
KWAJALEIN
AUSTRALIA
ROI-NAMUR
KWAJALEIN ATOLL
KWAJALEIN
ROI-NAMUR ISLAND
ROI-NAMUR ISLAND

KIERNAN REENTRY MEASUREMENT SYSTEM (KREMS) RADARS

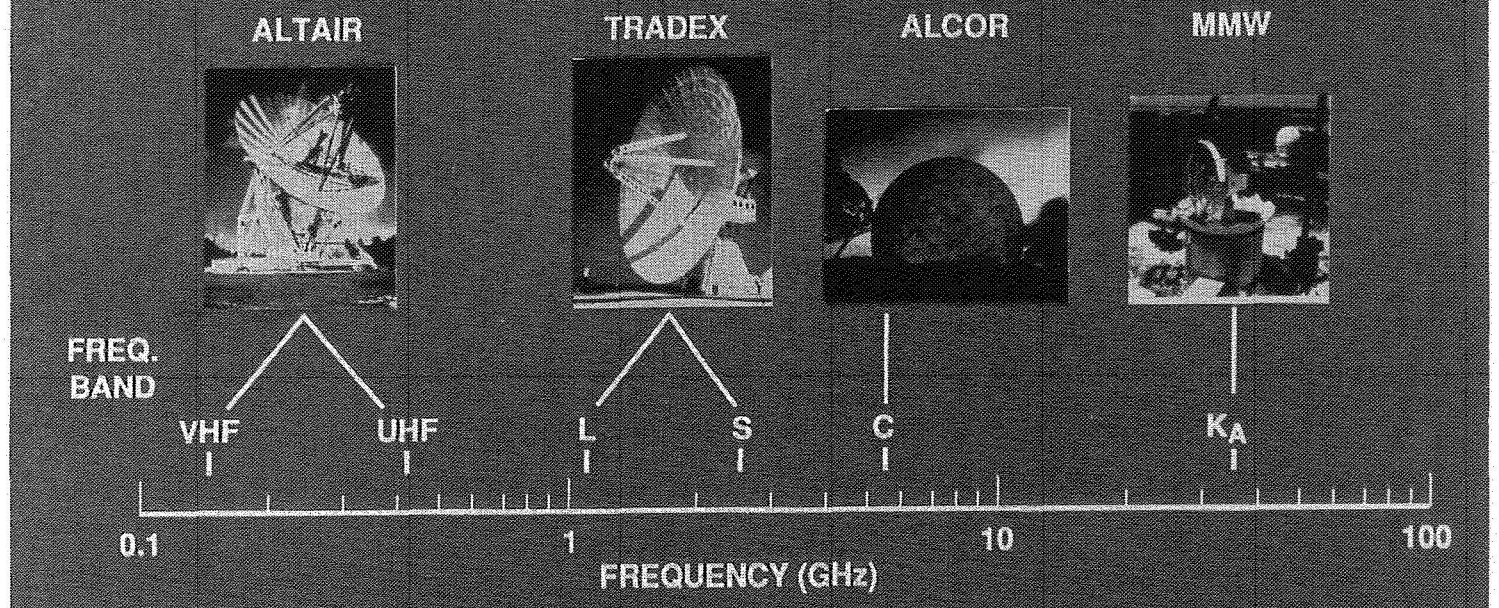

	ALTAIR		TRADEX		ALCOR	MMW
APERTURE DIAMETER (ft)	150		84		40	45
	VHF	UHF	L	S	C	K_A
PEAK POWER (MW)	7	5	2	2	3	0.025
SINGLE PULSE SENSITIVITY AT 200 km (dBsm)	–64	–73	–68	–56	–51	–45

178707-1

AEROMET LEARJET 36 FLY-BY
25 MAY 1990

GATES LEARJET 36

WING SPAN	12 m
MASS, EMPTY	4300 kg
MASS, MAX T.O.	8300 kg
FUEL FLOW AT 45,000 ft	1100 lbs/hr

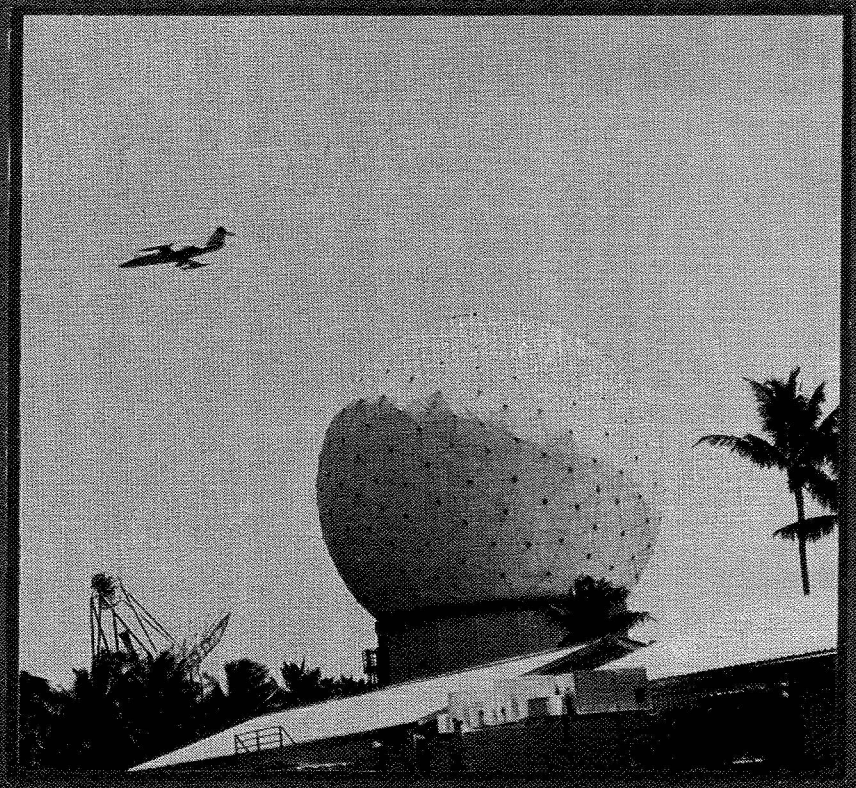

177348-4

439 MAW C-5A FLY-BY
15 JUNE 1990

LOCKHEED C-5A GALAXY

WING SPAN	68 m
MASS, EMPTY	150,000 kg
MASS, MAX T.O.	350,000 kg
FUEL FLOW AT 40,000 ft	18,000 lbs/hr

177345-5

FLIGHT PATH AND DATA RECORDING
TEST RUN AT 5,000 ft ALTITUDE

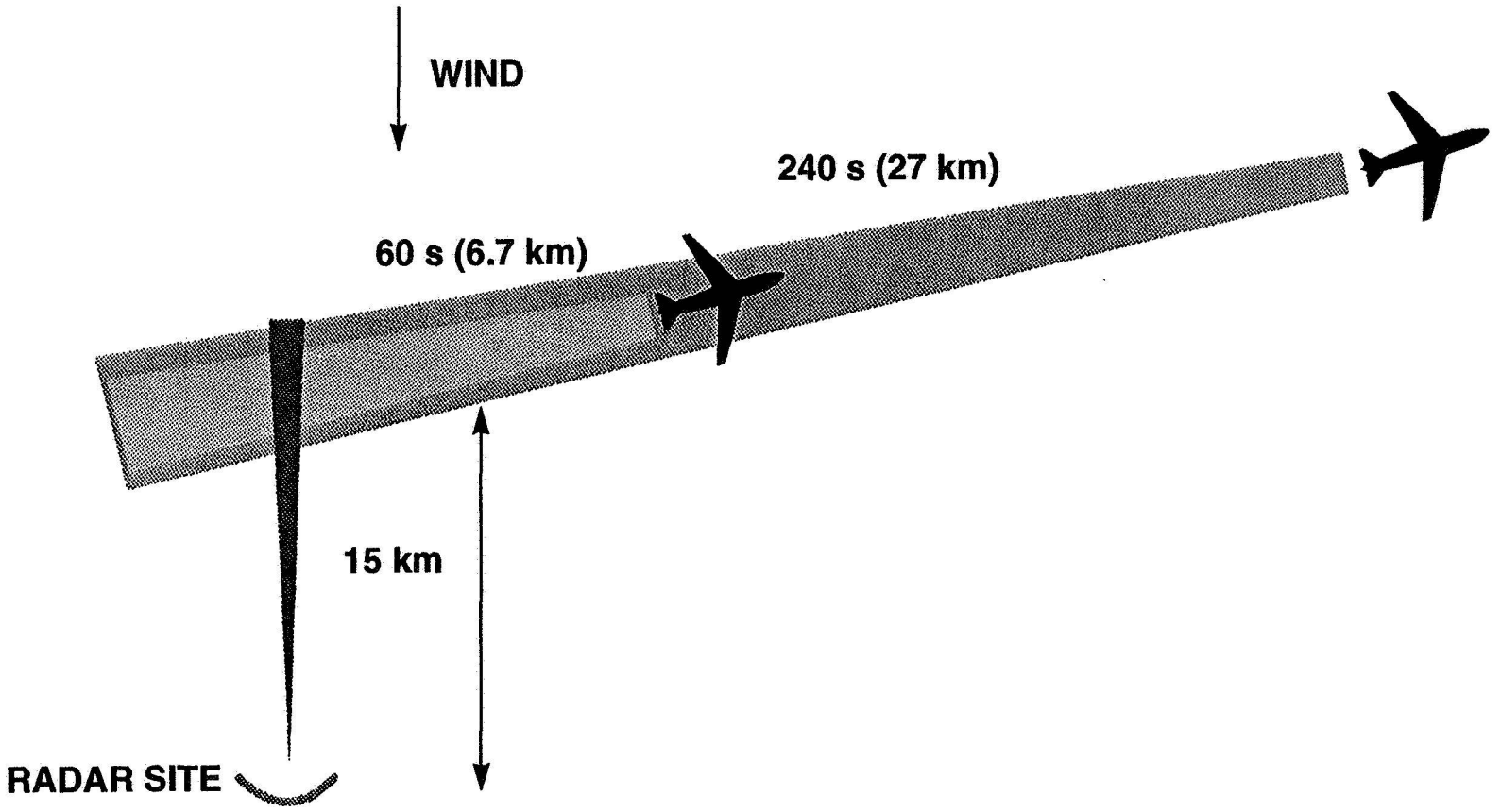

S-BAND RANGE-DOPPLER SLICE THROUGH C-5A WAKE

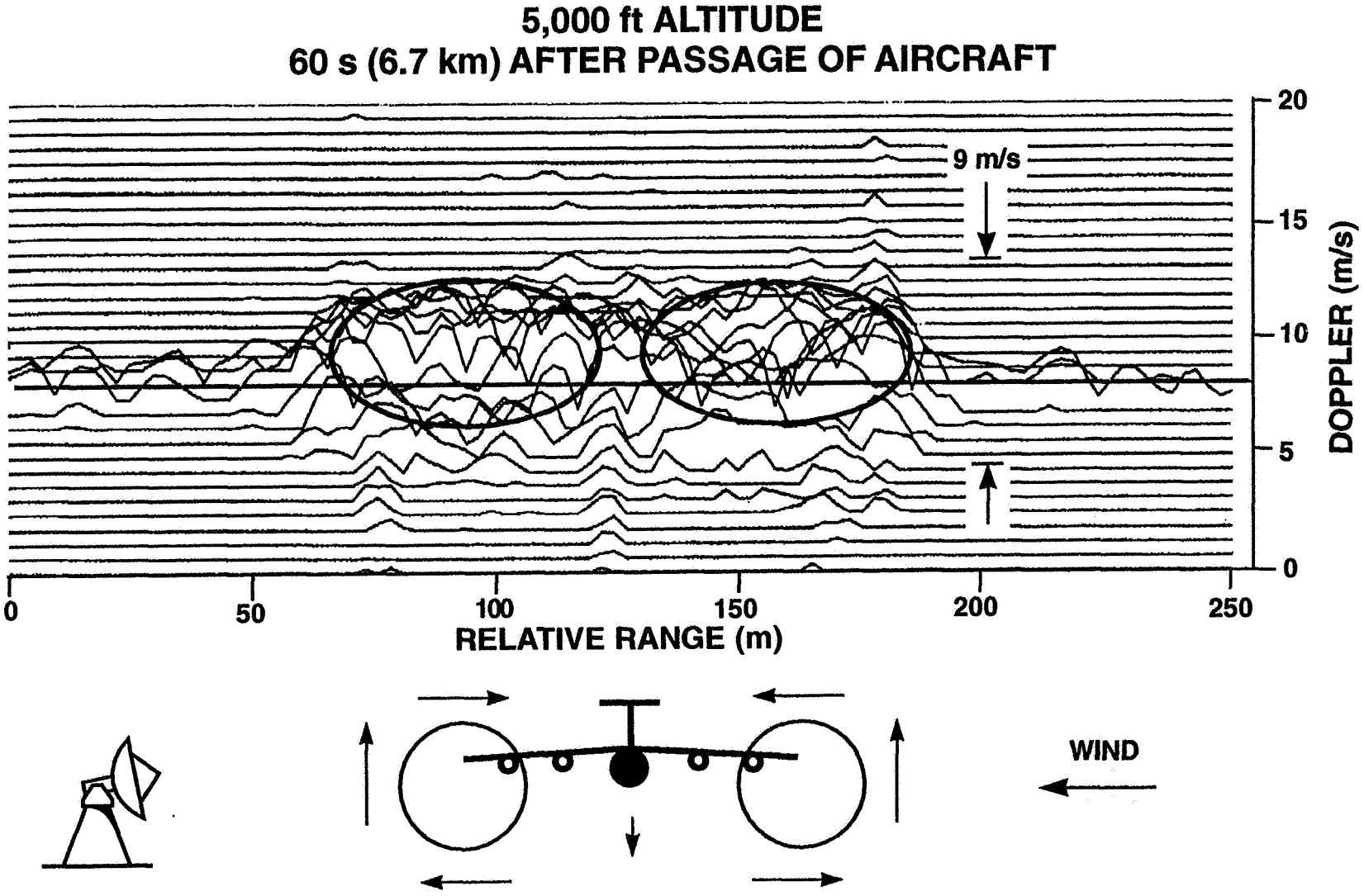

S-BAND RANGE-DOPPLER SLICE THROUGH C-5A WAKE

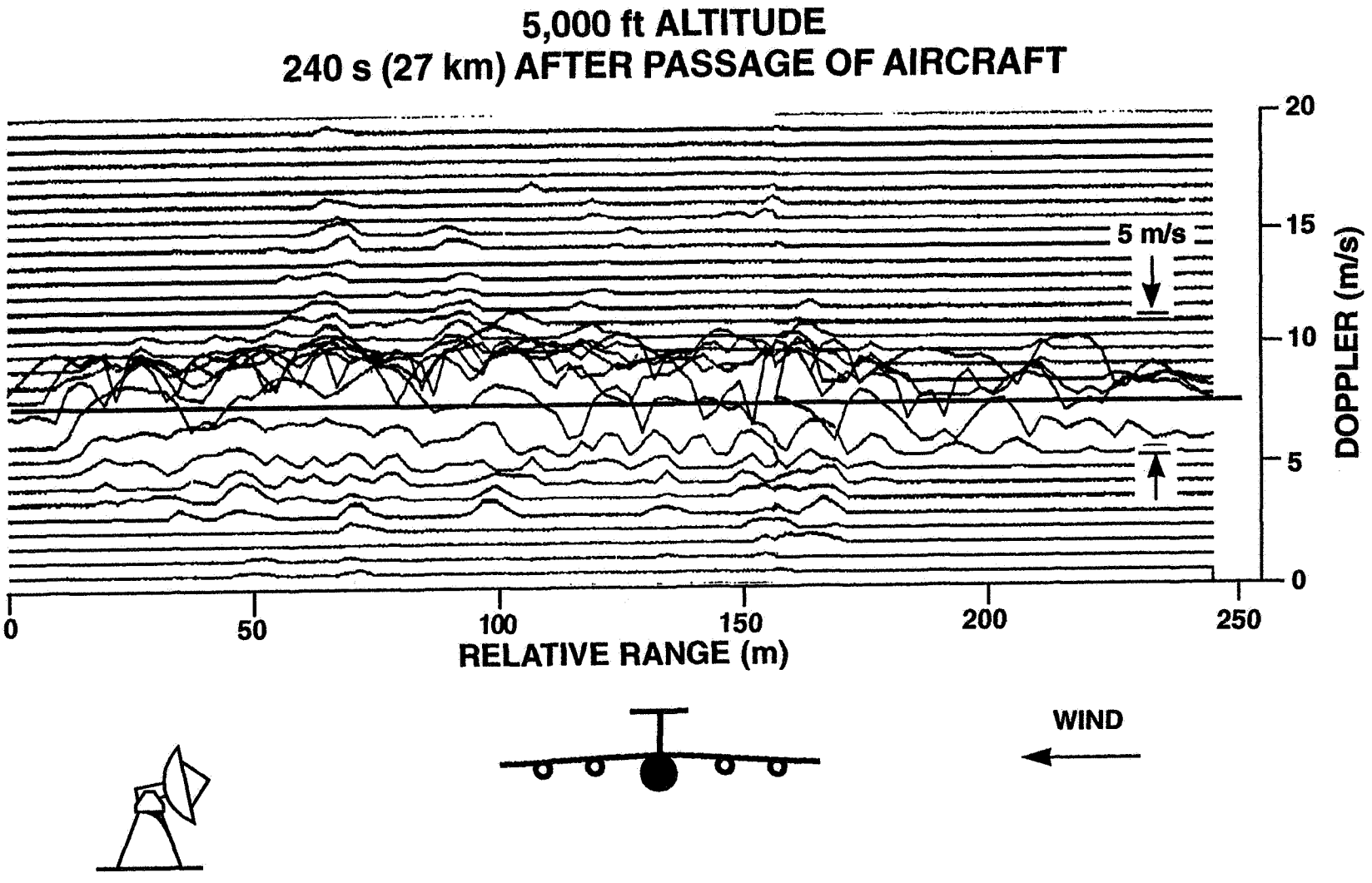

C-5A WAKE DATA

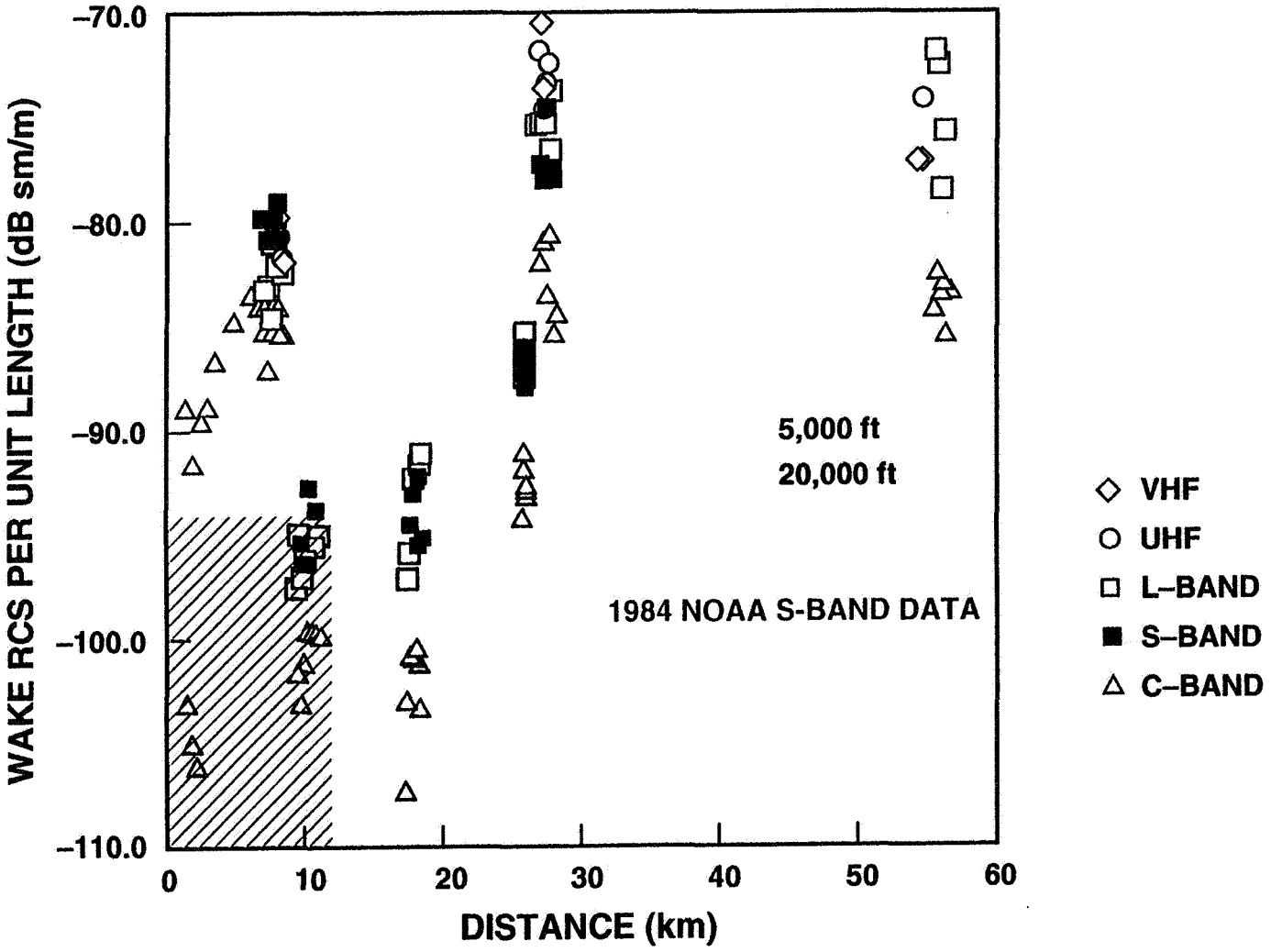

AIRCRAFT WAKE SIGNATURE
PRIOR MEASUREMENTS AND CALCULATIONS

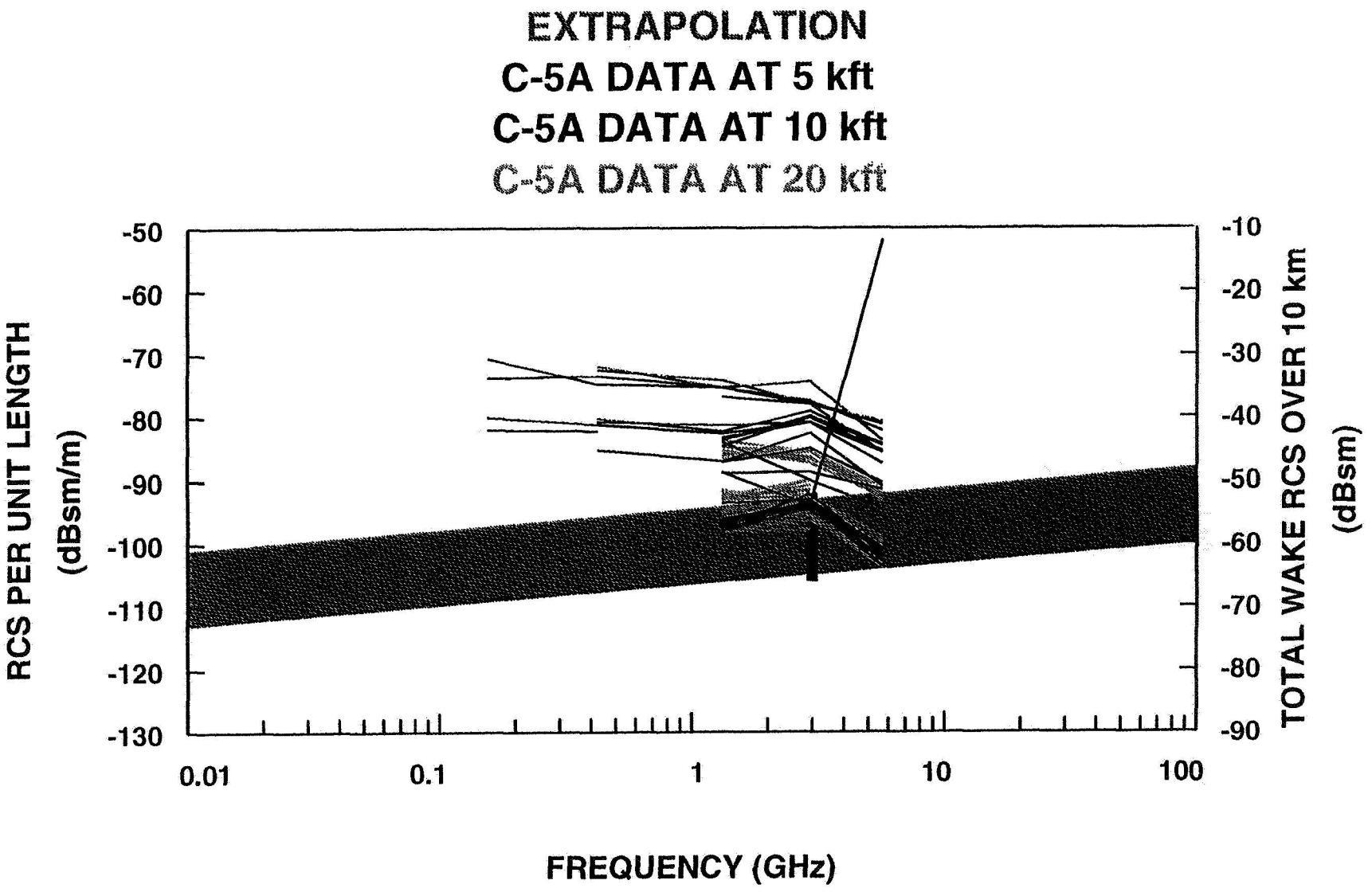

SUMMARY OF C-5A WAKE SIGNATURE DEPENDENCE

PARAMETER	DEPENDENCE	CONCLUSION
DISTANCE	INCREASES FOR CA. 10 km, THEN TRAILS OFF	RELATED TO TURBULENCE
FREQUENCY	LARGELY FLAT, FALLING OFF AT C-BAND	NOT PARTICULATES
ALTITUDE	DECREASES WITH HEIGHT; NOT SEEN ABOVE 27 kft	RELATED TO LOW-ALTITUDE CLIMATE
ENGINE THRUST	NONE: IDLE TO MILITARY RATED THRUST	WEAK EXHAUST CONTRIBUTION
FLAP SETTING	NONE: ZERO TO HALF FLAPS	INDEP. OF DETAILED VORTEX STRUCTURE
AIR SPEED	NONE: 100 kn VARIATION	INDEP. OF DETAILED VORTEX STRUCTURE

POSTULATED MECHANISM

- TURBULENT MIXING OF ATMOSPHERIC INDEX OF REFRACTION GRADIENTS
  - CONSISTENT WITH RCS DEPENDENCE ON
    - ALTITUDE
    - THRUST
    - TIME
    - FREQUENCY
- STRENGTH DEPENDS ON CLIMATE
  - STRONGEST IN TROPICS NEAR SEA LEVEL
- EXHAUST HEAT AND MOISTURE MAY GIVE LOWER LIMIT

SUMMARY

- PRIOR WORK SUGGESTED A VERY SMALL WAKE RCS
- AT KWAJALEIN
  - ENGINE EXHAUST COMPONENT NOT DISCERNIBLE
  - DOMINANT ATMOSPHERIC MIXING CONTRIBUTION
- NO USEFUL "TELL-TALE"
  - STRONG CLIMATE DEPENDENCE
  - LARGE AND COMPLEX SYSTEM
  - CLEAR AIR TURBULENCE CLUTTER

WSMR V. (KWA) WAKE RCS MEASUREMENTS

RADAR	MOTR	ALCOR	ALCOR/MOTR
Peak power	1 MW	3 MW	5 dB
Beam width	1°	5°	-14 dB
Duty factor	0.1%	5%	17 dB
Range	3km	15km	-14 dB
Beam-filling loss (100 m wake)	←		-10 dB
Relative sensitivity to wake C_n^2 i.e. MOTR more sensitive			-16 dB

AIRCRAFT	A-7	LEARJET 36	C-5A	
	22 klbs	10 klbs	330 klbs	dry

QUESTION #3

Can a radar detect and quantify the VORTEX STRENGTH?

OBVIOUS ANSWER - In principle - YES, WITH ENOUGH RANGE OR ANGULAR RESOLUTION?

MY QUESTION FOR THE AERODYNAMICISTS?

WHAT IS ENOUGH RESOLUTION?

(e.g. 1m range by 50 m (cross range))

ATMOSPHERIC DATA FOR WAKE RCS MEASUREMENTS

	WSMR	KREMS
Rawinsondes	AM, PM	1130, from Kwaj.
Weather reports	Met. Station, Before & after fly-bys	Met. station on Kwaj. Mornings, before missions.

Wake Vortex Detection at Denver Stapleton Airport with a Pulsed 2-micron Coherent Lidar.

S. Hannon and A. Thomson,
Coherent Technologies, Inc.

No abstract, original needed

WAKE VORTEX DETECTION AT DENVER STAPLETON WITH A PULSED 2 μm COHERENT LIDAR

WINDSHEAR REVIEW MEETING, '93

30 SEPTEMBER 1993

STEPHEN M. HANNON AND J. ALEX THOMSON

COHERENT TECHNOLOGIES, INC.
BOULDER, COLORADO

OVERVIEW

- HISTORICAL PERSPECTIVE
- PROGRAM SUMMARY
- MEASUREMENT OBJECTIVES
- SYSTEM DESCRIPTION
- WAKE VORTEX SIGNAL PROCESSING
- EXAMPLE RESULTS
- SUMMARY AND FUTURE DIRECTIONS

HISTORICAL PERSPECTIVE

- FAA AND NASA PROGRAMS IN 1960's AND 1970'S
  - EVALUATE HAZARD TO FOLLOWING AIRCRAFT DUE TO PERSISTENT WAKE VORTICES OF LARGE COMMERCIAL AIRLINERS
  - CW CO_2 DOPPLER LIDAR MEASUREMENTS OF WAKE VORTICES
  - FUNDING REDUCED/ELIMINATED IN MID-1970'S

- CURRENT FAA AND NASA PROGRAMS
  - URGENT NEED TO SAFELY INCREASE AIRPORT CAPACITY
  - MODELING AND EXPERIMENTAL VALIDATION OF ENVIRONMENTAL EFFECTS ON WAKE PERSISTENCE
  - EVALUATION OF COHERENT LASER RADAR FOR ONBOARD AND GROUND-BASED WAKE DETECTION AND MONITORING

- OTHER (EUROPEAN) PROGRAMS
  - CW CO_2 DOPPLER LIDAR MEASUREMENTS OF WAKE VORTICES AT FRANKFURT AIRPORT

- WAKE VORTICES AS AN UNEXPLOITED OBSERVABLE
  - DETECTION AND TRACKING USING PULSED DOPPLER SYSTEMS
  - FALSE ALARM MITIGATION

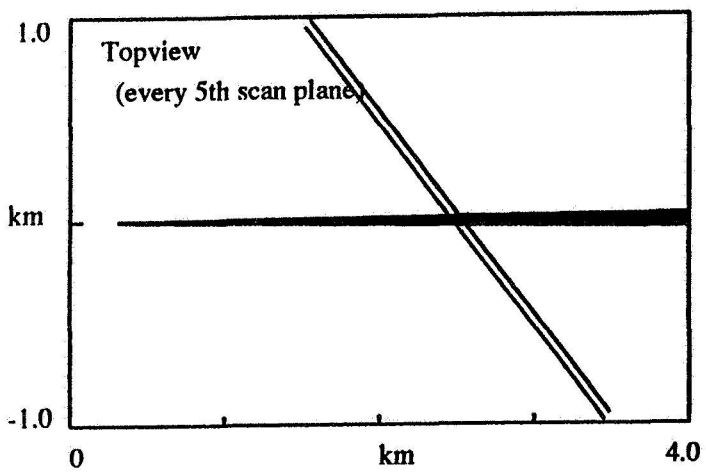
1.0
Topview
(every 5th scan plane)
km
-1.0
0
km
4.0

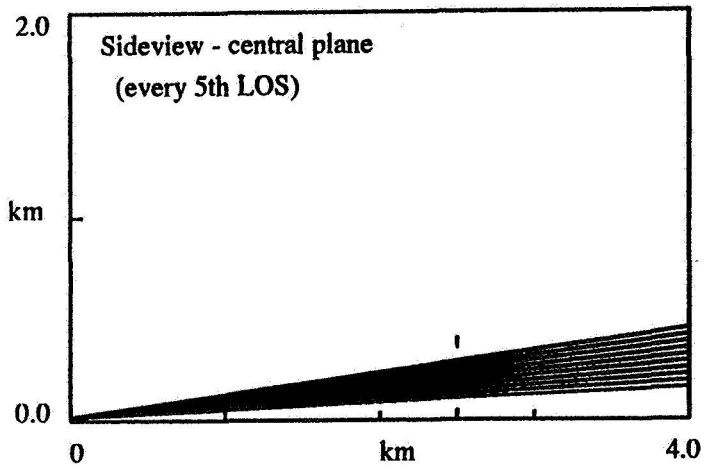
2.0
Sideview - central plane
(every 5th LOS)
km
0.0
0
km
4.0

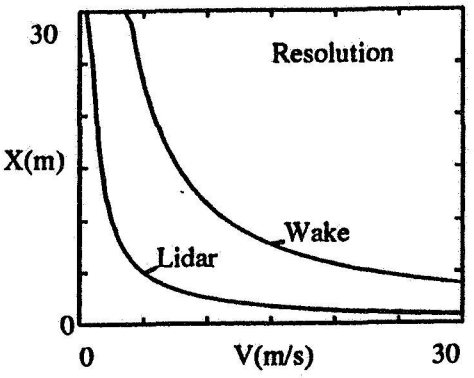
30
Resolution
X(m)
Wake
Lidar
0
0
V(m/s)
30

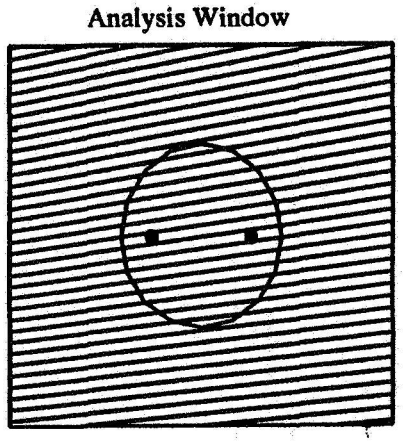
Analysis Window
256 m by 128 m

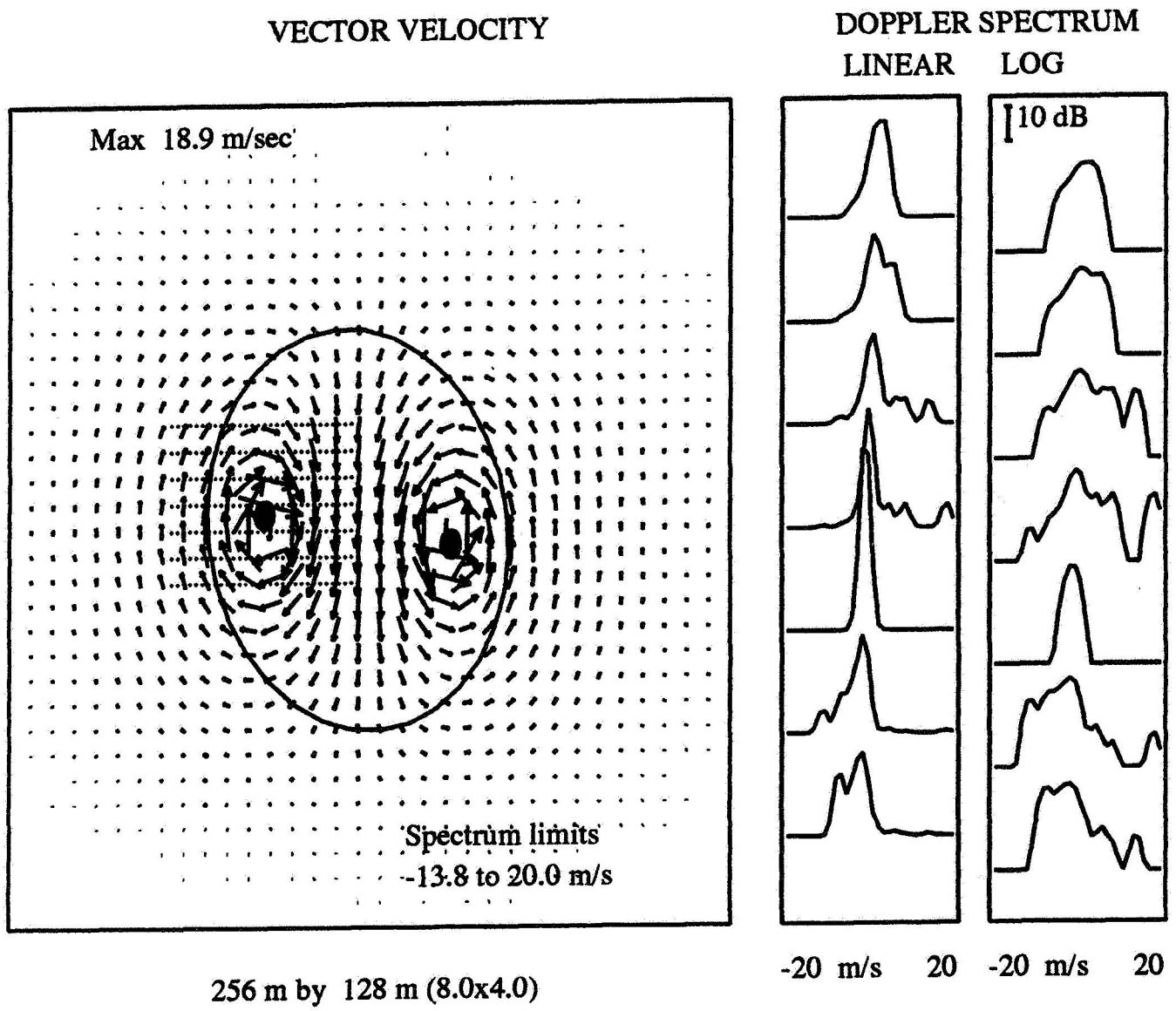
VECTOR VELOCITY
DOPPLER SPECTRUM
LINEAR
LOG
Max 18.9 m/sec
10 dB
Spectrum limits
-13.8 to 20.0 m/s
-20 m/s 20
-20 m/s 20
256 m by 128 m (8.0x4.0)

DETECTED DOPPLER SIGNATURE (512 m by 128 m)

VELOCITY (max 3.34 m/s)

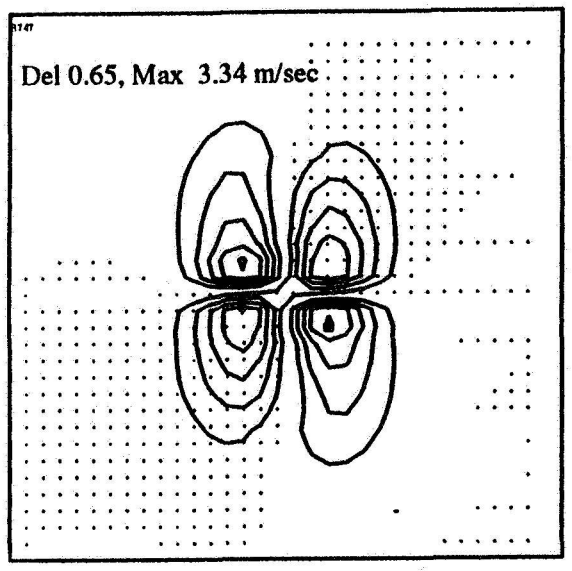

WIDTH (max 5.07 m/s)

realization (Vrms= 0.72, Wrms= 0.79 m/s)

MATCHED FILTER OUTPUT (512 m by 128 m)

VELOCITY (27.39 db)

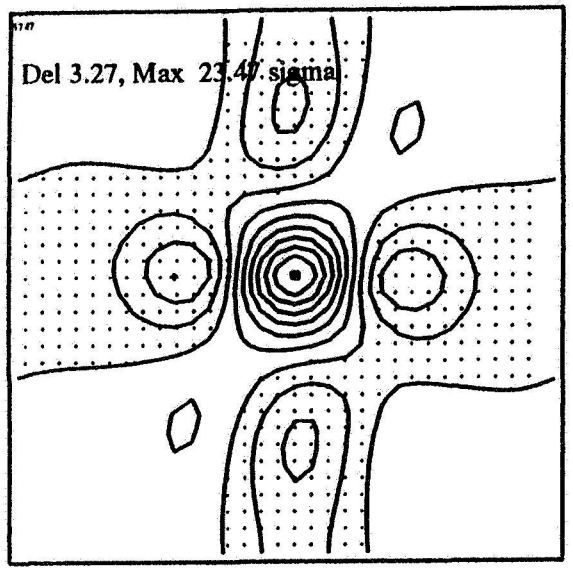

DELTA WIDTH (26.16 db)

realization

NASA PHASE I PROGRAM OBJECTIVES

OVERALL: RELATE WAKE HISTORY TO LOCAL ENVIRONMENT

- SYSTEM REQUIREMENTS AND CONCEPT DEFINITION
  - SYSTEM SIZING
  - MEASUREMENT PLANNING
  - PRELIMINARY ALGORITHM DEVELOPMENT (VECTOR WIND RETRIEVAL)

- PERFORM FIELD MEASUREMENTS
  - EXISTING MOBILE 2.09 μm COHERENT LIDAR SYSTEM*
  - STAPLETON INTERNATIONAL AIRPORT
  - DEMONSTRATE ABILITY TO CREATE USEFUL DATABASE

- DEVELOP PRELIMINARY SYSTEM SPECIFICATION FOR A DEDICATED SYSTEM

MEASUREMENT OBJECTIVES

OBJECTIVE: RELATE WAKE HISTORY TO LOCAL ENVIRONMENT

- MONITOR EMBEDDING WINDFIELD
  - VERTICAL PROFILE OF HORIZONTAL VECTOR WIND
  - LOW-ANGLE LOS WIND DISTRIBUTIONS (3° PPI)
  - TRANSVERSE VECTOR WIND RETRIEVAL IN VERTICAL SCAN PLANES
- MONITOR LOCAL METEOROLOGY
  - GROUND MET OBSERVATIONS
  - RAS TEMPERATURE PROFILES
  - LIDAR MEASUREMENTS
  - RADAR WIND PROFILE (LIMITED UTILITY)
  - RAWINSONDE LAUNCHES (LIMITED UTILITY)
- HIGH-RESOLUTION VELOCITY FIELD ANALYSIS IN VERTICAL SCAN PLANES
  - VORTICITY FIELD RETRIEVAL
  - RELATE VORTICITY SOURCES TO WAKE CIRCULATION DECAY
- AXIAL VELOCITY SIGNATURE
  - DIRECT AND INFERRED MEASUREMENT USING MULTIPLE VERTICAL SCAN PLANES

CTI FAA/TASS PROGRAM SUMMARY

OBJECTIVE: *ASSESS THE UTILITY OF SOLID-STATE COHERENT LIDAR TO THE TASS PROGRAM*

APPLICATIONS: WAKE VORTICES; DRY AND WET MICROBURST WINDSHEAR; GUSTS; VERTICAL AND GENERAL WIND PROFILING

- ASSESS OVERALL SYSTEM UTILITY
  - MULTIFUNCTION SYSTEM

- FIELD DEMONSTRATION MEASUREMENTS
  - GENERAL SYSTEM CAPABILITY
  - SNR PERFORMANCE AS A FUNCTION OF ENVIRONMENTAL CONDITIONS
  - WAKE VORTEX AND MICROBURST WINDSHEAR MEASUREMENTS
  - KSC AND STAPLETON INTERNATIONAL AIRPORT

FAA TCO: James W. Rodgers

CTI FAA/TASS PROGRAM WAKE VORTEX MEASUREMENTS

OBJECTIVE: *ASSESS THE ABILITY OF PULSED SOLID-STATE COHERENT LIDAR TO DETECT AND TRACK WAKE VORTICES*

- EMPHASIS ON RELIABLE *DETECTION*
  - WAKE PHENOMENOLOGY LESS IMPORTANT
  - FOCUS ON WAKE, NOT WAKE+LOCAL WIND FIELD
  - WEATHER EFFECTS LIMITED TO SNR IMPACT
  - DEVELOPMENT OF DETECTION AND TRACKING ALGORITHMS
- MULTIFUNCTION REQUIREMENT
  - DEDICATED DEVICE BETTER SUITED TO UNDERSTAND PHENOMENOLOGY

FLASHLAMP-PUMPED 2.09 MICRON SOLID-STATE COHERENT LASER RADAR SYSTEM

- Tm,Ho:YAG
- INJECTION-SEEDED (MO/SO) CONFIGURATION
- PULSE ENERGY ~30 mJ/PULSE
- PULSE DURATION ~170 ns
- PRF ~5 Hz
- TRANSMIT APERTURE 10 cm
- PROCESSING BANDWIDTH ~50 MHz (50 m/s)
- REAL-TIME DATA ACQUISITION, PROCESSING, AND DISPLAY

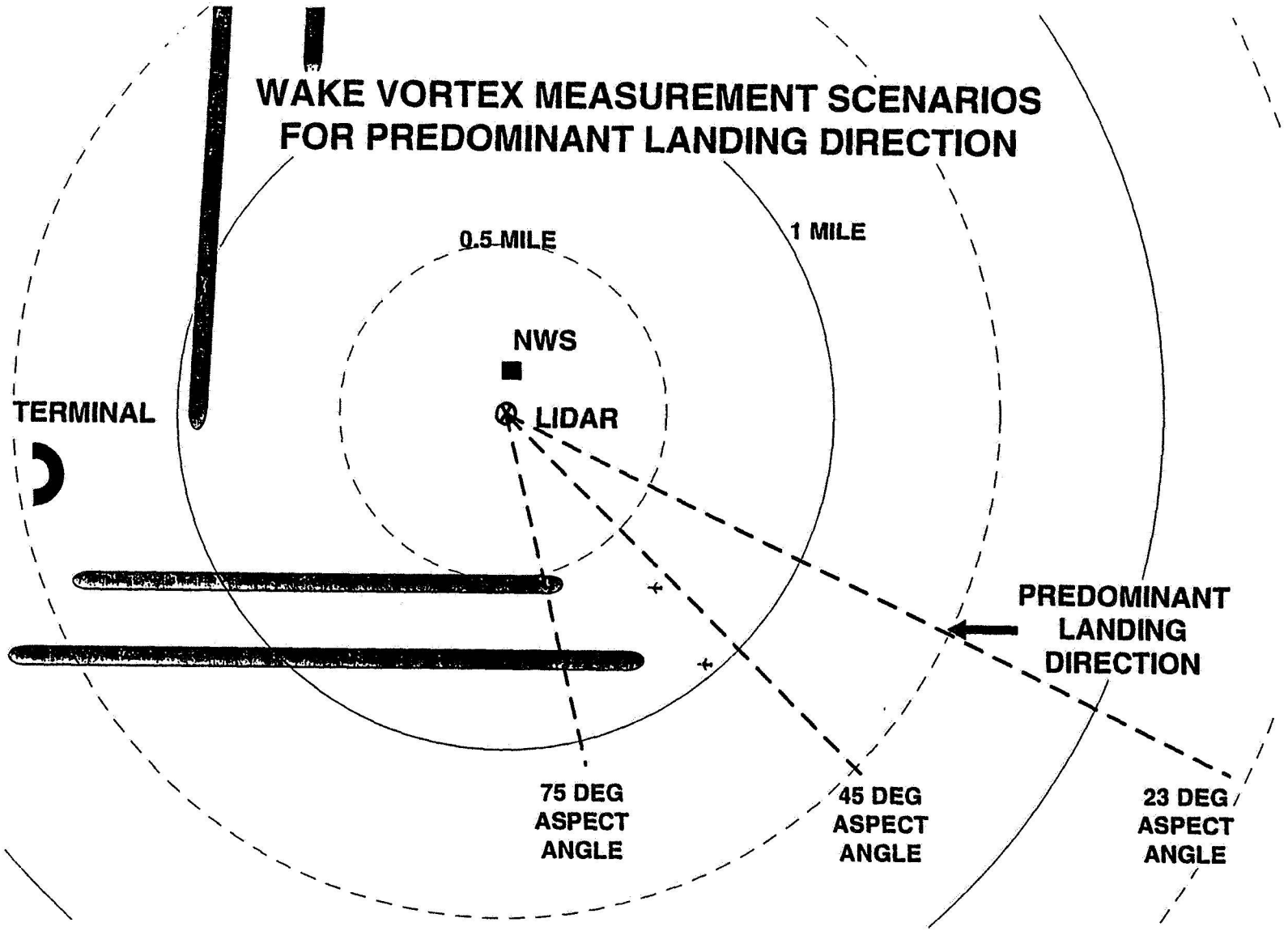
WAKE VORTEX MEASUREMENT SCENARIOS
FOR PREDOMINANT LANDING DIRECTION
0.5 MILE
1 MILE
NWS
LIDAR
TERMINAL
PREDOMINANT
LANDING
DIRECTION
75 DEG
ASPECT
ANGLE
45 DEG
ASPECT
ANGLE
23 DEG
ASPECT
ANGLE

MEASUREMENT APPROACH

- UTILIZE 3 VERTICAL SCAN PLANES
  - ASPECT ANGLES: 23°, 45°, 75° (DATA ALSO @ 90°)
  - 8-10 sec PER VERTICAL SLICE
  - 1-3 m VERTICAL SEPARATION OF LOS
  - 800-4000 m MEASUREMENT RANGE
  - PRIMARILY LANDING AIRCRAFT (B757, AIRBUS, DC10, OTHERS)

- MONITOR LOCAL METEOROLOGY
  - LOCATE ADJACENT TO NWS/STAPLETON
  - BUILD MET DATABASE WITH HELP OF NWS AND NOAA
  - 30-60 MINUTES OF DATA FOLLOWED BY VAD OR PPI SCAN

- REAL-TIME DATA QUALITY CHECKING
  - RANGE-RESOLVED SPECTRAL PROFILES
  - SPECTRAL WIDTH AND MEAN VELOCITY 'IMAGES'

RESTRICTIONS OF CURRENT DATABASE

- LOW PRF RESULTS IN COARSE LIFETIME QUANTIZATION (8-10 sec)

- ONE VERTICAL SCAN PLANE PER AIRCRAFT

- GEOMETRY RESTRICTS MINIMUM MEASUREMENT HEIGHT (10 m)
  - CHANGED LOCATION FOR LIMITED DATA SET WITHOUT GEOMETRY RESTRICTIONS

SIGNAL PROCESSING

STAGE 1 : PULSE PROCESSING (range, frequency)

spectrum: range, frequency display per pulse

spectrum moment or feature

0	area	SNR
1	centroid	mean velocity
2	width	local velocity variance, 'turbulence'
3,4,...		shape, peak velocity, ML band pass

STAGE 2 : SPACE - TIME PROCESSING

spectral moment, feature vs x,y,z,t

velocity/vorticity field

turbulence, shear field

Processing

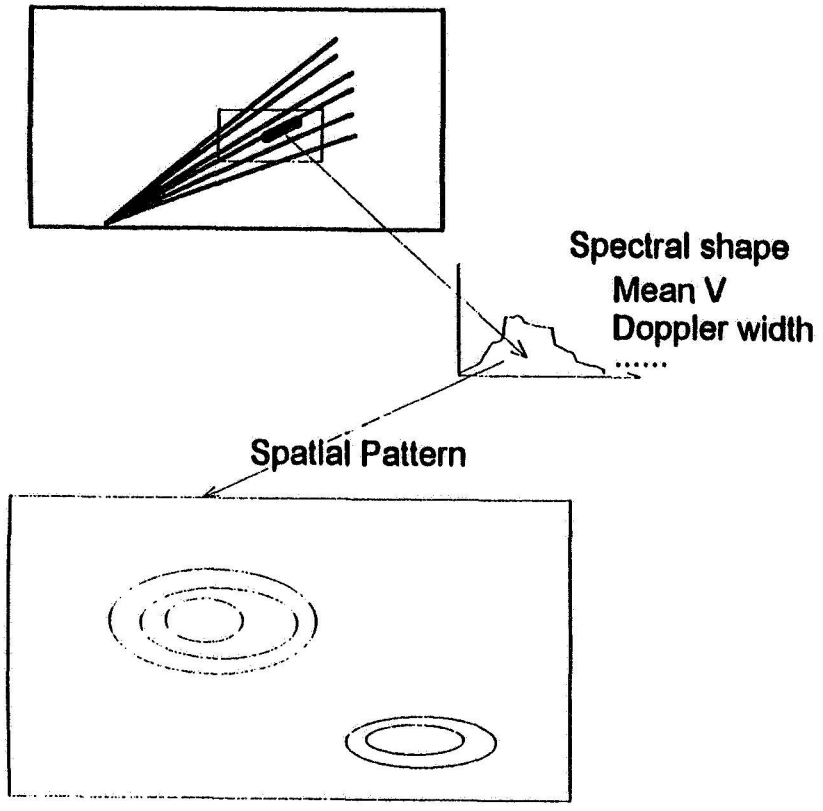
Spectral shape
Mean V
Doppler width
.....
Spatial Pattern

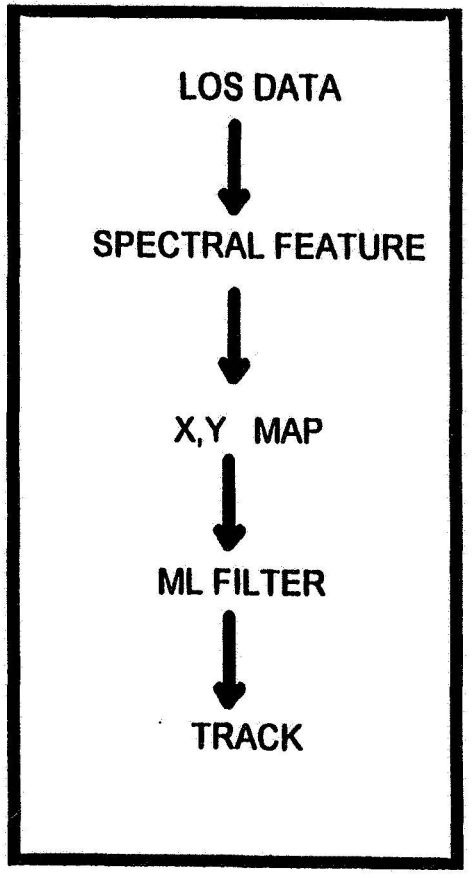
LOS DATA
SPECTRAL FEATURE
X,Y MAP
ML FILTER
TRACK

Maximum likelihood processing

Maximize likelihood of wake vs no wake

$$\Lambda = \text{Probability (wake)} / \text{Probability (no wake)}$$

$$\ln \Lambda = -0.5^* < \left(Data - \sum_i c_i F(x - x_i; a_i \right)^2 > /\Sigma^2 + 0.5^* < Data^2 > /\Sigma^2$$

Get noise covariance from no-wake data

$$\Sigma = < Data(x)^* Data(x') >$$

Choose vortex strengths first $(\partial\Lambda / \partial c_i = 0)$

$$\ln \Lambda = +0.5^* \sum_i < \left(Data(x)^* F(x - x_i) \right)^2 > /\Sigma^2 \qquad ; \quad < F^2 > \equiv 1$$

Matched filter is prime analysis quantity

$$Data(x)^* F(x - x_i)$$

MAXIMUM LIKELIHOOD DETECTION

Calculate the likelihood that a wake is present

- fit model to measured data
- choose model parameters to maximize probability that data and model agree
- for Gaussian noise/background statistics:

$$\ln \Lambda = -0.5 * \left(Data - Model(parameters) \right)^2 / \Sigma^2$$

- Multiple vortex model

$$\ln \Lambda = -0.5 * \left(Data - \sum_i c_i F(x - x_i; a_i \right)^2 / \Sigma^2$$

MATCHED FILTER PROCESSING
DC10 - SLICE 3

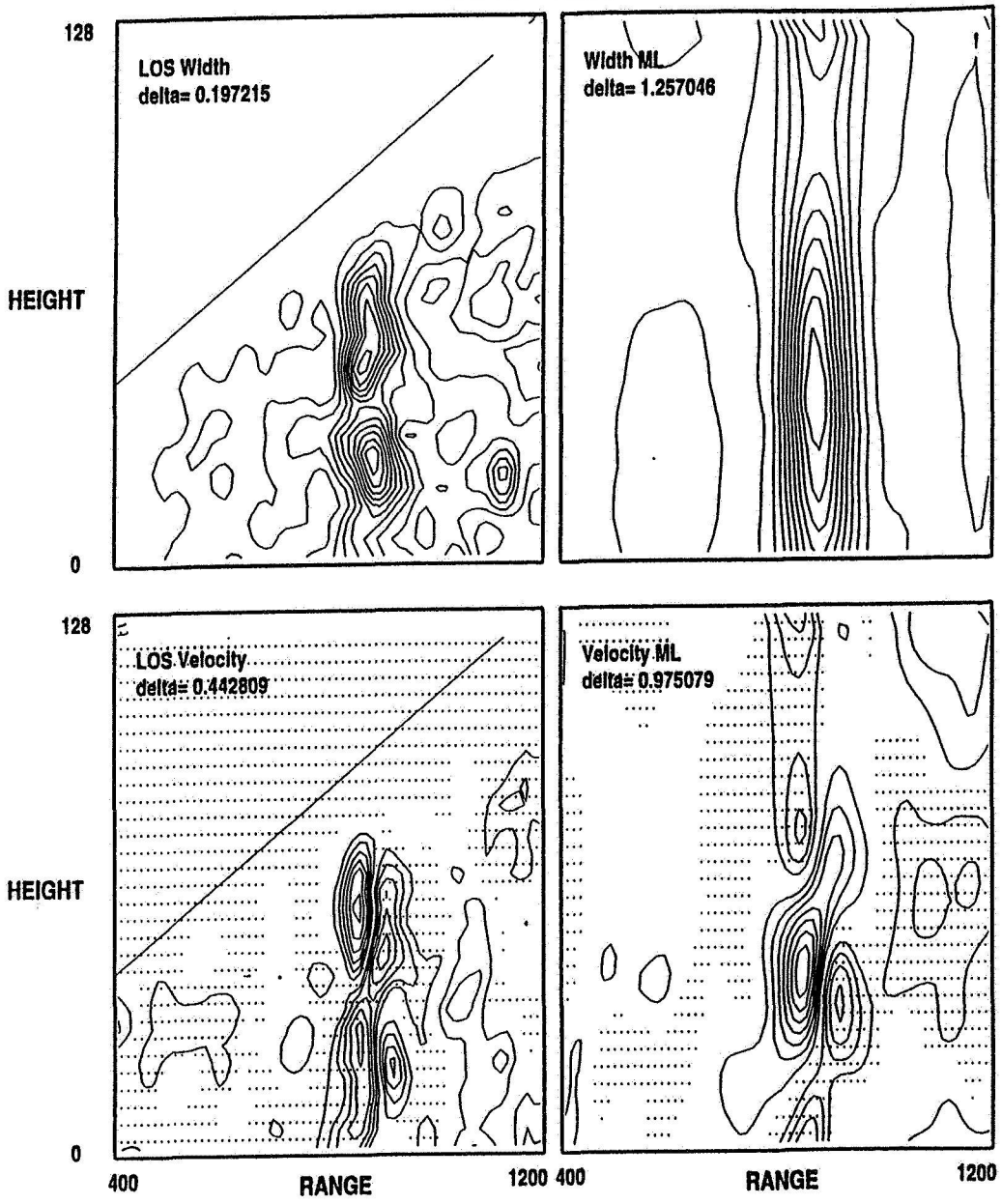

SPECTRAL PEAK PROCESSING FOR VORTEX TRACKS

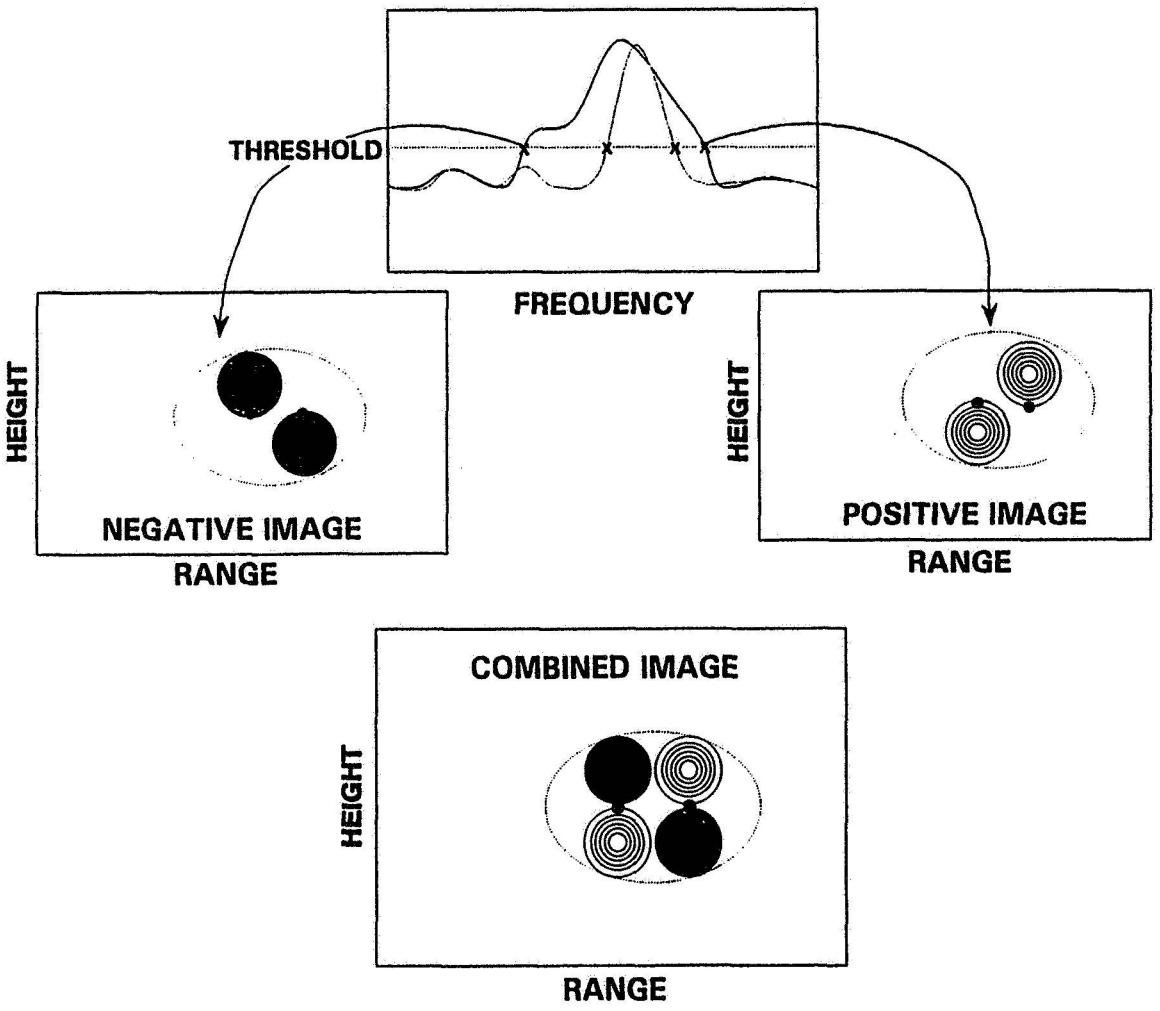

SPECTRAL TRACKING RESULTS - DC10

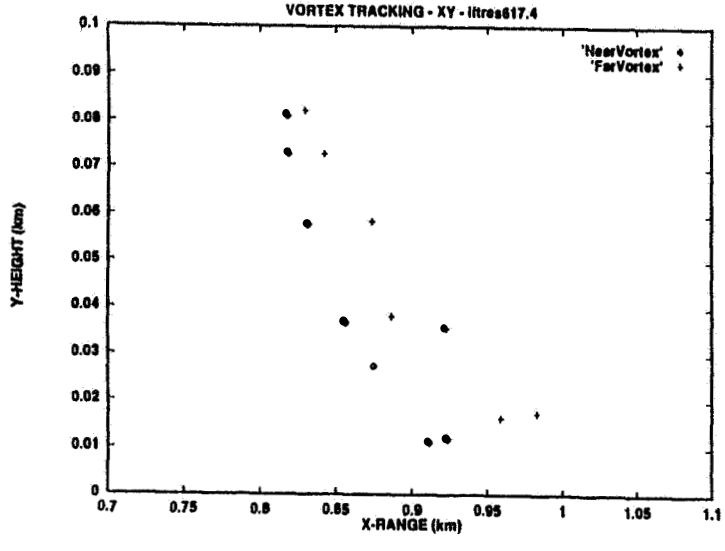

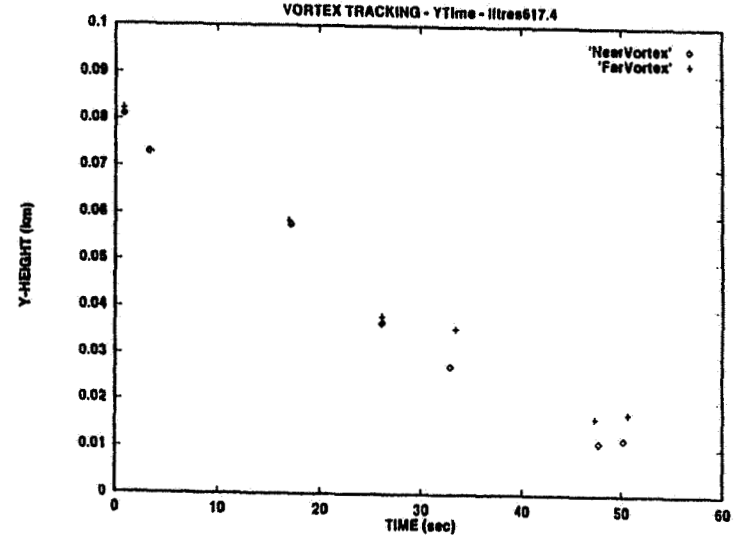

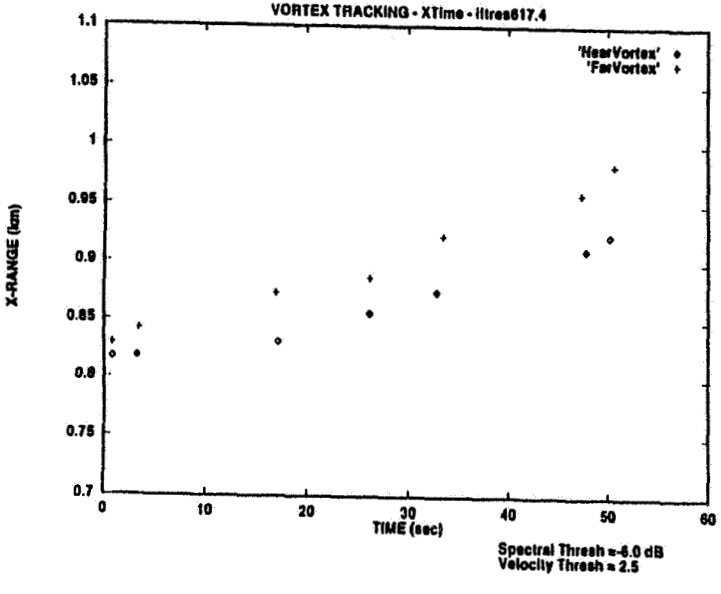

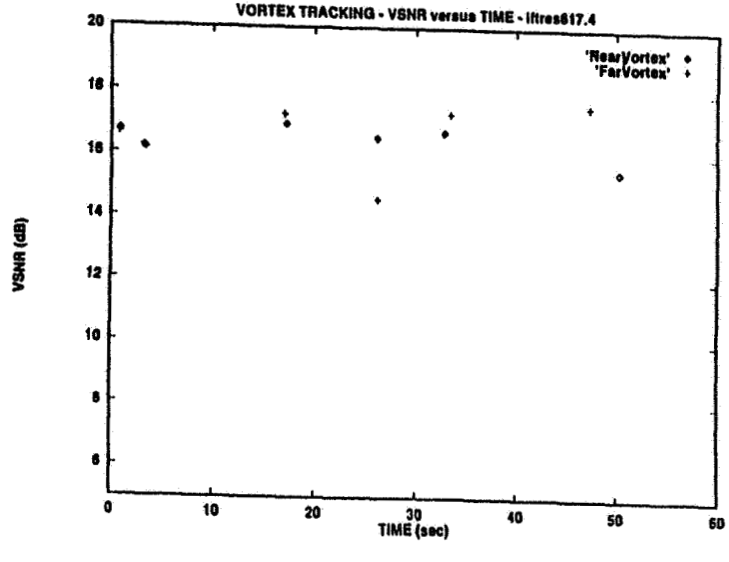

STAPLETON MEASUREMENTS—SUMMARY

- STRONG WAKE VORTEX SIGNATURES FOR MODERATE TO LARGE AIRCRAFT
  - ~300+ LANDINGS
  - DETECTION RELIABILITY DEPENDS ON ALGORITHM ROBUSTNESS

- LARGE VORTEX DATABASE COMPILED
  - THREE SCAN PLANES (ASPECT ANGLES)
  - LARGE AMOUNT OF METEOROLOGICAL DATA
  - CORRELATIONS BETWEEN ENVIRONMENT AND WAKE PERSISTENCE

- MULTIPLE SCAN PLANES CAN POTENTIALLY BE USED TO DETERMINE AXIAL FLOW SIGNATURE
  - DATABASE SHOULD BE USEFUL TO ASSESS AXIAL FLOW: ANALYSIS NEEDED

SUMMARY OF DC10 WAKE VELOCITY VALUES AS A FUNCTION OF MEASUREMENT ASPECT ANGLE

Aspect Angle	Max Shear[1] (m/sec)	Max Pos Excursion[2] (m/sec)	Max Neg Excursion[2] (m/sec)	Excursion Δ (m/sec)
90°	20.3	12.5	-7.0	19.5
43°	22.0	11.7	-7.8	19.5
23°	25.5	13.3	-9.4	22.7

All values estimated from spectral content approx. 8 dB below peak
[1]Velocity shear over less than 100 m
[2]Relative to ambient mean

PLANS

- DATA ANALYSIS
  - SIGNIFICANT DATA BACKLOG
  - IMPLEMENT SPECTRAL MATCHED FILTER
  - DEVELOPMENT OF KALMAN APPROACH FOR TIME-SERIES VORTEX MEASUREMENTS
  - CORRELATE TRACKS AND WAKE CIRCULATION STRENGTH WITH ENVIRONMENTAL PARAMETERS
  - AXIAL FLOW ANALYSIS

Doppler Radar Detection of Vortex Hazard Indicators.

J. Nespor, E. Hudson, and R. Stegall,
Government Electronic Systems,
Martin Marietta,

and

J. Freedman,
MITRE Corp.

ABS: next page

DOPPLER RADAR DETECTION OF VORTEX HAZARD INDICATORS

J.D. Nespor, B. Hudson, R.L. Stegall and J.E. Freedman*
Government Electronic Systems
Martin Marietta MS 108-102
Moorestown, NJ 08057

*Current Affiliation: The MITRE Corporation, McLean,VA

ABSTRACT

Wake vortex experiments were conducted at White Sands Missile Range, NM using the AN/MPS-39 Multiple Object Tracking Radar (MOTR). The purpose of these experiments was twofold. The first objective was to verify that radar returns from wake vortex are observed for some time after the passage of an aircraft. The second objective was to verify that other vortex hazard indicators such as ambient wind speed and direction could also be detected. The present study addresses the Doppler characteristics of wake vortex and clear air returns based upon measurements employing MOTR, a very sensitive C-Band phased array radar. In this regard, the experiment was conducted so that the spectral characteristics could be determined on a dwell to-dwell basis. Results are presented from measurements of the backscattered power (equivalent structure constant), radial velocity and spectral width when the aircraft flies transverse and axial to the radar beam. The statistics of the backscattered power and spectral width for each case are given. In addition, the scan strategy, experimental test procedure and radar parameters are presented.

INTRODUCTION

The need to provide protection against wake vortex-induced turbulence hazards necessitates imposing large separations between heavy jets and other aircraft, resulting in a major constraint on ATC system capacity. In truth, an actual wake vortex hazard is rarely present—occurring only when ambient winds along the approach path are too weak to rapidly dissipate the vortices. Since today's ATC system lacks a sensor system that can indicate presence or absence of the wake vortex hazard, it must always be assumed that the hazard is present and the cost of reduced capacity is borne in the interest of safety. Previous research with microwave doppler radar has suggested the potential of this technology to monitor the winds and detect turbulence even in clear air conditions. This capability, if combined with the flexibility produced by the beam agility of phased array antennas, offers hope for an operational sensor system that can support an all-weather fail-safe solution of the vortex problem. This solution could be accomplished in the following three ways. First, radar can provide doppler wind field measurements covering the terminal area which, when combined with data from other meteorological sensors present, can enable highly accurate mesoscale, short-term wind condition forecasts. These forecasts looking 20 to 30 minutes ahead provide the lead time needed for air traffic controllers to adjust traffic separations to the vortex hazard as indicated by forecasted wind speed and direction in the final approach corridor. Second, the radar could perform continuous real-time monitoring of the wind conditions actually occurring along the final approach path, providing a means for verifying the forecasted hazard level and if necessary alerting the controller to increase separations. Third, for ultimate protection, the radar could provide a means for actually detecting the vortices and determining decay rate and motion and, if necessary, alerting the controller to wave-off the approaching aircraft.

The above described possibilities have stimulated interest in including wake vortex protection as a functional requirement for the FAA's recently announced Terminal Area Surveillance System (TASS). Encouraged by such interest, the Martin Marietta Co. has conducted an informal series of cooperative experiments with the White Sands Missile Range (WSMR) exploring the feasibility of including vortex protection functionality in an advanced multifunction terminal radar as envisaged for TASS. The aircraft test vehicles were limited to small jet aircraft (A-7), as heavier aircraft were not available. The sensor used was the AN/MPS-39, a C-Band pulse doppler phased array radar originally developed by MM for the WSMR range instrumentation complex. The AN/MPS-39 is an excellent tool for exploring how beam agility can be exploited to provide prediction, detection and location of vortex hazards for a multifunction airport radar. This paper reports on the experimental results. It first reviews the physical basis underlying the application of microwave radar to the vortex problem, then describes the test radar and the experimental setup. It then goes on to present results, recommendations for further work, and finally conclusions.

WAKE VORTEX AND OPTICALLY CLEAR AIR PHENOMENOLOGY

Scattering from fluctuations in the refractive index of the atmosphere has provided a very powerful tool in the application of radars to clear air turbulence (CAT) investigations. It has been clearly established [1] [2] and widely accepted that high powered, very sensitive microwave radars can detect echoes caused by backscattering from inhomogeneities of the refractive index in the atmosphere. The backscattered power is related to the intensity of the fluctuations in the refractive index within a narrow range of turbulent eddy sizes centered at one-half the radar wavelength. This region is known as the inertial subrange of the turbulence.

The theory of scattering of electromagnetic waves from refractive index in homogeneities has been developed by Tartarski. [3] For homogeneous and isotropic turbulence, Tartarski has shown that the structure constant can be expressed as $D_n(r) = C_n^2 r^{2/3}$. The scattering mechanism from homogeneous and isotropic turbulent media is similar to Bragg scatter in that a radar of wavelength λ scatters from a particular component of turbulence with eddy sizes equal to $\lambda/2$ [4]. Ottersten [5] has derived the following expression relating volumetric reflectivity to the intensity of refractive index variations:

$$n = 0.38\, C_n^2\, \lambda^{-1/3} \qquad (1)$$

where C_n^2 is the structure constant and is a measure of the intensity of the refractive index fluctuations, and λ is the radar wavelength. It has been established by Chadwick [6] et al. that the scattering model for clear air turbulence is applicable to scattering from wake vortex induced turbulence. In other words, the vortex induced turbulence is created at scale sizes of 5-10 meters during the wing tip roll-up process and then fractures to smaller sizes as the vortex dissipates. When the vortex induced turbulent scale size dissipates to the point where it becomes on the order of half the radar wavelength, the radar backscattered power then becomes proportional to the refractive index fluctuations.

For turbulence associated with wake vortices, the characteristics of the vortex are generated primarily by a discontinuity in the air flow traversing the wings. This causes a vortex flow to be shed along the wing tips. The velocity gradients that are generated across the width of the vortex core are the primary contributor to the refractive index fluctuations. The entrainment of the heat emissions and water vapor

from the engines leads to increased fluctuations in the refractive index of the vortex as it propagates through the atmosphere behind the aircraft producing it [7].

Continuous real-time monitoring of the low-altitude wind speed and direction has been demonstrated with the AN/MPS-39 radar. We believe the sensitivity of this radar to monitoring wind speed and direction results from refractive index inhomogeneities caused by convective cells produced by the heating of the earth's surface, as well as particulate scatter from small millimeter sized particles such as dust and insects which may be lifted by buoyant air parcels rising from the heated surface of the earth. Due to the size and nature of these particles, they are accurate tracers of air motion up to the boundary layer. It should be noted that there may be seasonal and geographical variations in the scattering mechanisms that produce the radar echoes for mapping the low altitude winds. This is an area that needs to be investigated further.

DESCRIPTION OF MULTIPLE OBJECT TRACKING RADAR (MOTR)

Background

The AN/MPS-39 Multiple Object Tracking Radar (MOTR) is a new precision instrumentation system designed to support range safety, weapon development, operational test and evaluation, and training exercises involving multiple participants. The first MOTR was delivered to the U.S. Army's White Sands Missile Range (WSMR) in May 1988 where it underwent extensive field testing culminating in final government acceptance in December of that year. Since then three other MOTR radars have been delivered to various DoD test ranges around the country. A photograph of the radar is shown in Figure 1.

Technical

The MOTR's transmission lens phased array antenna, mounted on an elevation over azimuth pedestal, enables it to accurately track up to ten targets while simultaneously processing two surveillance beams. Accuracies better than 0.2 mil rms angle and 1.0 yd rms range are achieved while tracking a 20 dB or greater signal-to-noise ratio target. A 5.0 dB or better signal-to-noise ratio is obtained while tracking a 6 inch diameter sphere with a 1.0 micro-second pulse width at 100 kiloyard range. MOTR is fully coherent and has built-in clutter suppression capability. The radar is mobile, and its design is based on Inter-Range Instrumentation Group (IRIG) timing, transponder, and frequency standards. Table 1 lists important MOTR system parameters.

As can be seen from Table 1, the radar has the following unique features that make it very well suited for vortex detection experiments:

1) High peak transmit power of 1 MW for high sensitivity.

2) Antenna beamwidth of 1° for good angular resolution of targets.

3) Very low antenna sidelobes -45 dB rms for reduced sidelobe clutter contamination.

4) Variable pulsewidth between 0.25 μsec and 1 μsec. This corresponds to variable range resolutions of between 37.5 meters to 150 meters.

5) The ability to electronically steer the beam reduces ground clutter contamination.

6) High system stability for high doppler resolution.

Modifications

MOTR software was extensively modified to support the wake vortex experiments and these changes have permanently been made part of all existing systems. MOTR additions consisted of a new mode to enable disk recording of 36 range gates of coherent in-phase and quadrature sum channel data and angle scan modifications to permit dwells of up to 256 pulse repetition intervals.

WSMR WAKE VORTEX EXPERIMENTAL OVERVIEW

During January-February of 1991, the AN/MPS-39 MOTR at WSMR, NM was used to conduct wake vortex detection experiments. Weather conditions during this time were characterized by mild daytime temperatures, rising to 55-60 degrees Fahrenheit on the average, with generally light winds. In general, during the winter months, the two dominant type air masses influencing WSMR weather are modified Maritime Polar and Modified Continental Arctic. The modified Maritime Polar was the system that dominated the weather patterns during this time. No precipitation in the region occurred during the days when fly-bys were being conducted.

Experiments were conducted using A-7 fighter aircraft flying out of Holloman, Air Force Base. Figure 2 is an elevation view of the geometry of the experiment. Figure 3 shows the location of the two space points that the aircraft flew through relative to the radar. Space Point 1 was located 3 kyds directly north of the radar, and space point 2 was located 3 kyds directly west of the radar. The aircraft flew a clockwise racetrack flight pattern and was vectored to the appropriate space point and altitude by the WSMR control tower. The experiment was set up such that the radar looked axially behind the aircraft for vortices as it flew through space point 2, and looked transverse to the aircraft flight direction as it flew through space point 1. The aircraft flew at an approximate speed of 180 knots with both flaps and landing gear down to simulate as close as possible a landing configuration. Each mission was composed of three separate data collection modes. These consisted of a pre-mission, target mission, and post mission data collection mode. The pre-mission data collection mode was performed approximately 15 minutes before the aircraft arrival. The intent was to record data on clear air returns prior to the aircraft's arrival. Data was then collected for at least 30 seconds immediately before the aircraft flew through the beam and for at least one minute after the aircraft flew through the beam. Another post-mission data collection mode was then taken for two minutes to determine the ambient wind conditions after the fly-by. Before and after each mission, a call was placed to the WSMR weather station located a half mile from the radar so that the temperature, humidity, pressure, wind speed and direction both at the surface and aircraft altitude could be monitored and used in subsequent data analysis. Visual observations were made of the two space points with personnel using binoculars during the entire mission. Two observers were employed; one monitored space point 1 and the other space point 2 for birds, insects, etc., flying through or around the beam.

Figure 4 shows the scan pattern employed by the radar for the axial passes (looking due west to space point 2). The radar electronically scanned a 3x3 array, the aircraft was vectored through the top middle beam. This scan strategy facilitated vortex detection even when the cross winds were strong enough to blow the vortex into the adjacent beams or, as they sank into the lower beams, when the wind conditions

were calm. Figure 5 shows the scan pattern employed by the radar for the transverse pass when the radar was looking due north to space point 1. For this scan, the radar electronically scanned a 6x1 array. The aircraft flew through the third beam from the top. This allowed for some uncertainty in the aircraft's altitude as it flew through the beam, and also allowed the vortex to be detected as it sank into the lower beams.

Data collection modes for clear air mapping were very similar to the vortex scan modes discussed above except the tests were conducted without an aircraft fly-by. Data was collected for up to three minutes in this mode at space points 1 and 2.

DATA ANALYSIS AND RESULTS

Table 2 compares the vortex characteristics of the A-7 aircraft used for this experiment against other well known aircraft types. As Table 2 indicates, the circulation strength of the vortex produced by the A-7 is significantly less than all the other aircraft presented. This is primarily a function of the lighter weight of the A-7 aircraft. With this in mind, this section presents the spectral characteristics of what is believed to be a vortex detected when the A-7 aircraft flew through space point 2 (axial to the beam). While several passes were conducted on this day with the A-7 aircraft, the pass presented herein represents the only data set collected to date that has been usable. This is because of experimental problems that occurred on the other passes on this day. Subsequently, constraints on range or aircraft availability have prevented us from reproducing these results. In addition, spectral characteristics from a very windy and a calm clear air day are presented.

Wake Vortex Spectral Processing

The experiment was set up such that 36 range gates were spread out over a 2 kyd range interval. Essentially, there were 18 range gates on either side of the designated space point. The radar was operating with a 1 microsecond pulse and a 1280 Hz pulse repetition frequency. For each range gate, 128 I & Q samples were recorded for each of the nine or seven beams at a given space point. Thus, the dwell time for each beam was 0.1 seconds, and each beam was revisited every 0.9 seconds over the course of a given data collection period. A 256 point FFT was then performed for each of the 36 range gates for all nine beams over the entire data collection interval. The time series data was weighted by minimum three-term Blackman-Harris weights to push the sidelobes below -70 dB. The periodogram at each range gate was then used to estimate the first three central moments such that

$$\hat{P} = \sum_{i=1}^{N} S(v_i) \tag{2}$$

where $\hat{P}$ is the estimate of backscattered power and N is the number of spectral lines. The backscattered power in dBsm was then converted to an equivalent structure constant C_n^2.

$$\hat{v} = \frac{\sum_{i=1}^{N} v_i S(v_i)}{\sum_{i=1}^{N} S(v_i)} \tag{3}$$

where $\hat{v}$ is the mean velocity estimate and N is the number of spectral lines.

$$\hat{w}^2 = \frac{\sum_{i=1}^{N} (v_i - \hat{v})^2 \; S(v_i)}{\sum_{i=1}^{N} S(v_i)} \tag{4}$$

where $\hat{w}^2$ is the spectrum width estimate, $\hat{v}$ is the mean velocity estimate and N is the number of spectral lines.

It should be noted that care was taken to remove the undesired ground clutter spectral components before each of the first three central moments were computed. This was accomplished by removing four spectral lines on either side of the zero velocity component.

Figures 6(a) through 6(c) show "waterfall" or Doppler history plots of a vortex produced by the A-7 aircraft as it was flying axially through the top left radar beam. These plots consist of the time history of the spectral characteristics for three range gates. For these plots, negative velocities represent motion toward the radar and positive velocities represent motion away from the radar. Time increments between each spectrum are 0.9 second. On this day at the time of this mission, it was exceptionally calm at the surface and winds were reported between 1 - 2 knots at 800 feet, the approximate altitude of the aircraft. There were no birds or insect swarms reported from the visual observations made during the course of this mission. Figure 6(a) shows no vortex in range gate 14, but it does show the target saturating the receiver as it goes through the beam at this range gate. This figure also substantiates the wind conditions reported by the WSMR meteorological station. Also note that there were approximately 10 seconds of data collected before the aircraft flew through the beam. No spectra induced by vortices shed by the A-7 are evident after the aircraft flies through the beam for this range gate. The dark narrow spectral lines centered around zero velocity are ground clutter. However, for Figure 6(b) which is a spectral history for adjacent range gate 15, vortex induced spectra appear about 8 seconds after the aircraft leaves the beam at 18:07:22 GMT. Figure 6(c) which is the spectral history for range gate 16, shows a larger amplitude in the spectra and again no wind induced spectra before the aircraft flies through this gate. It appears that the vortex is in this gate for approximately 10 seconds. The two spectra, one on each side of the zero doppler, may be evidence of vortex perturbations in either direction. These have been observed from the axial structure of the vortex by other researchers [10]. In addition, the axial flow perturbations are generally small compared with the flight speed. Near the center of the vortex, there may be perturbations on the order of 15% of the flight speed. For the spectral plots presented here the radial velocities were approximately 5

knots(about 5 percent of the flight speed). However, we reiterate that relating the complex vortex physics to the spectral characteristics is somewhat difficult. The spectra produced by the vortices appear in the succeeding range gates 17 and 18 as well for this upper beam.

Figures 7(a) through 7(e) show Doppler History plots for the beam directly below the upper left beam considered above. The first range gate where the vortex induced spectral characteristic occurs is number 13. We believe the vortex produced by the A-7 aircraft is sinking into the lower beams and into the closer-in range gates. This is consistent with results reported by other investigators [8] [9]. For Figure 7(a), the first evidence of vortex induced spectra occurs at 18:07:43 GMT approximately 21 seconds after the time the vortex appears in the upper beam. It should also be noted that the target returns shown in the plots for this beam are caused by the aircraft flying in the angular sidelobes of the antenna. For adjacent range gate 14 in Figure 7(b), the spectral amplitude is larger. In range gate 15 in Figure 7(c), two sets of spectra appear. One set of spectra occure earlier than the spectra in the upper beam and the other occurs later. The earlier spectra occur at approximately 18:07:26 GMT. The coherent return appears about 17 seconds earlier than it did in the upper beam. It is expected that the vortex returns would occur earlier in time at the farther out range gates in the lower beams because the aircraft flew through the lower beams earlier in time. In range gate 16 in Figure 7(d), the spectra occurring at the later time begins to decay while the spectra occurring earlier in time but at farther out range gates begins to grow. At range gate 17 in Figure 7(e), the spectra occurring later in time are almost fully dissipated while the spectra occurring earlier is larger in amplitude. By range gate 19, the spectra occurring earlier dissipates as well. Both sets of spectra lasted for about 10 seconds.

Figures 8(a) and 8(b) are Doppler History plots for the lowest beam. The first gate where vortex induced spectra occur is in range gate 12. The time associated with this spectra is approximately 18:07:45 GMT which is about the same time that was observed for the spectra in the beam above. This could be expalined by the overlap of the antenna beams at the 3 dB points. Figure 8(b) shows the spectra getting larger in amplitude and width, which is indicative of increased backscattered power for that gate. The spectra last for about 12 seconds and are spread out spatially over range gates 12 to 17. The apparent radar cross sections of the vortices presented for each of the three beams ranged from -65 dBsm to -80 dBsm. The equivalent structure constant, C_n^2 ranged from -116.7 to -135.4 dB. The apparent cross sections tended to increase as the vortex dropped into the lower beams. This might mean that the vortex grows spatially as it decays and occupies more of the pulse volume as it dissipates with time. The larger spatial extent of the vortex within the pulse volume could possibly explain the larger apparant cross sections in the lower beams.

The mean velocities tended to range from 1.1 m/s to 4.5 m/s. Spectral width tended to stay relatively constant and ranged from 2.75 to 3.7 m/s. We believe the data presented for this A-7 axial case to be consistent with what has been generally reported about vortex characteristics. However, specific radar data sets of axial looks at aircraft are nonexistent to the best of our knowledge. This makes making definitive statements difficult.

Clear Air Spectral Processing

Figures 9(a) through 9(c) show Doppler History plots of data collected on a very windy day on 5 May 1991. The wind direction at the surface was from the west at 270 and the wind speed was 15 knots with

gusts reported to 25 knots by the WSMR meteorological station. At 800 ft., the wind speed was reported at 25 knots with gusts to 30 knots. The radar was pointed due east and scanning a 3 x 3 pattern. The radial wind velocities of each of the three time history plots correlate very well with the speed and direction reported by the WSMR meteorological station. The plots show that the winds are moving away from the radar as one would expect with the prevailing westerly winds and the radar scanning due east. In addition, Figures 10(a) through 10(c) show the histograms of the first three central moments for the data collected that day. Figure 10(b) shows the average radial velocity to be at -428.04 Hz which corresponds to a wind speed of 23 knots moving away from the radar. This again correlates quite well with the meteorological station's report. Figure 10(a) shows the average structure constant to be -139 dB for this very windy day. In addition Figure 11(c) shows the average spectral width was 91.5 Hz which corresponds to 2.5 m/s or 5 knots.

Figures 11(a) through 11(c) show Doppler History plots of the data collected on a relatively calm morning on 6 May 1991. The wind direction at the surface was from the south at 190° and the wind speed was 5 knots. At 800 ft., the wind speed was reported at 8-10 kts. The radar was pointed due north to space point 1 and was scanning a 6 x 1 pattern. The Doppler History plots show very little activity for the three highest beams except for occasional gusts. Figures 12(a) through 12(c) show histograms of the first three spectral moments for the data collected on that day. Figure 12(b) shows the average radial velocity to be at -103.9 Hz which corresponds to 5 knots away from the radar. Figure 12(a) shows the average structure constant to be -143.5 dB, and Figure 12(c) shows the average spectral width to be 95 Hz which corresponds to 5.2 knots.

DART Plot Description

The Doppler History Plot was cumbersome to use when initially examining the data since it only provided information on one small segment of the scan volume. Several additional data representations were tried for visualizing over a larger volume. We learned that one of the dimensions that was necessary to include was time. We finally settled on a representation we called a DART (Doppler-Amplitude-Range-Time) plot. Figure 13 shows this plot. Using three axes and color, variations in amplitude and frequency of the spectral peak over range and time are easily seen allowing quicker identification of a potential vortex for more detailed analysis and a visualization of clear air phenomenon. Color indicates the doppler bin that the peak of the power spectrum occurs in. If the velocity is unambiguous, motion toward the radar is indicated by blue, motion away from the radar is indicated by red, and near zero velocity is indicated by green. The vertical axis is the amplitude of the peak of the power spectrum expressed in dBsm/doppler bin, i.e., the received energy is referenced back to the scattered. Time is shown on the horizontal axis and the 36 range bins are shown on the axis coming out of the page. When an aircraft flies through a beam it shows up on the DART plot as a high amplitude ridge. The order that the range bins is shown can be reversed so that both sides of the ridge can be seen. The DART plot is generated by estimating the power spectrum, as in the Doppler History plot, for each range gate. The doppler bin with the peak amplitude is located and the doppler bin is color coded. A varying color line is then drawn connecting the peak amplitudes of the 36 range bins with values less than -100 dBsm being shown at -100 dBsm in black. The processes are repeated for each time sample.

RECOMMENDATIONS FOR FUTURE EXPERIMENTS

In the course of this experiment, it has become clear that there are a number of useful areas for continued investigation. The effort thus far has demonstrated the highly variable and dynamic characteristics of vortex induced turbulence and optically clear air returns. We recommend the following areas for future investigation:

1) Carry out a series of experiments that insure the repeatability of the radar vortex returns presented in this paper and extend the experiments to include the more representative heavy commercial aircraft such as an MD-ll or Boeing 747.

2) Carry out experiments that will identify wake vortex signatures of heavy commercial aircraft and distinguish them from ambient winds.

3) Establish the reliability of monitoring wind speed and direction from ambient winds so that the conditions for wake vortices stalling can be predicted. A long-term investigation for determining wind speed and direction at low altitudes by microwave radar should be compared to a meteorological network of wind sensors to validate the reliability of monitoring winds.

4) The maximum range of detection should be established for heavy commercial aircraft.

5) A thorough study should be carried out to determine how well microwave radars detect vortices in rain, fog and other kinds of precipitation.

SUMMARY AND CONCLUSIONS

The experiments reported herein were an exploratory, limited scale feasibility investigation. They were performed by piggybacking on other scheduled WSMR missions so that resources could be obtained inexpensively. As such, we had to use aircraft that were already at WSMR which limited the aircraft population to A-7 jet fighters. Access to a heavy jet capable of producing the hoped-for very strong vortex radar echoes could not be provided without a formal testing program. Nevertheless, the tests did show definite evidence of detection of weak vortex echoes on an axial view for even the small A-7 aircraft which has an expected vortex backscatter cross section two orders of magnitude less than a heavy jet such as a MD-ll or Boeing 747. Also, the ability of microwave pulse doppler phased array radar to efficiently monitor low-level wind conditions in clear air was demonstrated. We find that these results point toward the feasibility of a multifunction radar playing an important role in TASS as a wide area indicator of wake vortex hazards. We believe the evidence and ultimate benefits to be substantial enough to warrant a serious FAA testing program that would: 1) validate and develop further the rôle of microwave radar as a vortex hazard indicator, and 2) establish appropriate operational concepts.

ACKNOWLEDGMENTS

The authors acknowledge the significant contributions to this project made by MM Aerospace engineer L. Gereffi. We also are deeply indebted to D. Sammon, T. Stevens, and their personnel for their enthusiastic support and cooperation during tests at White Sands Missile Range.

REFERENCES

[1] K.R. Hardy, "Studies of the Clear Atmosphere Using High Power Radar", Remote Sensing of the Troposphere Symposium, ed. by V. Derr, University of Colorado, 1972.

[2] K. R. Hardy and I. Katz, " Probing the Clear Atmosphere with High Power High Resolution Radars", Proc. IEEE, p.468, April 1969.

[3] V. I. Tatarski, Wave Propagation in a Turbulent Media, McGraw-Hill, Inc., New York, N.Y., 1961.

[4] M. I. Skolnik, Introduction to Radar Systems, McGraw-Hill, Inc., New York, N. Y., 1980.

[5] H. Ottersten, " Atmospheric Structure and the Radar Backscattering in Clear Air", Radio Science, Volume 4, No. 12, Dec. 1969, pp. 1179-1193.

[6] R. B. Chadwick, J. Jordan and T. Detman, "Radar Detection of Wingtip Vortices", 9th Conference of Airospace and Aeronautical Meteorology, June, 1983, pp. 235-240.

[7] J. D. Friedman, "Airborne Wake Vortex Detection", March 1974, pp. 3-7 through 3-9.

[8] R. B. Chadwick and A. J. Bedard, Jr., Private Communications, April, 1991.

[9] W. H. Gilson, Private Communications, 1991.

[10] J. N. Hallock and W.R. Eberle, ed., "Aircraft Wake Votices: A State of the Art Review of the United States R&D Program, U. S. Department of Transportation, FAA, DOT-TSC-FAA-77-4, February 1977.

Table 1. MOTR System Parameters

Parameters	Value
Radar Frequency	C-Band (5.4 to 5.9 GHz)
Antenna:	
Directive Gain	45.9 dB
Beamwidth	1.05°
Scan Volume	60° cone plus cusps
Transmitter Power:	
Peak	1.0 MW
Average	5.0 kW
Range	0.5 to 8192 kyd
System PRF (Selectable)	80, 160, 320, 640, 1280 Hz
Object PRF (Selectable)	20, 40, 80, 160, 320, 640, 1280 Hz
Pulsewidth (Selectable):	
Non-Chirp	0.25, 0.5, 1.0 μs
Chirp (Expanded)	3.125, 12.5, 50 μs
Chirp (Compressed)	0.25 μs
Pedestal Servo:	
Position Servo	Rate-aided Type 2
Maximum Rate:	
Azimuth	800 mils/s
Elevation	300 mils/s
Maximum Acceleration	200 mils/s/s
Tracking Filters:	
Coordinates	Cartesian (XYZ)
Types	Alpha-Beta, Alpha-Beta-Gamma
Bandwidth	PRF/2 to 0.1 Hz

TABLE 2
AIRCRAFT AND VORTEX CHARACTERISTICS

AIRCRAFT CHARACTERISTICS								VORTEX CHARACTERISTICS			
Aircraft	Engine Location and Number/ Wing	Weight Lbs.	Wing Span Ft.	Area $Ft.^2$	Aspect Ratio	Take-off Speed MPH	Landing Speed MPH	Γ Vortex Strength $Ft.^2/sec$	Vortex Diameter Ft.	V_θ Tangential Velocity Ft./sec	Vortex Rate of Descent Ft./sec
B-707	Wings 2	258,000	145.75	2892	7.36	195	157	4165	10.0	132.4	5.4
B-727	Rear 3	169,000	108	1650	7.67	159	152	3309	5.3	200x	4.9
B-747	Wings 2	710,000	195.6	5500	6.95	195	163	7700	20.0[s]	122[c]	6.6
DC-9	Rear 2	108,000	89.3	914	7.40	165	154	2500	4.0[c]	200x	4.5
DC-10	Wings 1 and Rear 1	410,000	155	3550	6.8			5595	9.4[c]	190x	5.8
L-C5A	Wings 2	764,000	222.7	6200	7.20	161	150	7260	20.0[c]	115[x]	5.1
L-1011	Wings 1 and Rear 1	409,000	155	1755	6.4			5581	7.9[c]	225[x]	5.7
A-7	2	22,000	38.9			200	180	958	2.5[c]	37.7	2.25
C130	2	80,000	132.0				250	1353			

x = experimentally recorded maximum tangential velocity in tower fly-by at NAFEC

c = calculated parameter

s = estimated parameter

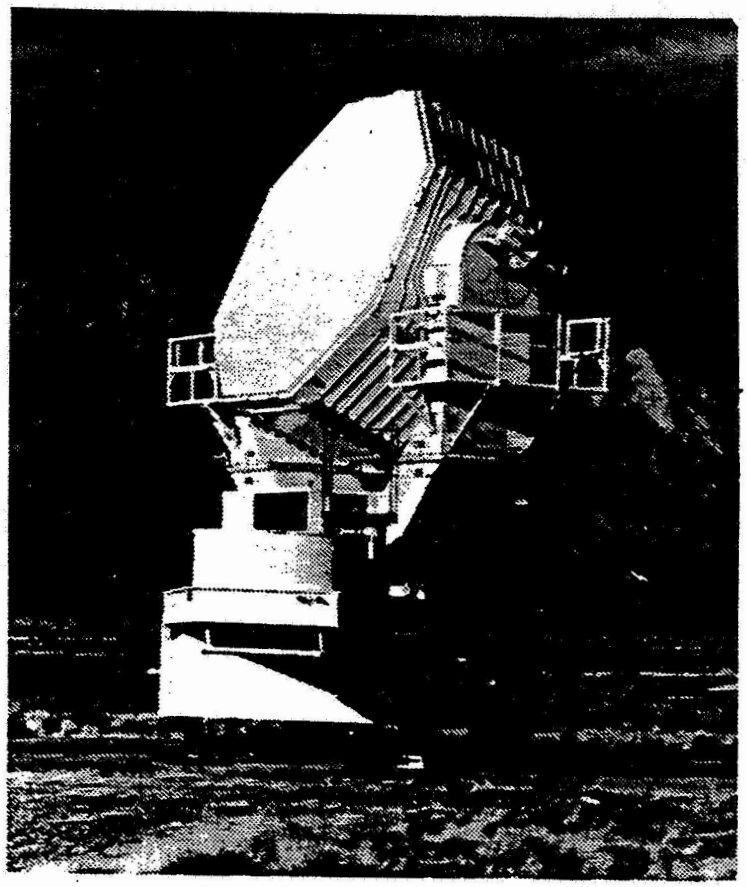

Figure 1. MOTR in Operation (US Army Photograph)

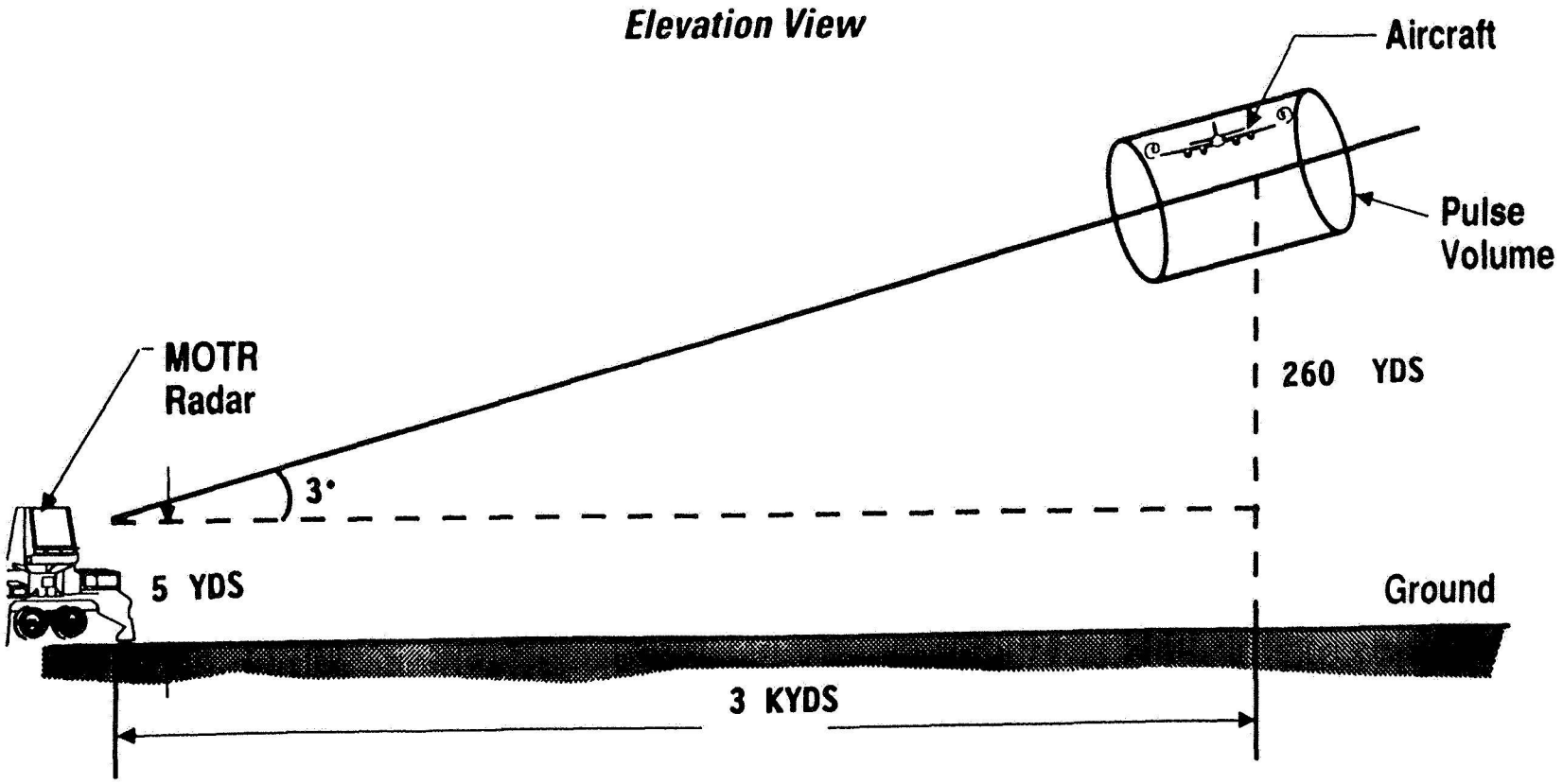

FIGURE 2 TEST SITE CONFIGURATION

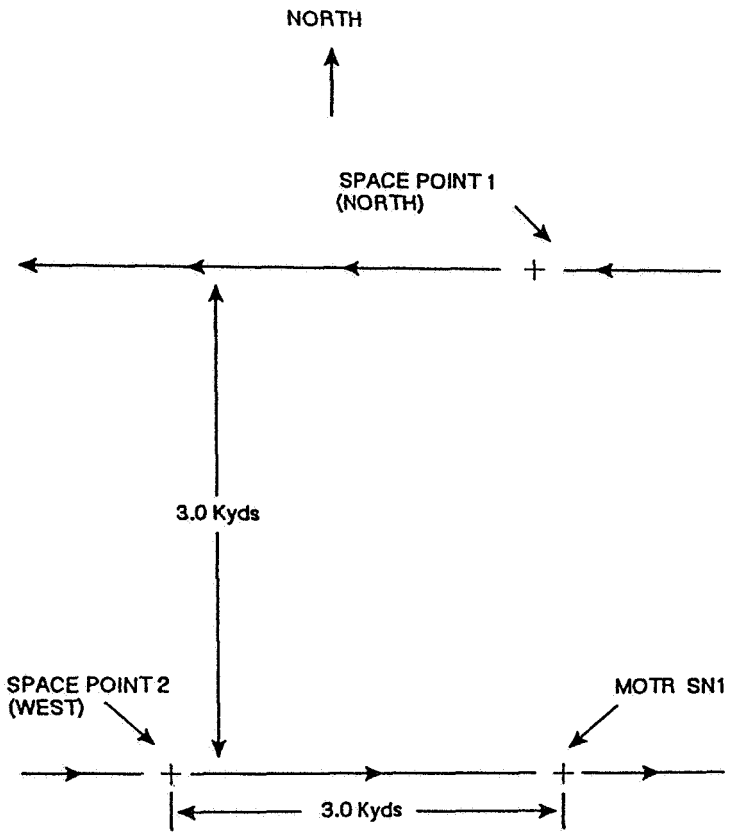

FIGURE 3
WAKE VORTEX TEST SITE LAYOUT

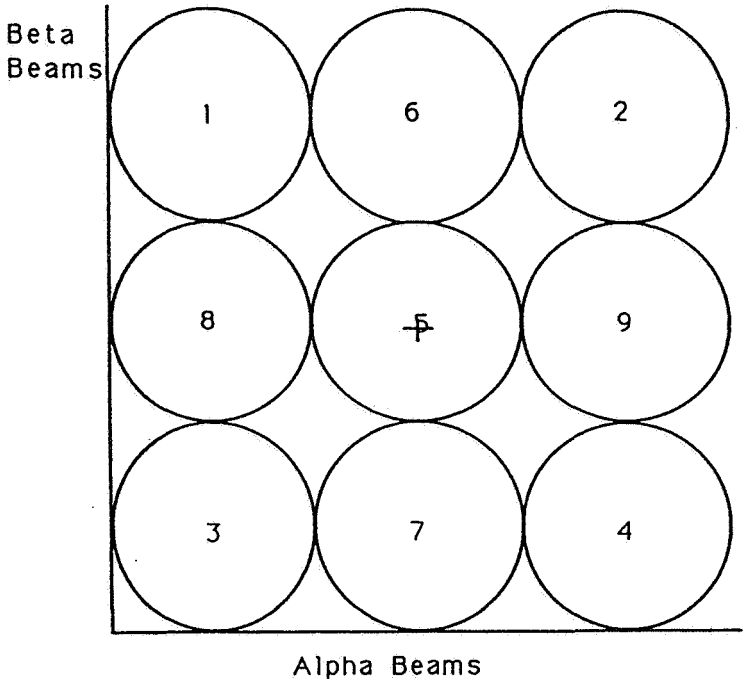

FIGURE 4 3X3 SCAN PATTERN USED FOR AXIAL PASSES

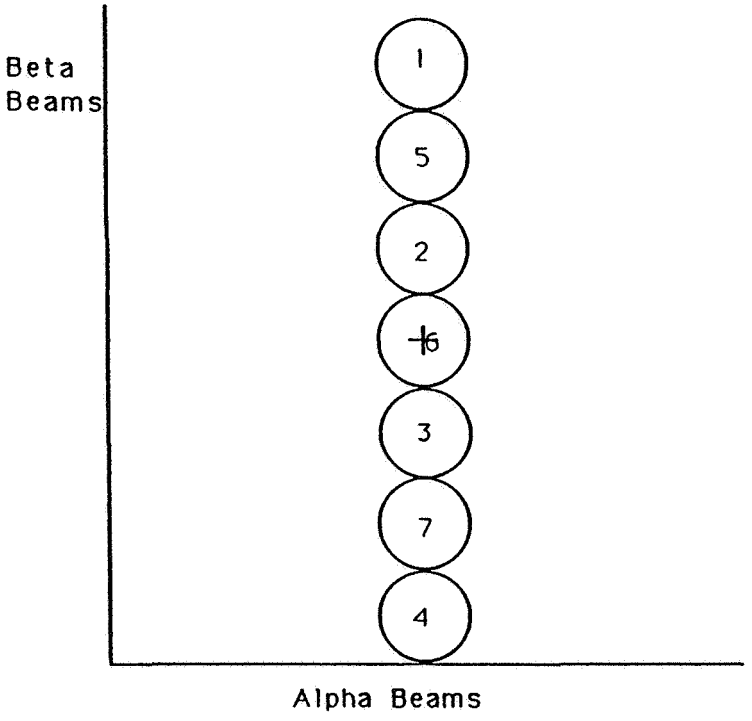

FIGURE 5 1 X 7 SCAN PATTERN USED FOR TRANSVERSE PASSES

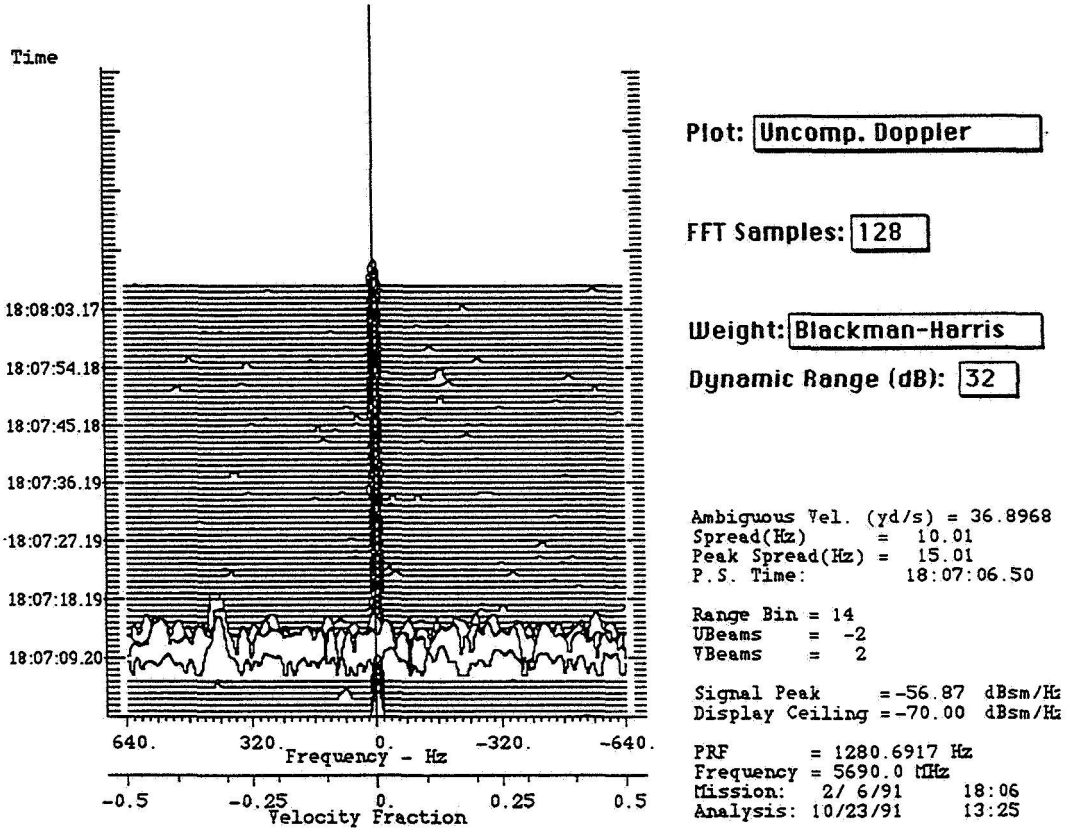

Figure 6(A). Doppler time history plot for A-7 fly-by, upper beam, range gate 14, axial case.

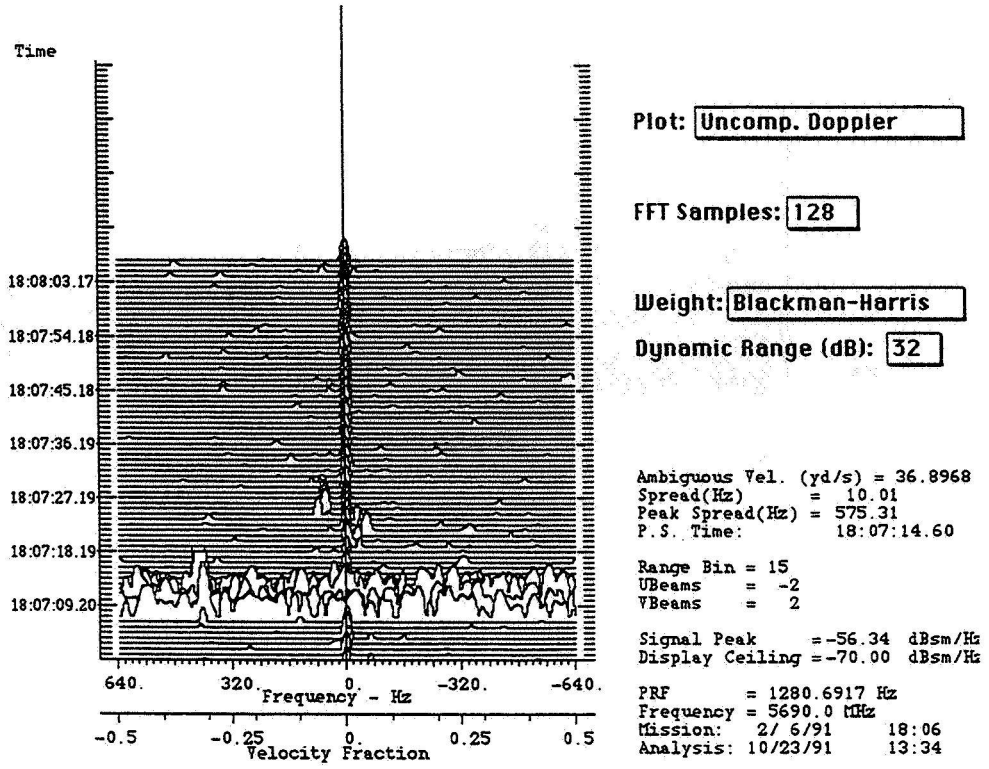

Figure 6(B). Doppler time history plot for A-7 fly-by, upper beam, range gate 15, axial case.

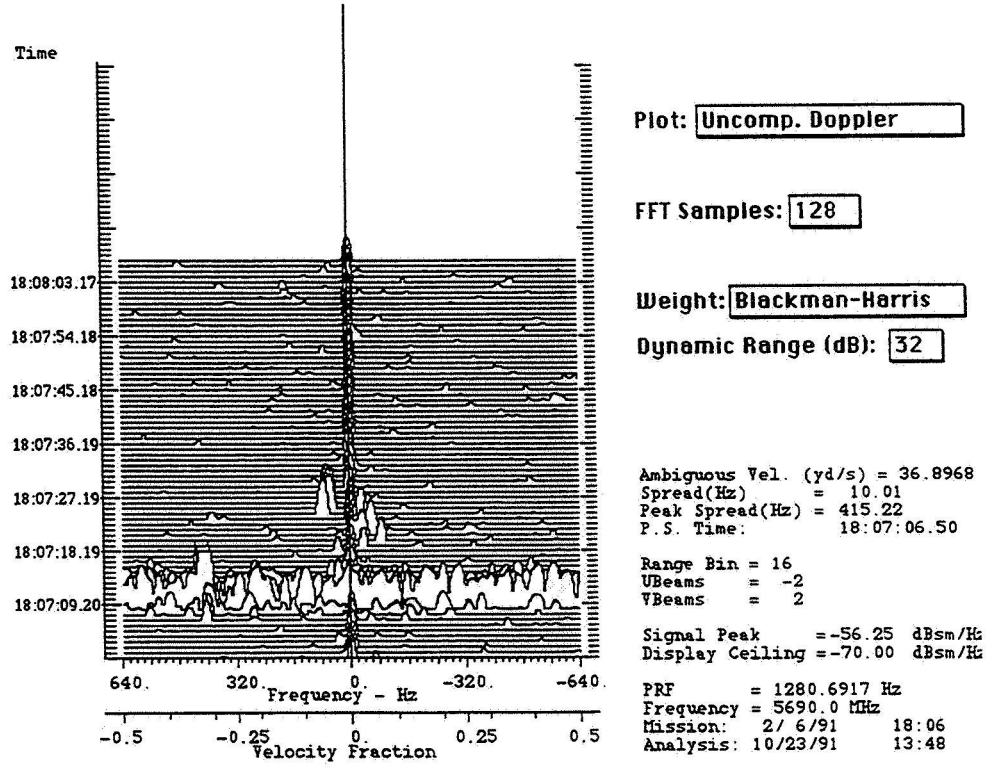

Figure 6(C). Doppler time history plot for A-7 fly-by, upper beam, range gate 16, axial case.

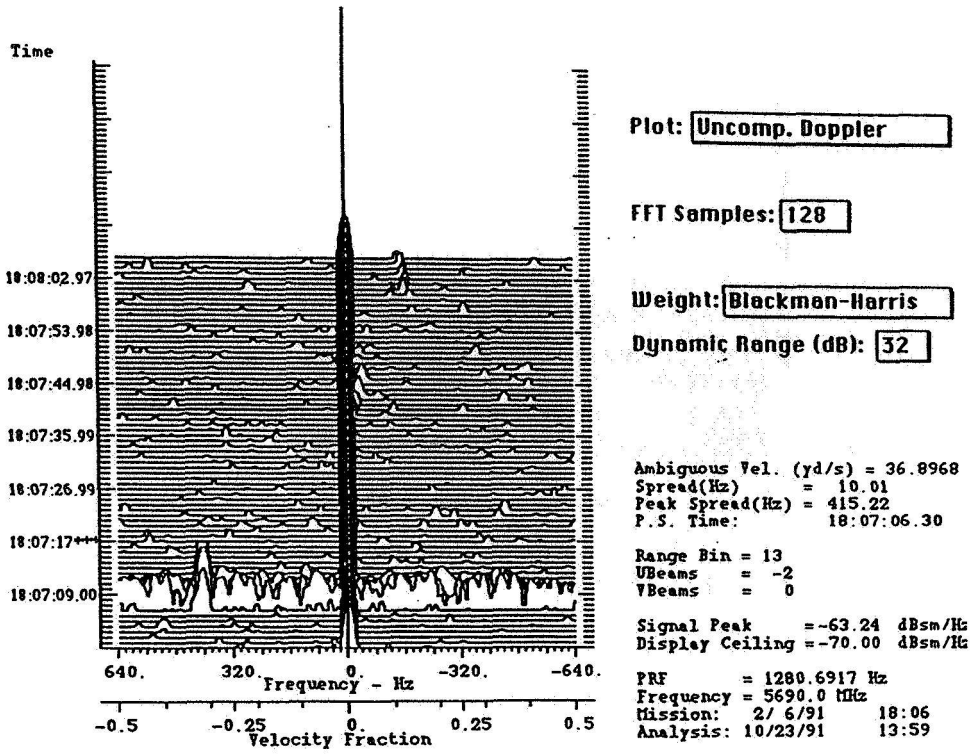

FIGURE 7(A) DOPPLER TIME HISTORY PLOT FOR A-7 FLY-BY, MIDDLE BEAM, RANGE GATE 13, AXIAL CASE

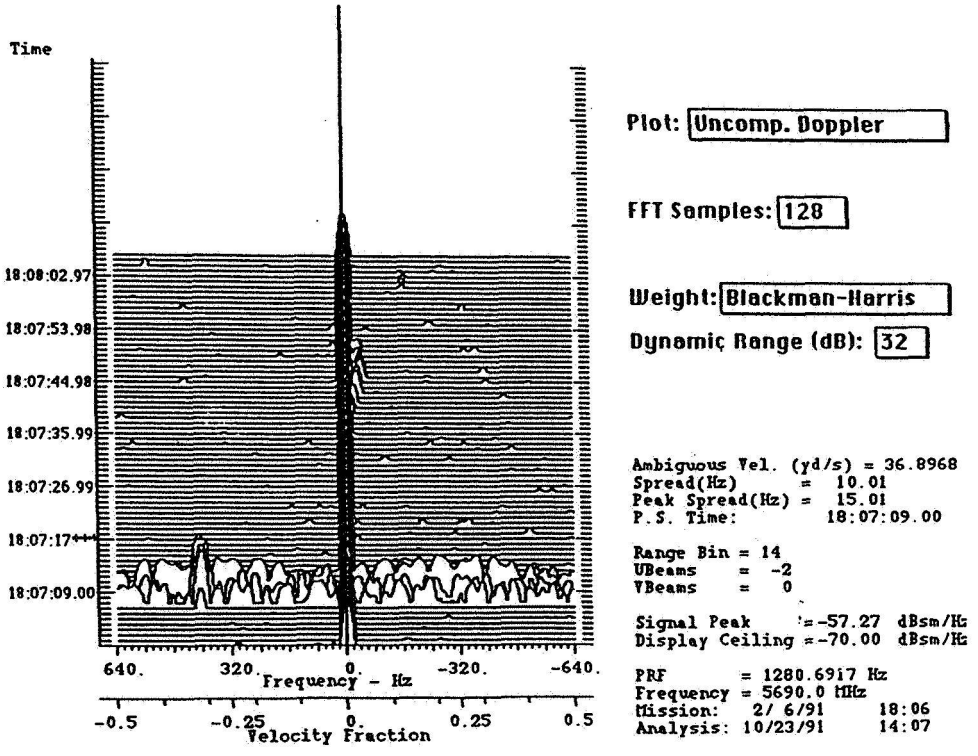

FIGURE 7(B) DOPPLER TIME HISTORY PLOT FOR A-7 FLY-BY, MIDDLE BEAM, RANGE GATE 14, AXIAL CASE

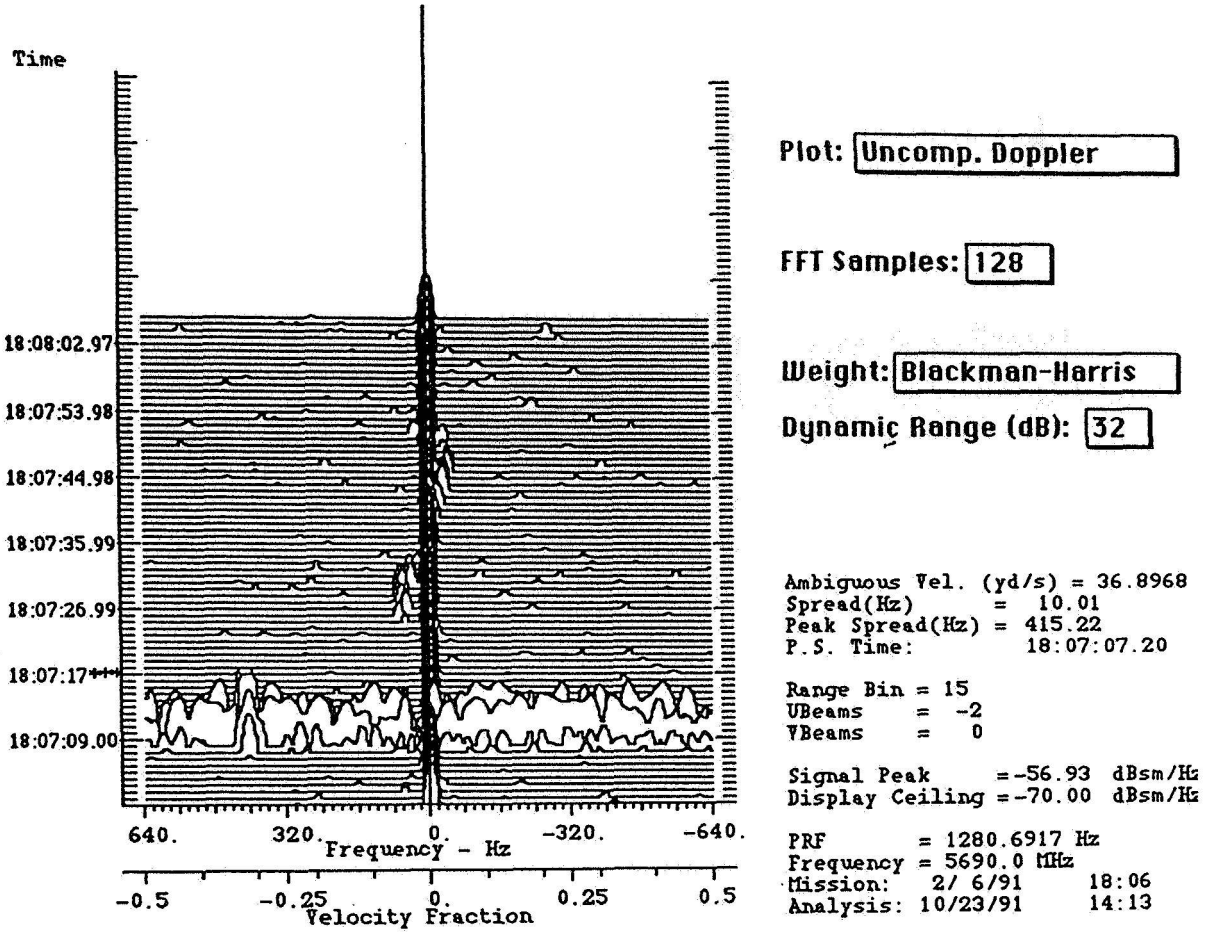

FIGURE 7(c) DOPPLER TIME HISTORY PLOT FOR A-7 FLY-BY, MIDDLE BEAM RANGE GATE 15, AXIAL CASE

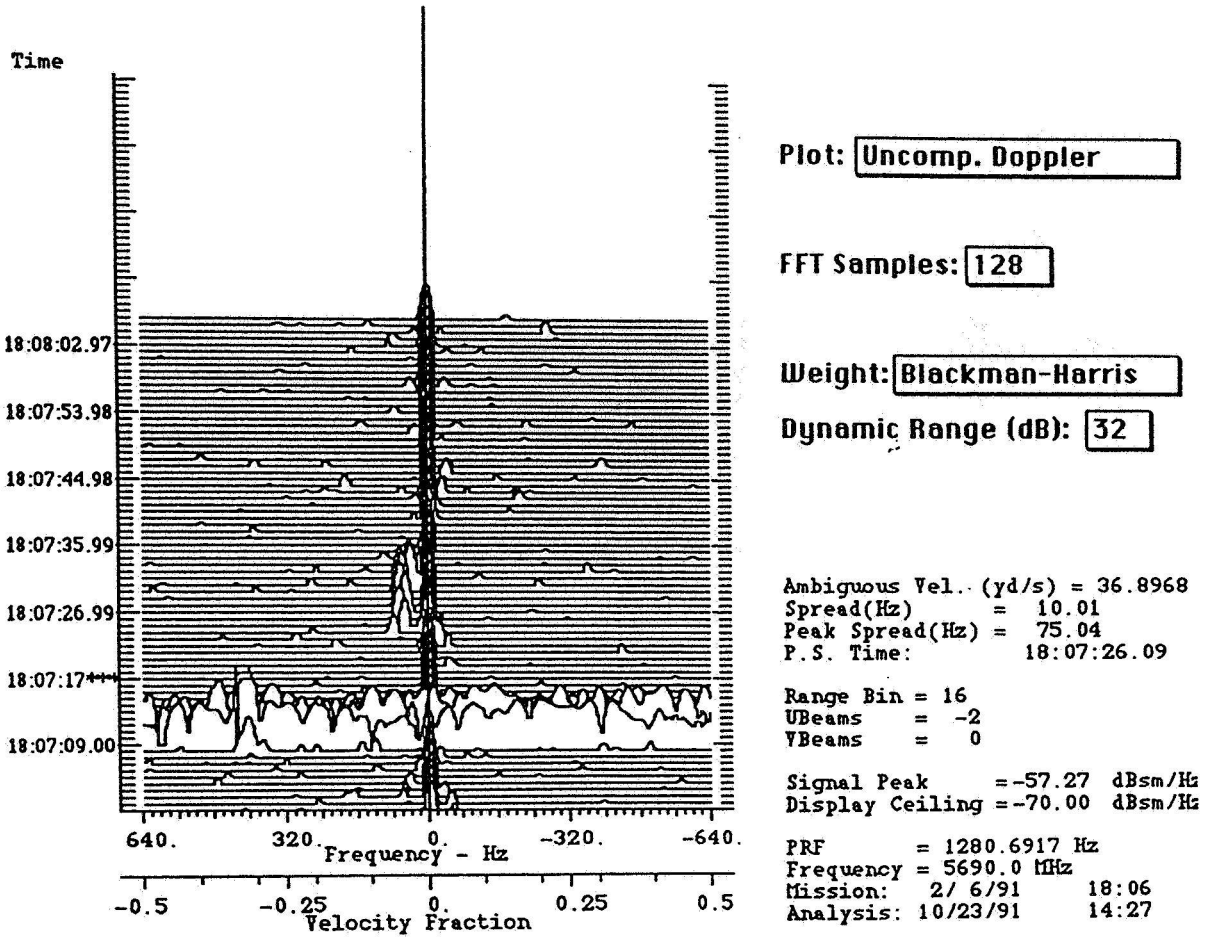

FIGURE 7(D) DOPPLER TIME HISTORY PLOT FOR A-7 FLY-BY MIDDLE BEAM, RANGE GATE 16, AXIAL CASE

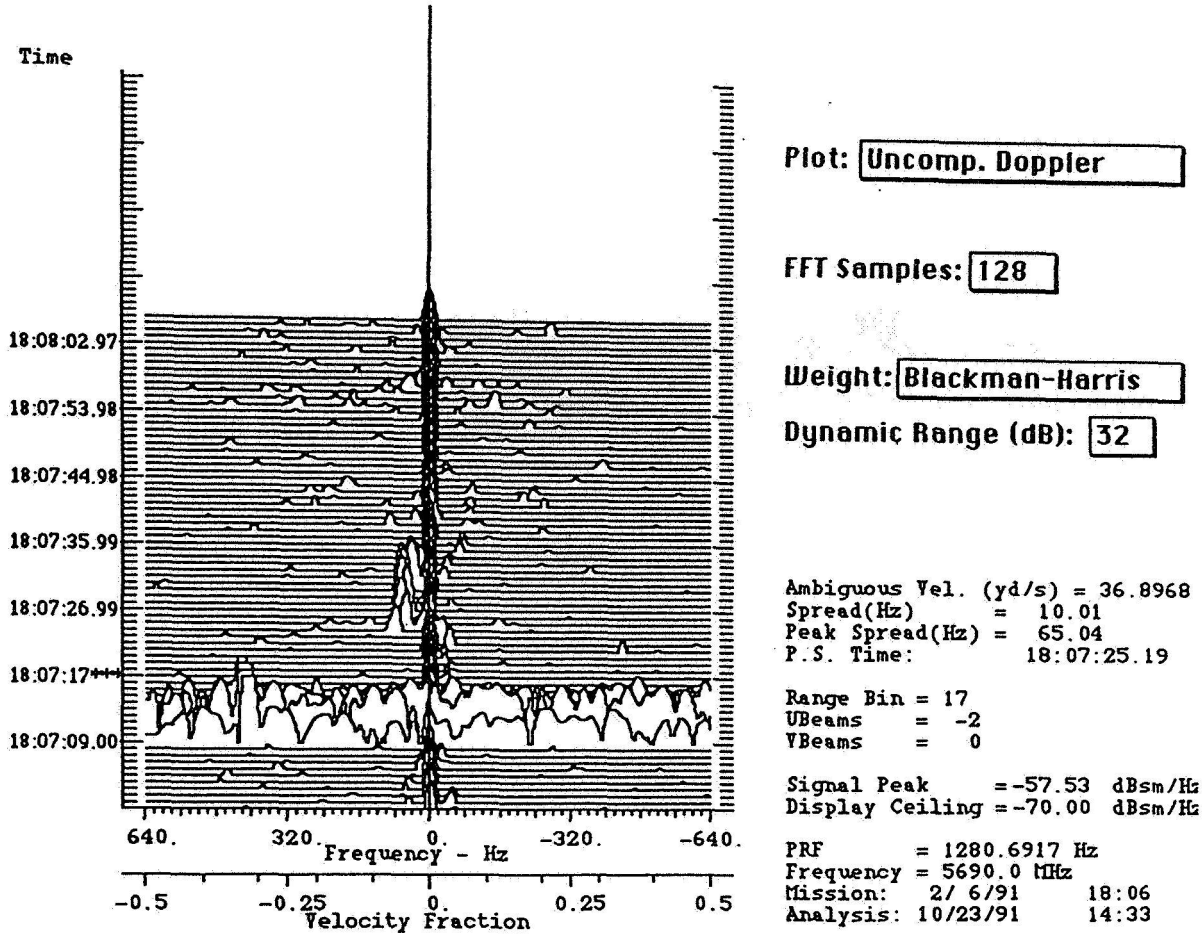

FIGURE 7(E) DOPPLER TIME HISTORY PLOT FOR A-7 FLY-BY, MIDDLE BEAM, RANGE GATE 17, AXIAL CASE

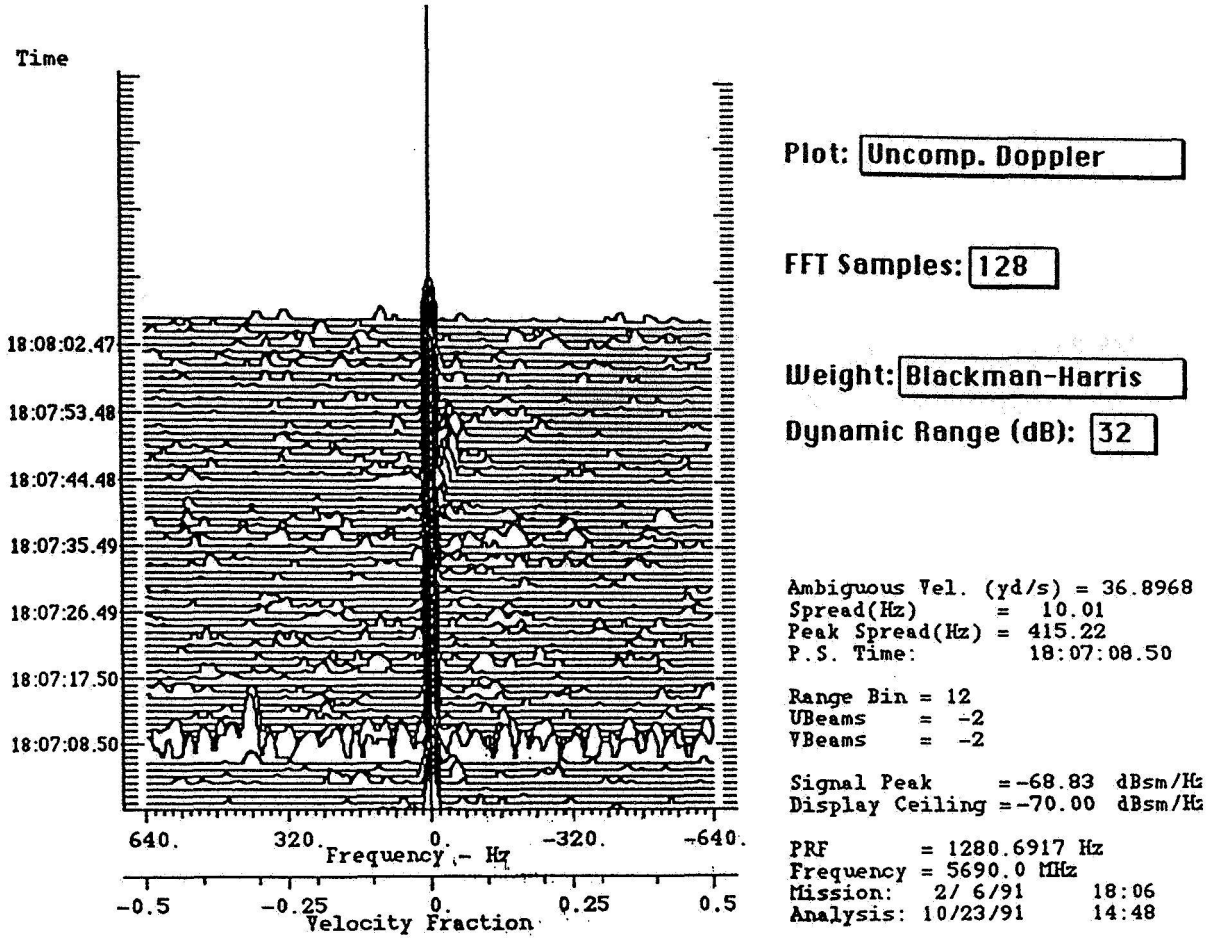

FIGURE 8(A) DOPPLER TIME HISTORY PLOT FOR A-7 FLY-BY, LOWER BEAM, RANGE GATE 12, AXIAL CASE

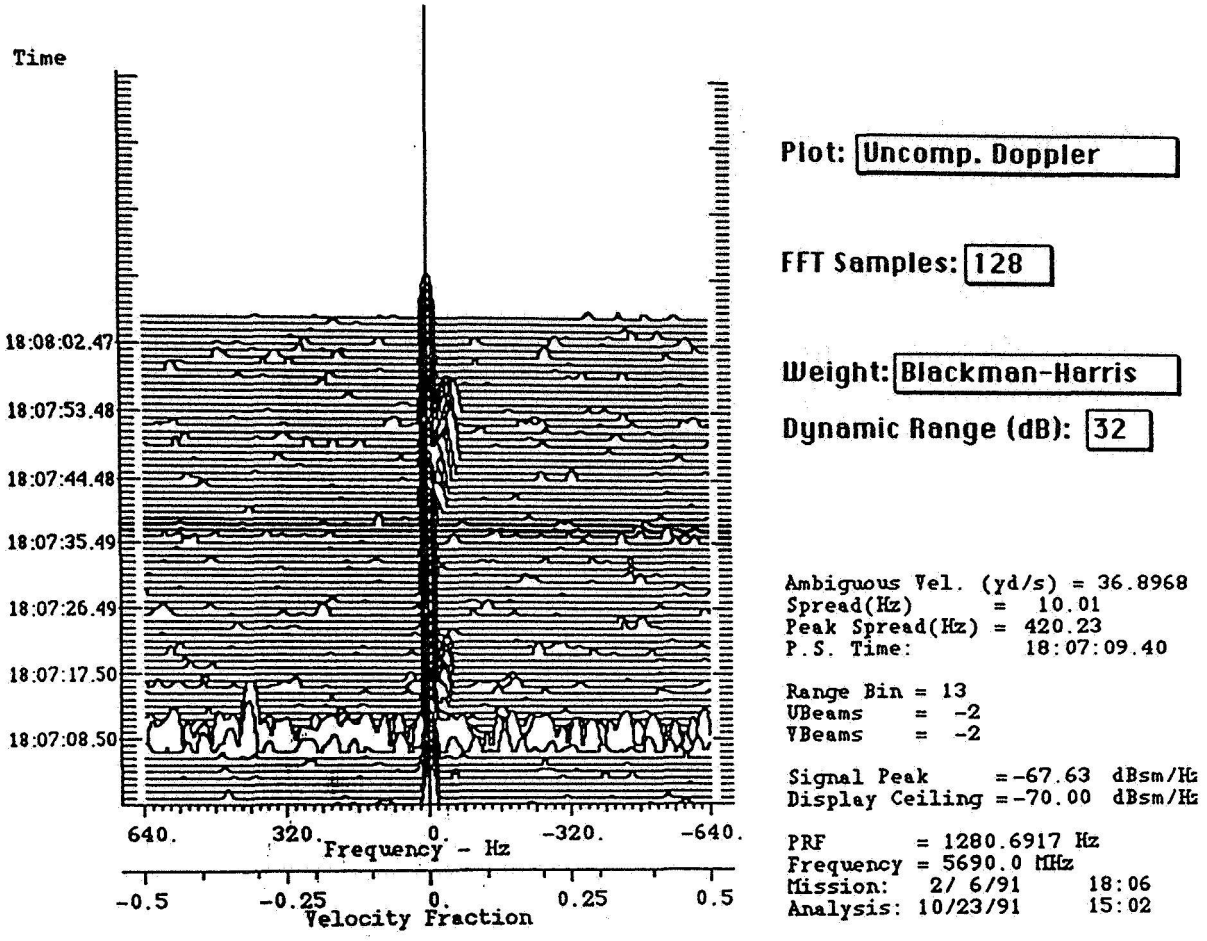

FIGURE 8(B) DOPPLER TIME HISTORY PLOT FOR A-7 FLY-BY, LOWER BEAM, RANGE GATE 13, AXIAL CASE

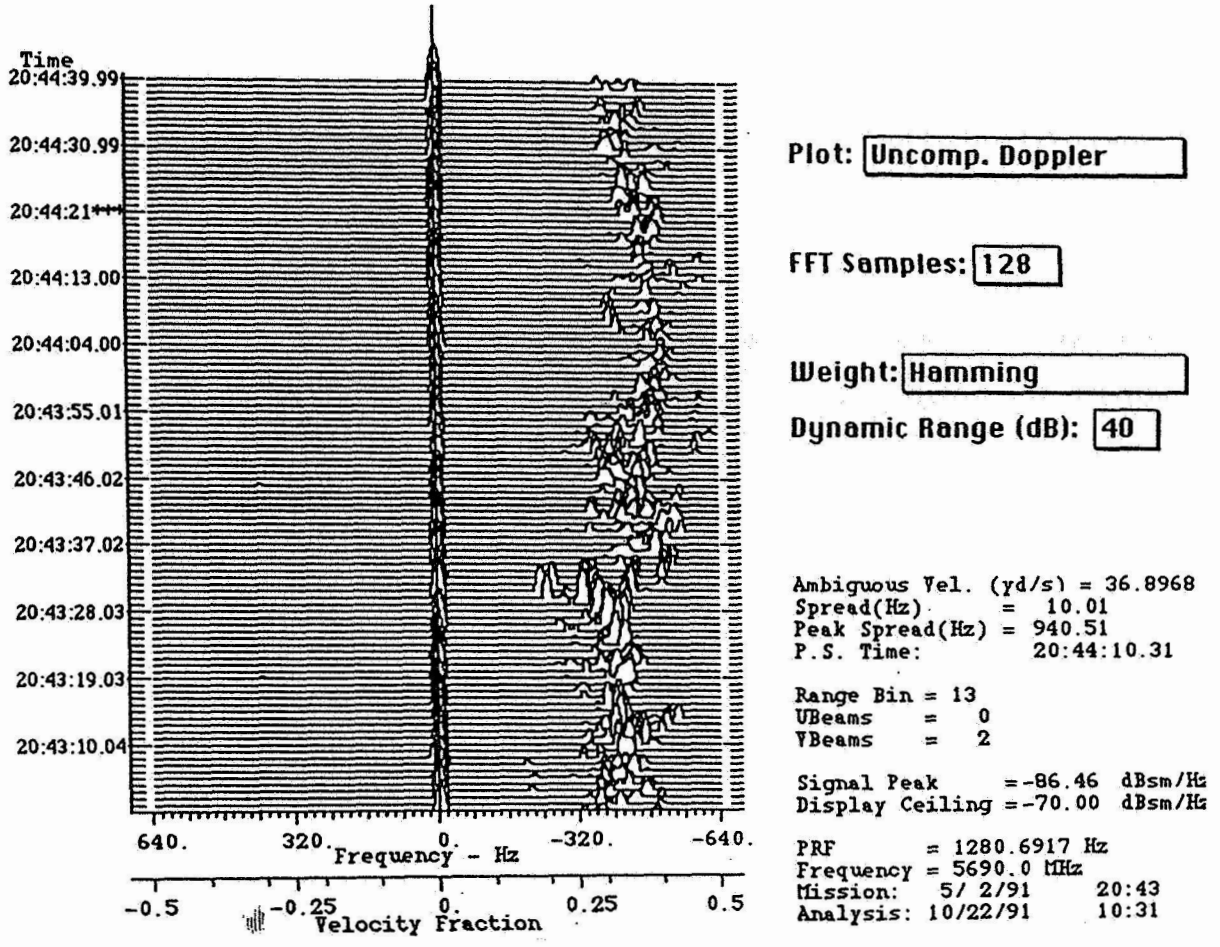

FIGURE 9(A) DOPPLER TIME HISTORY PLOT FOR WINDY DAY, UPPER BEAM, RANGE GATE 13, EAST LOOK

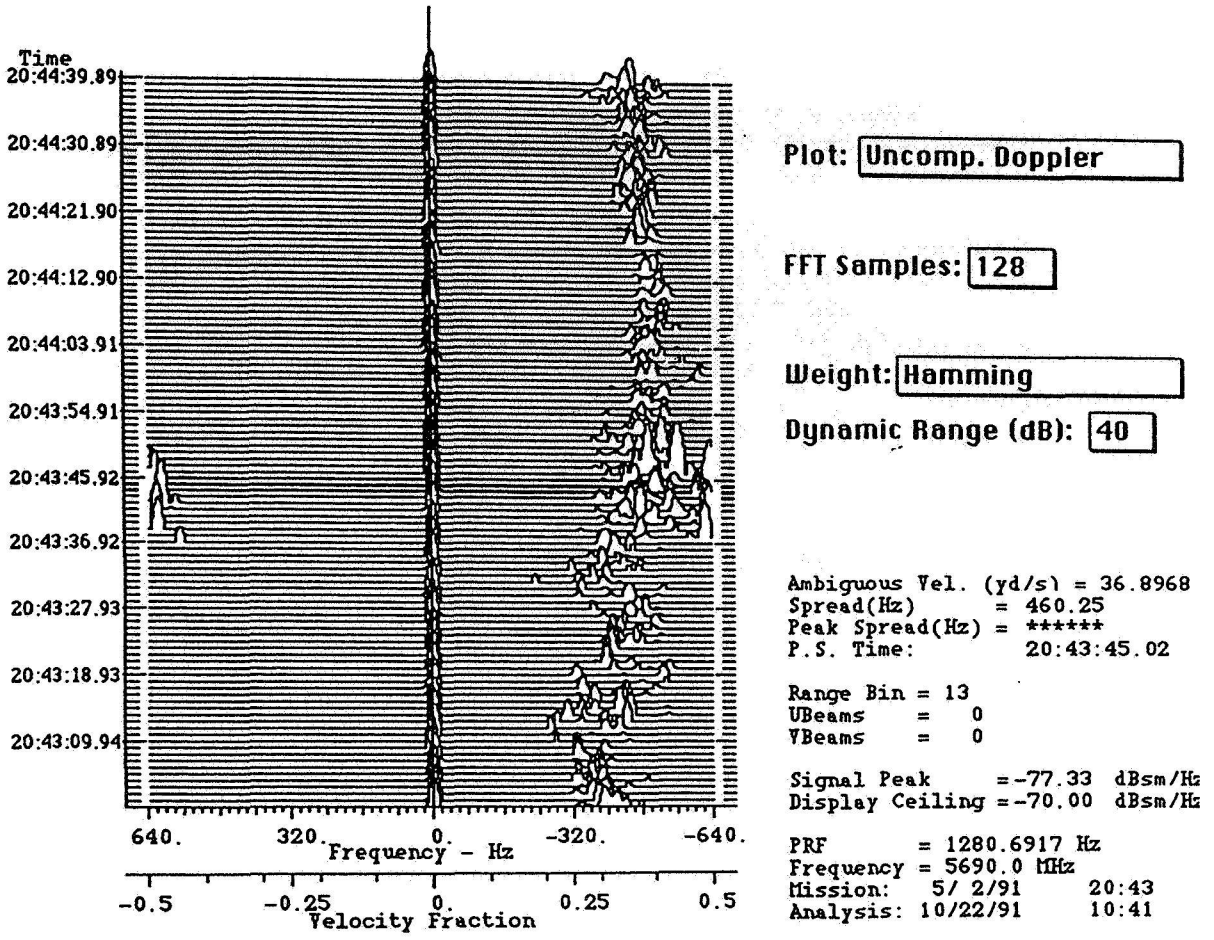

FIGURE 9(B) DOPPLER TIME HISTORY PLOT FOR WINDY DAY, MIDDLE BEAM, RANGE GATE 13, EAST LOOK

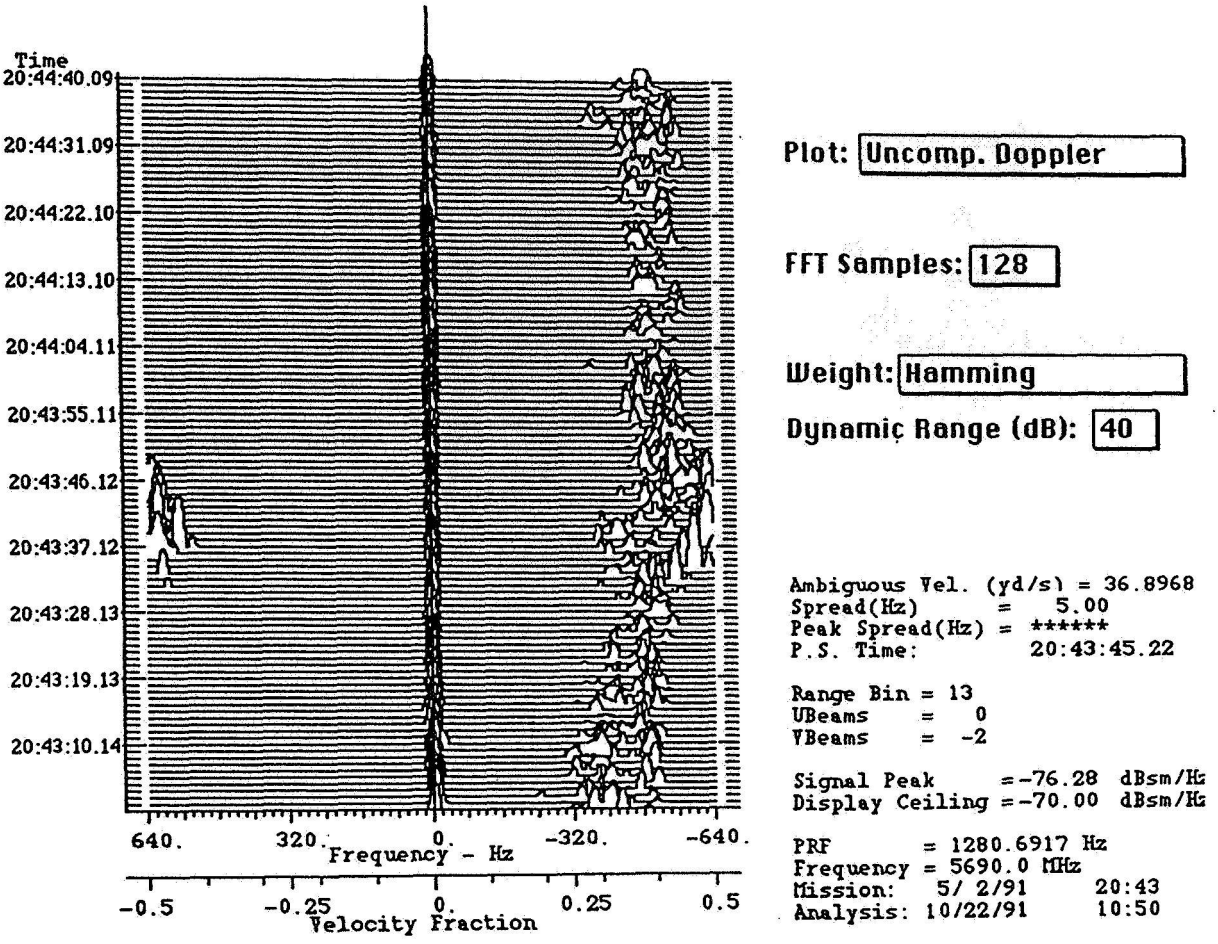

FIGURE 9(c) DOPPLER TIME HISTORY PLOT FOR WINDY, LOWER BEAM, RANGE GATE 13, EAST LOOK

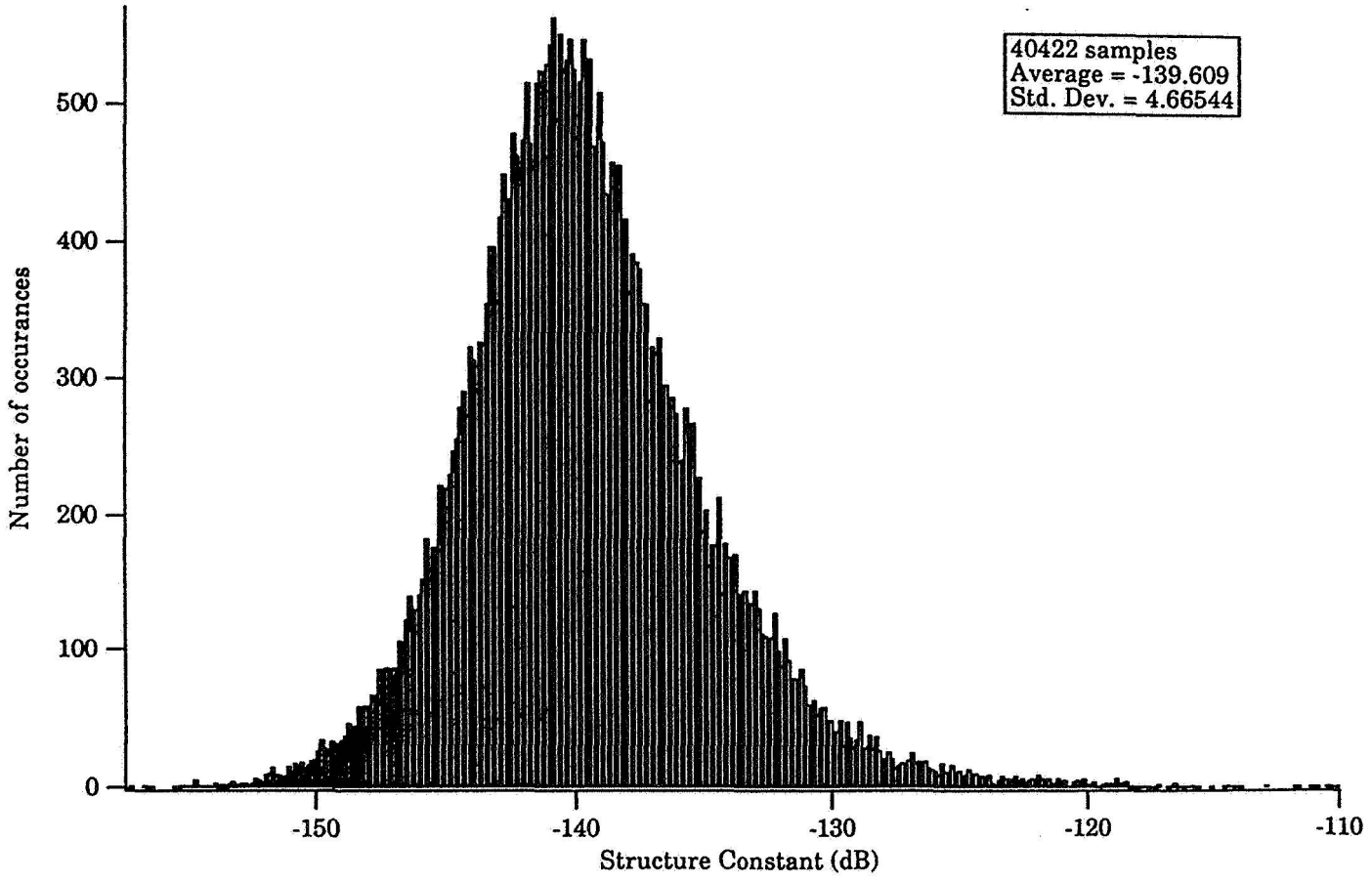

FIGURE 10(A) HISTORGRAM OF STRUCTURE CONSTANT FOR WINDY DAY

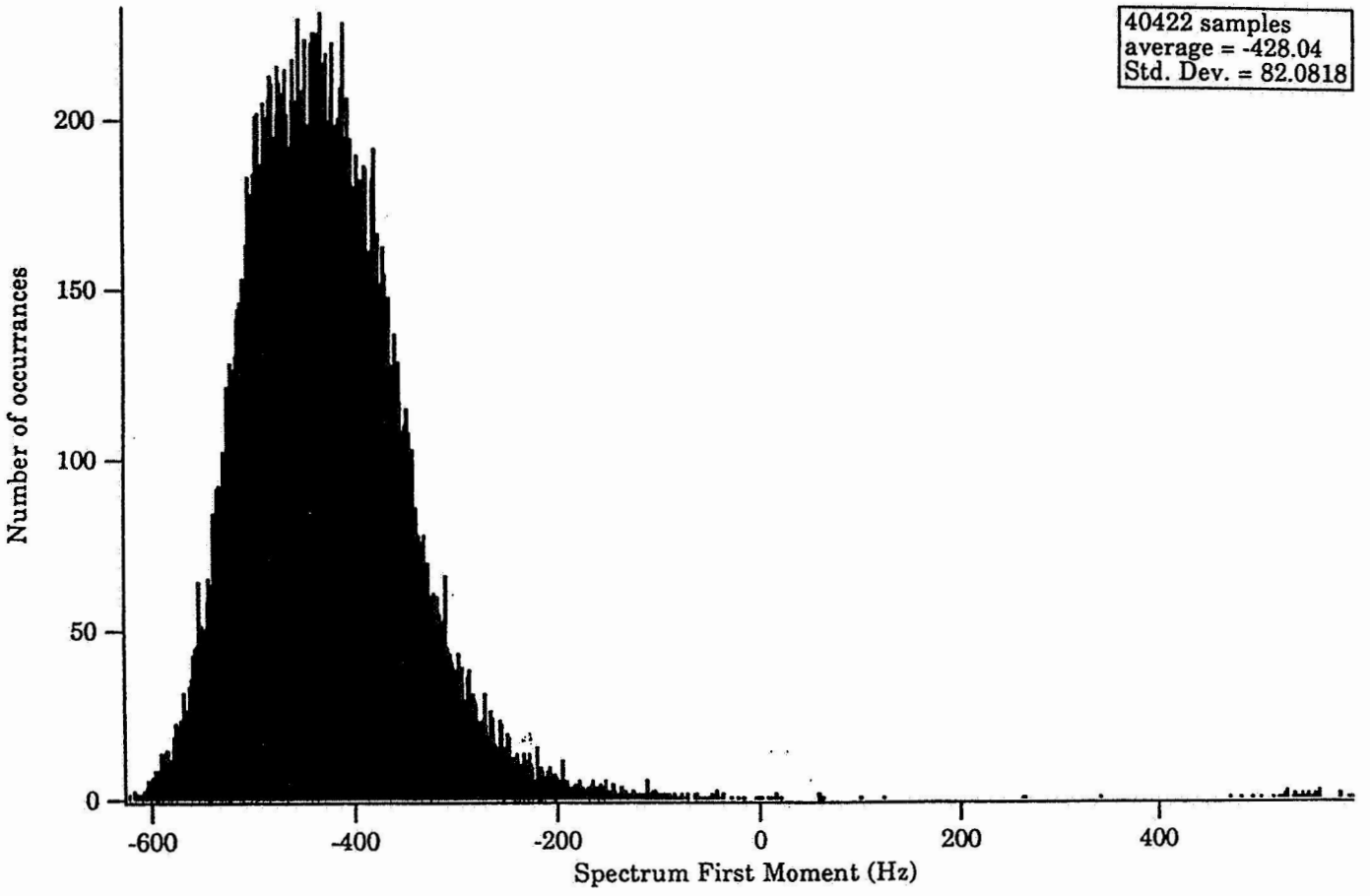

FIGURE 10(B) HISTOGRAM OF RADIAL VELOCITY FOR WINDY DAY

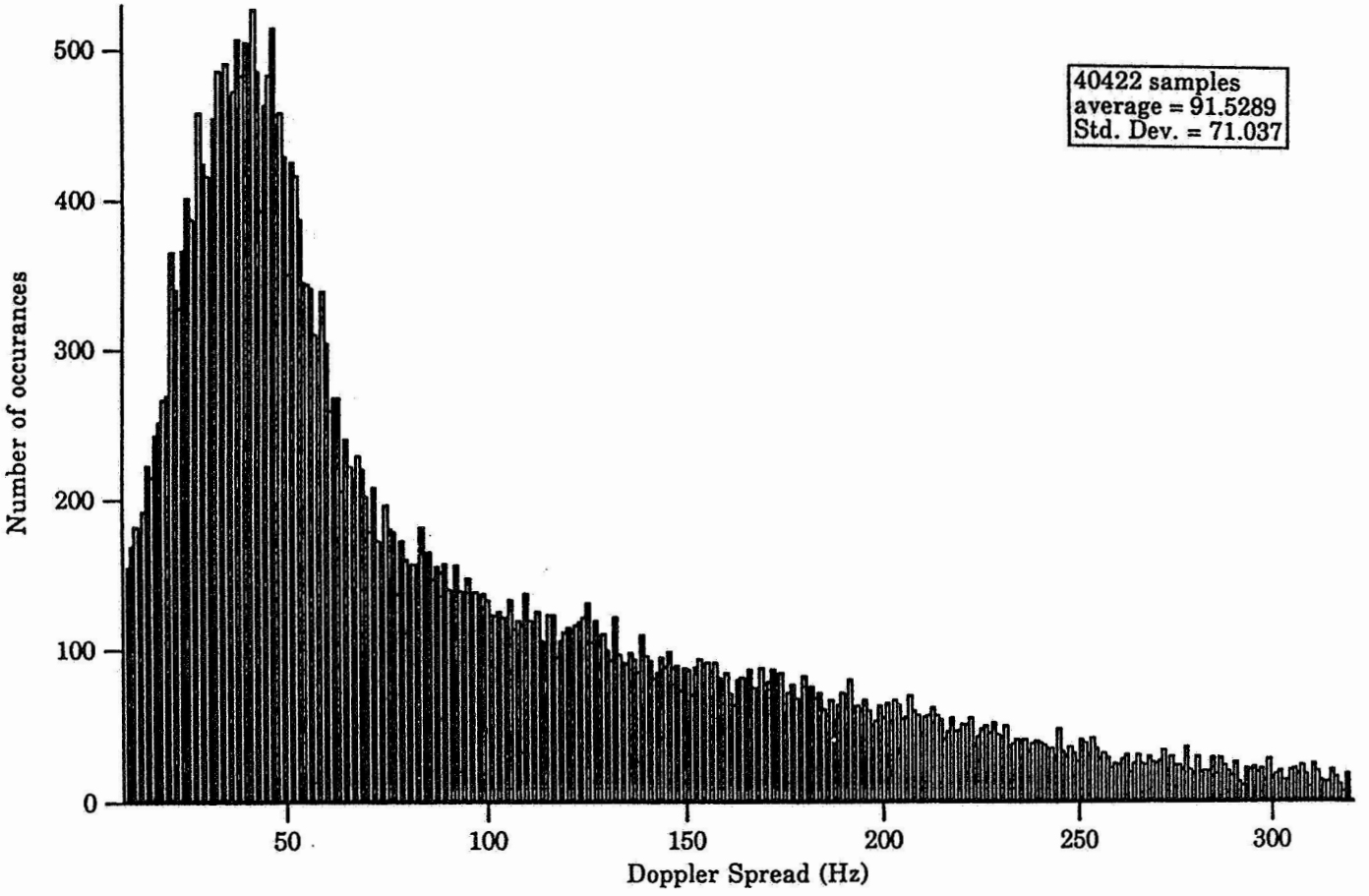

FIGURE 10(c) HISTORGRAM OF SPECTRAL WIDTH FOR WINDY DAY

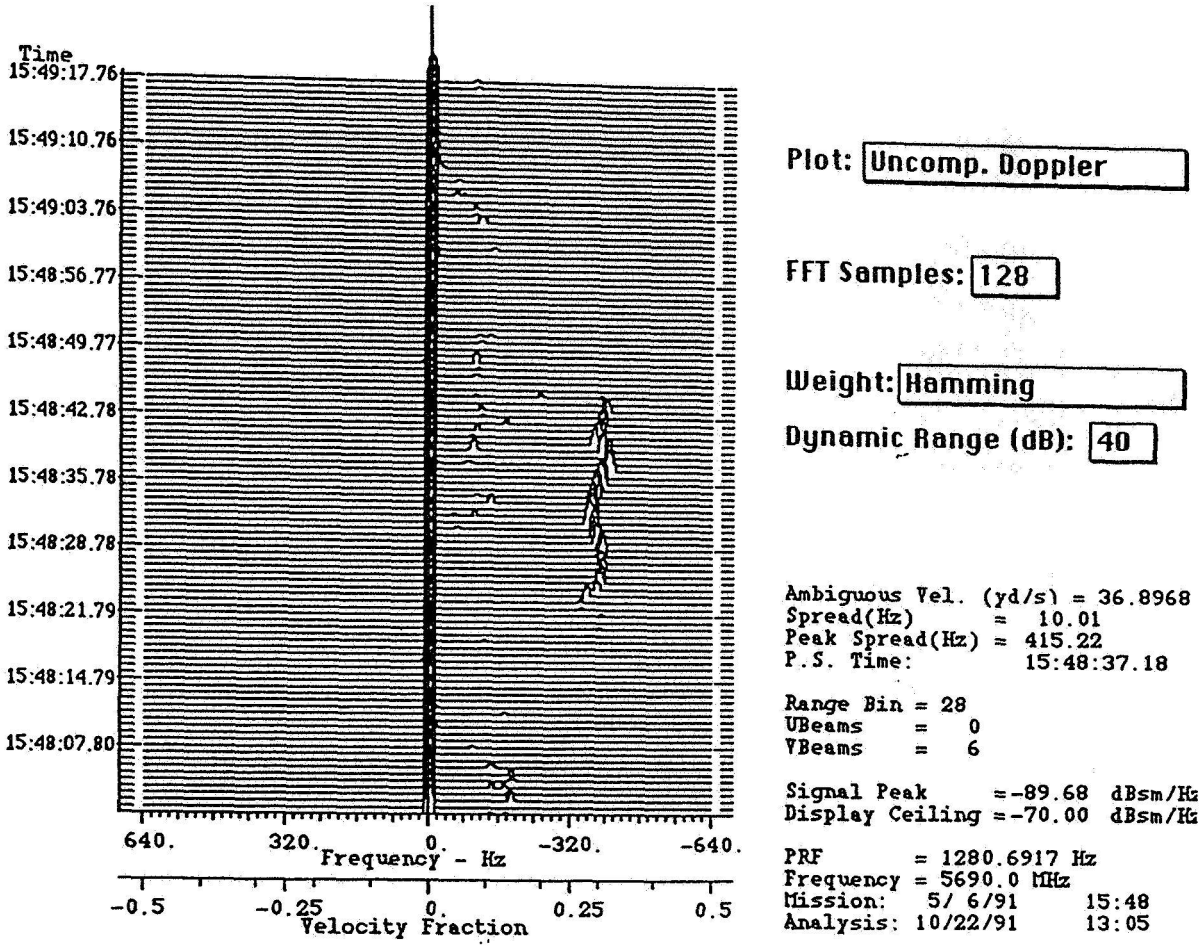

FIGURE 11(A) DOPPLER TIME HISTORY PLOT FOR CALM DAY, UPPER BEAM, RANGE GATE 28, NORTH LOOK

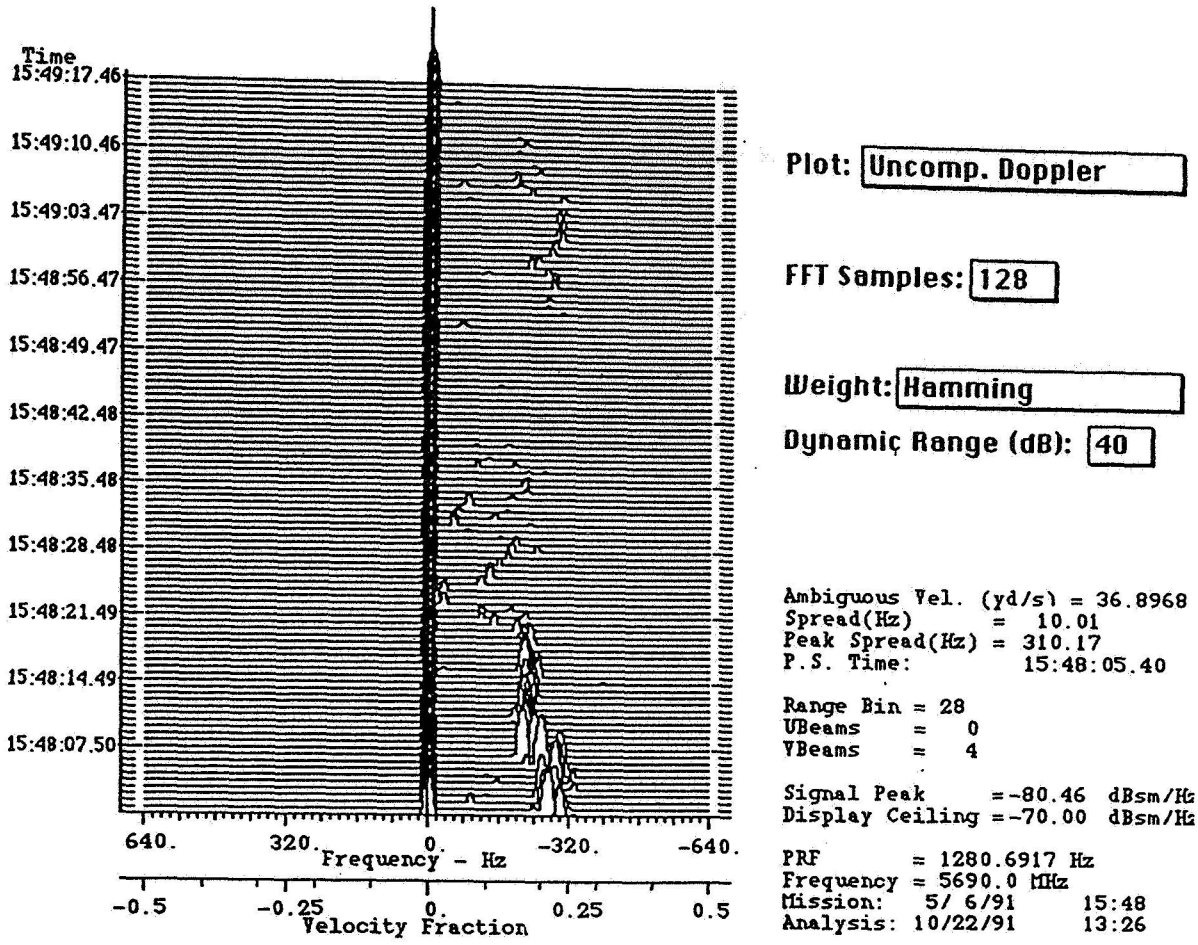

FIGURE 11(B) DOPPLER TIME HISTORY PLOT FOR CALM DAY, MIDDLE BEAM, RANGE GATE 28, NORTH LOOK

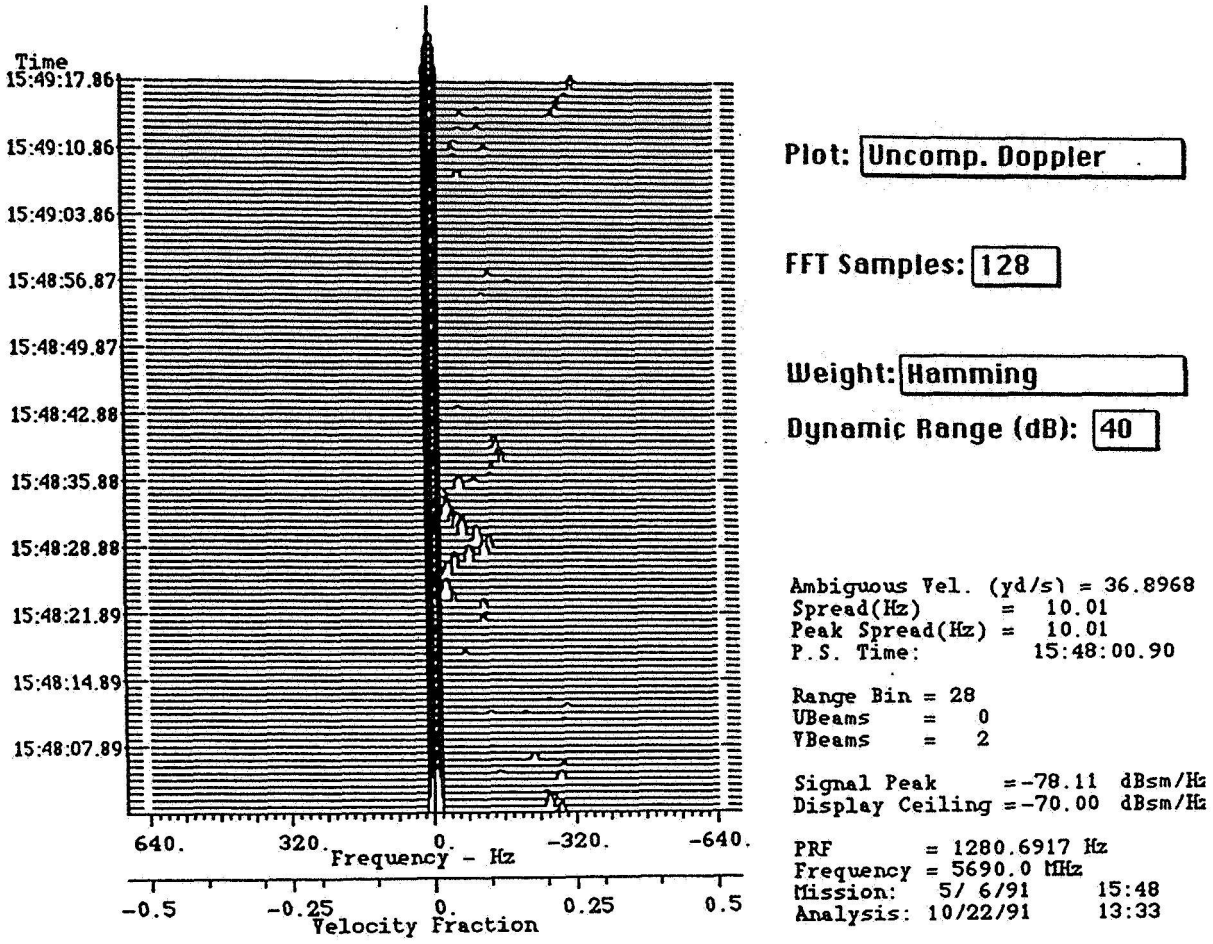

FIGURE 11(c) DOPPLER TIME HISTORY PLOT FOR CALM DAY, LOWER BEAM, RANGE GATE 28, NORTH LOOK

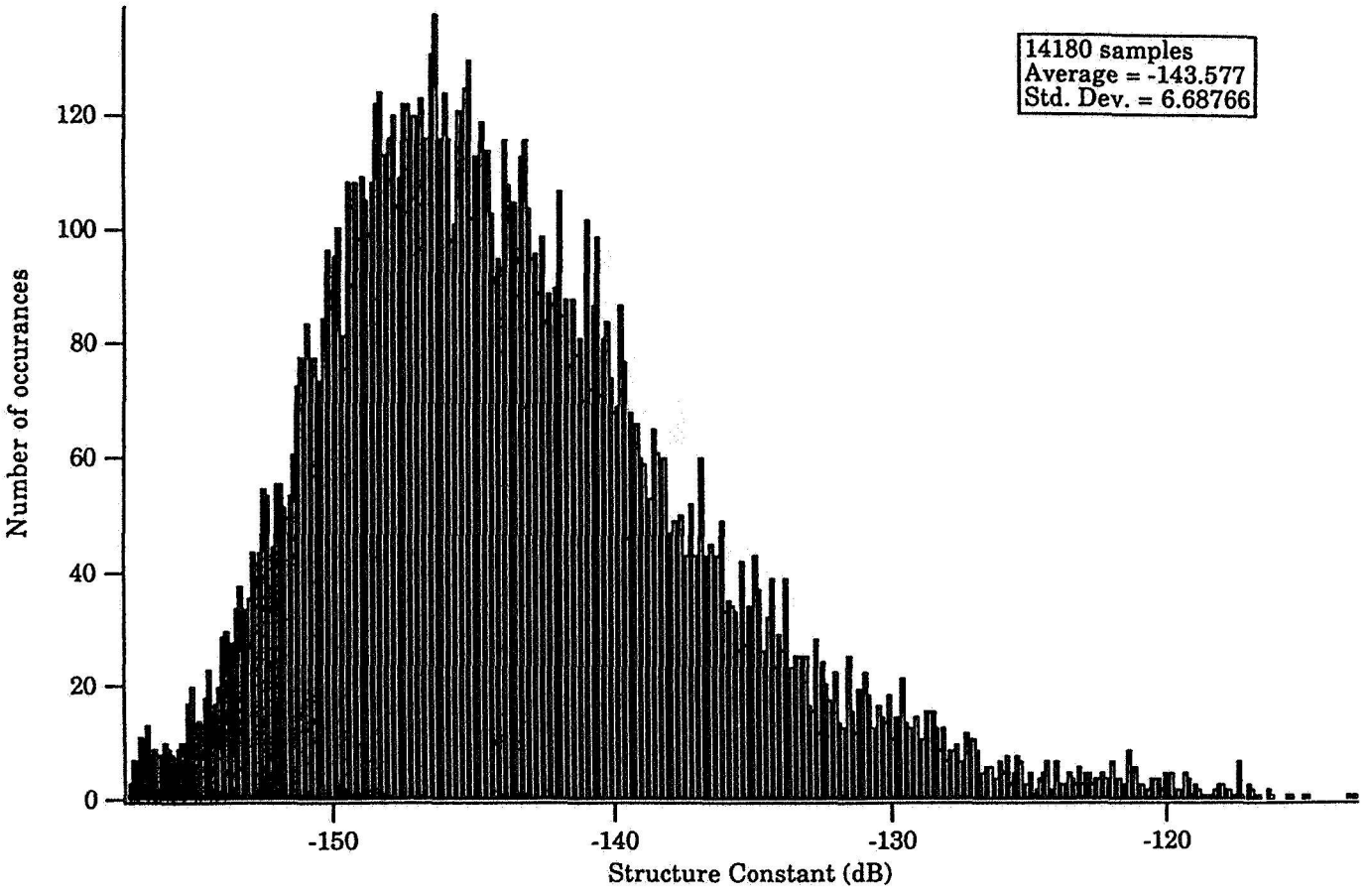

FIGURE 12(A) HISTOGRAM OF STRUCTURE CONSTANT FOR CALM DAY

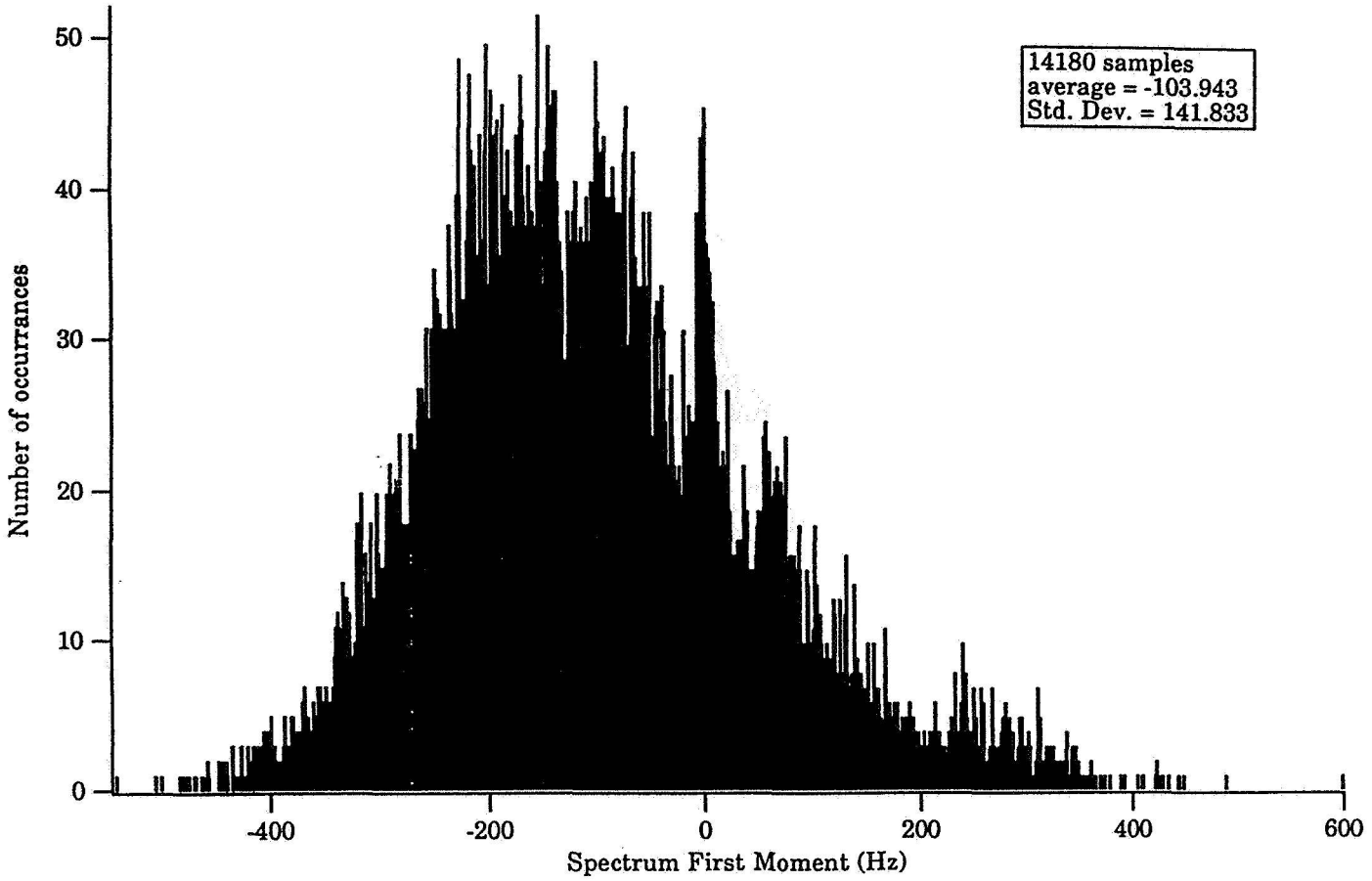

FIGURE 12(B) HISTORGRAM OF RADIAL VELOCITY FOR CALM DAY

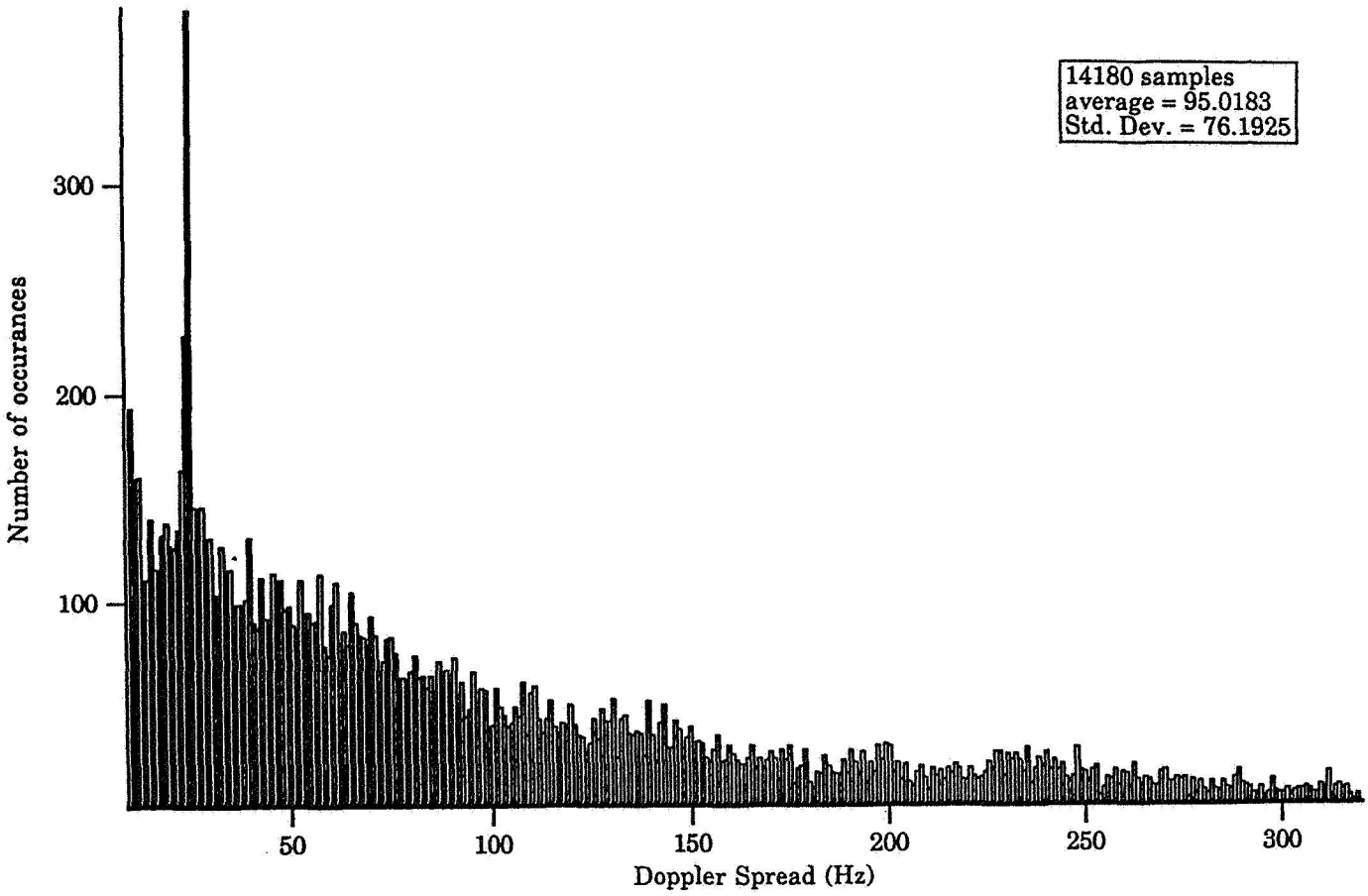

FIGURE 12(c) HISTORGRAM OF SPECTRAL WIDTH FOR CALM DAY

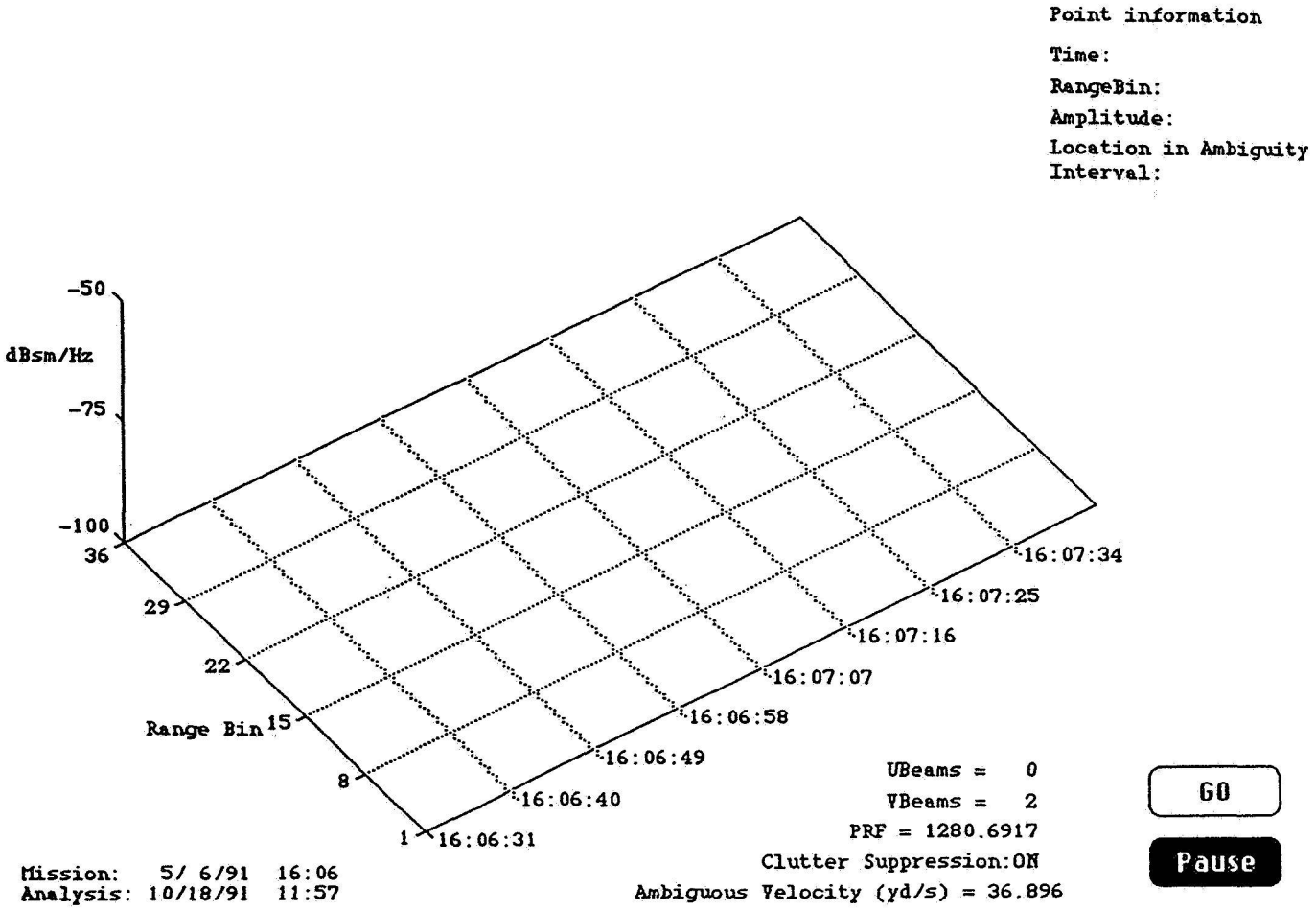

FIGURE 13 DOPPLER AMPLITUDE RANGE TIME (DART) PLOT

Remote Sensing of Turbulence in the Clear Atmosphere with 2-micron Lidars.

R. Martinson,
Lightwave Atmospherics, Inc.,
and
J. Flint,
Schwartz Electro-Optics, Inc.

Remote Sensing of Turbulence in the Clear Atmosphere with 2 μm Lidars

by

Robert J. Martinsen and John H. Flint†

Lightwave Atmospherics, Inc.
2 Susan Road, Marblehead, MA 01945
(617) 639-2536

†Schwartz Electro-Optics, Inc.
45 Winthrop Street, Concord, MA 01742
(508) 371-2299

LIGHTWAVE ATMOSPHERICS, INC.

SEO RESEARCH DIVISION

Motivation

- **Passenger safety/comfort**
- **Economic performance**
- **Reduce structural failures due to fatigue and instability**
- **Benefits civil and military aviation, HALE and UAVs**

LIGHTWAVE
ATMOSPHERICS, INC.

SEO RESEARCH DIVISION

Research Summary

- We report on the development of an eye-safe, airborne lidar that exploits the decorrelation of the heterodyne signal to detect CAT.

- A 1-watt average power transmitter is shown to be capable of detecting CAT to over 20 km in subvisual cirrus - an environment highly correlated with instabilities of stratified shear layers.

- In the absence of subvisual cirrus, a 4 km detection range is maintained, allowing 40 seconds of warning at 200 knots.

LIGHTWAVE ATMOSPHERICS, INC.

SEO RESEARCH DIVISION

Turbulent Motions in the Clear Atmosphere

- **Turbulence in PBL is driven primarily by convective over-turning and terrain-induced centrifugal instabilities.**

- **"CAT comprises all turbulence in the free atmosphere that is not in, or adjacent to, visible convective activity."** National Committee for CAT, 1966.

- **Principal mechanism => Kelvin-Helmholtz instability (KHI).**

- **Most CAT is confined to a 100 - 1000 m thick layer, several square kilometers in extent, and persists for 10's of minutes.**

LIGHTWAVE ATMOSPHERICS, INC.

SEO RESEARCH DIVISION

Kelvin-Helmholtz Instability

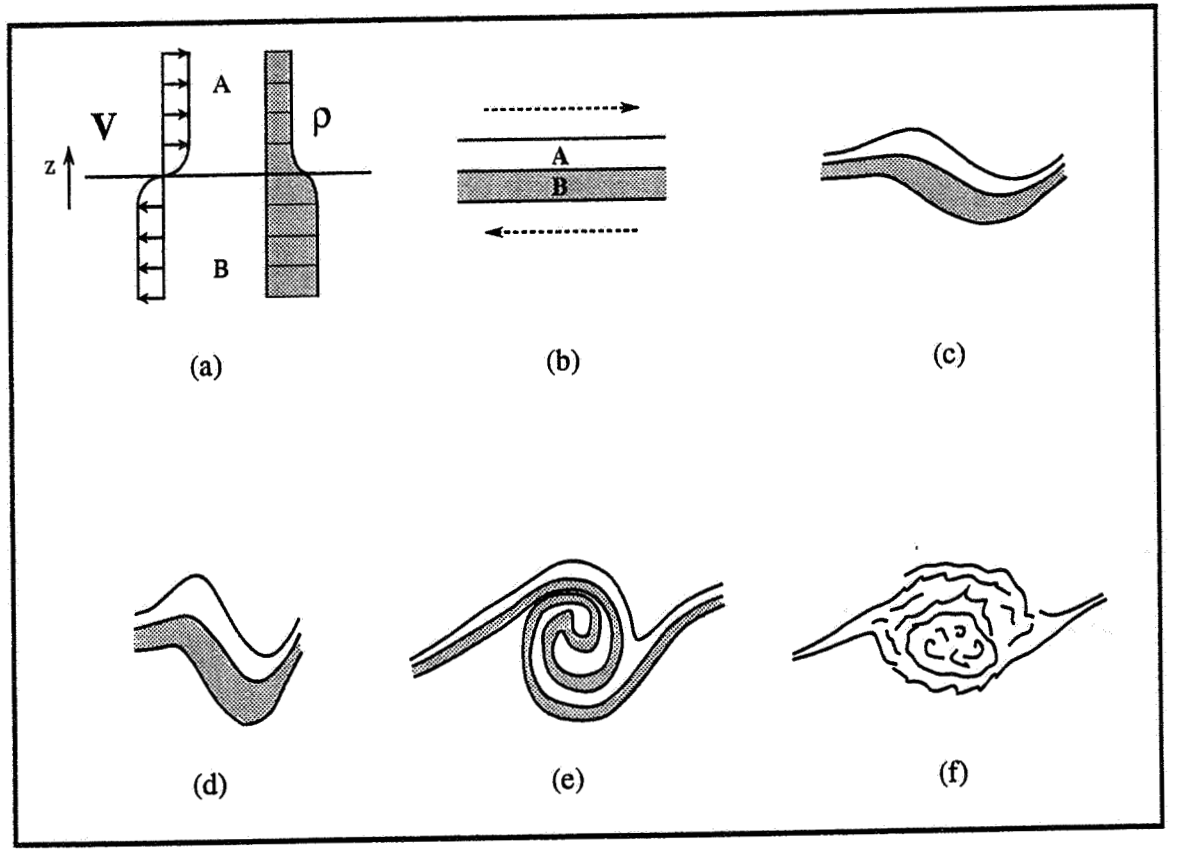

LIGHTWAVE ATMOSPHERICS, INC.

SEO RESEARCH DIVISION

Turbulence - Spectral Width Correspondence

Turbulence Classification	Velocity Width,† σ_v	Frequency Width,†† σ_f
Natural Background	≤ 0.5 m/s	≤ 0.5 MHz
Light	0.5 - 1.0	0.5 - 1.0
Moderate to Strong	1.0 - 8.0	1.0 - 8.0
Extreme	≥8.0	≥8.0

† **Ref. H. Sauvageot, *Radar Meteorology, Artech House.***

†† **For a 2 μm Lidar.**

LIGHTWAVE ATMOSPHERICS, INC.

SEO RESEARCH DIVISION

Simulations of Doppler Broadened Lidar Signals

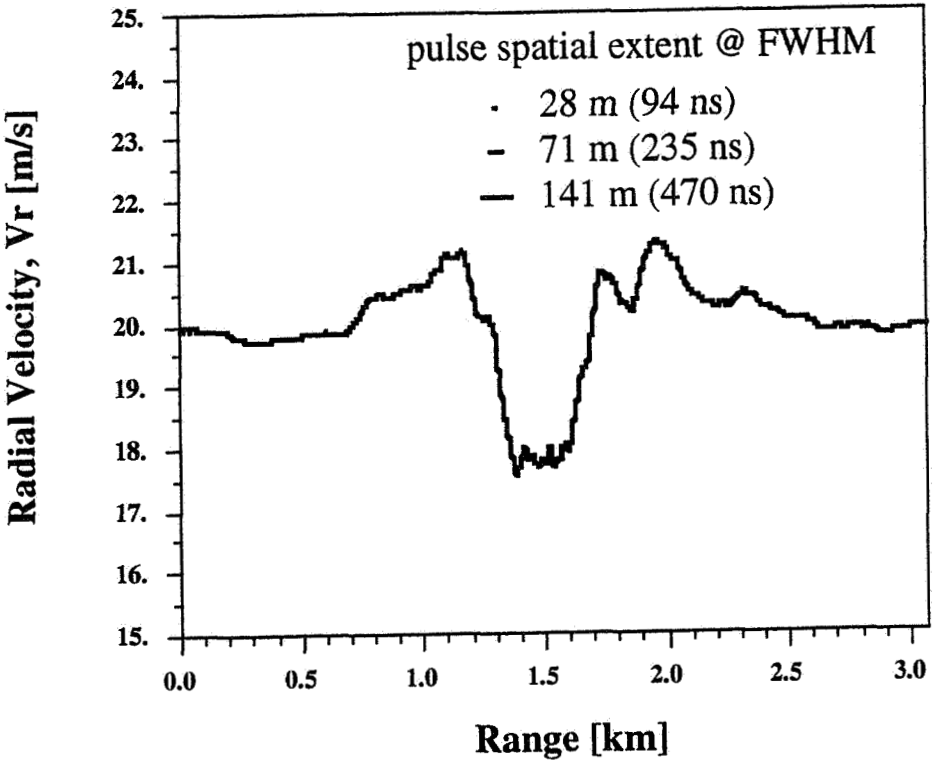

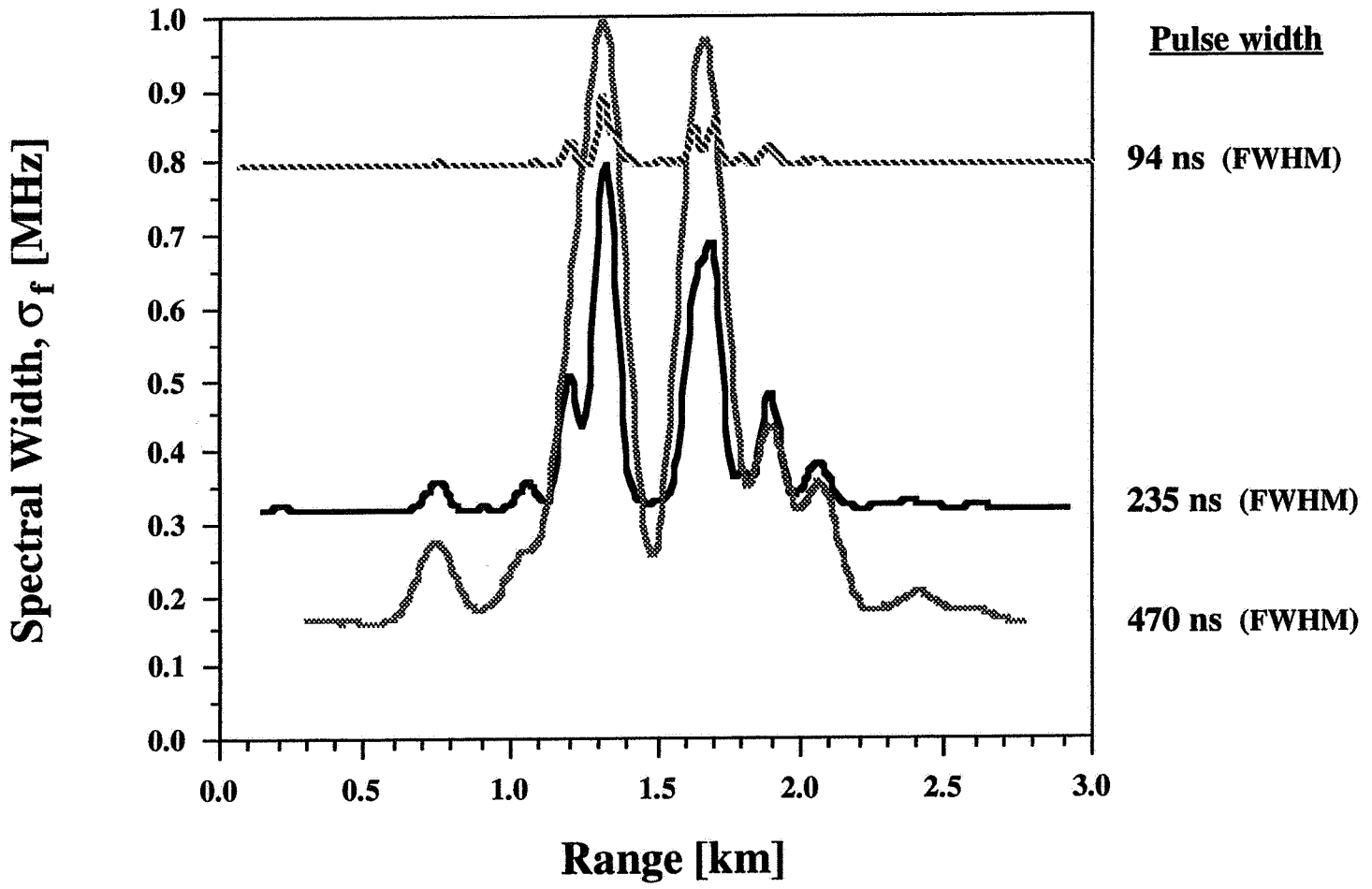

$\Longrightarrow$ **Spectral broadening response of a longer pulse is more effective for detecting the sheared velocity profiles that characterize the onset of CAT development.**

LIGHTWAVE ATMOSPHERICS, INC.

SEO RESEARCH DIVISION

Simulations of Doppler Broadened Lidar Signals

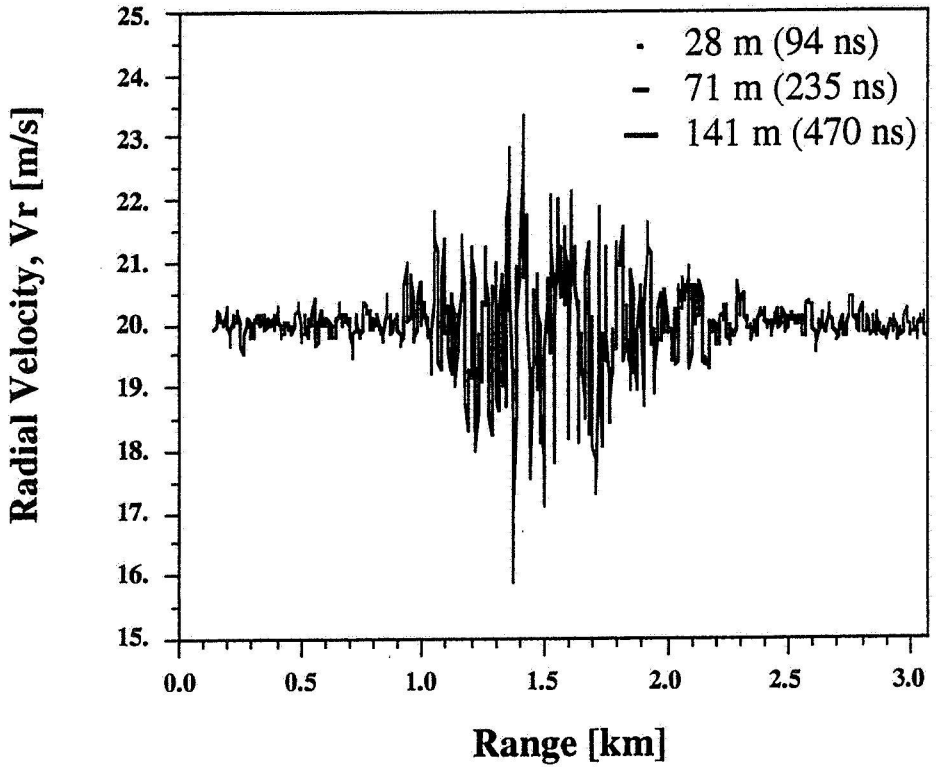

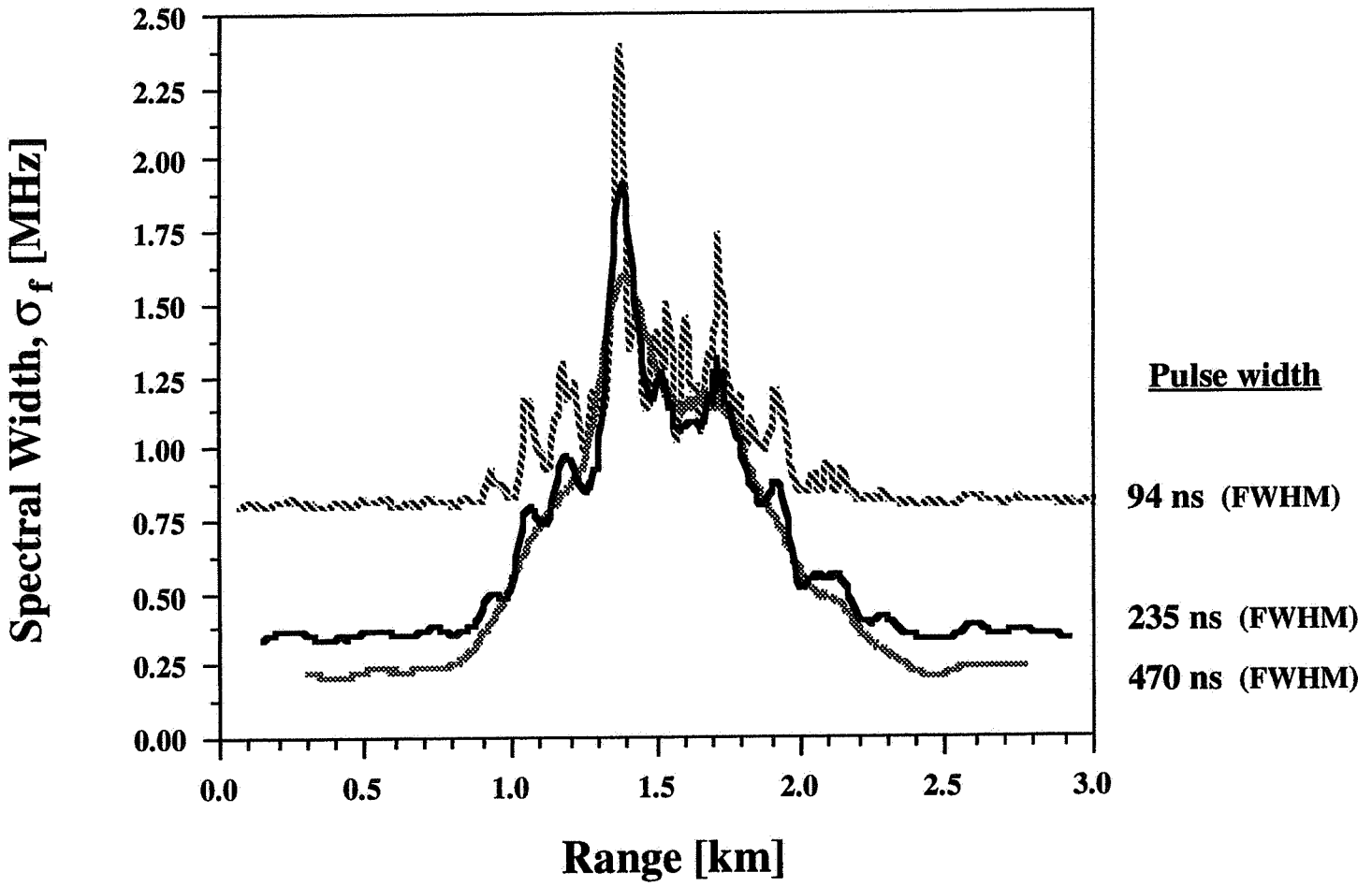

$\Longrightarrow$ **Fine scale turbulence broadens Doppler spectrum by similar amounts (beyond transform limit) for the pulse widths studied.**

LIGHTWAVE ATMOSPHERICS, INC.

SEO RESEARCH DIVISION

Decorrelation of the Heterodyne Signal

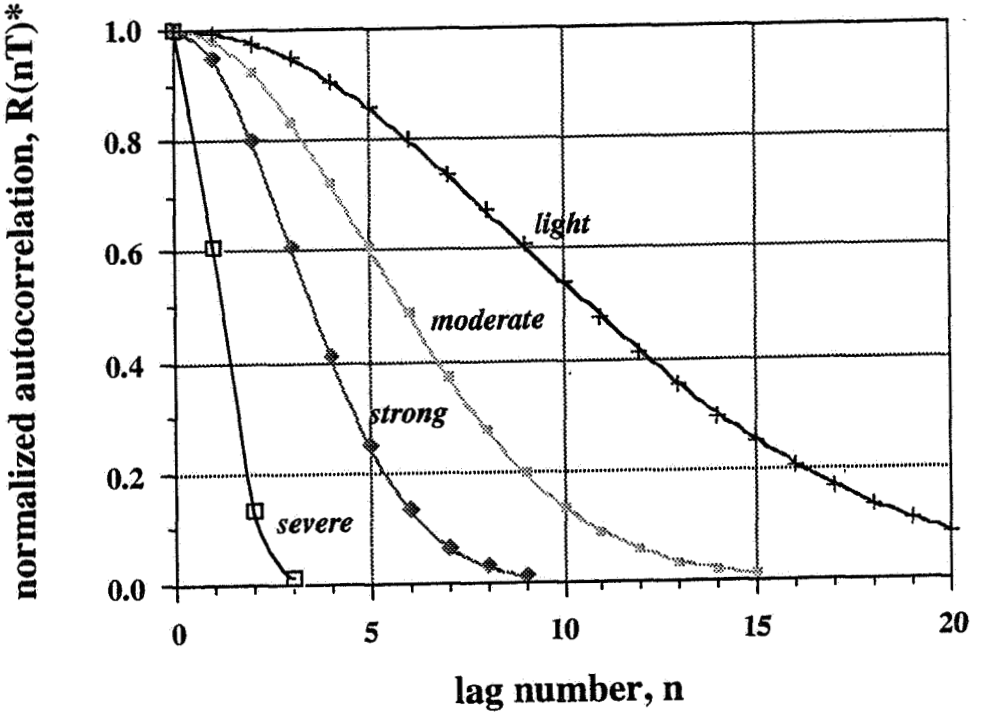

LIGHTWAVE ATMOSPHERICS, INC.

SEO RESEARCH DIVISION

Significance of Subvisual Cirrus Aerosols

.... Correlation with turbulent regions of the atmosphere.

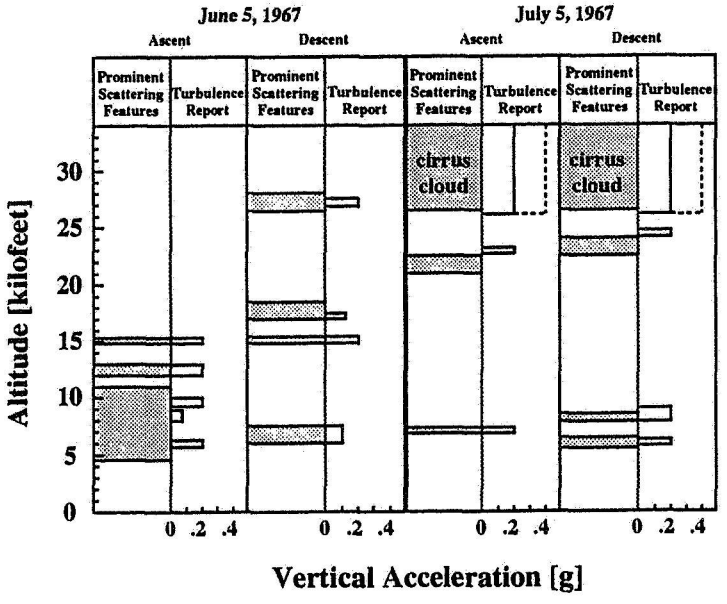

Adapted from J.D. Lawrence, et al., Clear Air Turbulence and its Detection, eds., Y-H Pao and A. Goldberg, New York, Plenum Press, 1969, pp 481-495.

.... Scattering environment is dramatically enhanced.

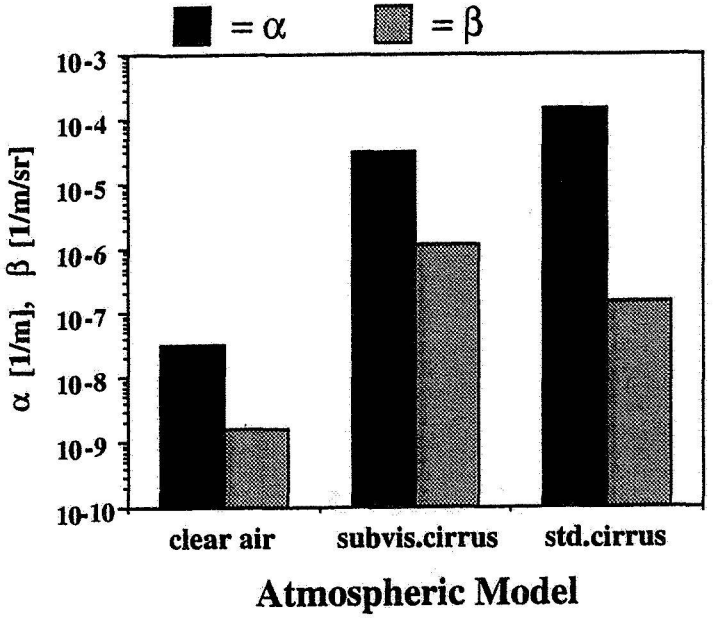

Derived from *Backscat* version 2.0, Lidar Backscatter Simulation Code, J.R. Hummel, et al., SPARTA, Inc.

LIGHTWAVE ATMOSPHERICS, INC.

SEO RESEARCH DIVISION

Coherent Lidar Performance Evaluation

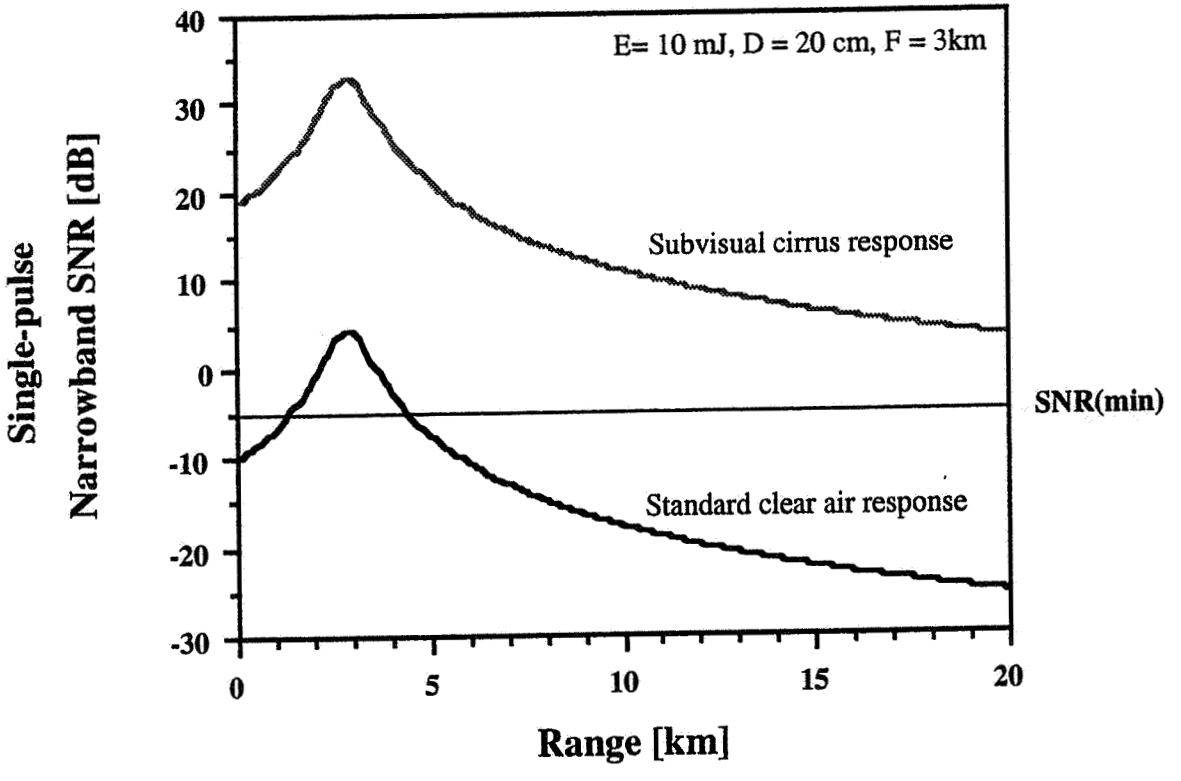

LIGHTWAVE ATMOSPHERICS, INC.

SEO RESEARCH DIVISION

Minimum Warning Time for 1 W Average Power Transmitter

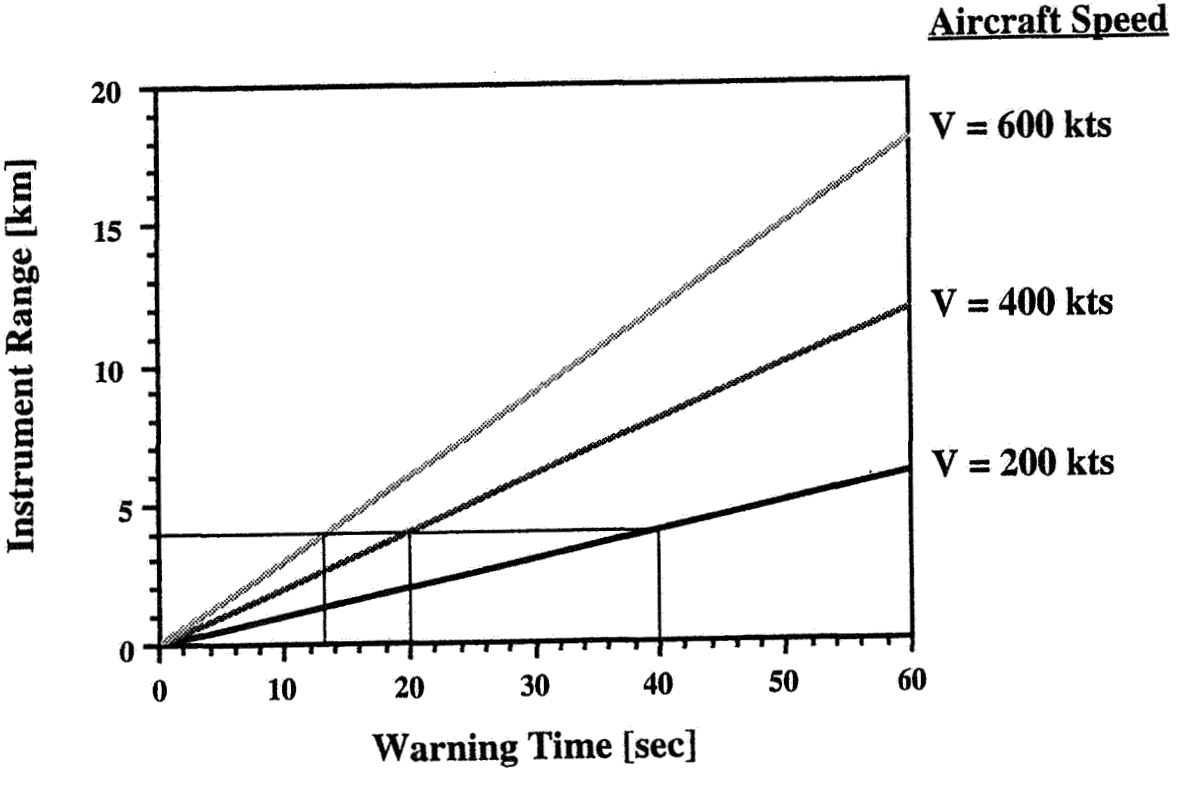

LIGHTWAVE ATMOSPHERICS, INC.

SEO RESEARCH DIVISION

Principal Findings

- Spectral broadening appears to be a reliable CAT discriminant and time domain processing of σ_v can be performed in real-time.
- Relationships have been established between the decorrelation of the heterodyne signal and the severity of turbulence in a range gate.
- The spatial extent of the transmitted pulse should be adapted to the size of the aircraft for optimal sensitivity/resolution of CAT threats.
- Compact lidar under development: 10 mJ / 100 Hz 2μm transmitter coupled to 20 cm telescope focused at 3 km range.

LIGHTWAVE ATMOSPHERICS, INC.

SEO RESEARCH DIVISION

Acknowledgements

- This research was supported by the Defense Advanced Research Projects Agency (DARPA) under the Small Business Innovative Research (SBIR) program, contract number DAAH01-92-C-R097.

- The authors gratefully acknowledge many useful discussions with Bob Lee and Tayyab Khan of Lassen Research on spectral moment estimation, Steve Alejandro of USAF Phillips Lab for backscatter data at 2 μm , and Geoff Koenig and John Hummel of Sparta for informative discussions about the dynamical formation and physical properties of subvisual cirrus aerosols.

omit

Session 7:
SYNTHETIC AND ENHANCED VISION SYSTEMS.

Chair: T. Campbell,

NASA Langley Research Center.

Session 7:

SYNTHETIC AND ENHANCED VISION SYSTEMS.

Chair: T. Campbell, NASA Langley Research Center.

ESAS (Enhanced Situation Awareness Systems). A. Lambregts, Boeing Commercial Airplane Co.

Overview of Westinghouse Enhanced Vision Technology Activities. W. Patterson, Westinghouse Electric Corp.

Evaluation of Candidate Millimeter Wave Sensors for Synthetic Vision. N. Alexander, J. Echard, and B. Hudson, Georgia Tech Research Insitute

Passive MMW Camera for Low Visibility Landings. M. Shoucri, TRW Applications Technology Div.

Synthetic Vision System Flight Test. L. Jordan, Honeywell Technical Center

Enhanced Synthetic Vision Systems. C. Taylor, Lear Astronics Corp.

ESAS (Enhanced Situation Awareness Systems).

A. Lambregts,
Boeing Commercial Airplane Co.

Enhanced Situation Awareness System

The Boeing Research Approach

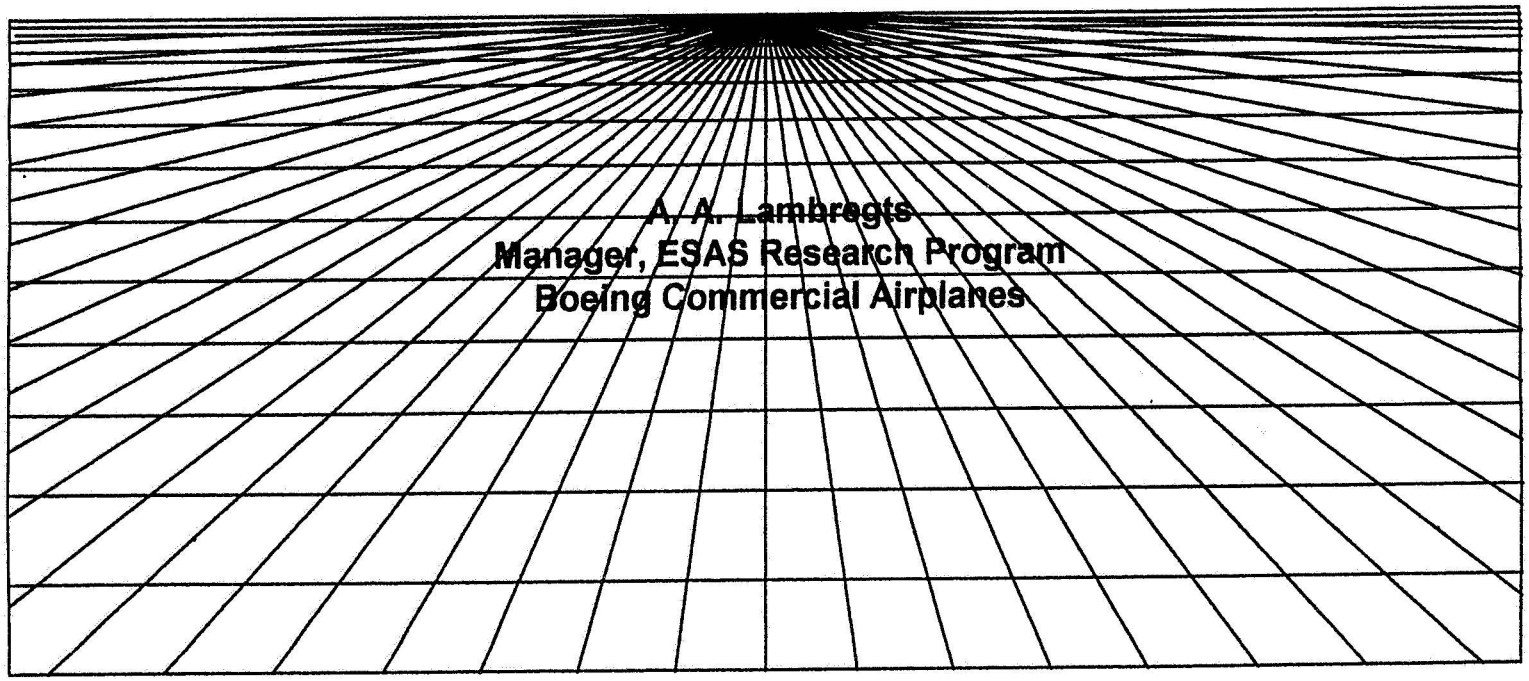

Airline Fiscal Morass Erases Profits and Crimps Fleet Plans

JAMES OTT/WASHINGTON

— S. airlines, deepl... and th...

Compromise plan is likely as labor and management drive to resolve ownership and restructuring problems and return the airline to profitability

Not ... soured the start o...

Storage of 175 Transports Shows Poor Airline Industry State

MOJAVE, CALIF.

The approximately... transp... ...mmercial airline ... World War 2-era Marine Corps base about 100 mi. north of Los Angeles, ... sprawling desert airport has becom... prominent open-air commercial airc... storage facility. Both new and ag... transports are parked here, most victi... kets and bankrupt airlir... ...new Air Canada Boe... ...l temporarily until mar... ...ive, will b...

American Stretches Boeing, McDonnell Douglas Deliveries

FT. WORTH

American Airlines and Boeing tenta... ...Ya...

3,918	1.
–2,078	– 1.
2,457	0.
130	28.
1,846	0.
2,381	0.
1,443	2.
8,656	N.

Source: Avitas

...now on firm contract, but did not envi... ...ders. Originally...

DEBT AND EQUITY PERCENT CHA... FOR SELECTED U.S. CARRIERS

PERCENT CH...

Source: AVITAS, Inc.

Long Term Debt and Shareholders' Equity
IBM Vs. ATA Member Carriers (1990)

Shareholders'

Boeing Reducing 737 Production In Response to Delivery Stretchouts

SAN FRANCISCO

Produc... ...record 2... ...will be reduced f... ...h quarter of next year... ...company said intend... ...compensate for... ...rate of demand...

In response to the deman... ...es to stretch deliveries... ...has been only one outstan... ...firm 737 order, thus ... ...protecting its ability to ... ...accurately demand... ...said Product... ...by suppliers about... ...are reflected by... ...The 737 slowdown will begin ... ...industry in early to mid-1992, he said. ...The company currently is producing ... ...commercial transports at a rate of 18 per ...month—a company record.

American Airlines ... ...tions for 33 of the transports. The carrier also stretched delivery of 44 757s on firm order, for two years.

"We think the market demand is still there," a Boeing official said.

While some 737 options have been canceled, the production slowdown is mostly

LAYOFFS, CUTBACKS, ALLIANCES FOR AEROSPACE

EDITORIALS

The Endangered Species

T T· S. major scheduled airlines have dropped to a peril- ... ...

The industry faces enormous capital requirements but there is far less confidence that these needs can ... met

...lated As a ...are f ...shelf ...th ...new ...main Th ...react At th ...lecti ...storm ...begin ...airpl Th ...aircr ...them ...airlir ...viron ...them Wi ...inves ...com ...comr

AIRCRAFT ORDERS ROSE IN '92; BUT SO DID DEFERRALS

Delays, the Hidden Costs

Delays Impose Many Costs on the Airline System Many of Them Hidden as "Unavoidable"

ATC delays
in Europe
$4.2 billion (U.S.)
in 1988

"...65,000 tonnes of fuel wasted by delays..."
British Airways

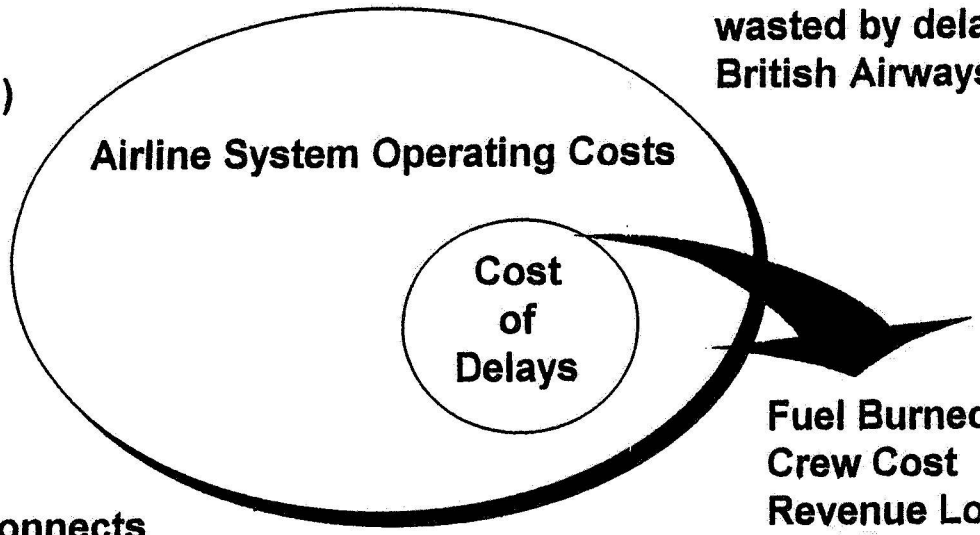

"...baggage misconnects may cost $30M per year..."
American Airlines

Fuel Burned
Crew Cost
Revenue Lost Passenger Accommodations
Oversized Fleet
etc.

Enhanced Situation Awareness

MAJOR TECHNOLOGY INITIATIVE

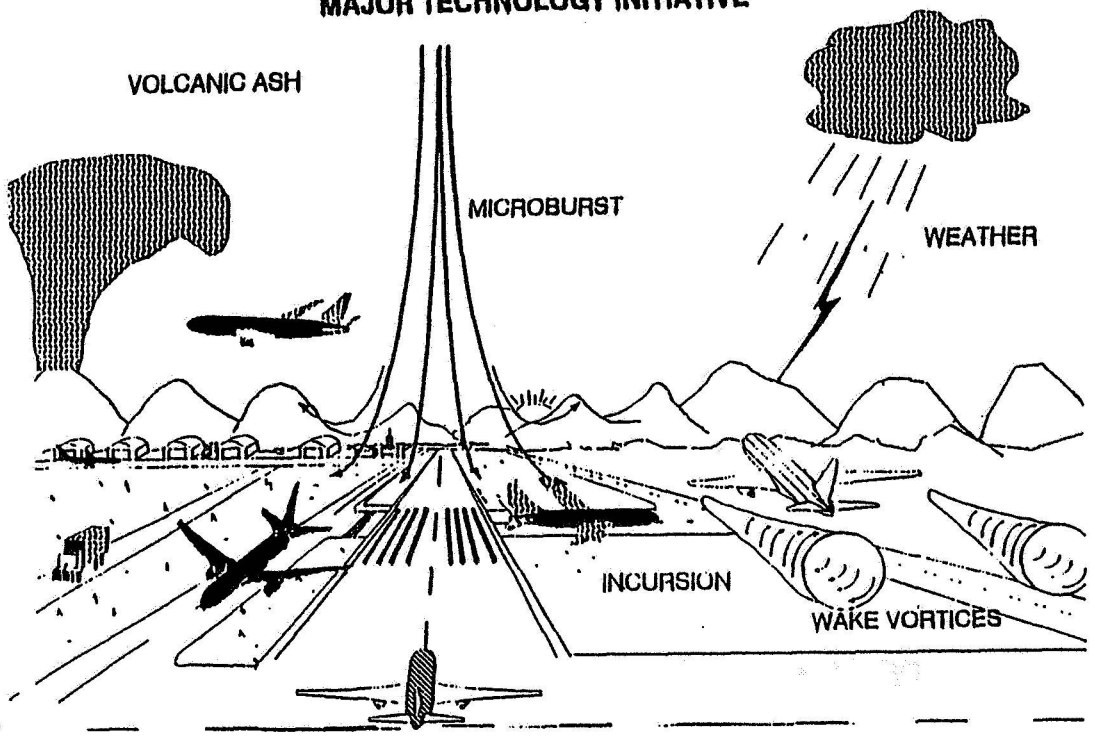

WHAT IS IT?

AN ONBOARD SENSOR/PROCESSOR/DISPLAY SYSTEM PROVIDING:

- EXPANDED CAPABILITY TO OPERATE WITH REDUCED WEATHER MINIMA
- PILOT AWARENESS OF HAZARDS ON GROUND AND IN-FLIGHT

ENHANCED SITUATION AWARENESS SYSTEM

CONSIDERED FUNCTIONAL CAPABILITIES:

NEAR TERM

- Landing, Taxi, Takeoff Operations in CATIIIA Weather with
  - Type II ILS/MLS
  - Type I ILS/MLS
- Look Ahead GPWS
- Ground Obstacle Alerting
- Predictive Windshear

LONG TERM

- Operations in CATIIIB Weather with Minimal Ground Facilities
- Atmospheric Hazards Alerting: I.e., Wake Vortex, Cat, Dry Hail, etc.
- Full Terrain Awareness

ESAS Flight Crew Integration
System Building Blocks

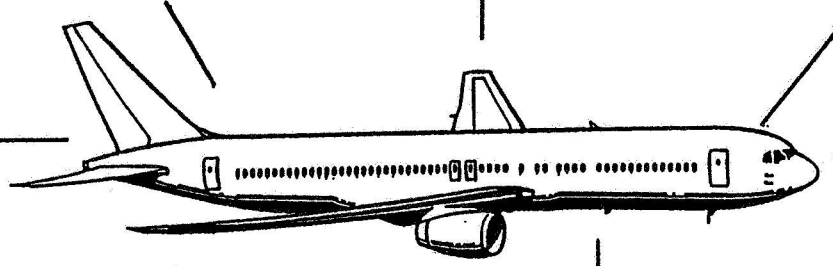

GPS
- Position information
- Update avionics
- Interface with database
- Traffic awareness
- Taxi guidance

ESAS Processor
- Integrate data sources
- Merge data
- Produce images

TCAS
- Collision avoidance
- Traffic awareness
- Separation

Data Link
- Changes in clearance
- Weather information
- Traffic awareness
- Update databases

Flight Crew Interface
- Information pathway for all components
- Displays, controls & procedures
- All flight phases
- Situation awareness

Database
- Terrain information
- Strategic planning
- Obstacle awareness
- Airport representation
- Taxi guidance

Sensor(s)
- Multi-function implementation
- Active and passive
- Imaging
- Enhanced Vision System
- Atmospheric hazards
- Positioning
- All flight phases

Enhanced Situation Awareness

Candidate Solution Identification Process

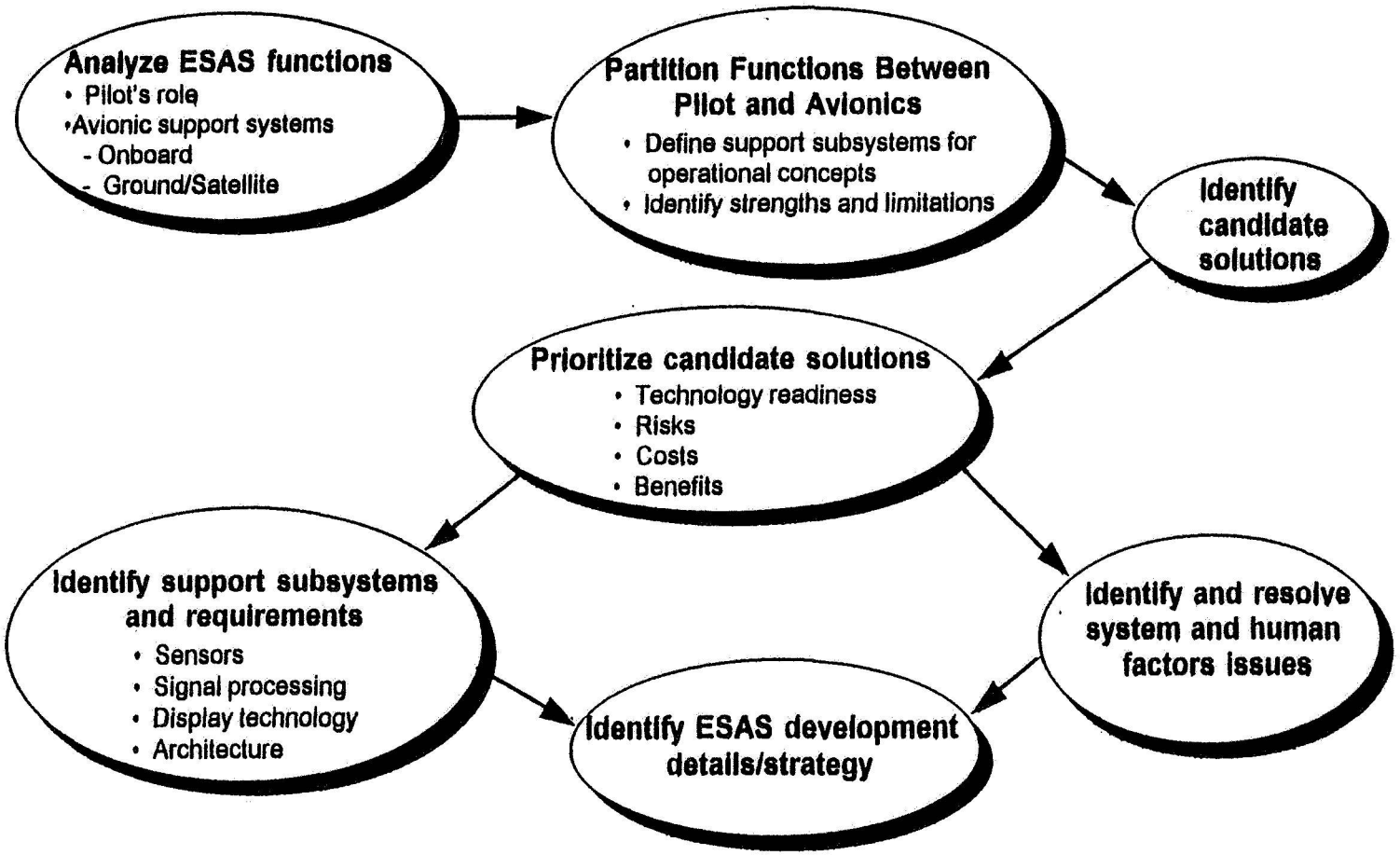

ESAS ECONOMIC BENEFIT ANALYSIS PROCESS
MULTI-DISCIPLINE APPROACH

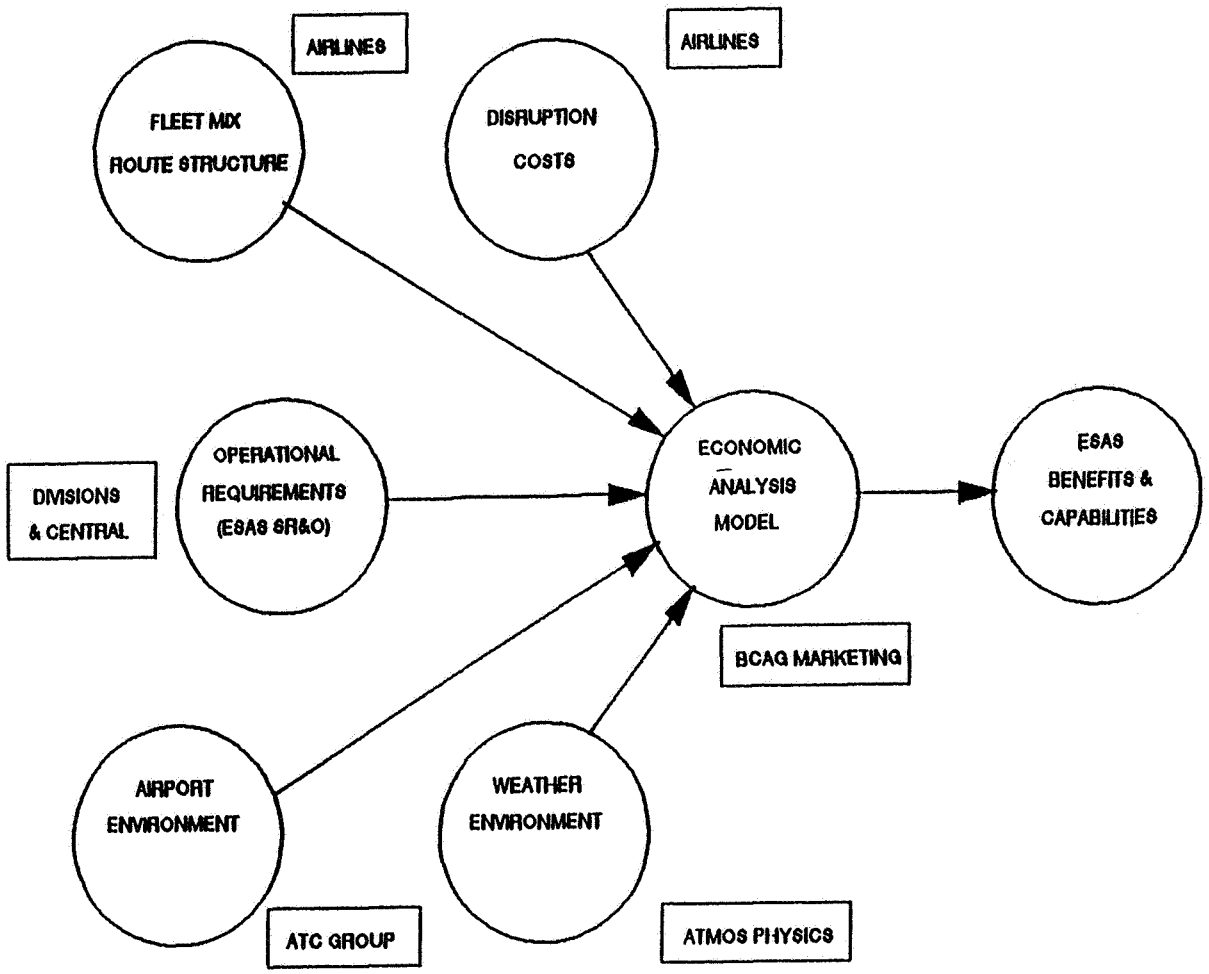

ESAS Phased-Approach Plan

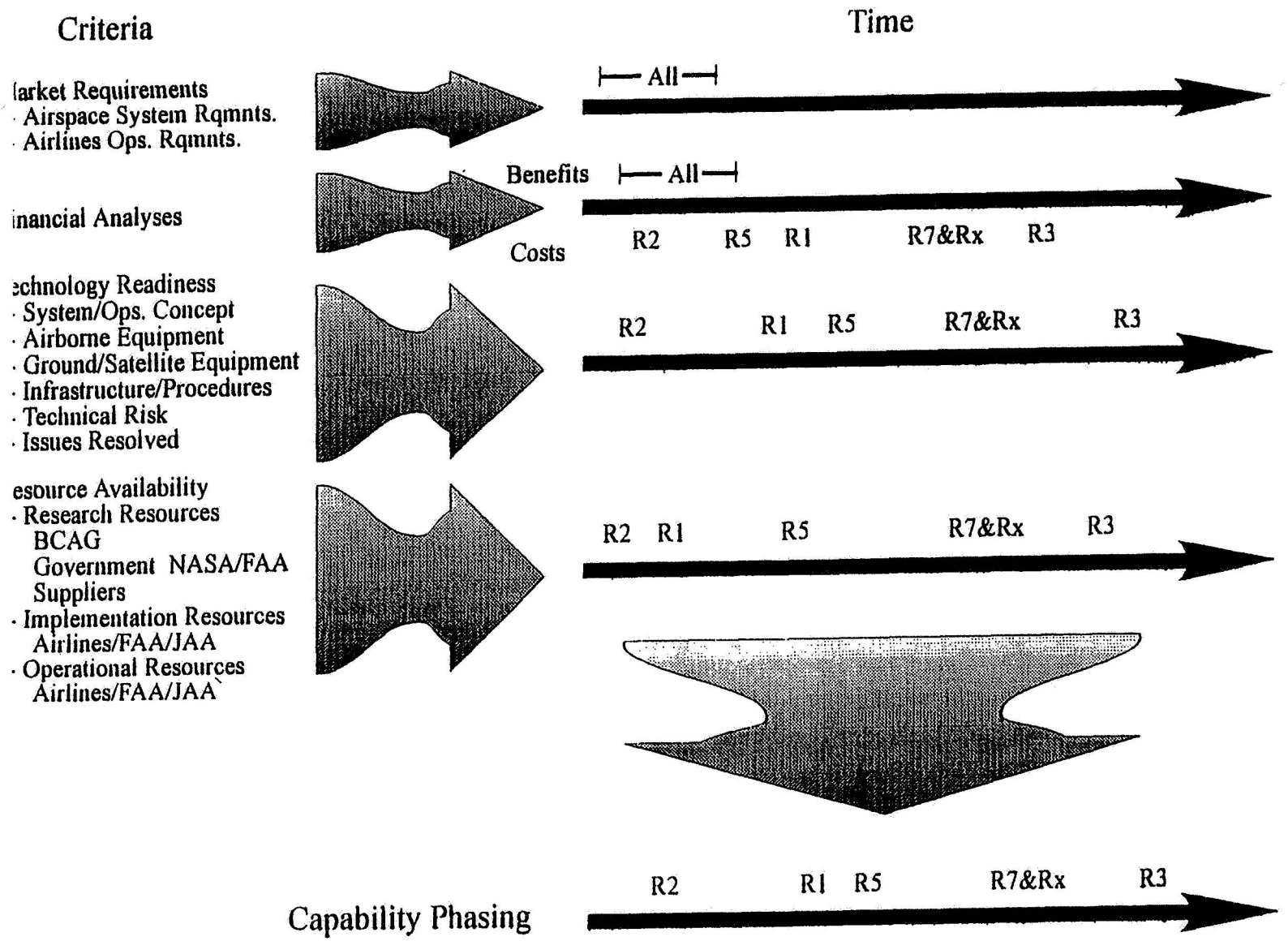

Enhanced Situation Awareness

Initial ESAS Operational Envelope

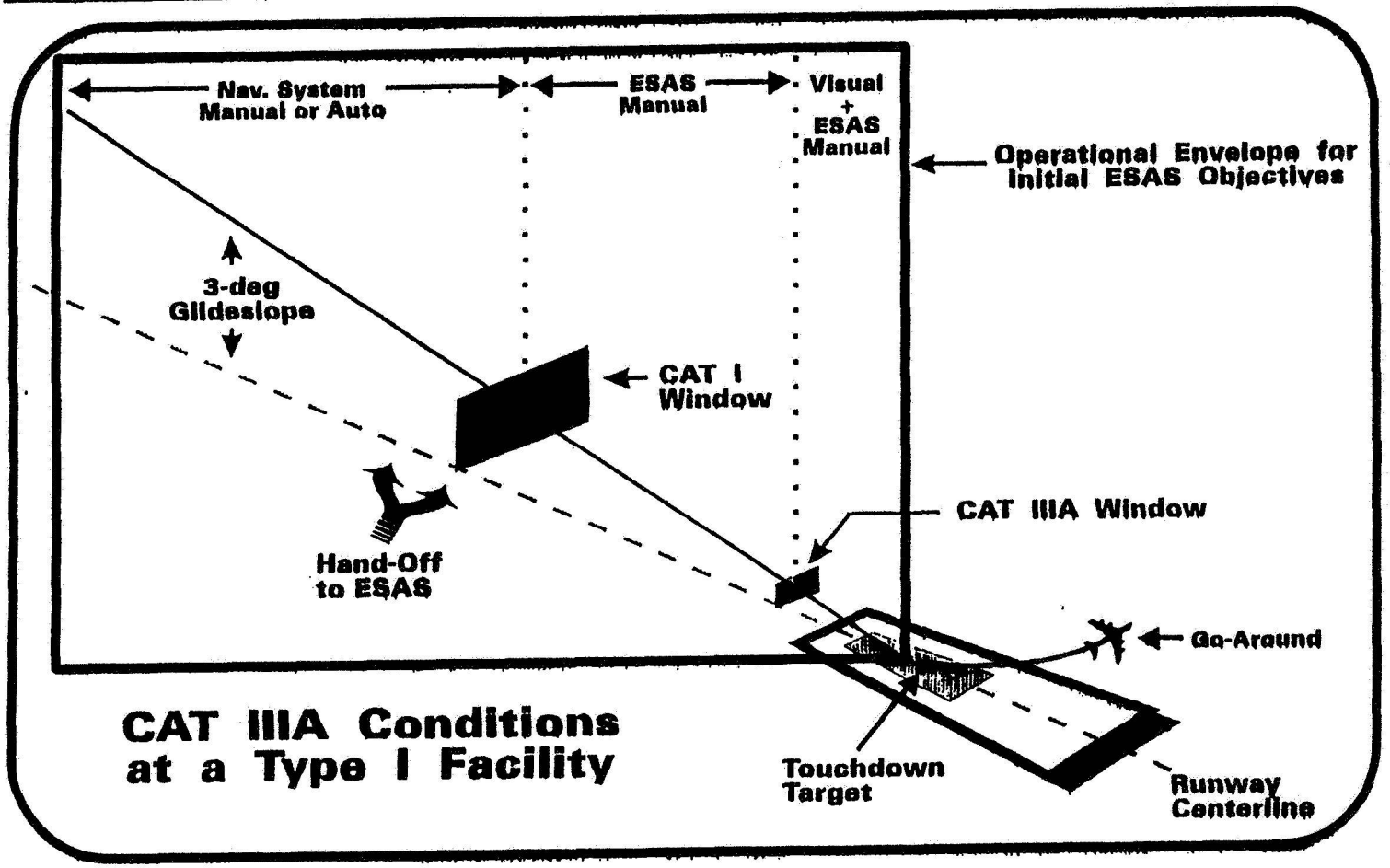

Enhanced Situation Awareness

Critical System Issues

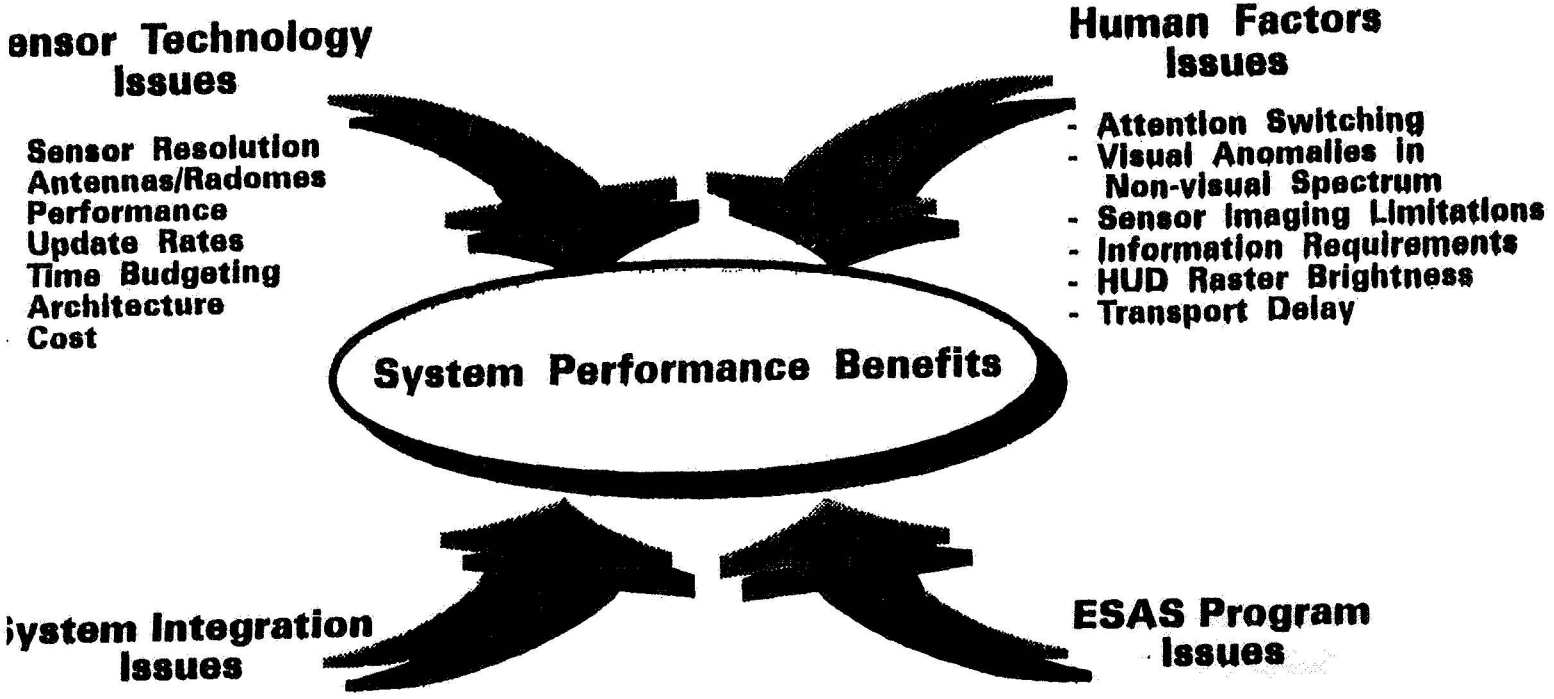

Enhanced Situation Awareness

Major System Risks

- Capability of Crew to Transition from HUD to Outside View
- Impact of Visual Anomalies in a Non-Visual Spectrum Image
- Limitations of the Sensor Imaging Capability
  - Resolution
  - Image Quality
  - Transport Delay
- Brightness of Raster Imagery on the HUD
- Radome

Enhanced Situation Awareness

Risk Reduction Strategy

- Let technology do what it does best
  - Radar is best at detecting objects not imaging
  - HUD very good at displaying stroke symbology
- Provide the crew with the information they need to do their job
- Display a sensor-based "wire frame" representation of the runway environment instead of a sensor generated raster image
- Display sensor detected obstructions as distinct symbols rather than indistinct blobs

Enhanced Situation Awareness

How New Strategy Addresses Major Risks

- Runway "Wire Frame" Representation Will Not Have Visual Anomalies Created by Imaging Non-visual Spectrum Energy
- Since the Display Will Present the Information and Filter the Noise, It Should be Less Difficult to Transition to the Outside Scene
- Sensor Imaging Is Not Required Thus Imaging Technology Limitations Are Not a Risk
- The "Wire Frame" Representation Will Be Drawn With Stroke and We Already Know How to Make a Stroke Written HUD Bright Enough
- If the Weather Radar Can Provide All Functions, We Already Know How to Build the Radome

Enhanced Stiuation Awareness System

System Evolution

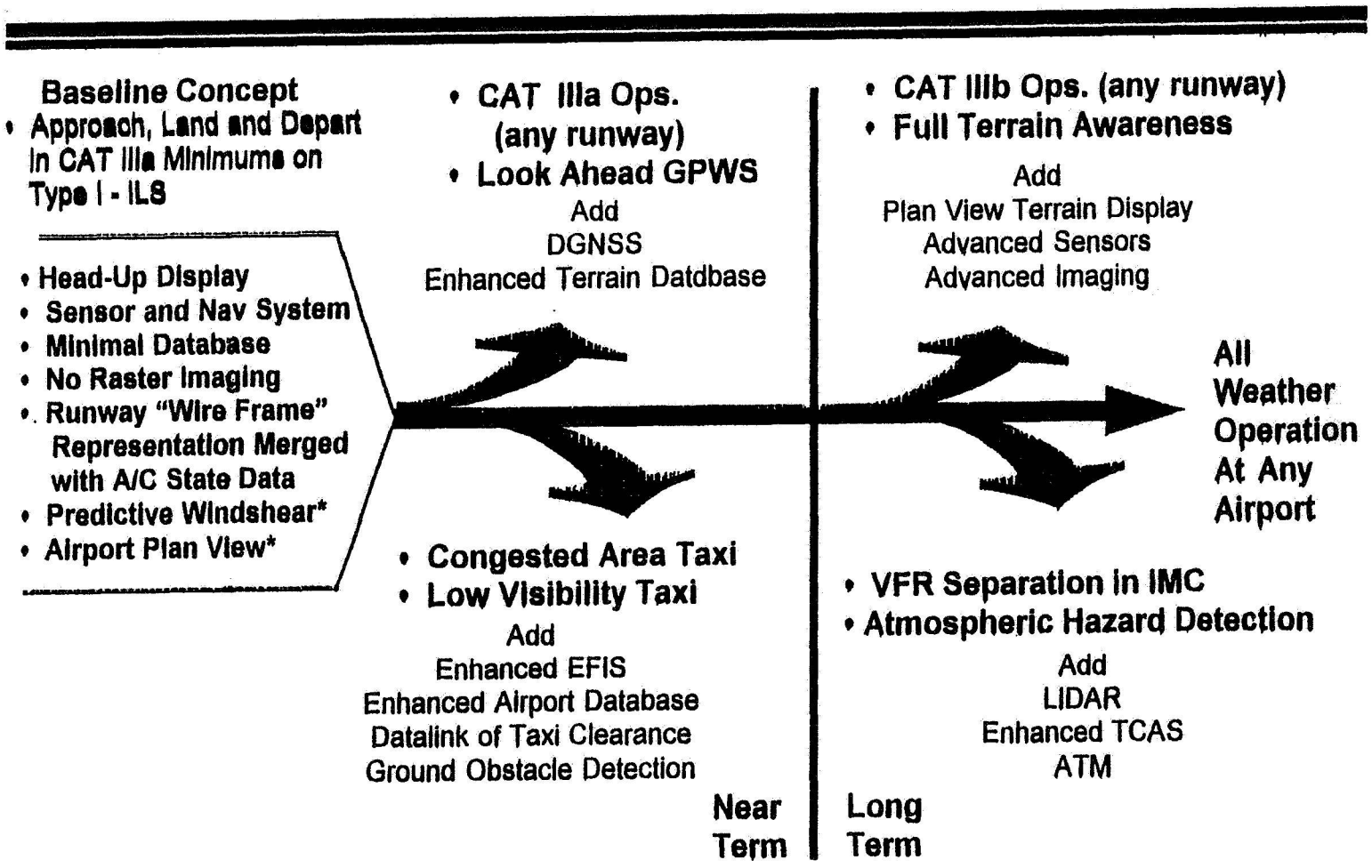

omit

Overview of Westinghouse Enhanced Vision Technology Activities.

W. Patterson,

Westinghouse Electric Corp.

OVERVIEW OF WESTINGHOUSE EVS TECHNOLOGIES

5TH (and Final)

COMBINED MANUFACTURERS' & TECHNOLOGISTS

AIRBORNE WINDSHEAR

REVIEW MEETING

Session 7

30 Sept 1993

Westinghouse ESG
Walter Patterson

OUTLINE

BEYOND WINDSHEAR

SENSOR OBJECTIVES

MODAR APPROACH

MODAR EVS RELATED FEATURES

X-BAND MAPS

E-O ACTIVITIES

SUMMARY

EVS/SVS

- **OBJECTIVES**
  - Safely increase all weather terminal area efficiency
- **EVS ROLE**
  - Obtain credit for lower operating minimums
    - FAR 91.175 Rules
    - Obstacle Avoidance
- **QUANTIFY BENEFITS/COST**
  - Upgrade old aircraft to CAT III on CAT III
  - CAT IIIa on Type I
  - CAT I, II on Non-equipped runways
  - Fog severity, haze, mist, night
  - Unimproved runways
- **AGREED WEATHER PHENOMENOLOGY**
  - Impartial Data Base
- **POTENTIAL TECHNOLOGY TRANSITION EFFORTS**
  - HSCT
  - T.A.P.

Beyond Predictive Windshear

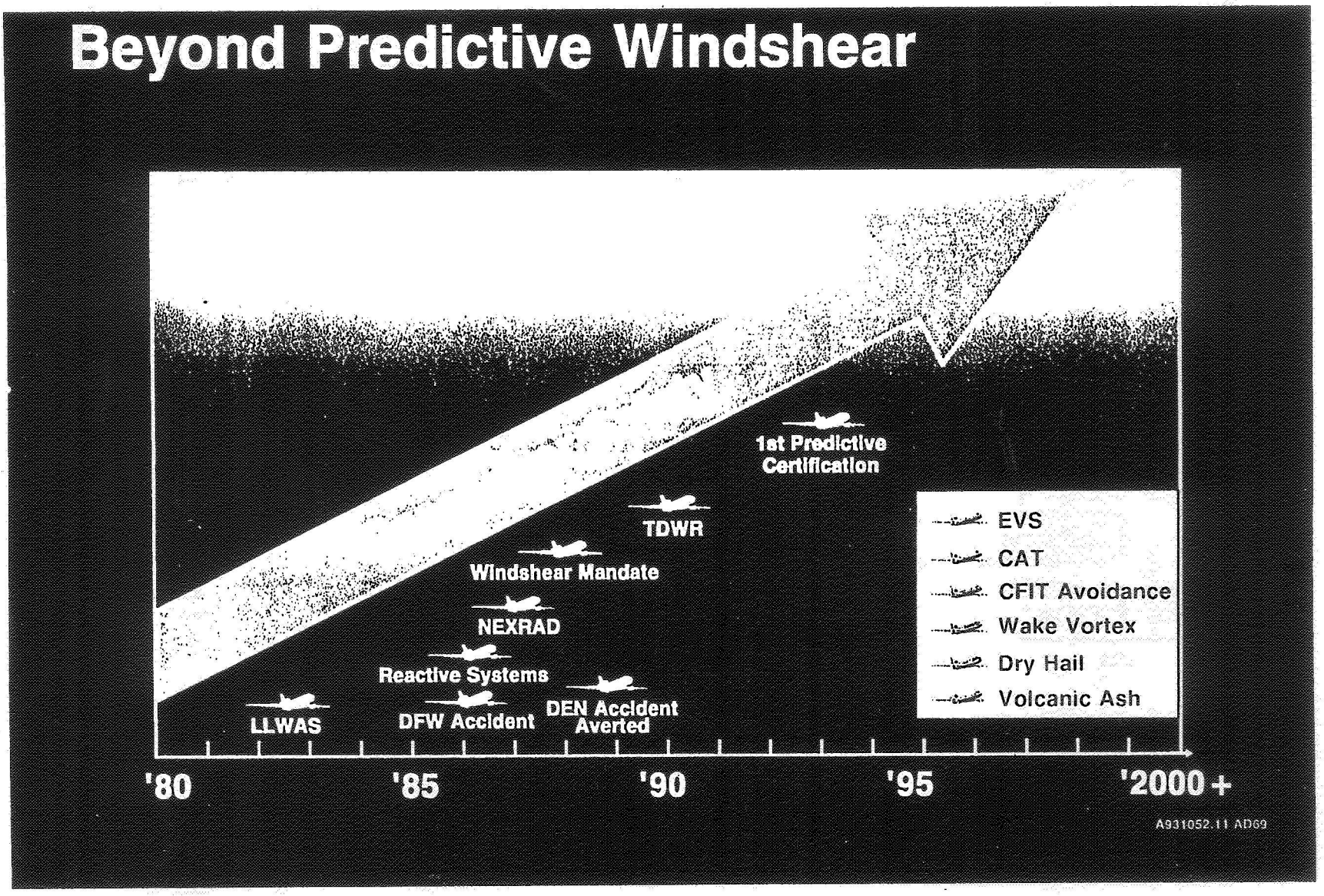

Honeywell Westinghouse GEC AVIONICS

ESAS:

- Reduce costs by increasing operational efficiency
- Increase safety

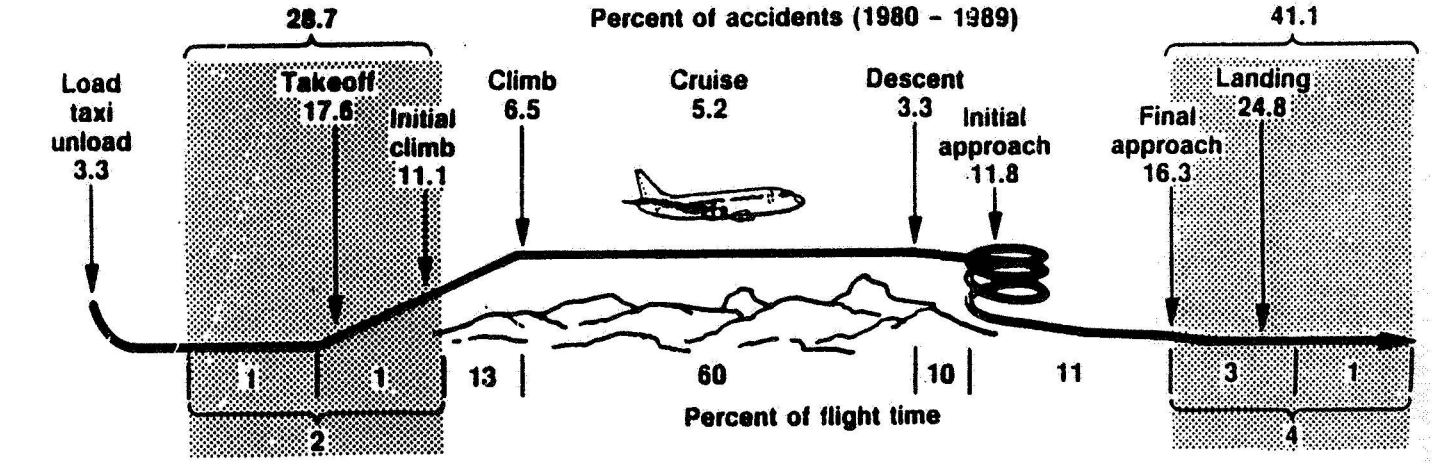

Functional Requirements

- Taxiway obstacle avoidance
- Take-off aids
- Windshear detection
- Obstacle avoidance
- Wake vortex
- Weather avoidance
- Clear air turbulence detection
- Navigation
- Volcanic ash detection
- Air target display
- Windshear detection
- CFIT
- Landing aids
- Obstacle avoidance
- Taxiway obstacle avoidance
- Wake Vortex

P5820 07 03

[1]Assumed 1.6 hour flight leg

EVS SENSOR OBJECTIVES

- **Obstacle Detection Avoidance**

- **Augment Navigation Aids, Integrity Monitor**

  Raw Image

  Scene Match Data Base

  VASI/RASI

MODAR

- X-Band Radar/Processing System
  - Improved Weather
  - High Integrity Windshear
- Modularly Architected for ESAS Functions
  - Core Sensor
  - Adjunct Sensors
- X-Band Multiple Function Growth
  - EVS
  - Obstacle Avoidance
  - CFIT
- MODAR X-Band EVS Features
  - Coherent Over Multiple Channels - Frequency Diverse
  - Dual Bandwidth Map/Image Resolution
  - Partitioned for Single/Dual Receivers - Monopulse
  - Solid-State Power Managed, Fault Tolerant Transmitter
  - Processor Architected and Partitioned0 for Growth
  - Extensive Performance Monitoring Bit
  - Dual Use Technology Hardware and Software

MR-3000 . . . Improved Weather Radar (WXR) with Predictive Windshear (PWS)

Modular Radar Core Modules	Unique Modules
TX	
Receiver	
Exciter	
Proc.-GP	
Proc.-DSP	
Sync.	
Mas. Osc.	

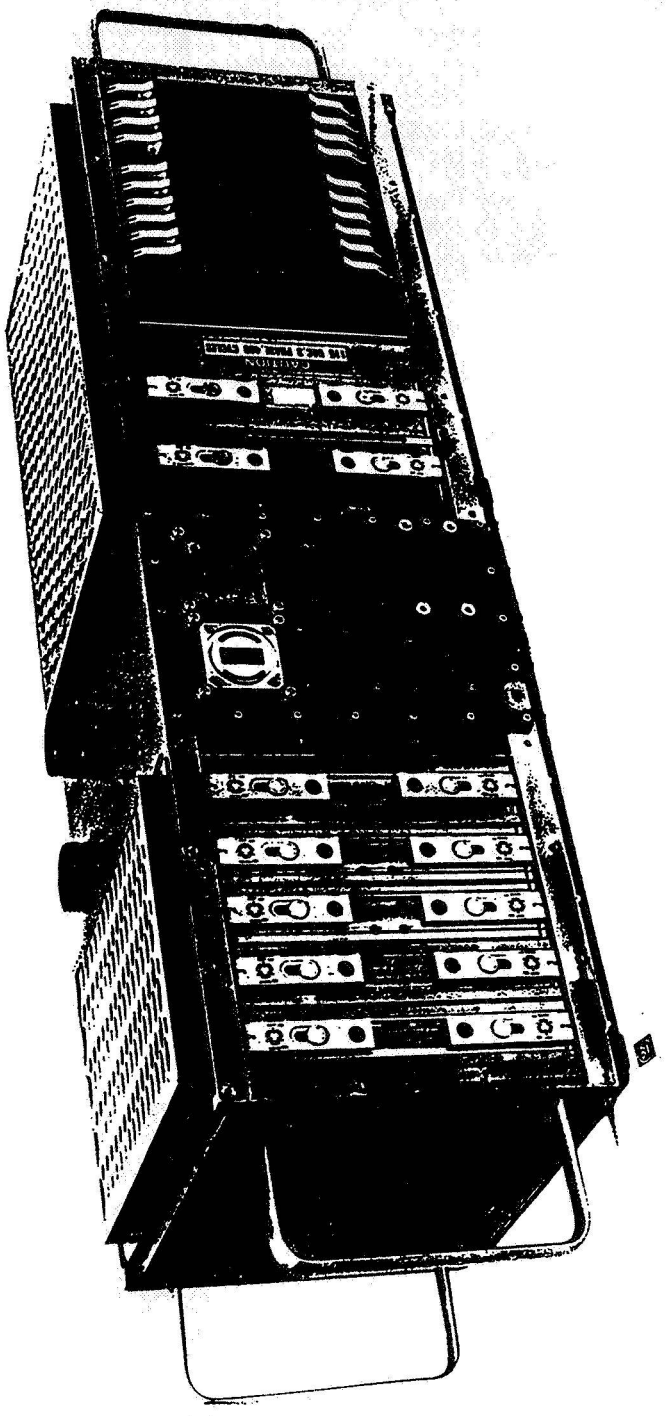

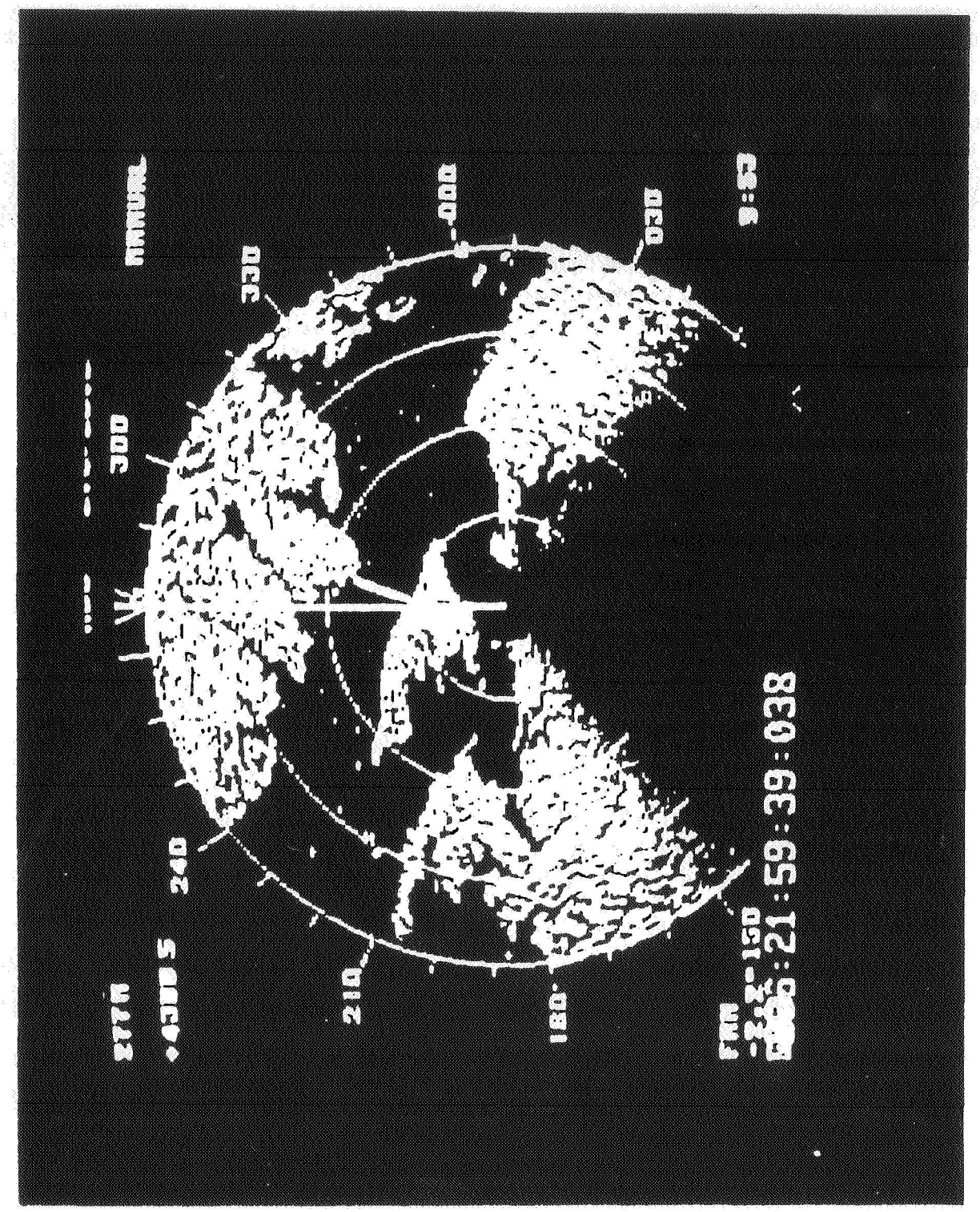
300
330
000
030
240
210
180
150
21:59:39:038

16:29.01N
ARMD
210
220
11:45
122M
PEM
20:59:31:308

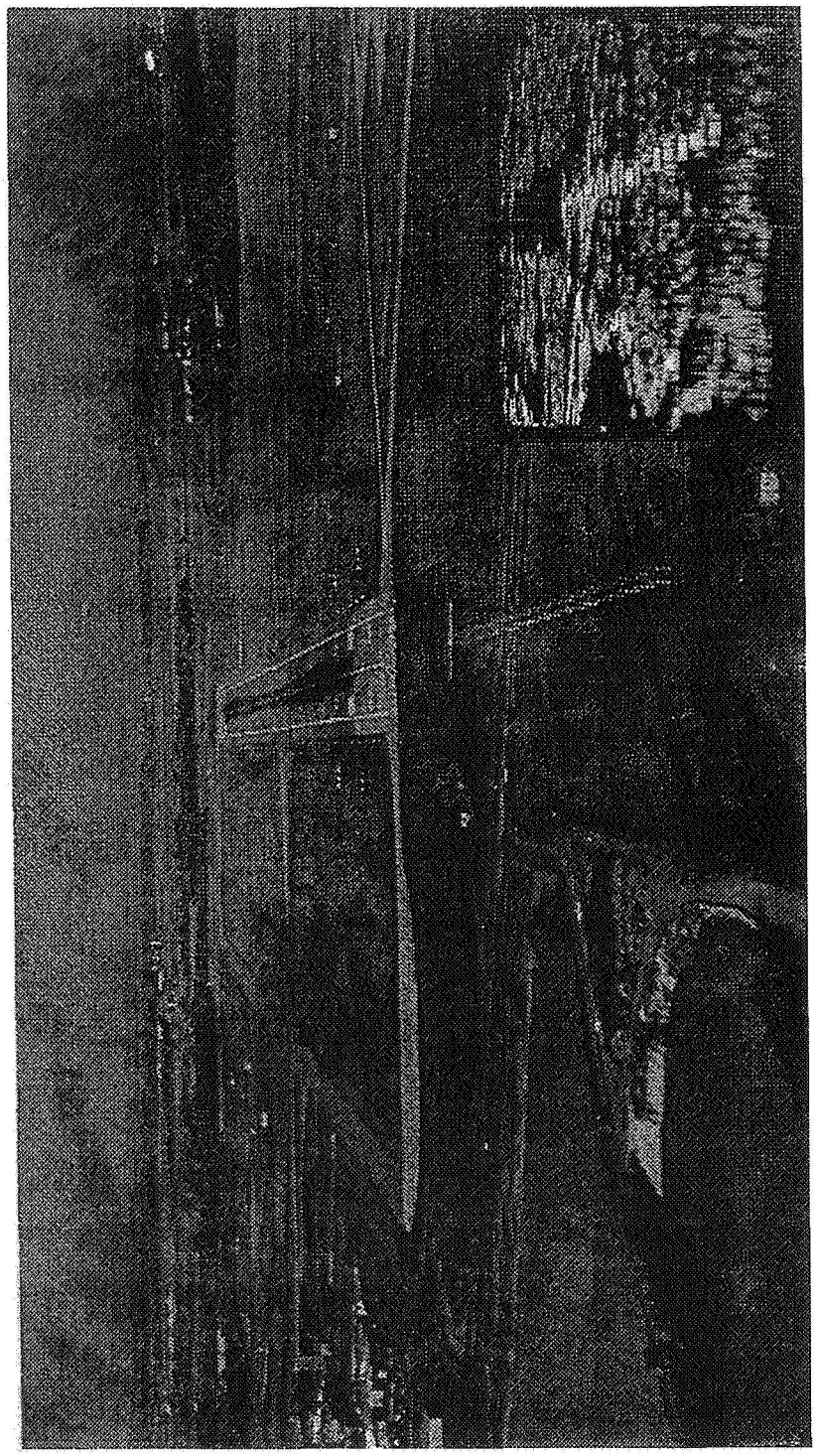

MODAR 4000 - HI RESOLUTION MAP - BWI RUNWAY 10 APPROACH

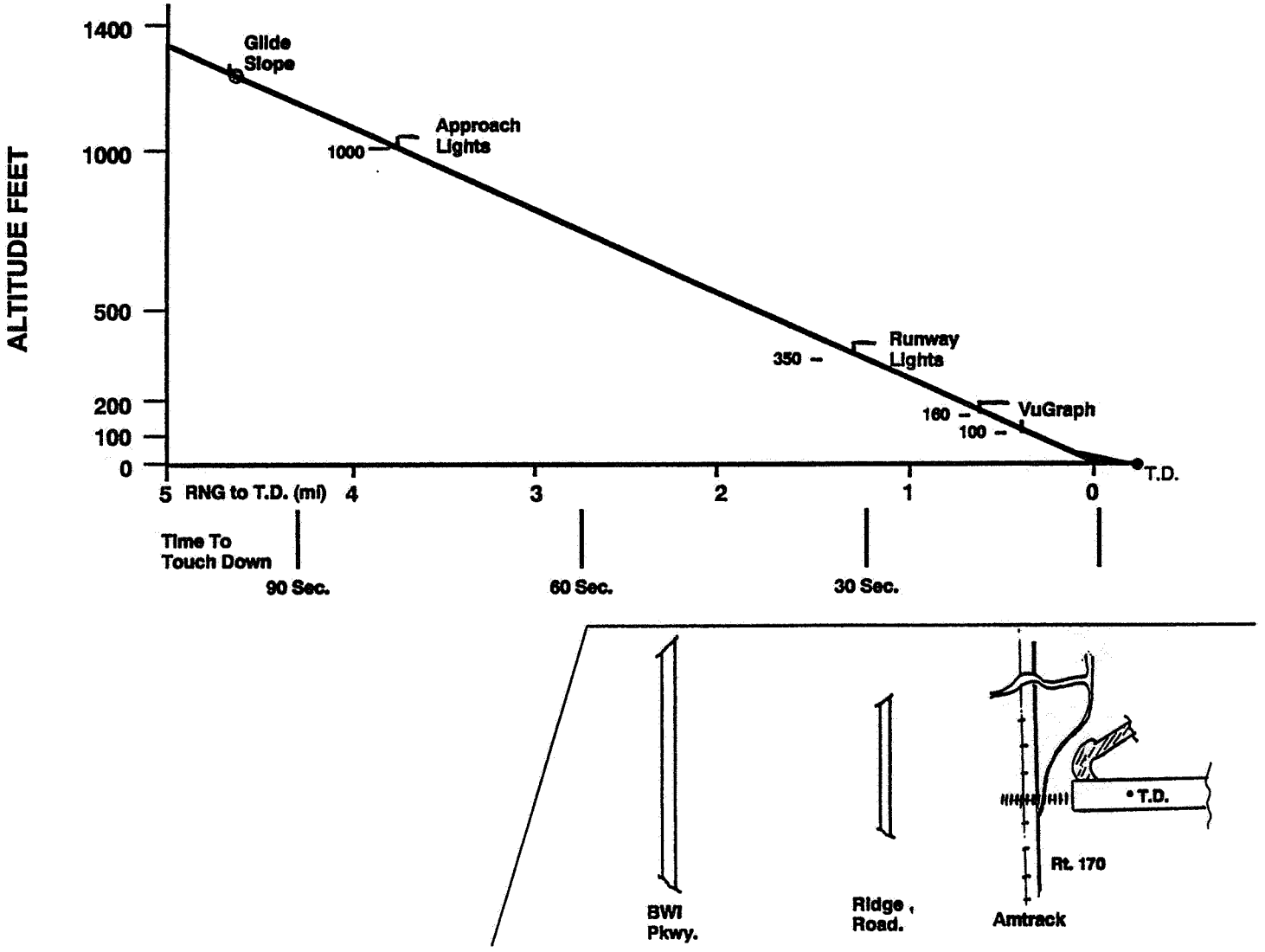

MANUAL
DEO
M301
28:5
FAN

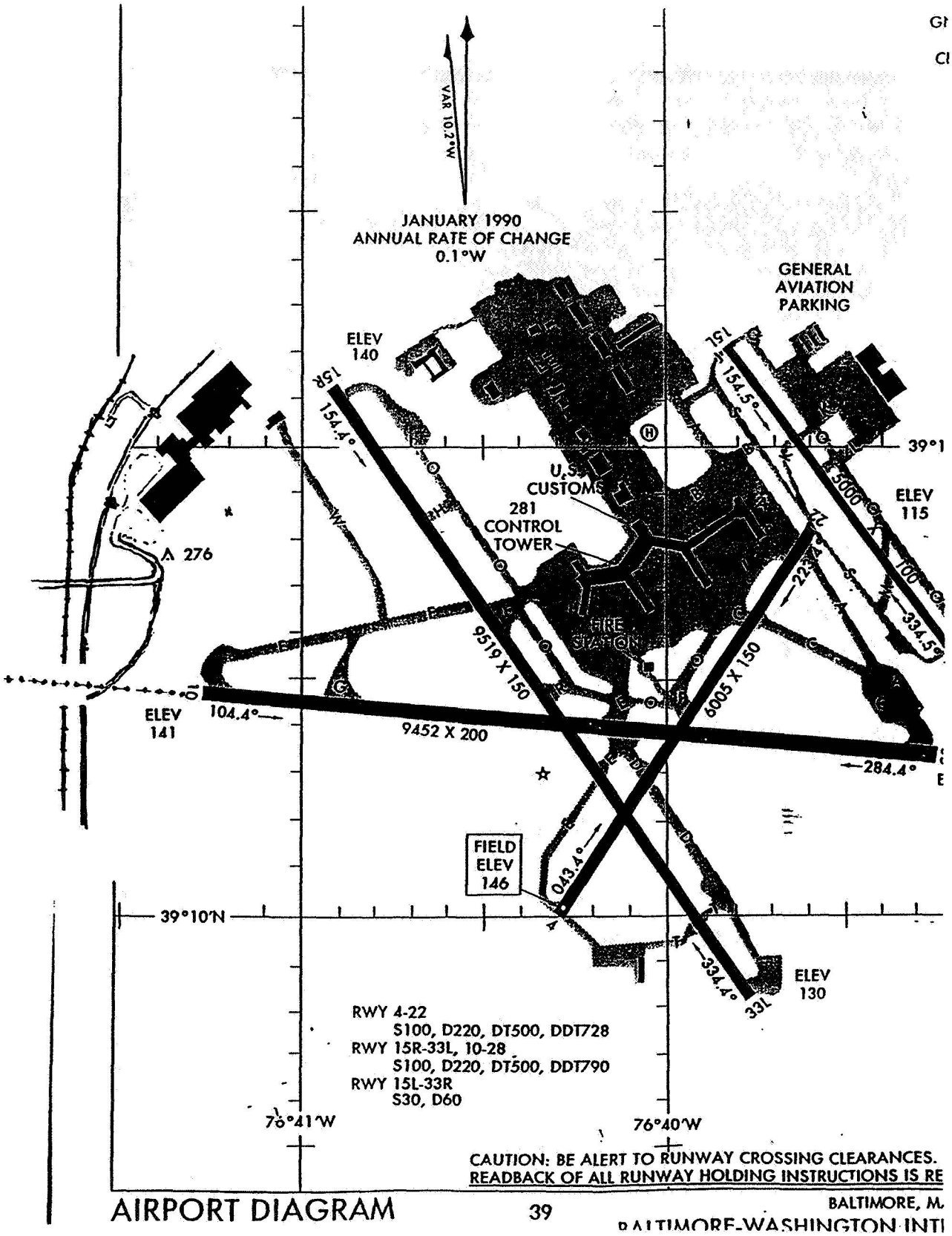
VAR 10.2°W
JANUARY 1990
ANNUAL RATE OF CHANGE
0.1°W
GENERAL
AVIATION
PARKING
ELEV
140
15R
154.4°
15L
154.5°
39°1
U.S.
CUSTOMS
281
CONTROL
TOWER
ELEV
115
3000
100
334.5°
22
A 276
FIRE
STATION
9519 X 150
6005 X 150
ELEV
141
10
104.4°
9452 X 200
284.4°
FIELD
ELEV
146
043.4°
39°10'N
334.4°
33L
ELEV
130
RWY 4-22
S100, D220, DT500, DDT728
RWY 15R-33L, 10-28
S100, D220, DT500, DDT790
RWY 15L-33R
S30, D60
76°41'W
76°40'W
CAUTION: BE ALERT TO RUNWAY CROSSING CLEARANCES.
READBACK OF ALL RUNWAY HOLDING INSTRUCTIONS IS RE
AIRPORT DIAGRAM
39
BALTIMORE, M.
BALTIMORE-WASHINGTON INTI

ESAS

Westinghouse Test Aircraft

The addition of meteorological instrumentation provides truth data for Synthetic Vision development

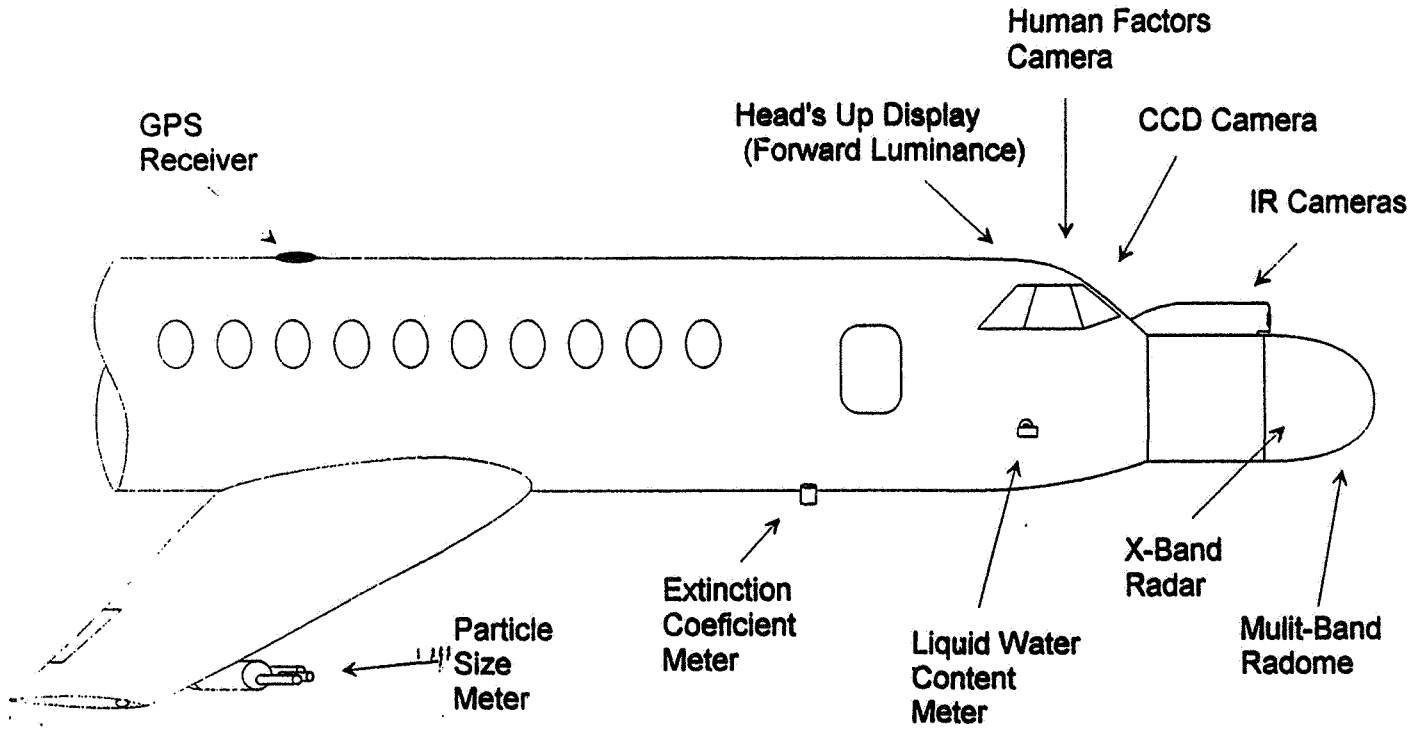

ENHANCED VISION SYSTEM TECHNOLOGY
INFRARED MODELING

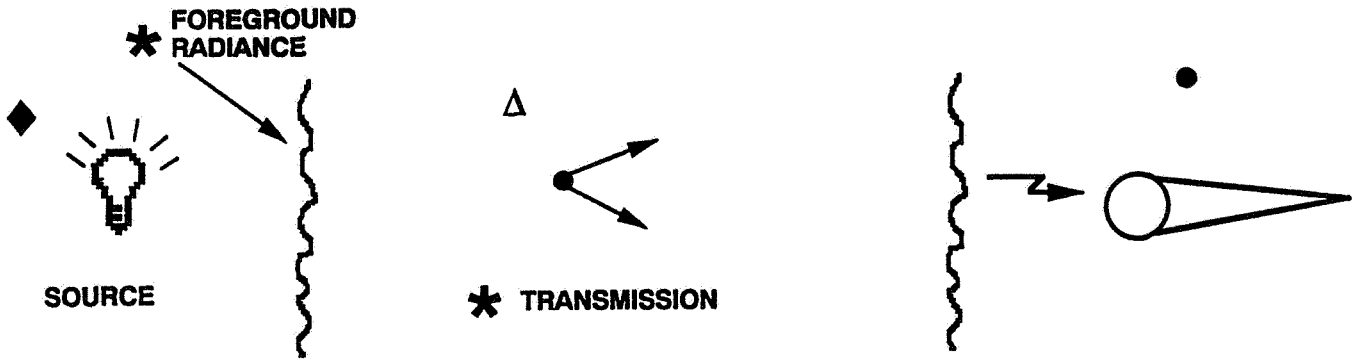

◆ TARGET ⟹ MEASUREMENT / EMPIRICAL

✱ LOWTRAN
Δ MIE SCATTER
} ⟹ SIMPLIFIED MODEL

● SENSOR CHARACTERIZATION

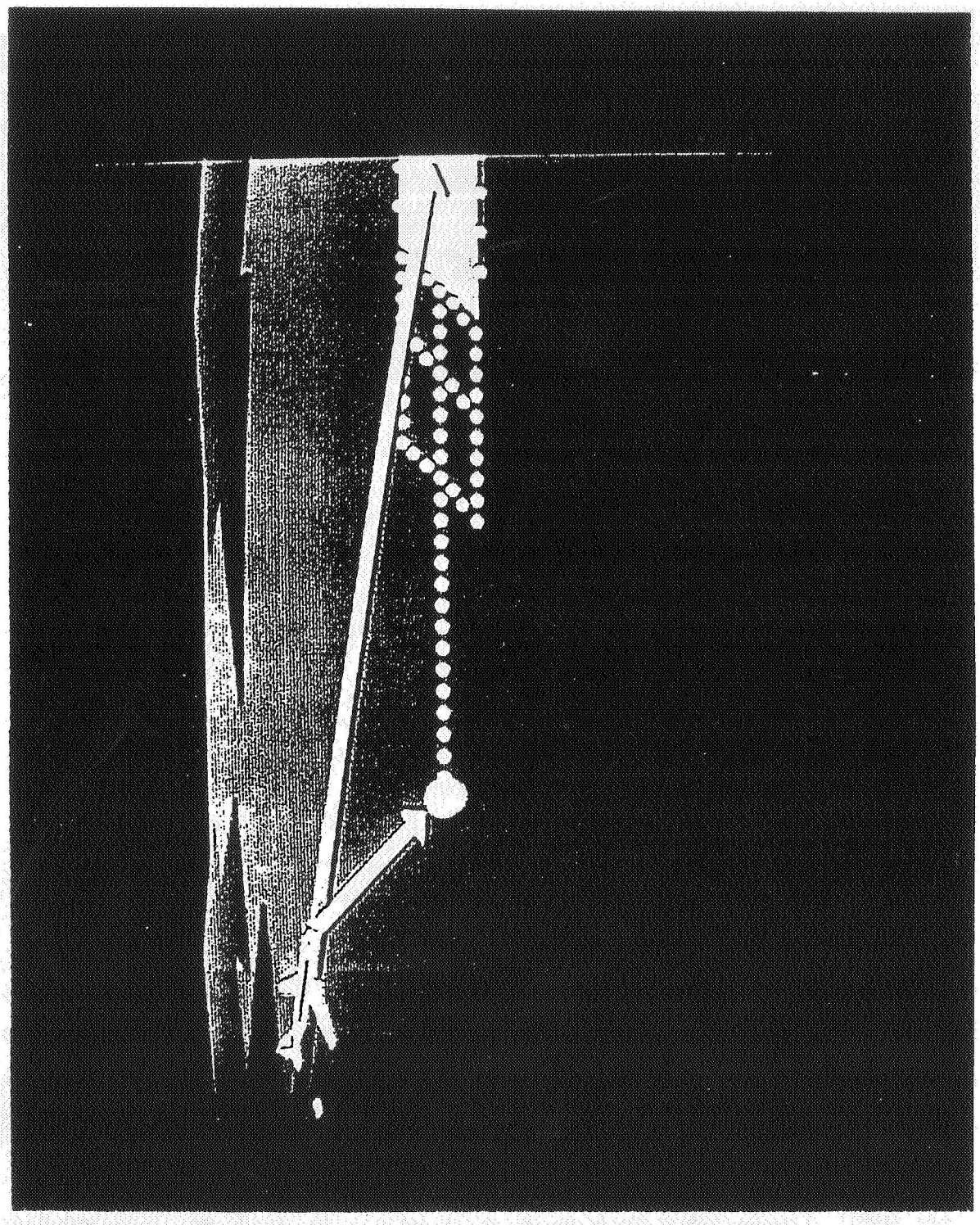

1–5 um PtSi
Visible
CCD

1–5 um PtSi
Visible
CCD

MODAR APPROACH TO EVS

- **X-Band Enabling Technology**
- **Supporting EVS Features Incorporated**
- **Processing Technology Provides High Resolution Map Basis for X-Band EVS**
- **Modular Architecture Set For Pre-Planned Growth**
- **Incrementally Achieve Lower Minimums with X-Band**
- **Augment with other Sensors as Justifiable Infrared and MMW**
  - **Independent Apertures and Front Ends**
  - **Shared Signal and Image Processing**

Evaluation of Candidate Millimeter Wave Sensors for Synthetic Vision.

N. Alexander, J. Echard,

and B. Hudson,

Georgia Tech Research Insitute

ABS: next page

Evaluation of Candidate MMW Sensors for Synthetic Vision

Neal T. Alexander, Brian H. Hudson, and Jim D. Echard
Georgia Tech Research Institute
7220 Richardson Road
Smyrna, GA 30080

The goal of the Synthetic Vision Technology Demonstration (SVTD) Program was to demonstrate, and document the capabilities of current technologies to achieve safe aircraft landing, take off, and ground operation in very low visibility conditions. As part of the technology evaluation process, the Georgia Tech Research Institute (GTRI) was a primary participant in two of the major thrusts of the program: (1) sensor evaluation in measured weather conditions on a tower overlooking an unused airfield and (2) flight testing of sensor and pilot performance via a prototype system installed in a test aircraft.

GTRI supported tower testing of six different millimeter wave (MMW) radar sensor configurations and two infrared (IR) sensors at an instrumented tower facility at Wright-Patterson AFB in the 1991-1992 time frame. Sensors tested included a Honeywell 35-GHz MMW imaging radar, a Norden 95-GHz MMW target detection and tracking radar, a Lear Astronics 94-GHz MMW imaging radar, a 3-5 micron Kodak IR imaging camera, and a 3-5 micron Mitsubishi IR camera. The tower tests were performed under varied meteorological conditions including clear, fog, rain, and snow. As tower-test contractor, GTRI provided engineering services, including test planning, equipment preparation, field-test support, sensor data analysis, sensor performance modeling, and technical documentation of test results.

Three of the sensors evaluated in the tower tests were subsequently utilized in the flight-test evaluation program, which was performed during 1992 using a functional prototype SV system mounted in a specially configured Gulfstream II aircraft. During these flight tests, the observed performance of the prototype SV system was documented in actual and simulated weather conditions. The prototype system evaluated under this program included both a MMW radar sensor and an IR imaging sensor to detect and image the runway and surrounding area, as well as both a HUD and a head-down display to present the images and flight symbology to the pilot. GTRI's primary role in the flight test program was to perform analysis of raw radar data frames (snapshots). The effort focused almost exclusively on data snapshots captured by the Honeywell MMW radar. GTRI also participated in experiment design and test planning, characterization of the radar sensors, radar modeling, radar calibration, and weather data analysis.

The presentation first briefly addresses the overall technology thrusts and goals of the program and provides a summary of MMW sensor tower-test and flight-test data collection efforts. Data analysis and calibration procedures for both the tower tests and flight tests are presented. The remainder of the presentation addresses the MMW sensor flight-test evaluation results, including the processing approach for determination of various performance metrics (e.g., contrast, sharpness, and variability). The variation of the very important contrast metric in adverse weather conditions is described. Design trade-off considerations for Synthetic Vision MMW sensors are presented, and the presentation concludes with recommendations for future research to address the remaining unresolved issues.

Evaluation of Candidate MMW Sensors for Synthetic Vision

Neal T. Alexander
Brian H. Hudson
Jim D. Echard

Synthetic Vision Technology Demonstration (SVTD) Program

Georgia Tech Research Institute
Georgia Institute of Technology
Atlanta, Georgia 30332

30 September 1993

GTRI SVTD Support Program (1)

- Demonstrate capabilities of current technologies to achieve safe landing, take off, and ground operations in low-visibility conditions

- Major thrusts

  Sensor tower tests
  - Static Tests
  - Overlooking runway
  - Measured weather conditions

  Flight testing
  - Sensor and pilot performance
  - Prototype system installed in aircraft

GTRI SVTD Support Program (2)

- Tower tests: 1991-1992
  - Radars: Honeywell 35 GHz pulsed
    Lear Astronics 94 GHz FMCW
    Norden 95 GHz pulsed
  - IR: Two IR cameras
  - Data Runs: 35 GHz (82), 95 GHz (174)
  - Weather: Clear, rain, snow, fog
- Flight tests: 1992
  - Radars: Honeywell 35 GHz pulsed
    Lear Astronics 94 GHz FMCW (limited)
  - IR: Kodak 3-5 mm focal plane camera
  - Approaches: 35 GHz (96), 94 GHz (11)
  - Weather: Clear (46), fog (41), snow (8), rain (1)

Data Analysis & Calibration (1)

- Calibrate MMW Sensors
  - Measure radar system gains and losses
  - Inject RF signal to develop receiver transfer function
  - Locate calibrated reflectors within runway scene

- Reduce Radar Sensor Data
  - Convert raw data into equivalent received power
  - Extract values from areas of interest within scene

Data Analysis & Calibration (2)

- Develop Sensor Figures of Merit
  Contrast, sharpness, and variability

- Calculate Radar Phenomenology Values
  RCS for runway and bordering grass
  Volumetric RCS and path attenuation for precipitation

Flight Test Data Analysis Methodology (1)

- Analyze discrete radar snapshots (full azimuth scan) at selected ranges

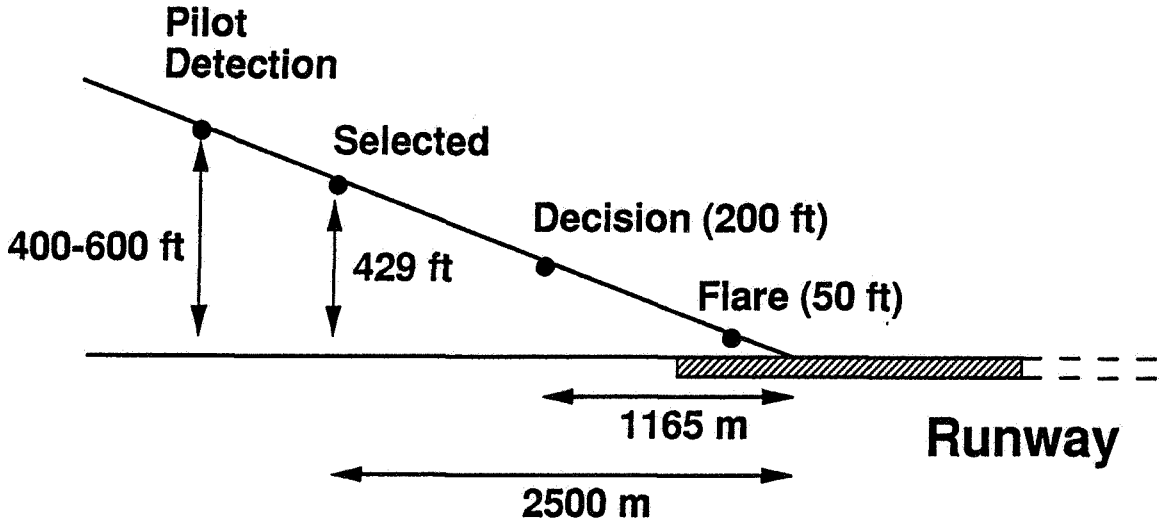

Flight Test Data Analysis Methodology (2)

- Weather data
  - Water drop size distributions
  - Liquid water content (LWC) for fog
  - Rainfall rate
  - Equivalent rainfall rate for snow
- Airport ground truth
  - Runway description
  - Terrain description
- Radar calibration
  - MMW Receiver calibration
  - Radar reflectors at selected runways

SVS Technology Demonstration

MMW Sensor Evaluation

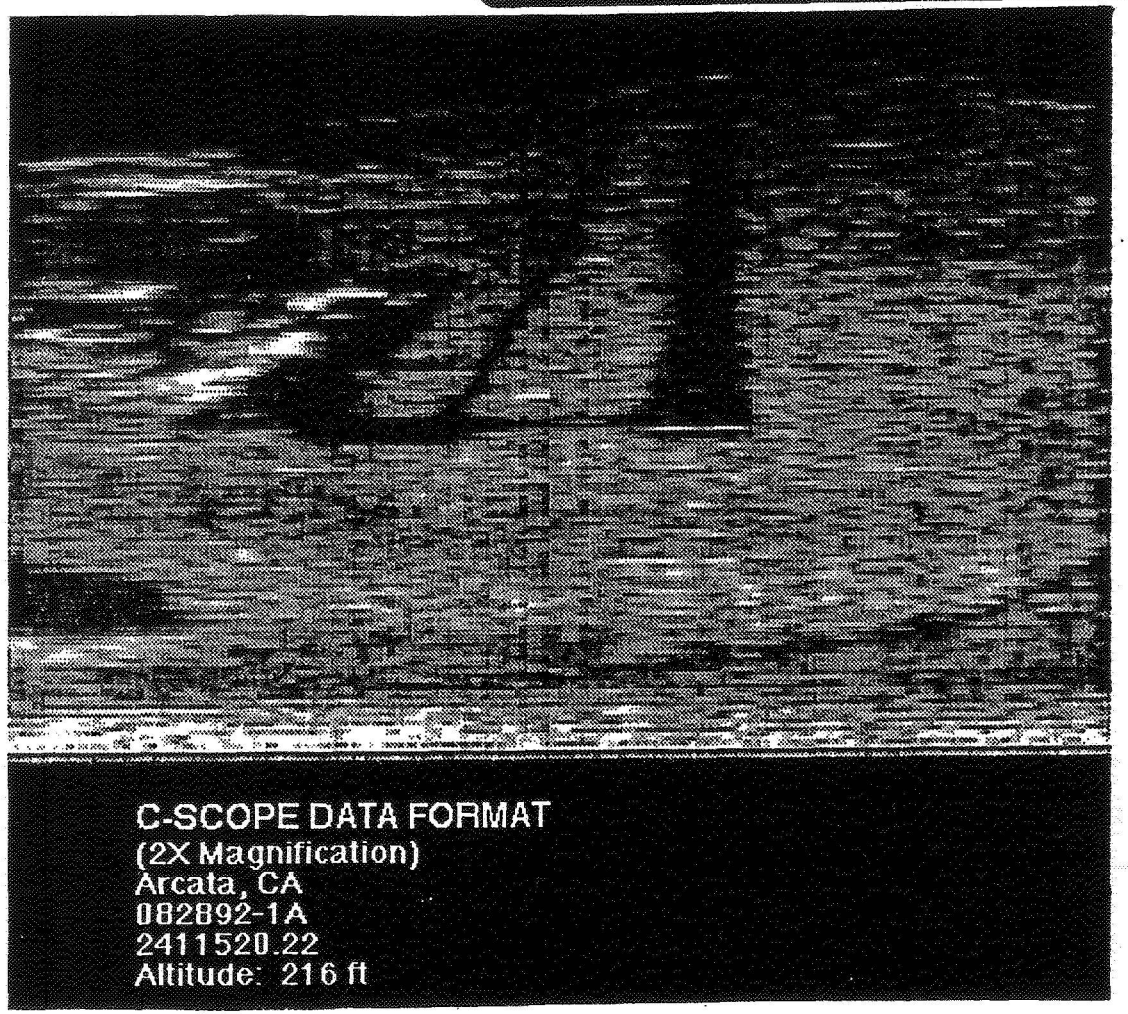

SVS Technology Demonstration

MMW Sensor Evaluation

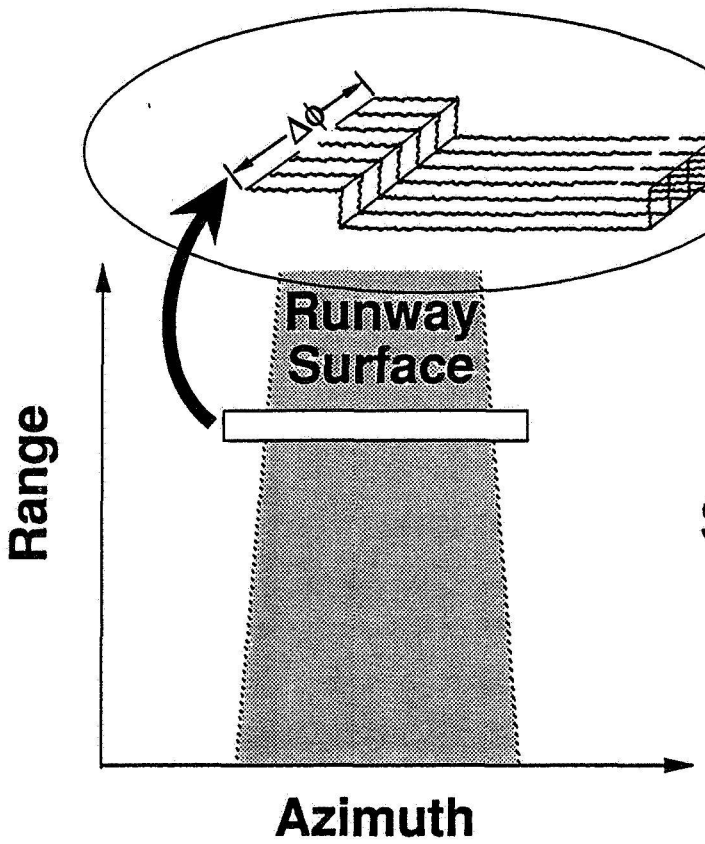

Radar Data Processing for Contrast, Sharpness, and Variability

Definitions of Contrast, Sharpness, and Signal-to-Variability Ratio

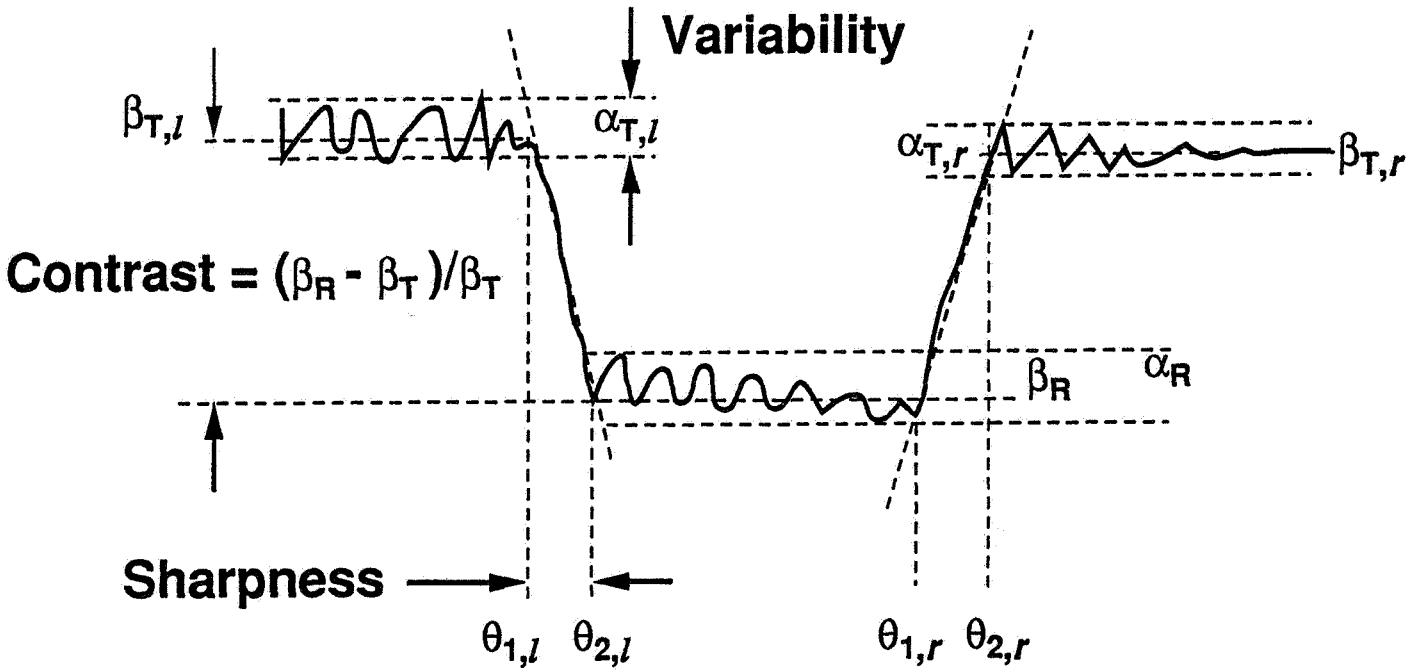

SVS Technology Demonstration

MMW Sensor Evaluation

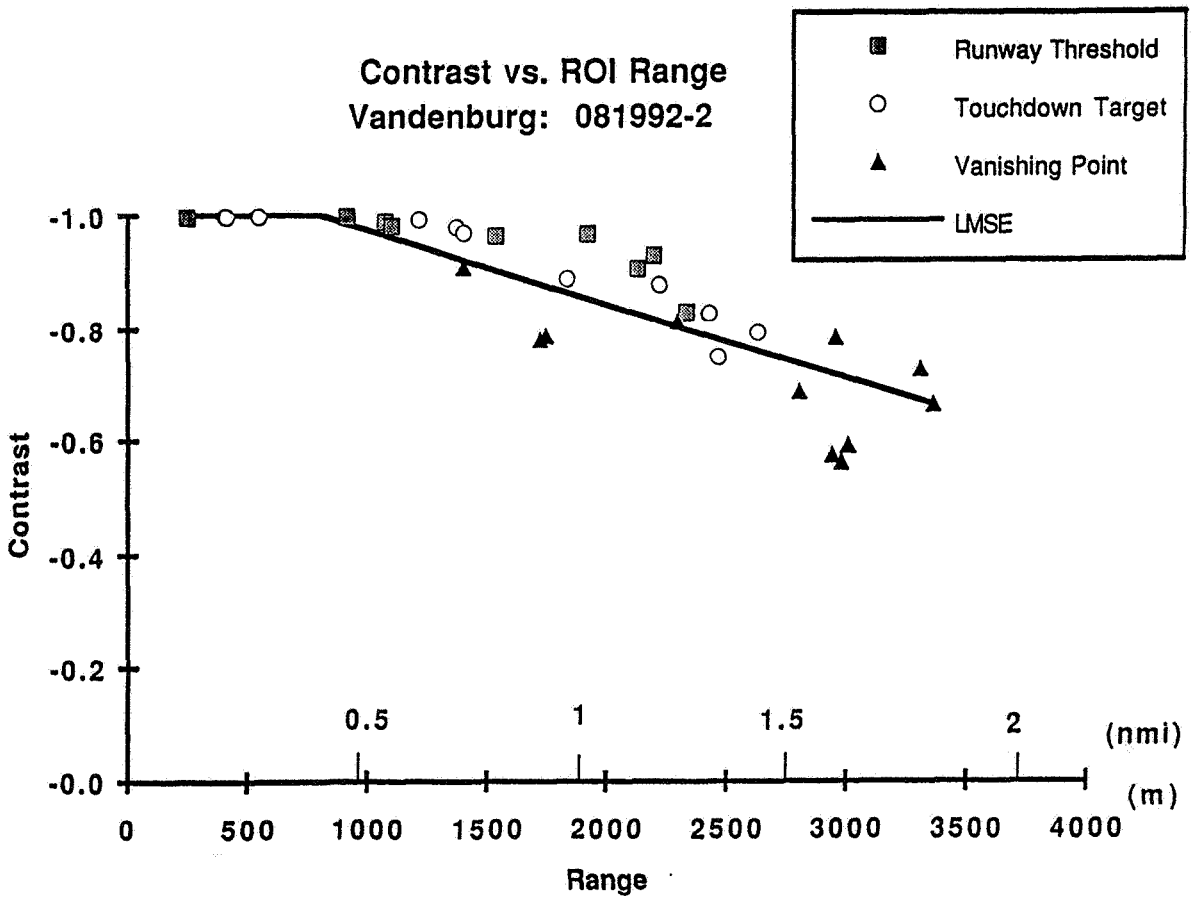

MMW Sensor Evaluation

Contrast vs. ROI Range
Clear Weather Approaches

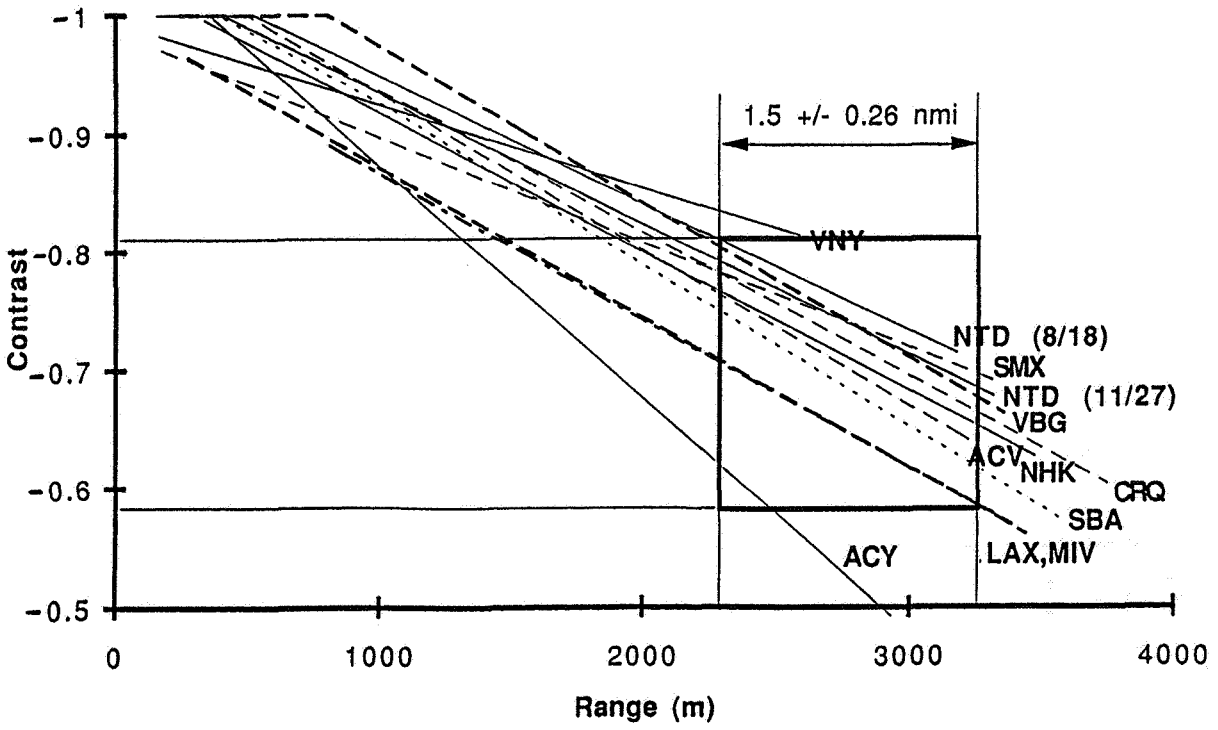

Weather Effects on Contrast (35 GHz)

- Fog
  - Excellent weather penetration (no effect)
  - (Most delays due to fog)
  - (Greatly reduced visual range)
- Rain
  - Poor penetration for rain rates > 8 mm/hr
  - Drop size distribution dependence
  - (Visual range reduction in very heavy rains)
- Snow
  - Falling snow not a problem
  - Accumulated snow effect significant
  - Runway must be cleared to improve contrast

Design Tradeoff Issues (1)

- MMW Band
  - 95 GHz: higher az resolution for given aperture
  - 35 GHz: superior weather penetration

- Azimuth and Range Resolution
  - High res (0.3° az by 7 m range): sharper images
  - Low res (1° az by 20 m range): higher contrast

Design Tradeoff Issues (2)

- Antenna Scan Rate
  - High rate (10 Hz): reduced image update latency
  - Low rate (5 Hz): more dwell time for integration

- Antenna Polarization
  - Circular: reduced rain backscatter/better image
  - Linear: higher return from grass clutter

Future Research Needs

- Use SVTD data to predict performance of future candidate MMW sensors
- Develop better models for performance of MMW sensors in weather
- Validate performance of future candidate MMW sensors based on the test and evaluation methodology established in the SVTD program
- Refine image quality metrics
- Examine techiques for image enhancement

Passive MMW Camera for Low Visibility Landings.

M. Shoucri,

TRW Applications Technology Div.

No abstract
Corrigendum needed

A Passive Millimeter Wave Imaging Sensor for Aircraft Landing in Poor Visibility Conditions

TRW

Fifth (and Final) Combined Manufacturers' and Technologists'
Airborne Windshear Review Meeting
NASA-LaRC
September 28-30, 1993

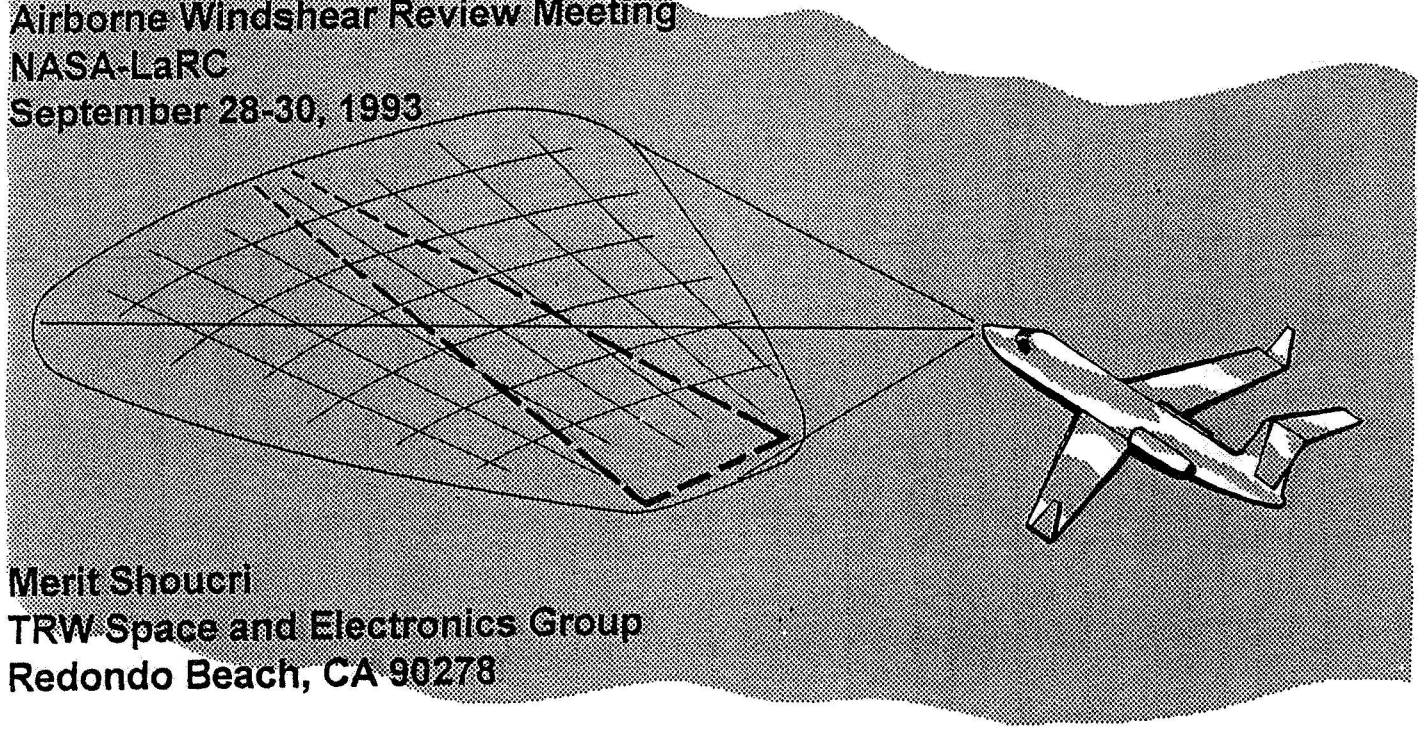

Merit Shoucri
TRW Space and Electronics Group
Redondo Beach, CA 90278

A Camera that sees through fog

- System Engineering
- Sensor Hardware
- Synthetic Vision System

Camera Images Are Obtained from Naturally Occurring Millimeter Waves

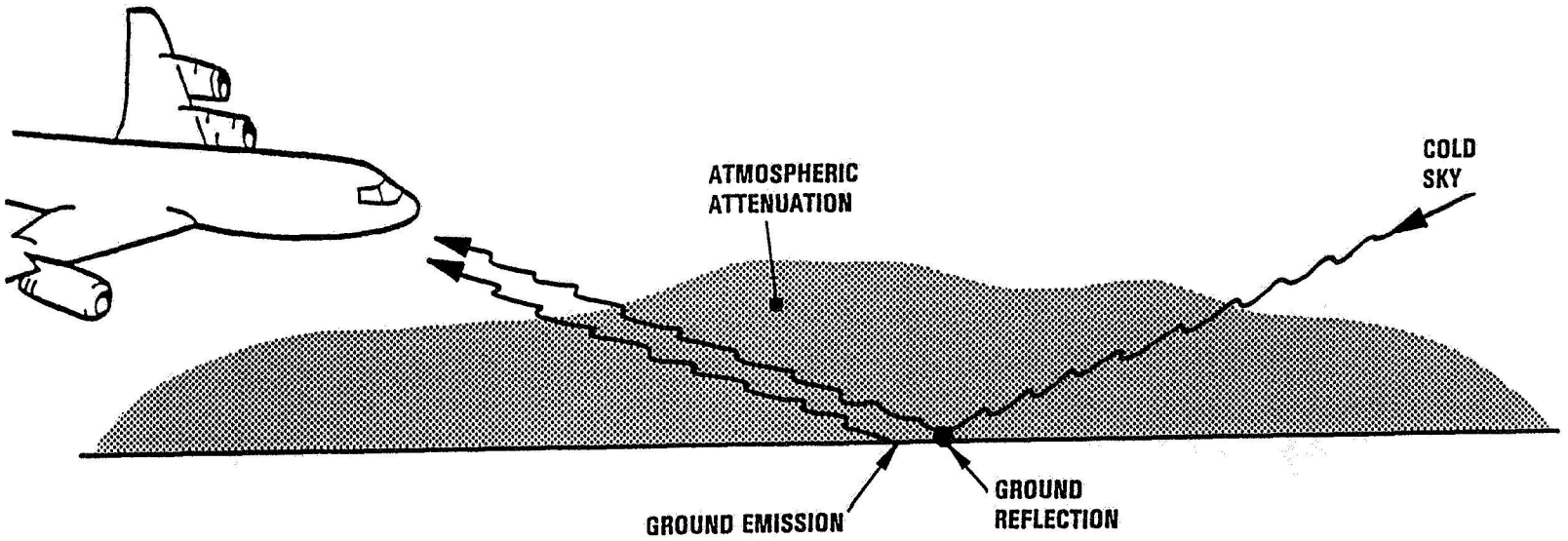

Scene contrast is provided by difference in material reflectivities, temperature and sky illumination of the scene

Passive MMW Sensing

$$T_{obs}(\theta; p) \sim T_a(\theta) + \{e(\theta; p)\, T_{scn} + [1 - e(\theta; p)]\, T_{sky}(\theta)\} / L_a(\theta)$$

- $T_{obs}(\theta; p)$: OBSERVED MMW TEMPERATURE AT GIVEN ANGLE Θ AND PLOARIZATION p
- $T_a(\theta)$: ATMOSPHERIC EMISSION EQUIVALENT RADIOMETRIC TEMPERATURE BETWEEN SCENE AND SENSOR
- $e(\theta; p)\, T_{scn}$: SCENE EMITTED RADIOMETRIC TEMPERATURE
- $T_{sky}(\theta)$: REFLECTED SKY (OR BACKGROUND) RADIOMETRIC TEMPERATURE
- $L_a(\theta)$: ATMOSPHERIC ATTENUATION BETWEEN SCENE AND SENSOR

Attenuation by Atmospheric Gases, Rain and Fog (from Preissner, 1979)

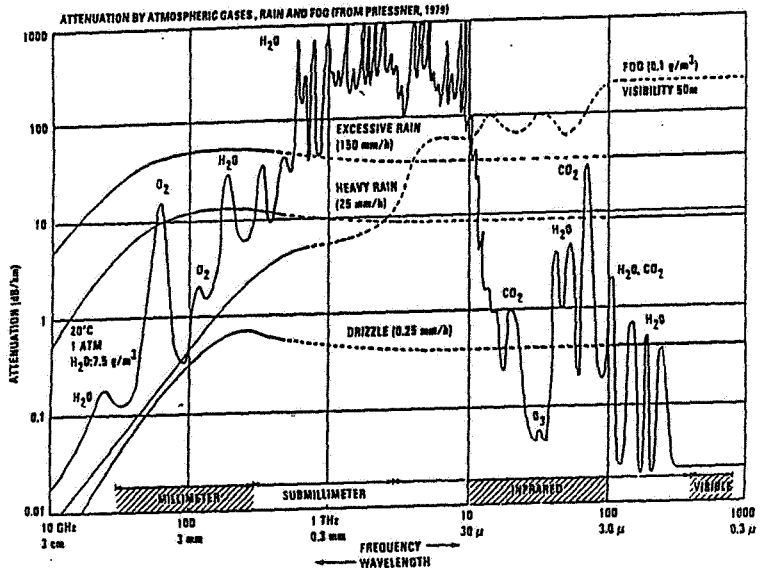

Millimeter Waves Give the Strongest Observed Radiometric Signals

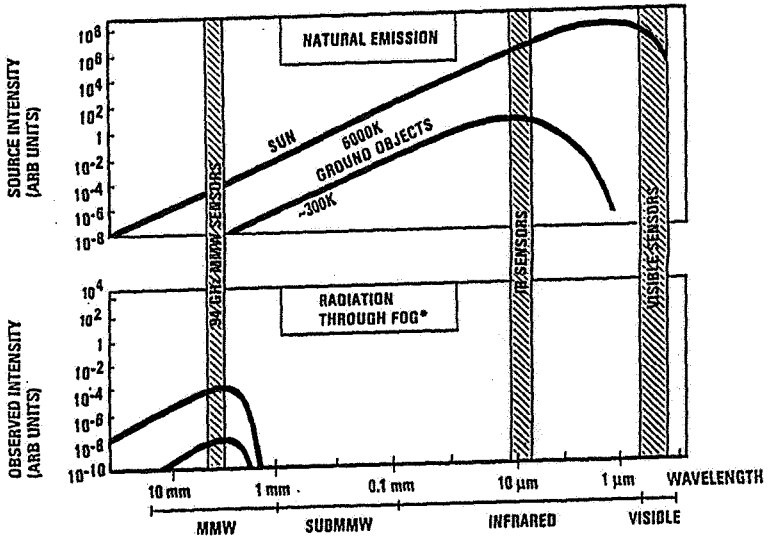

Fog Penetration Using 94 GHz MMW Propagation Window

CLEAR

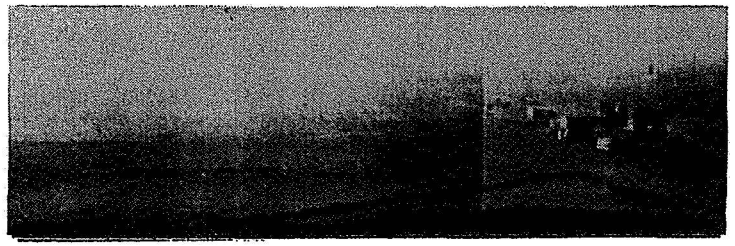

FOG, 120 M VISIBILITY

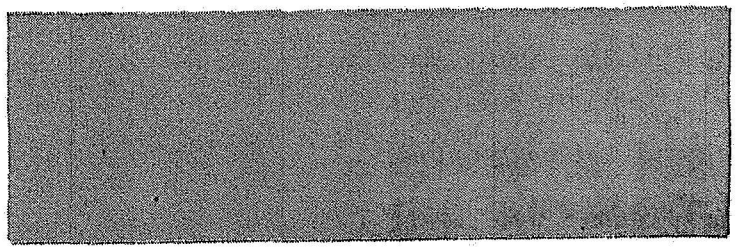

VISUAL LIGHT PHOTOGRAPHY

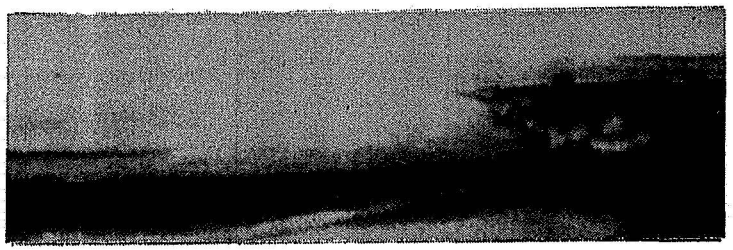

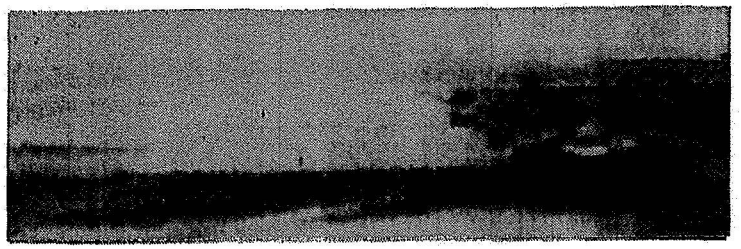

94 GHz RADIOMETRIC IMAGERS

SHAFTER, AIRPORT, CALIFORNIA

Passive MMW Radiometry Gives Day/Night Navigation and Landing Capabilities

TRW

Visible Light Photograph

Day

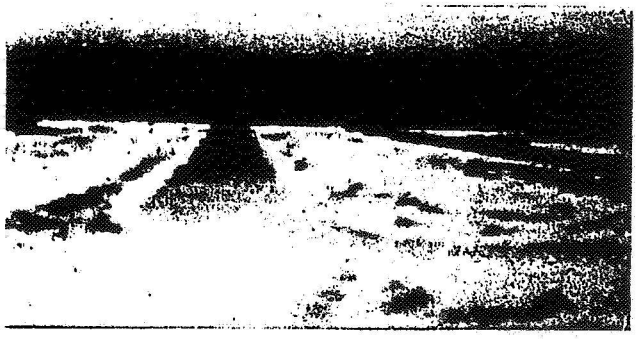

Night

94 GHZ RADIOMETRIC IMAGE AT TRUCKEE-TAHOE AIRPORT

94 GHz Image of Long Beach Harbor

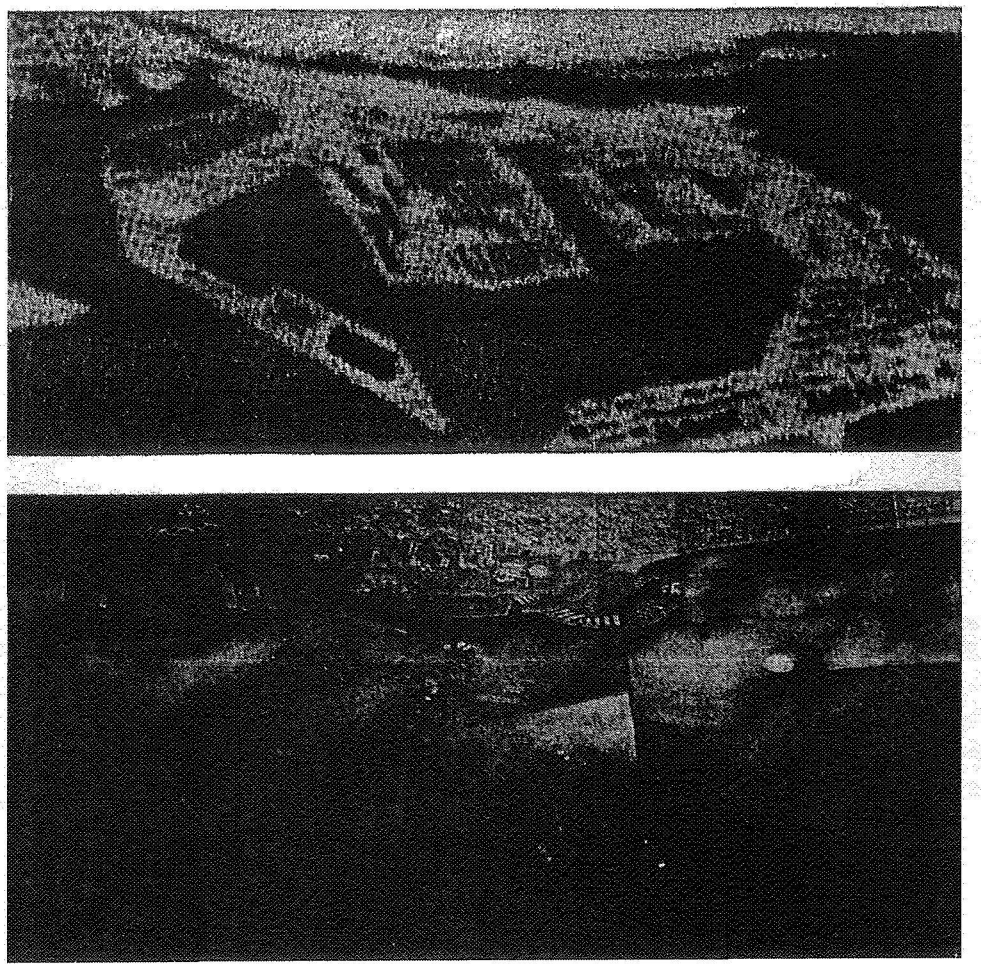

Aircraft Is Clearly Visible on Taxiway

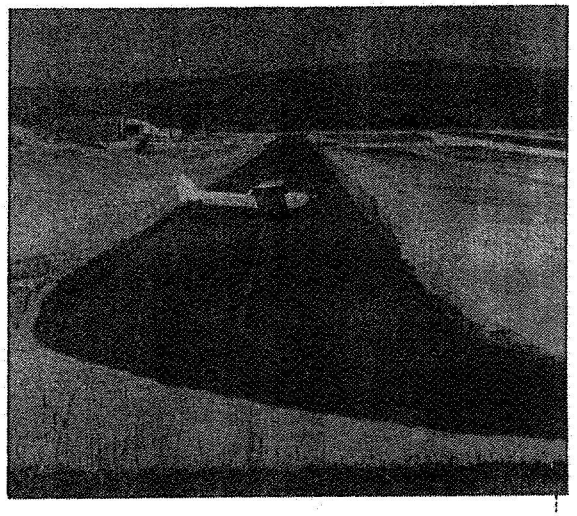

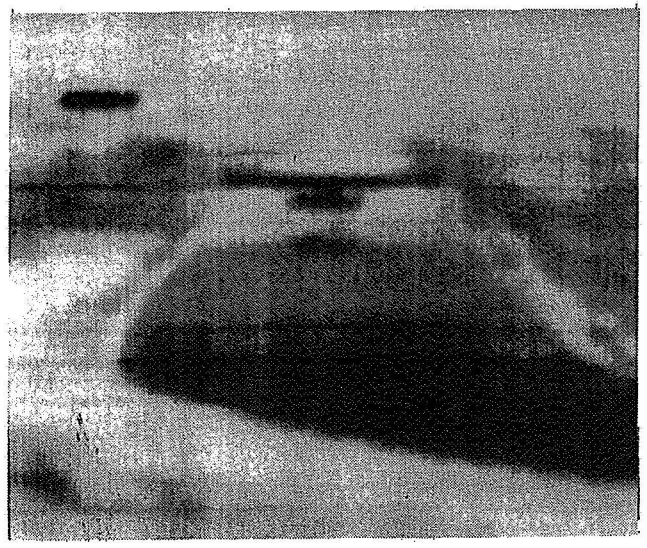

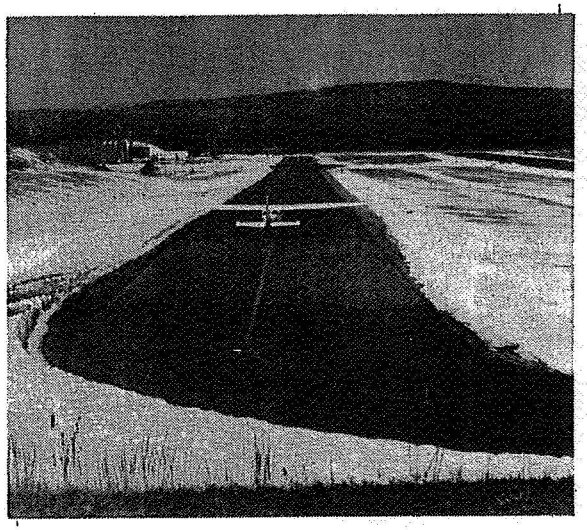

15° x 15° field of view with 6 mR resolution. Aircraft is 390 feet from camera

Ground Tracking of Aircraft in Airfield

Brunswick, Maine NAS

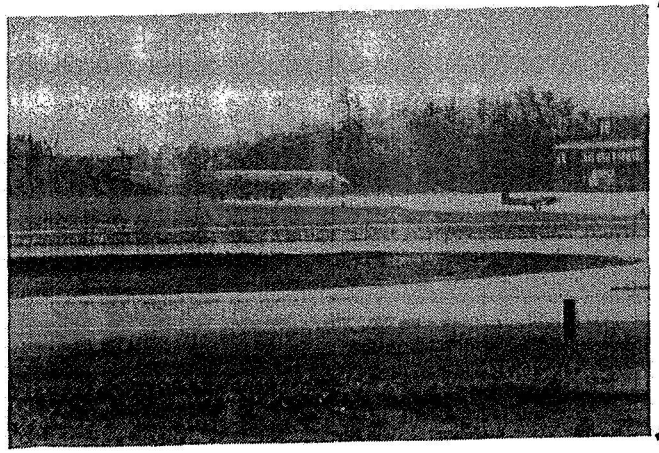

VISIBLE LIGHT MAGNIFIED IN CLEAR WEATHER

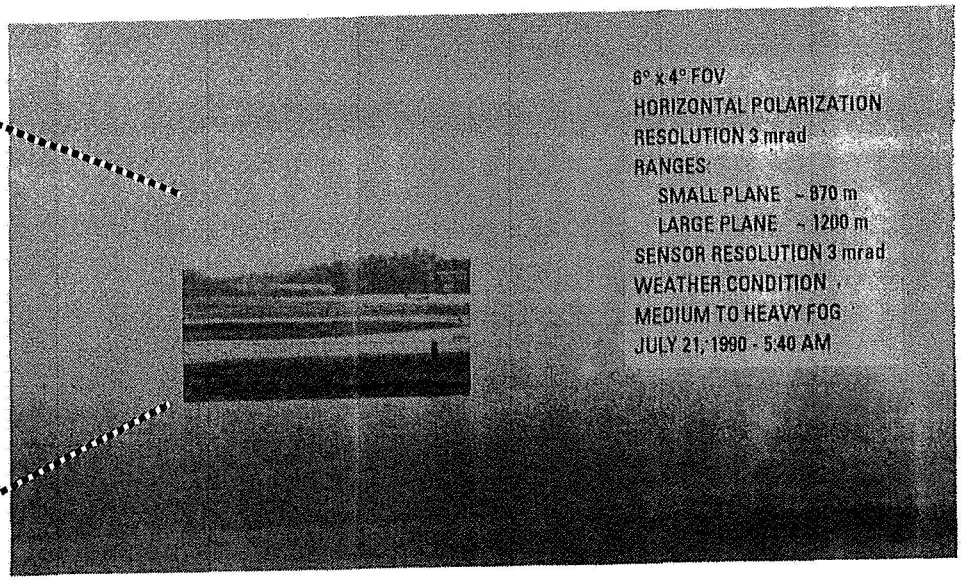

VISIBLE LIGHT IN FOG

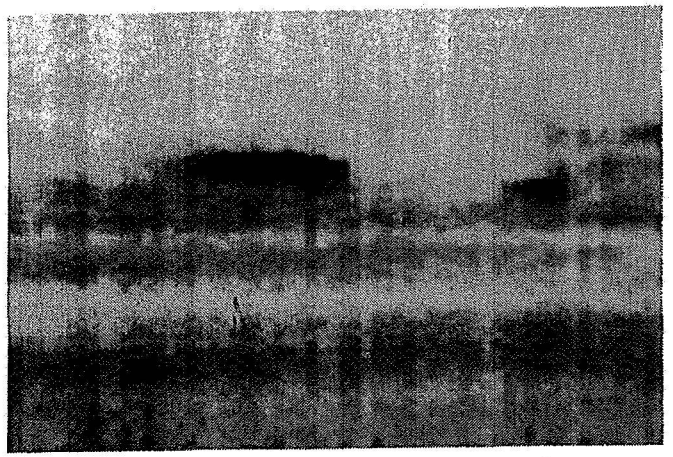

94 GHz RADIOMETRIC IMAGE IN FOG

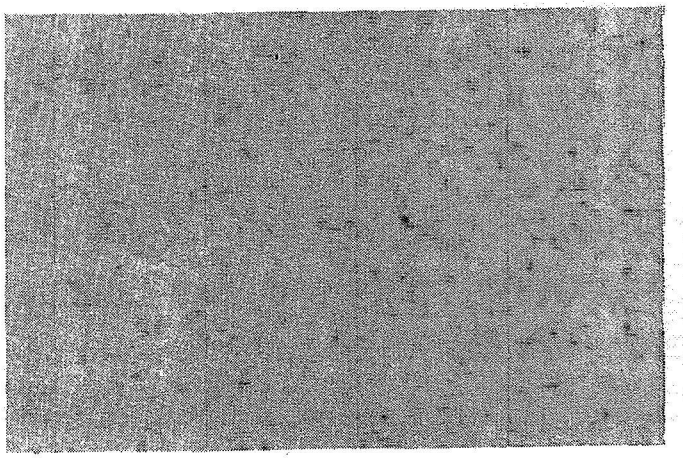

IR RADIOMETRIC IMAGE IN FOG

Passive Millimeter Wave Radiometric Image
(Building E2 at a Range of 180 Meters)

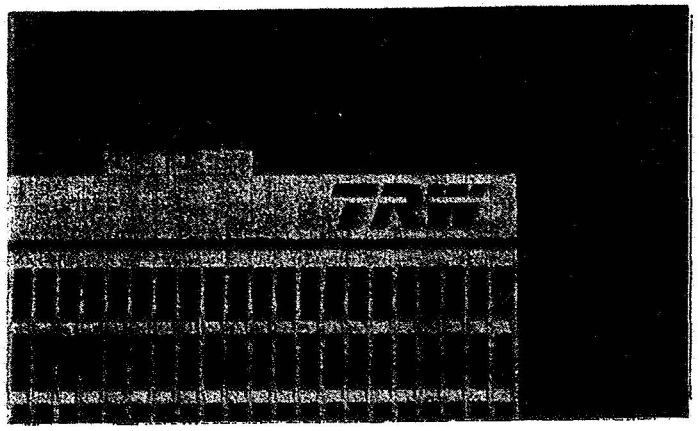

VISIBLE LIGHT PHOTOGRAPH

94 GHz RADIOMETRIC IMAGE

End-to-End Passive MMW Scene Simulation

A State-of-the-Art Capability to Predict Radiometric Scenes for a Wide Variety of Weather/Ground Conditions and Platform Operating Modes

PHENOMENOLOGY MODEL
- Atmospheric Propagation Model
- Atmospheric Weather Model
- Surface/Terrain Physics Model
- Ray Tracing Algorithm

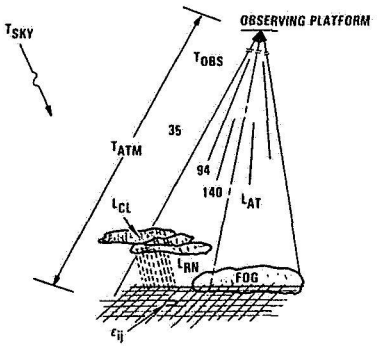

SENSOR MODEL
- Sensor Optics Model
- Detector Model
- Mechanical/Electrical Effects Model

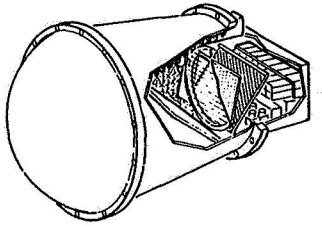

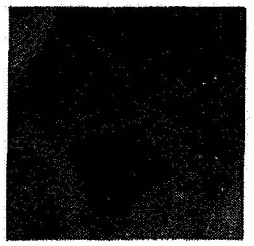

IMAGE PROCESSING MODEL
- Image Enhancement Techniques
- Image Restoration Techniques
- Defination of Real-Time Algorithms and Hardware

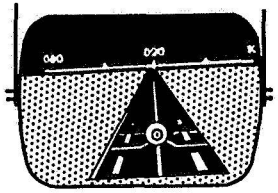

DISPLAY MODEL
- Frame-by-Frame Animation

The Phenomenology Model Includes All Aspects of the Passive MMW Scene

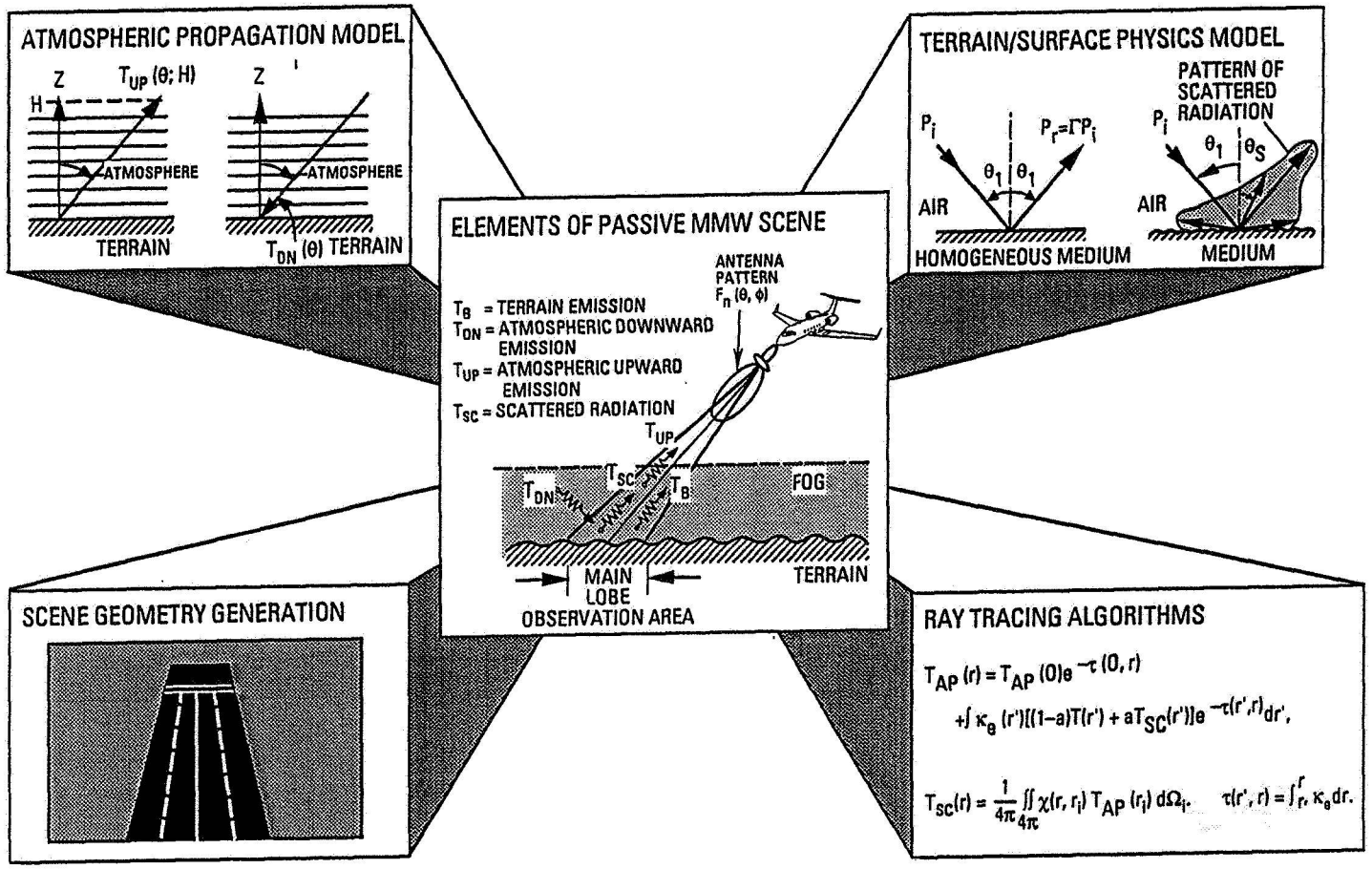

Scene Geometries Are Constructed Using the Combinatorial Geometry Technique

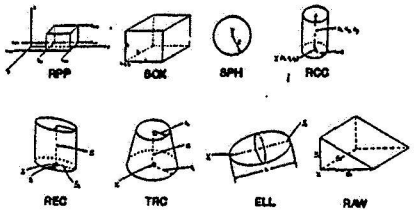

- Eight basic geometric shapes constitute the building blocks for 3–D complex–shaped objects

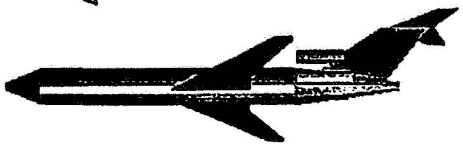

- The building blocks are *combined via union, intersection* and exclusion operations to form 3–D scene objects

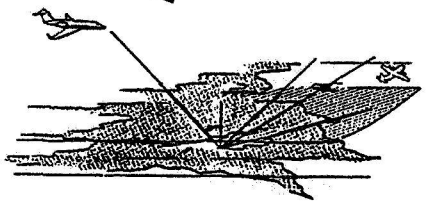

- The combinatorial geometry package determines ray intercepts with scene objects, providing the specific surfaces and propagation distance for the scene

Synthetic Vision Research Underway at LaRC

NASA/TRW *ASSIST* PROGRAM

GOAL: Provide Flight Sensor/Display Technology to Enable Safe & Efficient Aircraft Operations Under Restricted-Visibility Conditions

Pictorial Display Augmented With Sensor-based Info.

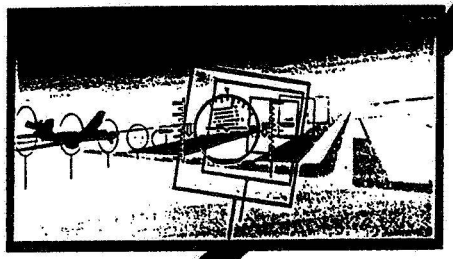

Flight

Sensor Image Augmented With Graphic Symbology

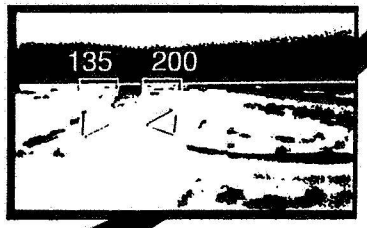

Simulation

Passive Millimeter Wave (PMMW) Sensor Imagery

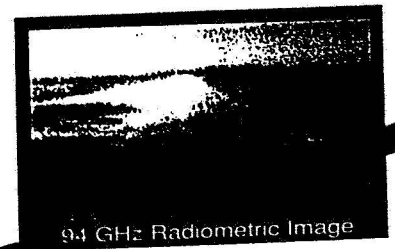

Modeling

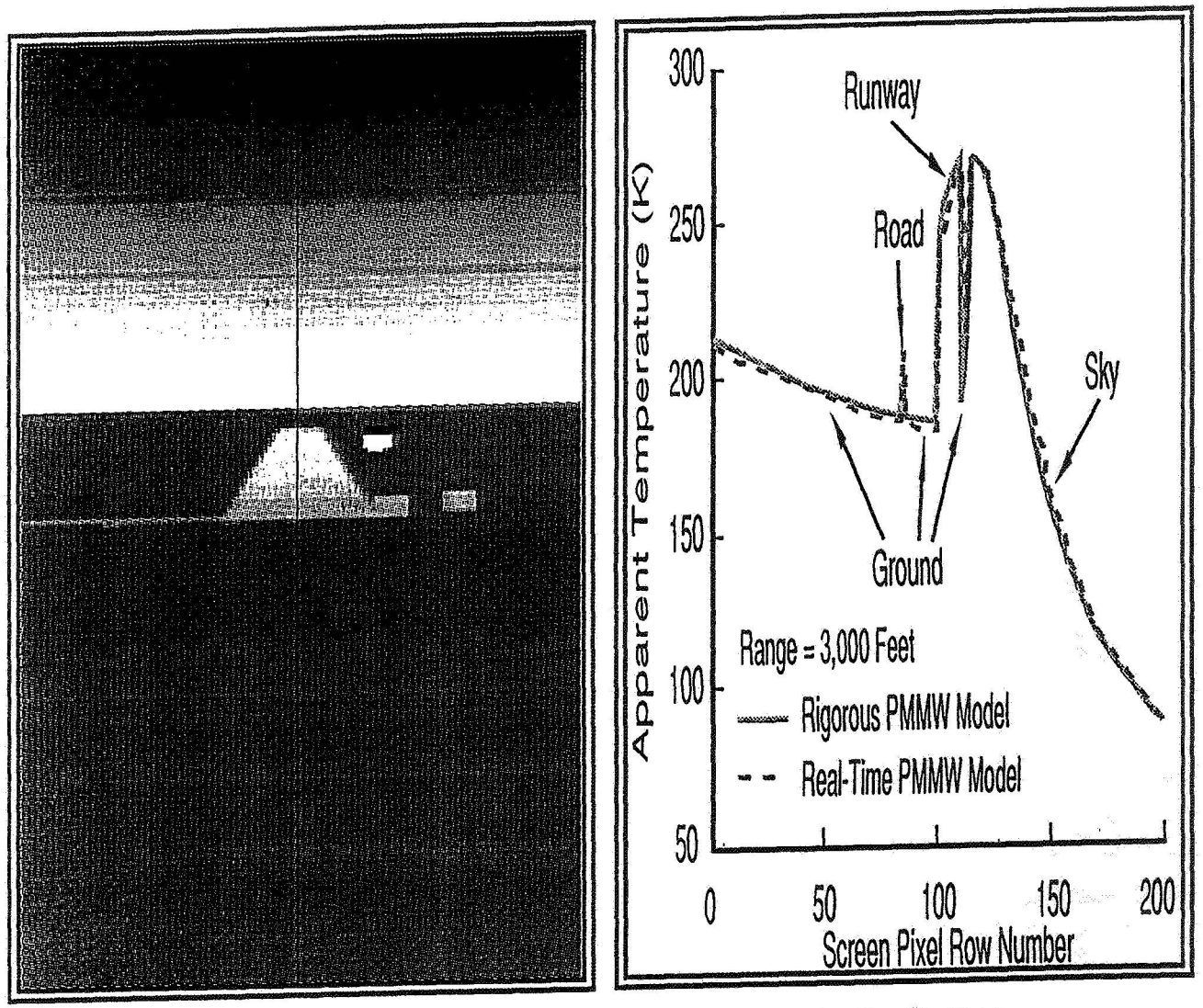

Validation of Real-Time PMMW Model Using Intensity Profile Test

The Development of MMW Staring 2-D Focal Plane Receiver Arrays is a Major Innovation that Permits Video Imaging at High Frame Rates

TRW

	Nominal 10,000 Pixels Image	Time Required to Obtain One Frame (Integration Time = 30 ms, MRT = 0.7 K)
Single element receiver scanner	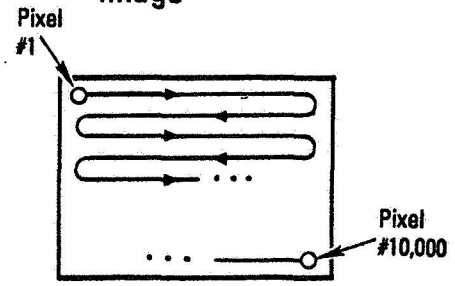	300 s
1-D receiver array push broom scanner	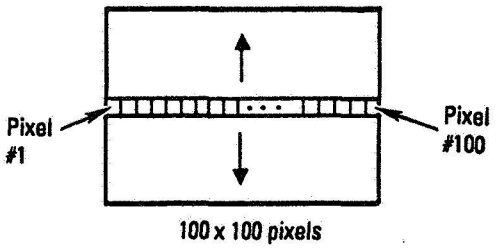	3 s
2-D staring receiver array	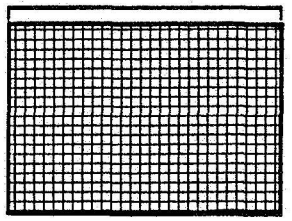	0.03 s

TRW has Over 10 Years Experience in Developing PMMW Systems

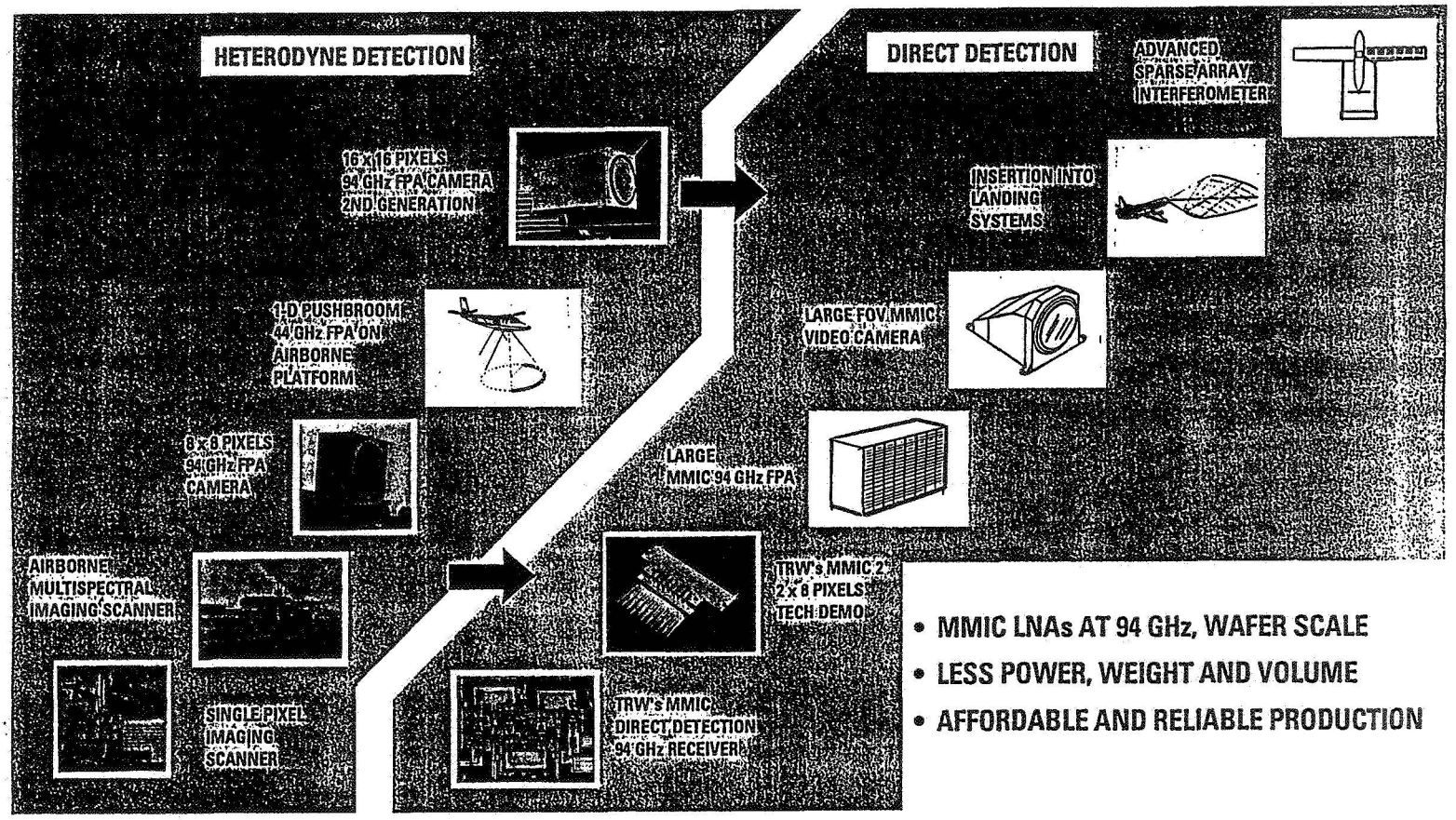

R1M 92.0129.03

Elements of Passive MMW Video Camera

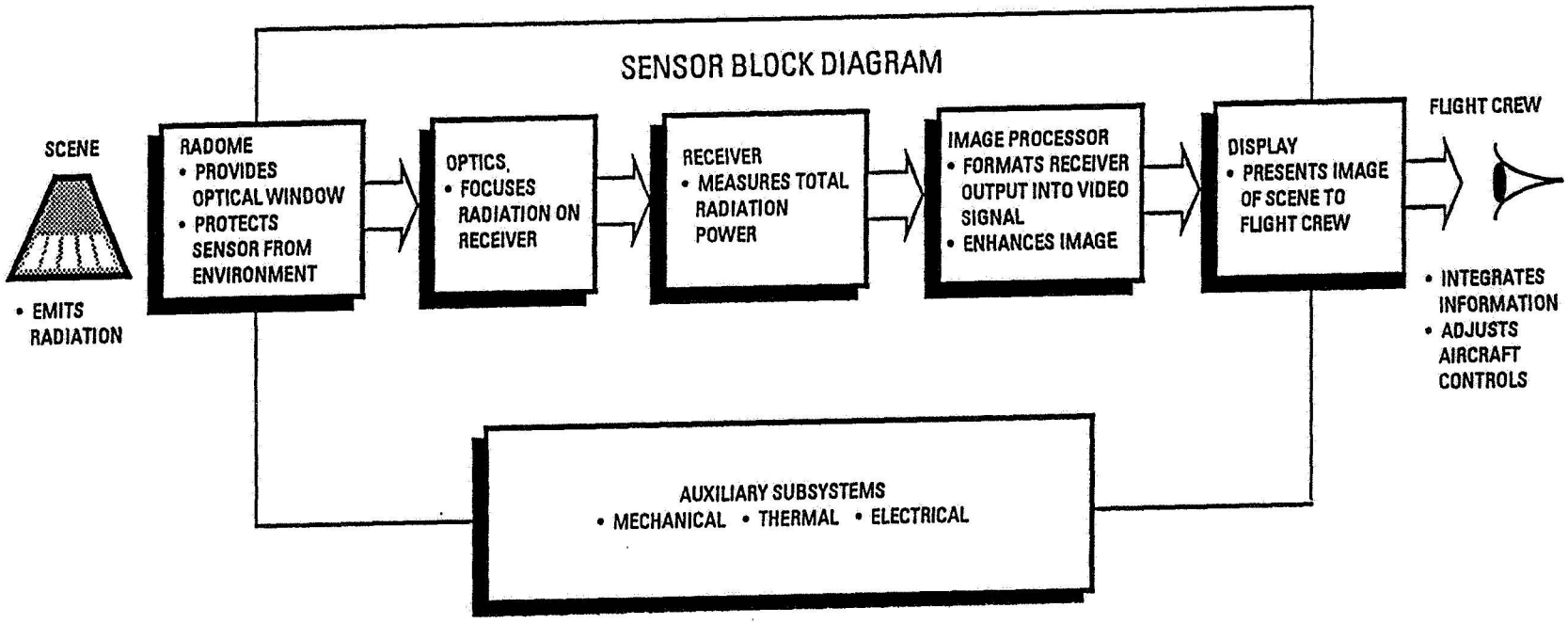

Product Description

Passive millimeter wave MMIC camera with real time imagery and ruggedized for field and flight tests

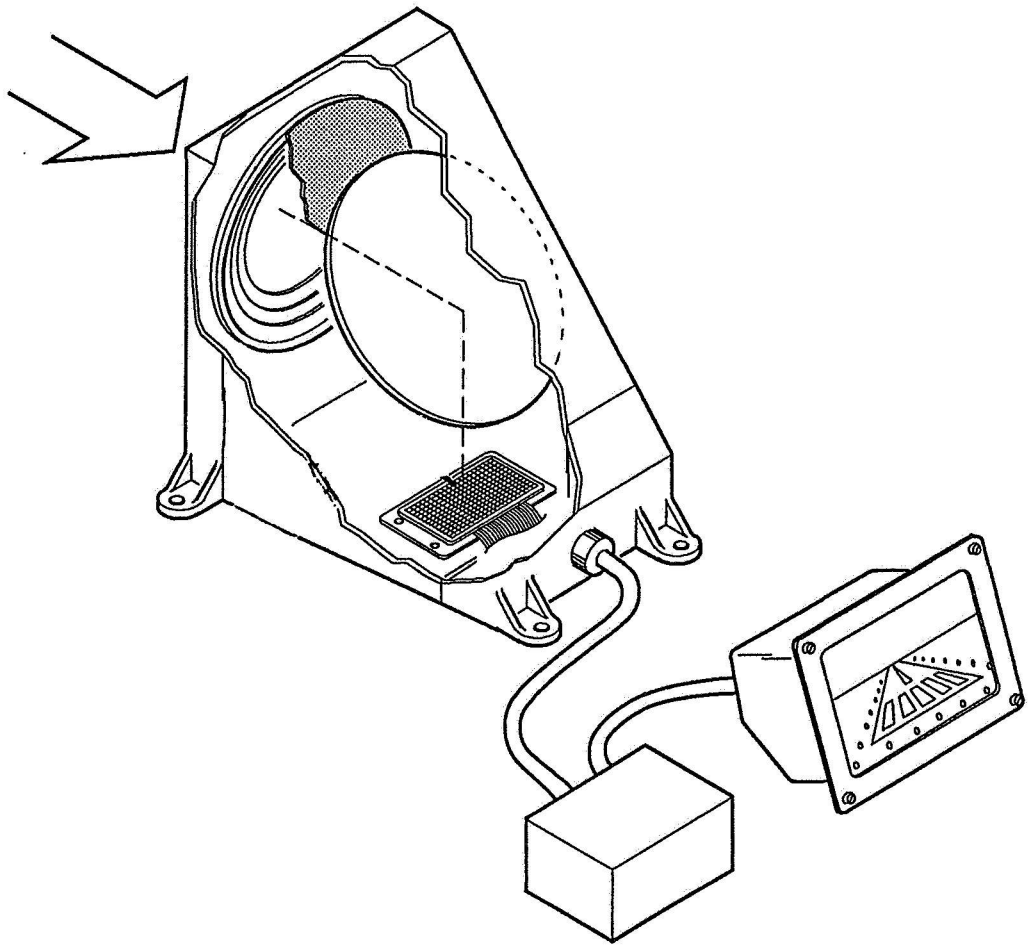

PMMW Camera is an Attractive Vision Sensor for Future Enhanced/Synthetic Vision Systems

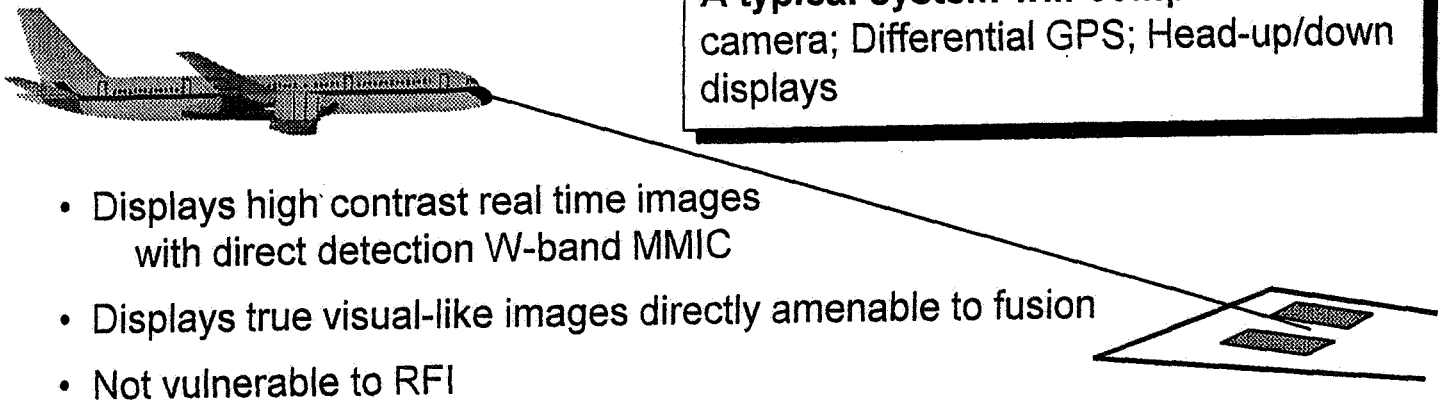

A typical system will comprise: PMMW camera; Differential GPS; Head-up/down displays

- Displays high contrast real time images with direct detection W-band MMIC
- Displays true visual-like images directly amenable to fusion
- Not vulnerable to RFI
- Does not radiate in airport environment
- No issues of minimum range, image latency or high processing overhead
- Operates with "W-band runway lights", similar to night aircraft operations
- Can be manufactured economically within four years

omit

Synthetic Vision System Flight Test.

L. Jordan,

Honeywell Technical Center

Synthetic Vision System Flight Test
Hardware

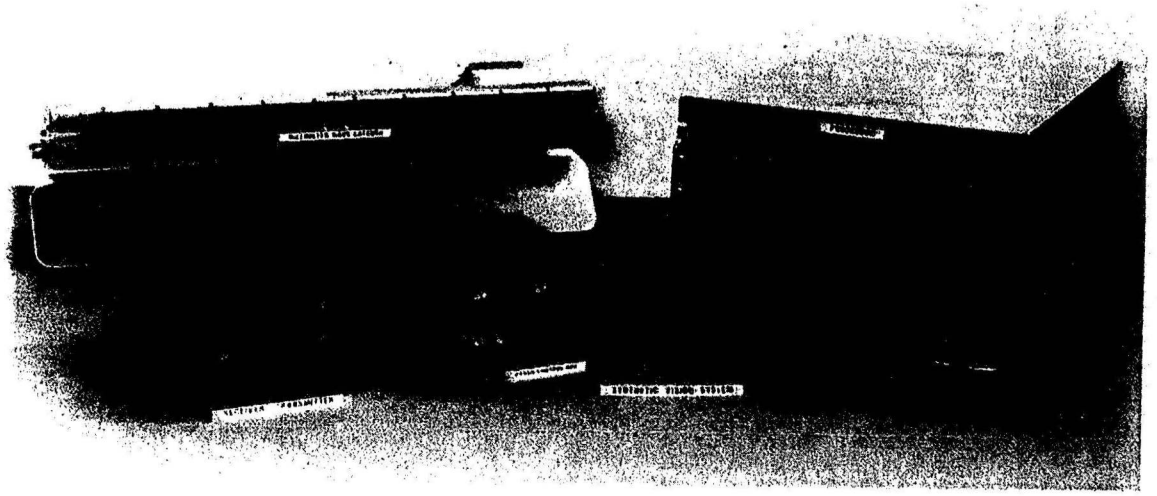

System Specifications

• Frequency	35 GHz
• Power out	1.1 kW (1 W avg.)
• Range	>3 mi
• Antenna dimensions	34 × 8 × 4 in.
• Scan area	30 deg (az.) by 26 deg (elev.)

Synthetic Vision System
Functional Block Diagram

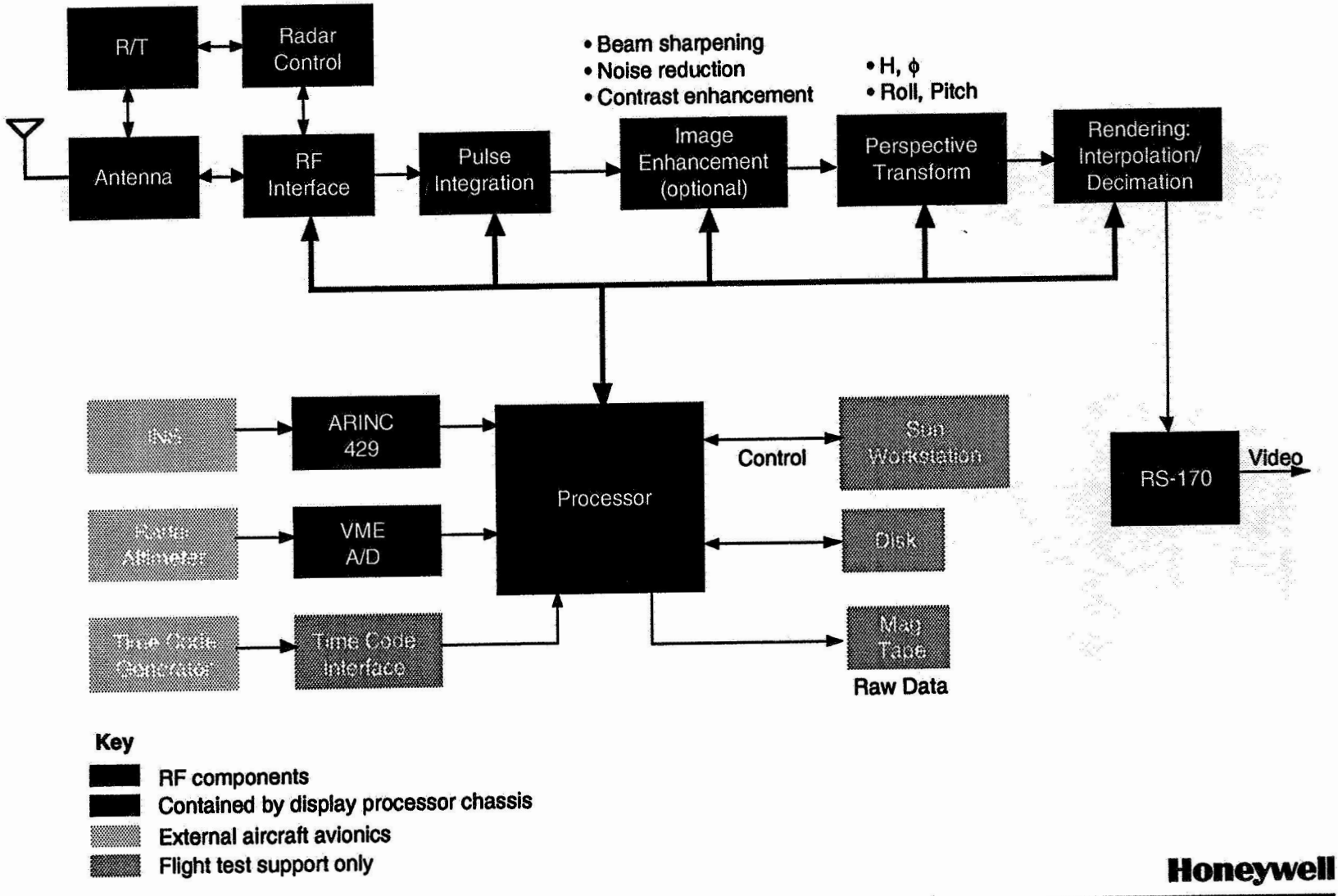

Honeywell

Synthetic Vision System Tower Test

Camera View from WPAFB Tower (Alt. = 290 ft)

Perspective Synthetic Vision Image Processed from Radar Data

Synthetic Vision System Flight Test

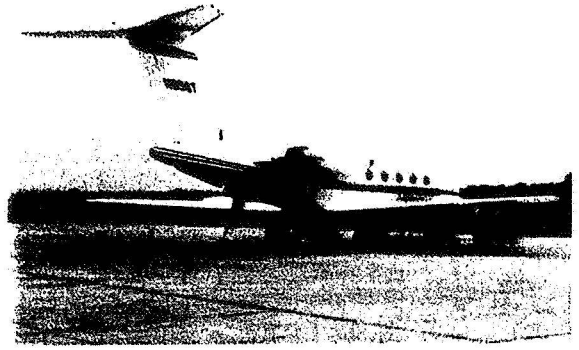

Test Aircraft

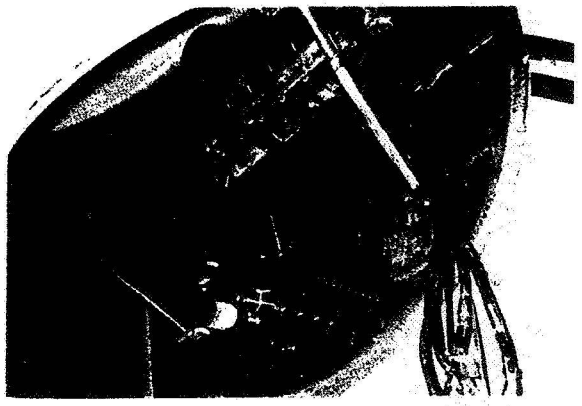

Antenna Mount

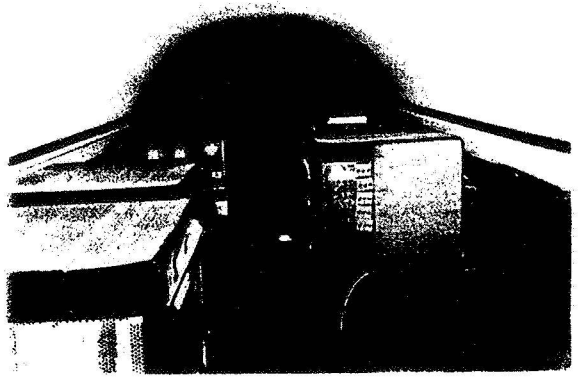

Flight Instrumentation

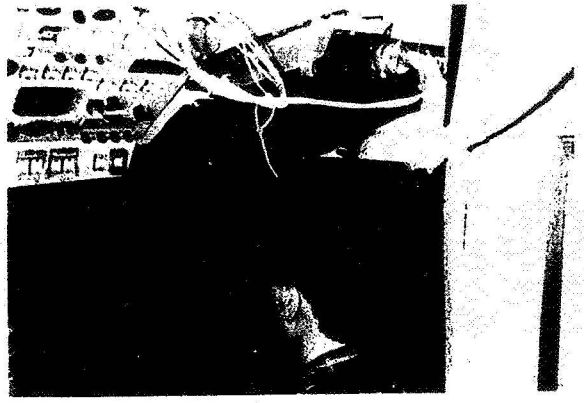

Cockpit/HUD

Approach to Vandenburg AFB
Honeywell 35 GHz SVS at 142' Altitude

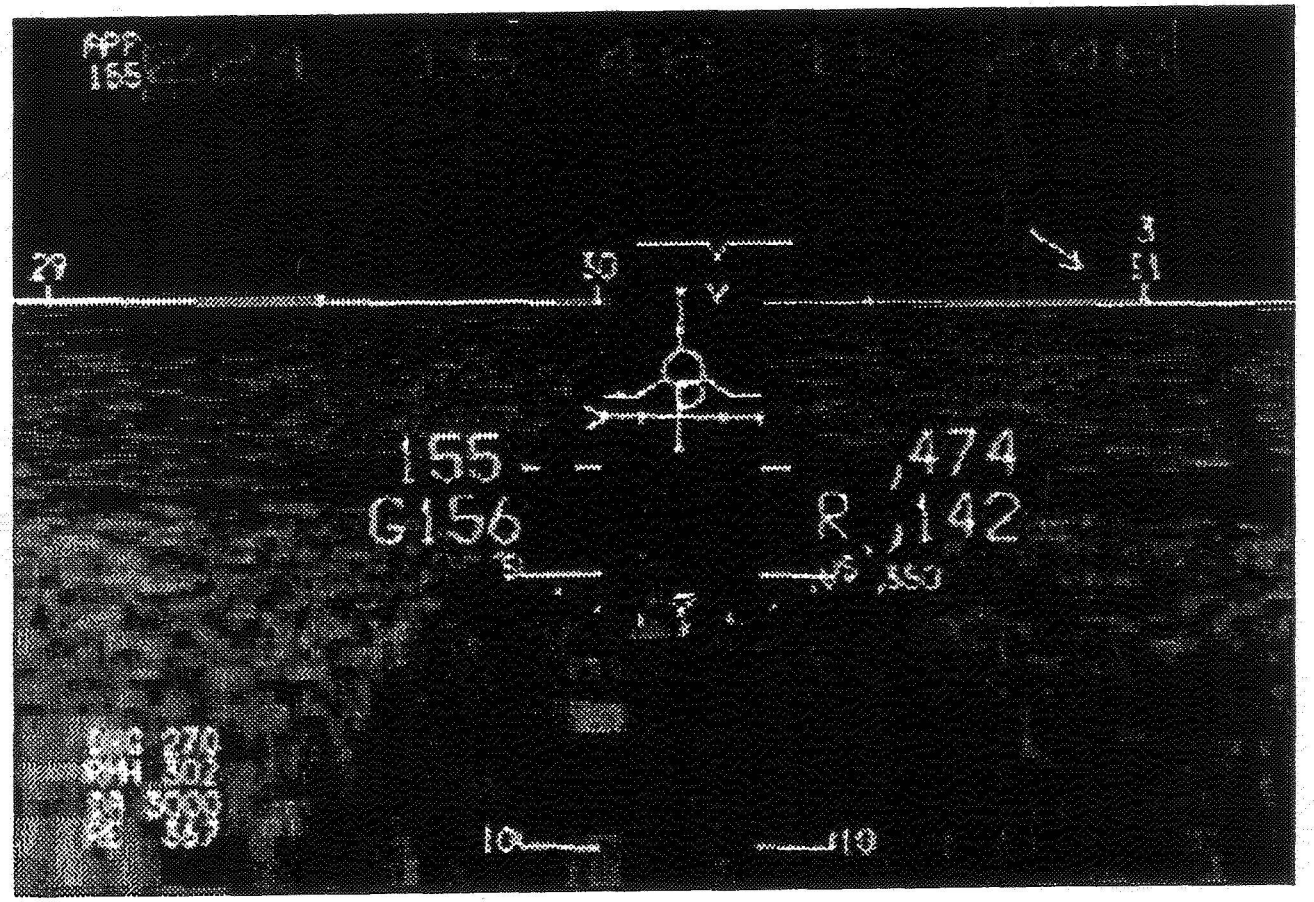

Honeywell

Imaging Radar
Issues and Lessons Learned

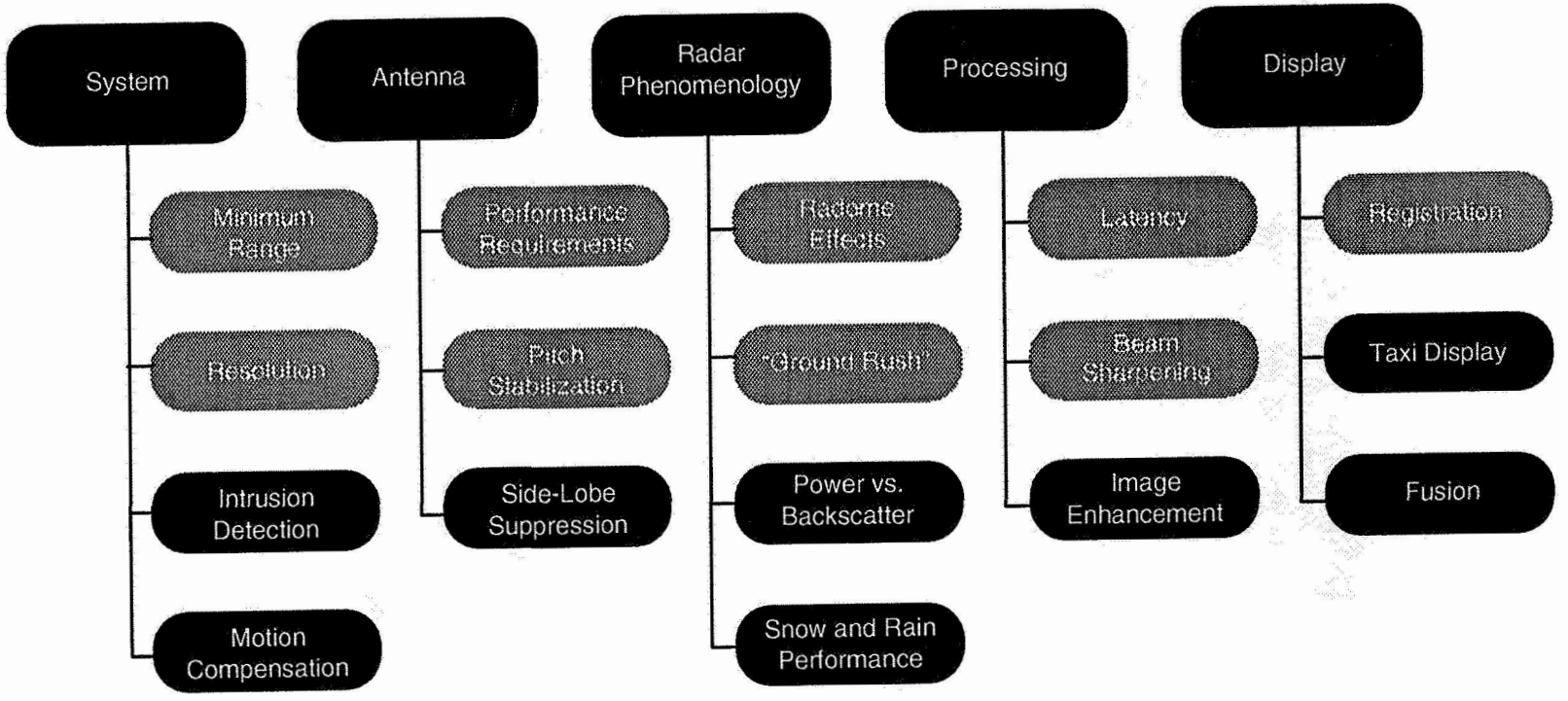

Beam-Sharpening Results

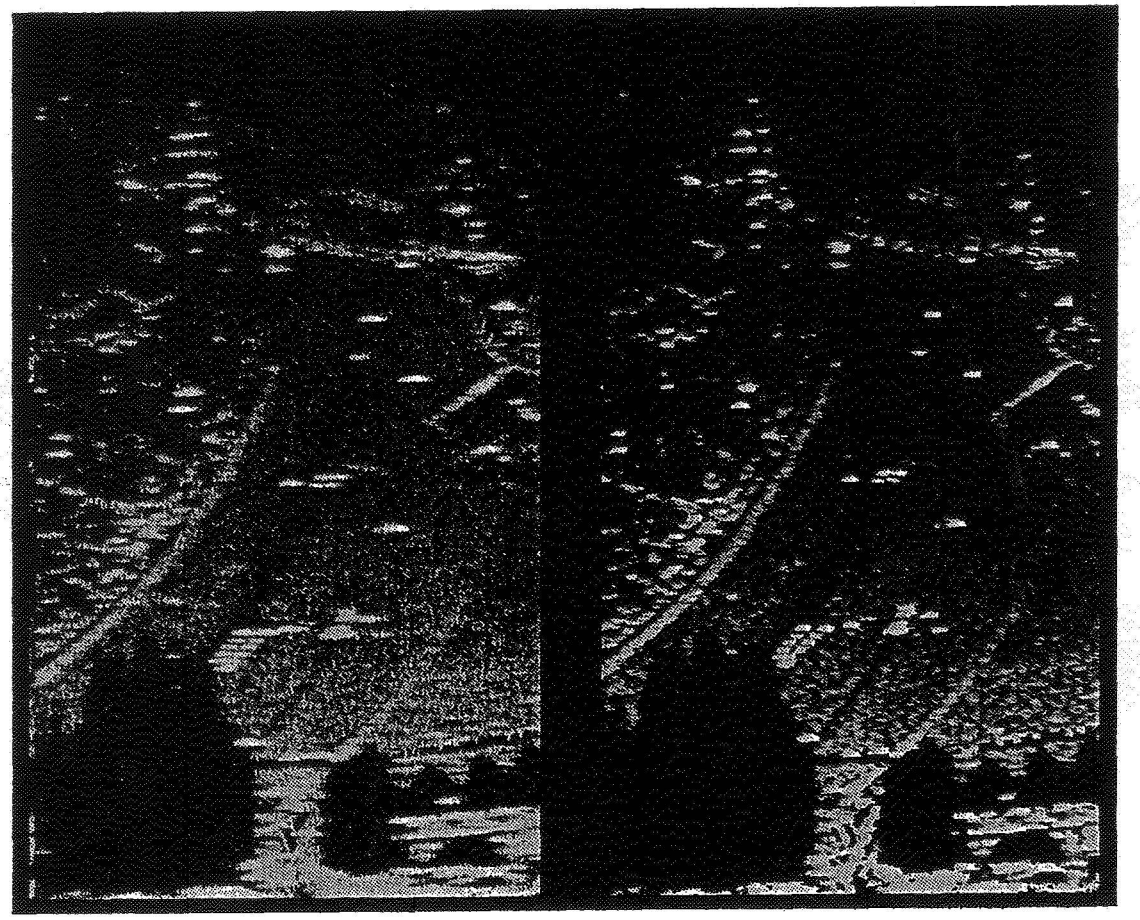

Runway/Taxiway Detection Results

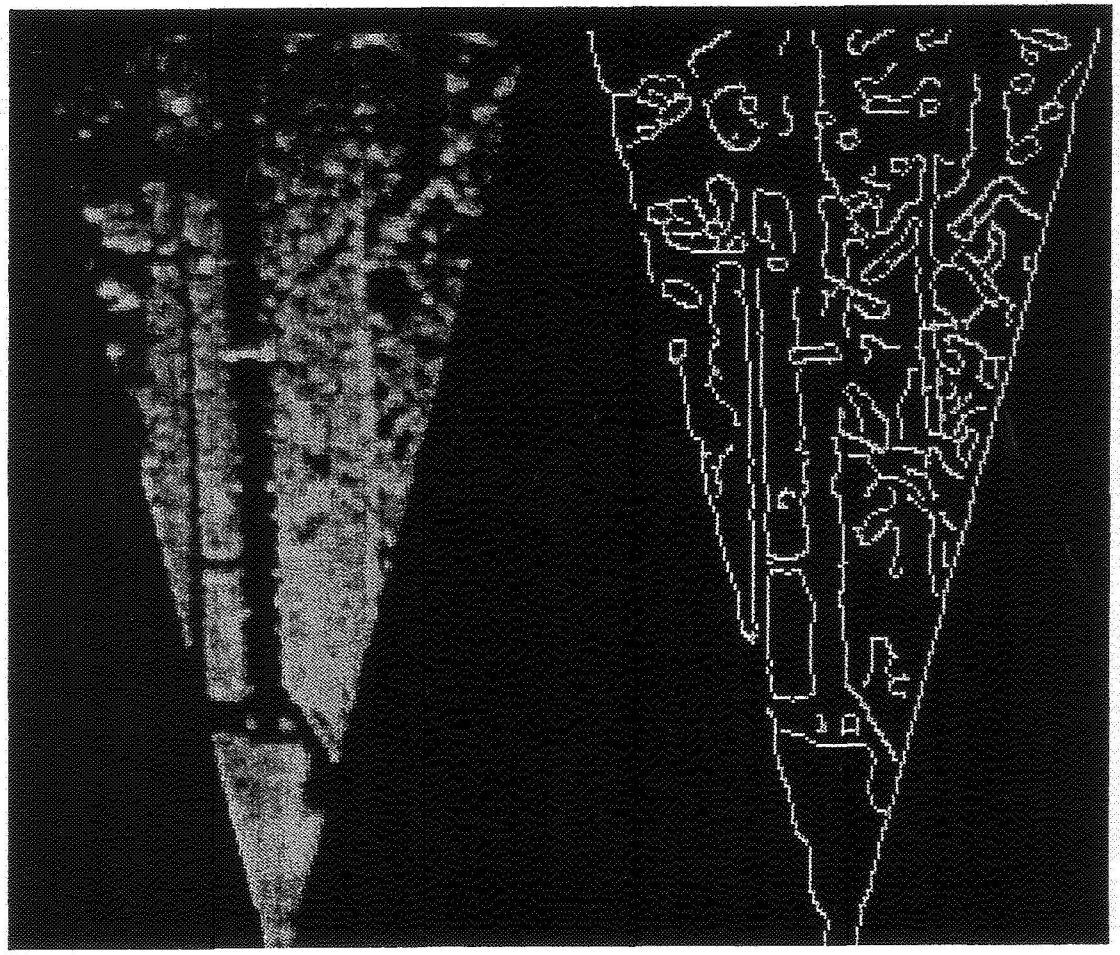

Runway/Taxiway Detection Results

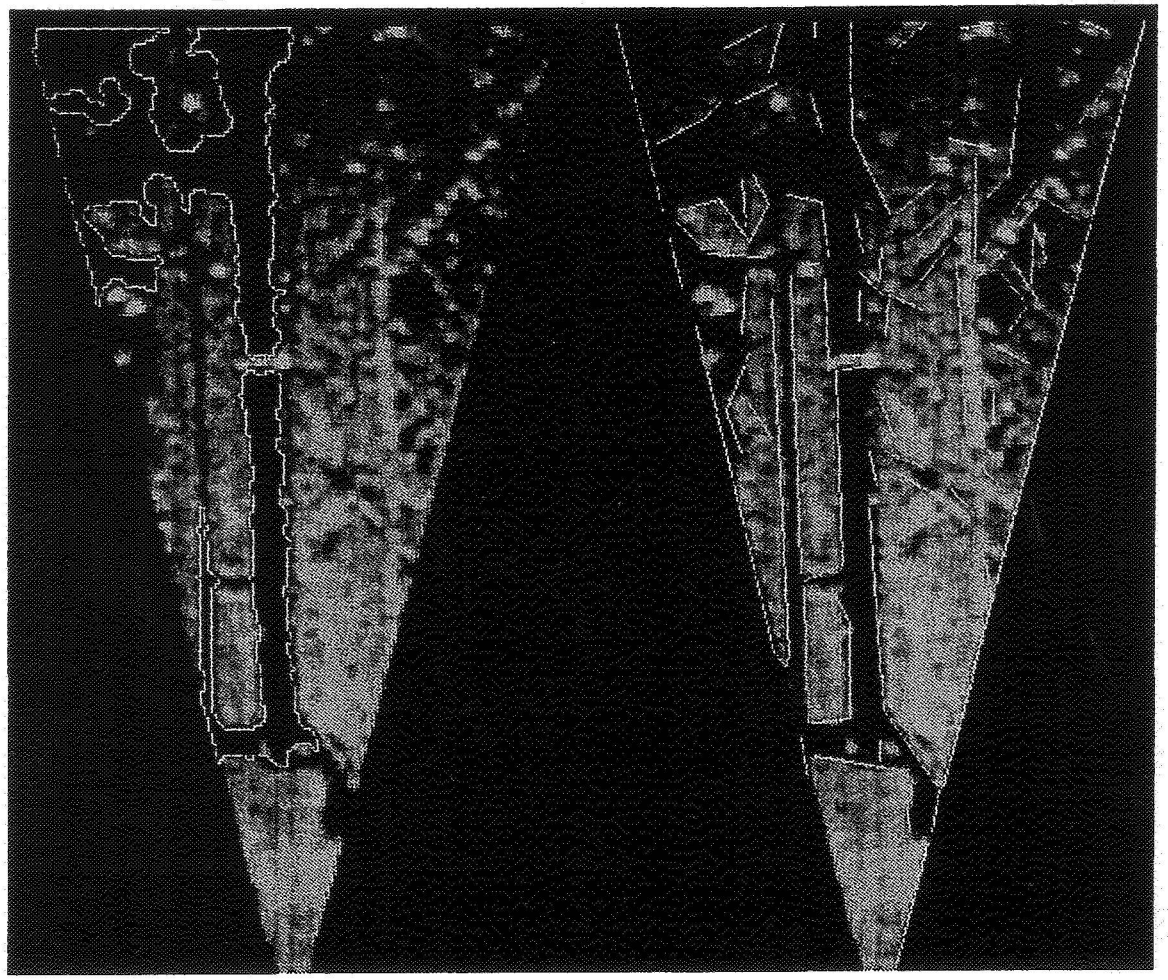

Autonomous Airplane
System Concept

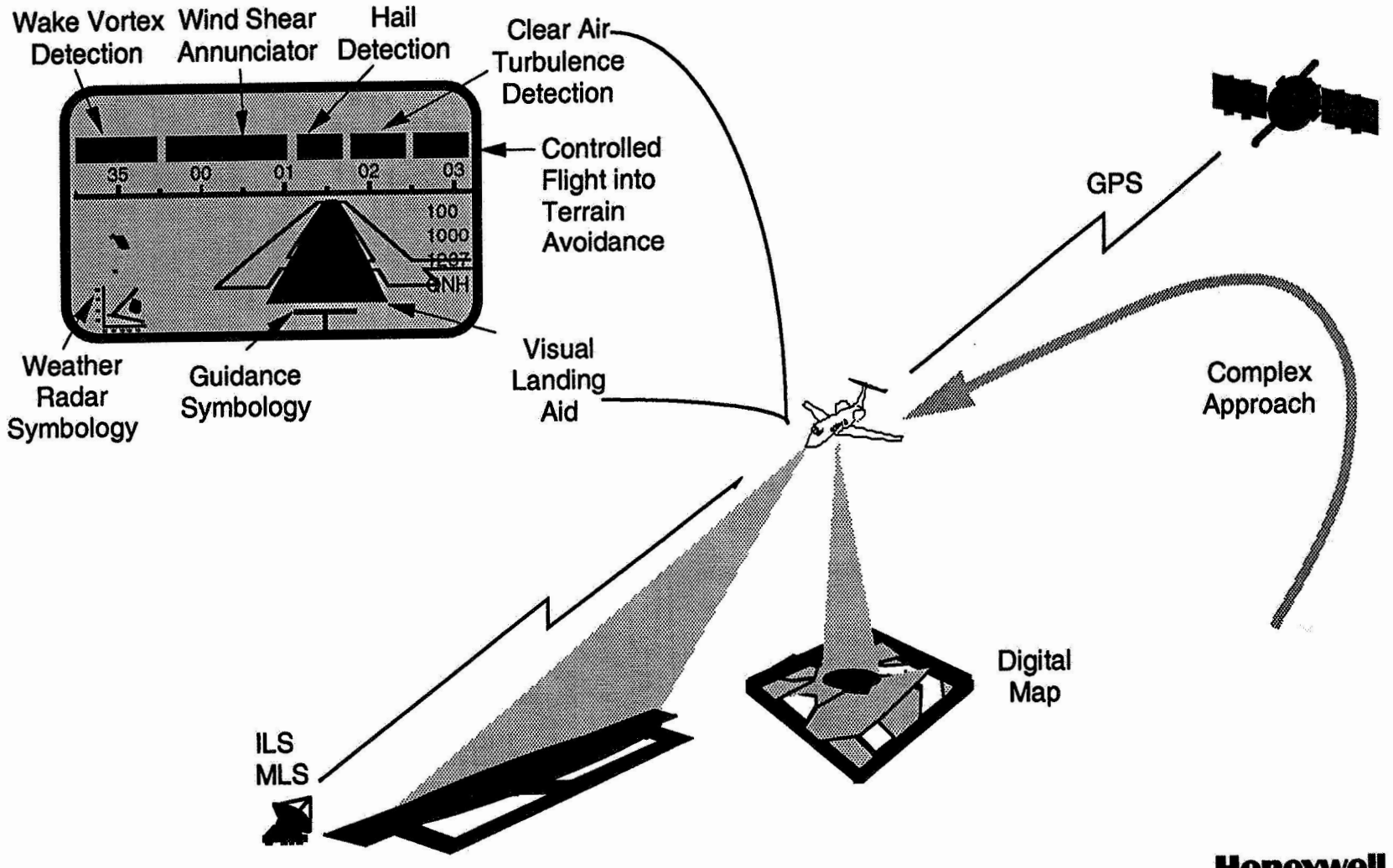

797

Honeywell

Autonomous Airplane
System Functions

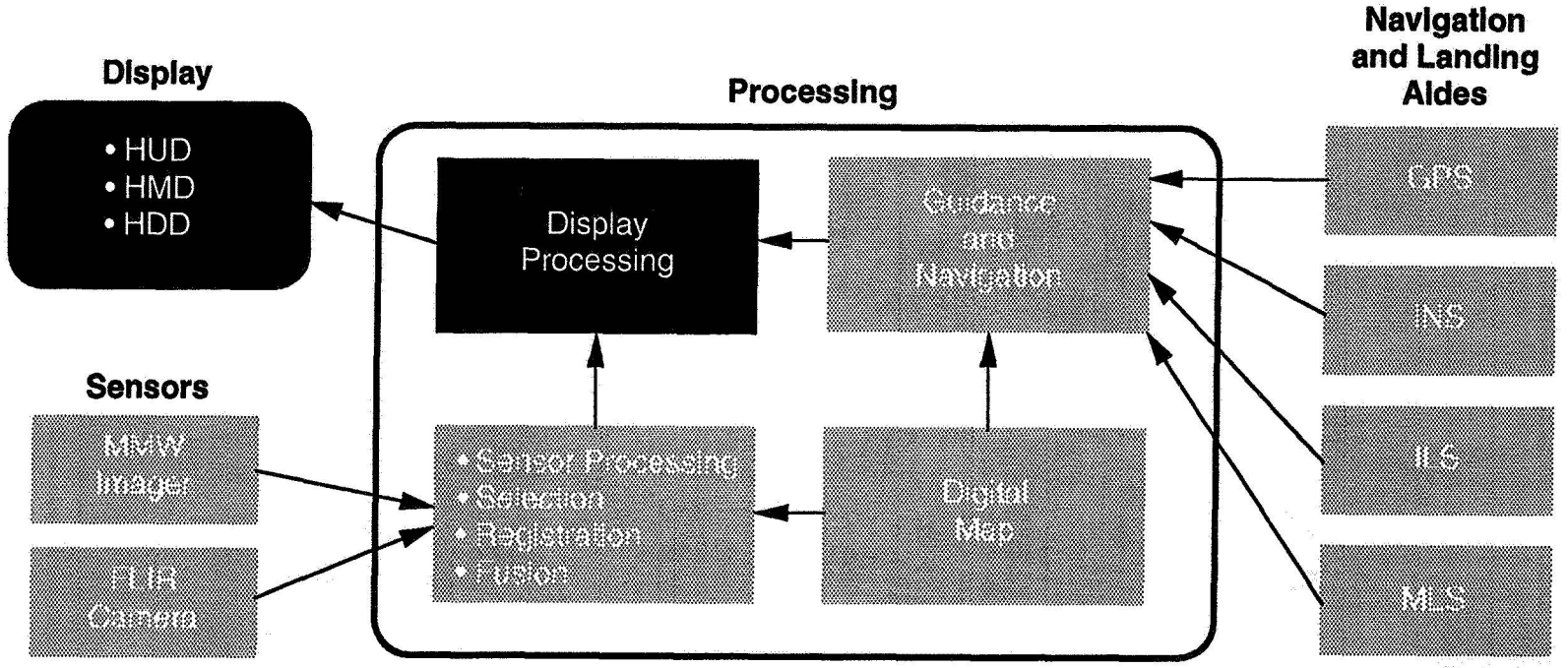

omit

Enhanced Synthetic Vision Systems.

C. Taylor,

Lear Astronics Corp.

Enhanced / Synthetic Vision Systems

Chris Taylor
Program Manager, Autonomous Landing Guidance
Lear Astronics Corp.

5th Combined Manufacturers'
and Technologists'
Airborne Wind Shear
Review Meeting

Paper 7-06

Lear Astronics ALG Team Program

- **Practical and Realistic**
  - Customer Driven
    - » Team Includes Two Commercial Air Carriers and USAF, who contribute to Operations Requirements Board
  - Entirely Within Existing FAR/JAR Requirements
    - » Requires no changes to existing regulations
  - Common Aperture W/X Radar
    - » Imaging Radar Add-On Kit To Existing Radar
    - » All Current Functions (Plus Windshear) Supported
  - Guidance To Touchdown
    - » Full-Time Guidance Thru Flare: Image Confirmation
  - Sensor Fusion
    - » Best Image By Combining Radar, Dual Band FLIR, Visual

Lear Astronics ALG Team Program

- **Applicability**
  - Retrofit To Commercial And Military Aircraft
    - » Basic Goal is Cat 3a Weather Performance On Type I ILS
    - » Provides All-Weather Capability At Most Facilities
  - Forward Fit Commercial And Military Aircraft
    - » Even GPS/Autoland Cannot Provide All-Weather Takeoff
    - » Pilot Currency / Training Still An Issue
    - » Provides Obstacle / Incursion Avoidance & Taxi Capability
  - Special Type Aircraft
    - » HSCT (No Conventional Forward Visibility)

Lear Astronics ALG Team Program

- Low-Power (200mW) FMCW, 94GHz Radar
  - Built On Solid Development And Test Foundation
    - » Field Test (Radar Test Vehicle)
    - » Tower Test (WPAFB Sensor Test Facility)
    - » Flight Test (200 Approaches, MADL Cessa 402)
  - Confirms Basic Technology Choices
    - » Low Power (Low Interference) Radar Capable Of Providing Suitable Imaging Performance (Actually Slightly Better In Fog)
      - Recognizable Runway Enviroment At >800'
      - Light Array / Runway At >400'
      - Edge/Centerline Lights At >100'
    - » 94GHz Resolution Highly Desirable
      - Lights/Edges/Detail Structures
      - Pigeon-Size Birds On Runway

Lear Astronics ALG Team Program

- **Summary**
  - Unique Team Of Industry And Government Leaders In Enhanced Vision / Autonomous Landing Guidance / Sensor Fusion
  - Unique Combination of Imaging Sensors (Active 94GHz Imaging Radar And Fused 3-5/8-12 Micron IR)
  - Unique Customer Focus / Regulatory Approach
  - Unique Database Of Information Gathered In Operationally Realistic Environment Driving Preproduction Designs
- **Enhanced Vision Is A Reality In 1993**
  - Successful Blind/Fog Approaches Using Image From Small-Aperture Radar Coupled With HUD Symbology